# THEORETICAL ANALYSIS OF NONLINEAR DIFFERENTIAL EQUATIONS IN APPLIED CHEMICAL SCIENCES



A thesis Submitted to the Bharathidasan University, Tiruchirappalli in partial fulfillment of the requirements for the award of the degree of

## **DOCTOR OF PHILOSOPHY IN MATHEMATICS**

# Submitted by

# R. SWAMINATHAN

Ref.No:007689/Ph.D.K1/Mathematics/P-T/(3-5)Jan-2019

Under the Guidance of

Dr. K. VENUGOPAL, M.Sc., M.Phil., PGDCA., Ph.D.,
Assistant Professor



PG & RESEARCH DEPARTMENT OF MATHEMATICS
GOVERNMENT ARTS COLLEGE
KULITHALAI – 639 120.
TAMIL NADU, INDIA

**FEBRUARY – 2022** 

# **CERTIFICATE**

## Dr. K. VENUGOPAL, M.Sc., M.Phil., PGDCA., Ph.D.,

Research Supervisor,
Assistant Professor,
PG & Research Department of Mathematics,
Government Arts College, Ayyarmalai,
Kulithalai- 639 120,

Karur (Dt). Mobile No: 9442358231 E-mail:drvenugopal2013@gmail.com



Date:

# **CERTIFICATE**

This is to certify that the thesis entitled, "THEORETICAL ANALYSIS **OF NONLINEAR DIFFERENTIAL EQUATIONS** IN **APPLIED CHEMICAL SCIENCES**" submitted to the Bharathidasan University in partial fulfillment of the requirements for the award of Degree of **Doctor of Philosophy** in Mathematics is a record of original research work done by Mr. R. SWAMINATHAN, Principal and Head of the Department of Mathematics, Vidhyaa Giri College of Arts and Science, Puduvayal during the period of his study in the Department of Mathematics Government Arts College, Ayyarmalai, Kulithalai under my Supervision and Guidance and the thesis has not formed the basis for the award of any Degree / Diploma / Associate Ship / Fellowship or other similar title to any candidate of any University and that the thesis represents independent work on the part of the candidate.

Dr. K. VENUGOPAL

Supervisor and Guide

# **DECLARATION**

## Dr. R. SWAMINATHAN M.Sc., M.Phil., Ph.D.,

Principal and Head,

Department of Mathematics,

Vidhyaa Giri College of Arts & Science,

Veerasekarapuram, Puduvayal – 630108.

Tamil Nadu, India.

Email:swaminathanmath@gmail.com

Date:

# **DECLARATION**

I hereby declare that the thesis entitled "THEORETICAL ANALYSIS OF NONLINEAR DIFFERENTIAL EQUATIONS IN APPLIED CHEMICAL SCIENCES" is my original work that has been carried out under the guidance and supervision of Dr. K. VENUGOPAL, M.Sc., M.Phil., PGDCA., Ph.D., Assistant Professor, PG & Research Department of Mathematics, Government Arts College, Ayyarmalai, Kulithalai - 639 120. This thesis is my independent research work and it has not formed the basis for the award of any Degree / Diploma / Associate ship / Fellowship or other similar title in any Indian or foreign University.

R. SWAMINATHAN

# Dr. K. VENUGOPAL, M.Sc., M.Phil., PGDCA., Ph.D.,

Research Supervisor,

Assistant Professor,

PG & Research Department of Mathematics,

Government Arts College, Ayyarmalai,

Kulithalai - 639 120,

Karur (Dt).

Mobile No: 9442358231

E-mail: drvenugopal2013@gmail.com



# PLAGIARISM FREE CERTIFICATE

This is to certify that the thesis entitled, "THEORETICAL ANALYSIS OF NONLINEAR DIFFERENTIAL EQUATIONS IN APPLIED CHEMICAL SCIENCES" submitted to the Bharathidasan University, Tiruchirappalli - 620 024, Tamil Nadu, India for the award of the degree of Doctor of Philosophy in Mathematics by Mr. R. SWAMINATHAN was Subjected to plagiarism check at Bharathidasan University Library and found 11% significance which is accepted 20% limit of Bharathidasn University guide lines. So, this is a plagiarism free thesis.

Dr. K. VENUGOPAL

Signature of Research Supervisor

# Curiginal

## **Document Information**

Analyzed document R.SWAMINATHAN-Ref.007689.pdf (D124407131)

**Submitted** 2022-01-10T07:59:00.0000000

 Submitted by
 Srinivasa ragavan S

 Submitter email
 bdulib@gmail.com

Similarity 11%

Analysis address bdulib.bdu@analysis.urkund.com

## Sources included in the report

W	URL: https://oarjpublication.com/journals/oarjet/sites/default/files/OARJET-2021-0106.pdf Fetched: 2021-10-31T17:12:05.2800000	88	8
W	URL: http://www.electrochemsci.org/papers/vol16/210452.pdf Fetched: 2021-04-10T09:23:06.7900000	88	12
W	URL: http://www.electrochemsci.org/papers/vol15/150605682.pdf Fetched: 2020-12-10T12:58:51.3900000	88	36
W	URL: http://www.tara.tcd.ie/bitstream/handle/2262/96803/210946.pdf?sequence=1&isAllowed=y Fetched: 2021-12-03T07:18:04.4870000	88	15
W	URL: https://www.math.ucdavis.edu/~kouba/CalcOneDIRECTORY/implicitdiffsoldirectory/ImplicitDiffSol.html Fetched: 2020-04-23T07:20:41.2230000	88	1

# **ACKNOWLEDGEMENT**

## **ACKNOWLEDGEMENT**

During my doctoral studies, I learned and experienced many things which have really shaped me as a person and expanded my knowledge. I would like to take this opportunity to thank all those who have contributed in any way to the completion of my Ph.D. work.

Foremost, I would like to express my sincere gratitude to my supervisor **Dr. K. VENUGOPAL**, Assistant Professor, PG & Research Department of Mathematics, Government Arts College, Ayyarmalai, Kulithalai, Tamil Nadu for his esteemed supervision, patience, knowledge, inspiration and great support during the period of my studies. I am impressed by his kind-hearted character and helping nature at all situation which is highly motivating me to do my research work effectively. I will never forget his company and suggestions throughout my life. I will remain ever grateful to him for teaching nonlinear equations in chemical and marine sciences to me till my thesis submission.

I express my deep sense of gratitude to **Dr. R. RAVICHANDRAN**, Principal, Government Arts College, Ayyarmalai, Kulithalai for the giving the opportunity and supporting to pursue my research degree.

I wish to record my feelings of gratitude and profound thanks to **Dr. R. KRISHNAKUMAR**, Associate Professor & Head PG and Research Department of Mathematics, Urumu Dhanalakshmi College (Autonomous), Tiruchirappalli for giving the opportunity and directing me in this interesting study. His endless support, encouragement and constructive criticism have been precious during this work. Moreover, I wholeheartedly thank him for the valuable comments and suggestions on the draft of journal articles and this thesis. His advice on both research as well as on my career has been priceless.

I am grateful to **Dr. N. RAJESH**, Assistant Professor, Department of Mathematics, Rajah Serfoji Government College (Autonomus) Thanjavur., Tamil Nadu, for her valuable advice and inspiration throughout this work.

I wish to place on record, the selfless, honest, sincere and dedicated support rendered by **Dr. L. RAJENDRAN**, Professor Academy of Maritime Education and training (AMET), Deemed to be University, Department of Mathematics, Kanathur, India.

I would like to place on record my gratitude and deep obligation to all other Research Scholars, PG and Research Department of Mathematics, Government arts College, Kulithalai for their scholarly advice and enlightened suggestions. It has been pleasant experience to learn and work together with them.

I record my sincere thanks to all the teaching and non-teaching staff members, PG and Research department of Mathematics, Government Arts College, Kulithalai, for their assistance in this work.

I thank silent support, encouragement and personal advice of my parents, Wife and Daughter were a great source of strength and inspiration in the long journey of the daunting task of shaping the thesis.

Last but not the least I am indebted to my supportive relatives, and my friends for their adore encouragement, enthusiasm, blessing, and so on in the entire course of my study.

A final word of thanks to all my friends and equals for their encouragement and untiring help rendered throughout.

R. SWAMINATHAN

#### **ABSTRACT**

In thesis theoretical analysis of nonlinear differential equations in applied chemical sciences are solved analytically and numerically. The application of HPM and VIM which is used to solve a broad range of nonlinear equations, especially in engineering as well as physical problems. Both methods are extremely useful and reliable, as shown by the examples in this chapter.

The mathematical models for mass transfer accompanied by a reversible homogeneous chemical reaction are focused. This model is based on a system of nonlinear equations containing a nonlinear term related to reversible homogeneous reactions. The concentration of species is obtained by solving the nonlinear equations using the homotopy perturbation method. Our approximate analytical results are also compared with the simulation result. A satisfactory agreement is observed between our analyst Also, a mathematical model describing the reduction of Hydrogen peroxide (H<sub>2</sub>O<sub>2</sub>) to water in a metal dispersed conducting polymer film is discussed. The model is based on a system of reaction-diffusion equations containing a nonlinear term related to Michaelis-Menten kinetics of the enzymatic reaction. The approximate analytical expressions corresponding to the substrate and product concentration for steady and non-steady-state conditions have been obtained using a new approach to the homotopy perturbation method (HPM).

A theoretical model of the sensitivity and resistance of amperometry biosensors with substrate inhibition kinetics are described. This model is based on the system of non-stationary diffusion equations containing a nonlinear term related to non-Michaelis-Menten kinetics of the enzymatic reaction. The influence of various parameters such as the thickness of enzyme layer, bulk substrate concentration, Michaelis-Menten and saturation constant on sensitivity and resistance of biosensor are discussed.

Theoretical analysis of nonlinear differential equations in applied chemical sciences is solved analytically in this thesis employing HPM, VIM, and the Taylors series method. Numerical methods (Matlab/Scilab) are also used to solve nonlinear problems in applied Chemical Sciences.

# **CONTENTS**

CHAPTER	TER TITLE		PAGE
			NO
	LIST OF T	ABLES	xvi
	LIST OF FIGURES		
	NOTATIO	NS AND ABBREVIATIONS	xxi
I	INTRODU	JCTION	1
	1.1 Mathen	natical modeling	1
	1.2 Models	based on nonlinear differential equations	1
	1.3 Asymp	totic approximation	2
	1.4 Some a	nalytical asymptotic methods	3
	1.5 Various	s nonlinear equations in chemical sciences	4
	1.5.1	Homotopy perturbation method and	
		variational iteration method for solving the	
		nonlinear equations with variable coefficients	
		in applied sciences.	4
		1.5.1.1 The Duffing equation	4
		1.5.1.2 The Riccati equation	4
		1.5.1.3 Fitzhugh–Nagumo equation	5
		1.5.1.4 The Thomas-Fermi equation	5
	1.5.2	Analytical solution of nonlinear problems in	
		homogeneous reactions occur in the mass-	
		transfer boundary layer: homotopy	
		perturbation method.	6
	1.5.3.	Analytical expressions for the concentration	
		and current in the reduction of hydrogen	
		peroxide at a metal-dispersed conducting	
		polymer film	7
	1.5.4	Sensitivity and Resistance of amperometric	
		biosensors in substrate inhibition processes	8
	1.6 Object	ives and scope of the present investigation	10
		zation of the research work	10

Ι	HOMOTOPY PERTURBATION METHOD AND	12
	VARIATIONAL ITERATION METHOD FOR	
	SOLVING THE NONLINEAR EQUATIONS WITH	
	VARIABLE COEFFICIENTS IN APPLIED SCIENCES	
	2.1 Introduction	12
	2.2 Homotopy perturbation method (HPM)	13
	2.3 Variational iteration method (VIM)	13
	2.4 Scientific Applications	13
	2.4.1. The duffing equations	14
	2.4.1.1. The analytical solution of Duffing equation	
	model using HPM	14
	2.4.1.2. The analytical solution of Duffing equation	
	using Variational iteration method	15
	2.4.2. The Riccati equations	16
	2.4.2.1. The analytical solution of Riccati equation	
	modelusing HPM	16
	2.4.2.2. The analytical solution of Riccati equation	
	model using Variational iteration method	18
	2.4.3. Fitz Hugh-Nagumo equation	20
	2.4.3.1. The analytical expression of the Fitzhugh-	21
	Nagumo equationusing HPM	
	2.4.4. The Thomas-Fermi equation	22
	2.4.4.1. The analytical solution of the Thomas-	23
	Fermi equation using HPM	
	2.5. Conclusions	28
	ANALYTICAL SOLUTION OF NON LINEAR	29
	PROBLEMS IN HOMOGENEOUS REACTIONS	
	OCCUR IN THE MASS-TRANSFER BOUNDARY	
	LAYER: HOMOTOPY PERTURBATION METHOD	
	3.1 Introduction	29
	3.2 Mathematical formulation of the problem	30
	3.3 Analytical expression of the concentration using	31
	homotopy perturbation method	

	3.4 Previous analytical results	32
	3.5 Numerical simulation and discussion	33
	3.6 Conclusions	35
IV	ANALYTICAL EXPRESSIONS FOR THE	47
	CONCENTRATION AND CURRENT IN THE	
	REDUCTION OF HYDROGEN PEROXIDE AT A	
	METAL-DISPERSED CONDUCTING POLYMER	
	FILM	
	4.1 Introduction	48
	4.2 Mathematical formulation	49
	4.3 Analytical expression for the concentration of	
	substrate and product for general case under non	
	steady condition	51
	4.3.1 Limiting case	52
	4.3.1.1 Case 1: Saturated (zero order) catalytic	<b>50</b>
	kinetics (High substrate)	52
	4.3.1.2. Case 2: Unsaturated (first order) catalytic	
	kinetics (Low substrate)	53
	4.4 Numerical simulation	58
	4.5 Results and discussion	61
	4.6 Differential sensitive analysis of kinetic parameters	63
	4.7 Estimation of kinetic parameters	66
	4.8 Conclusions	67
$\mathbf{V}$	SENSITIVITY AND RESISTANCE OF	72
	AMPEROMETRIC BIOSENSORS IN	
	SUBSTRATE INHIBITION PROCESSES	
	5.1 Introduction	72
	5.2 Mathematical formulation of the problems	73
	5.3 Approximate analytical expression of concentration of	
	substrate and product	75
	5.3.1 Approximate solution using Taylor series method	75
	5.3.2 Approximate solution using new homotopy	<b>-</b> -
	perturbation method	75 76
		76

	5.3.3 Sensitivity of biosensor	77
	5.3.4 Resitanceof biosensor	77
	5.3.5 Thickness of the membrane	
	5.4. Result and Discussion	78
	5.4.1 Sensitivity	78
	5.4.2 Resistance	80
	5.5 Conclusions	81
VI	CONCLUSIONS AND FUTURE ENHANCEMENT	88
	6.1 Conclusions	88
	6.2 Scope of future work	89
	REFERENCES	90
	LIST OF PUBLICATIONS	102
	REPRINT OF PUBLICATIONS	

# LIST OF TABLES

		Page
Table No.	· Title	
2.1	The values of $u'(0) = M$ for various Padé approximant	27
3.1	Comparison of numerical solution of concentration of species $a(z)$ with the analytical solutions by Homotopy perturbation method and Taylor series method for $K^* = 1$ , $\mu = -3$ and for different values $\varepsilon$ .	36
3.2	Comparison of numerical solution of concentration of species $b(z)$ with the analytical solutions by Homotopy perturbation method and Taylor series method for $K^* = 1$ , $\mu = -3$ and for different values $\varepsilon$ .	37
3.3	Comparison of numerical solution of concentration of species $S(z)$ with the analytical solutions by Homotopy perturbation method and Taylor series method for $\varepsilon = 2, \mu = -1$ and for different values $K^*$ .	38
3.4	Comparison of our analytical expression of concentration of species $a$ with the numerical result for various values of the parameter $\mu$ and some fixed values parameter $\epsilon=2, \mu=-1$ using Eqn. (3.15).	39
3.5	Comparison of our analytical expression of concentration of species $b$ with the numerical result for various values of the parameter $\mu$ and some fixed values parameter $\varepsilon = 2, \mu = -1$ using Eqn. (3.16).	39
3.6	Comparison of our analytical expression of concentration of species $S$ with the numerical result for various values of the parameter $\mu$ and some fixed values parameter $\varepsilon = 4, \mu = -1$ using Eqn. (3.17).	40
3.7	Comparison of our analytical expression of concentration of species $a$ with the numerical result for various values of the parameter $\mu$ and some fixed values parameter $\varepsilon = 2, K^* = 1$ using Eqn. (3.15).	40
3.8	Comparison of our analytical expression of concentration of species $a$ with the numerical result for various values of the parameter $\varepsilon$ and some fixed values parameter $\mu = -1, K^* = 4$ using Eqn. (3.15).	41

Tabla Na		
Table No.	Title	no
3.9	Comparison of our analytical expression of concentration of species $b$ with the numerical result for various values of the parameter $\mu$ and some fixed values parameter $\varepsilon = 2$ , $K^* = 10$ using Eqn. (3.16).	41
3. 10	Comparison of our analytical expression of concentration of species $b$ with the numerical result for various values of the parameter $\varepsilon$ and some fixed values parameter $\mu = -2$ , $K^* = 50$ using Eqn. (3.16).	42
3. 11	Comparison of our analytical expression of concentration of species $S$ with the numerical result for various values of the parameter $\varepsilon$ and some fixed values parameter $\varepsilon = 4$ , $K^* = 100$ using Eqn. (3.17).	42
3.12	Comparison of our analytical expression of concentration of species $S$ with the numerical result for various values of the parameter $\varepsilon$ and some fixed values parameter $\mu = -2$ , $K^* = 500$ using Eqn. (3.17).	43
4.1	Summary of analytical expression of concentration of substrate, product and current for non-steady state condition when $\xi=1$	55
4.2	Summary of analytical expression of concentration of substrate, product and current for steady - state condition when $\xi=1$ .	56
4.3	Comparison of our analytical result of dimensionless substrate $u(\chi, \tau)$ with the numerical simulation for various value of $\tau$ and $\chi$ using Eqn. (4.17) when $\phi=1$ and $\alpha=0.5$	59
4.4	Comparison of our analytical result of dimensionless product $v(\chi,\tau)$ with the numerical simulation for various values of $\tau$ and $\chi$ using Eqn. (4.18) when $\phi=0.1$ , $\alpha=0.5$ , $\beta=0.05$ , $\gamma=0.01$ and $\xi=1$	60

Table No.		
Table No.	Title	no
5.1	Comparison of numerical solution of concentration of substrate with the analytical solutions obtained by hyperbolic function method and Taylor series method for $\alpha = 0.1, \beta = 0.1$ and for different values of $\phi_s^2$ .	82
5.2	Comparison of numerical solution of concentration of product with the analytical solution obtained by hyperbolic function method and Taylor series method for $\alpha=0.1$ , $\beta=0.1$ , $\phi_s{}^2=1$ and for different values of $\phi_p{}^2$ .	82

# LIST OF FIGURES

Figure	Title	
No.		
2.1	The exact solution of Fitzhugh–Nagumo equation $u(t)$ (Eq.	22
	(2.4.3.14)), versus <i>t</i> with numerical solution	22
2.2	Comparision of Padé approximant [11/11] solution of	
	Thomas-Fermi equation with numerical solution for different	27
	initial condition.	
3.1	Comparison of concentrations $a(z)$ , $b(z)$ and $S(z)$ (Eqns.	
	(3.15)-(3.17)) with simulation results for various values of	34
	parameters $\varepsilon$ , $K^*$ and $\mu$ .	
3.2	Comparison of concentrations $a(z)$ , $b(z)$ and $S(z)$ (Eqns.	
	(3.15)-(3.17)) with simulation results for various values of	35
	parameters $\varepsilon$ , $K^*$ and $\mu$ .	
4.1	Schematic diagram for the reduction of hydrogen peroxide to	49
	water.	49
4.2	Plot of dimensionless concentration of substrate $u(\chi, \tau)$	
	versus dimensionless thickness $\chi$ calculated using Eqn.	
	(4.17) for different values of (a) Thiele modulus $\phi$ , (b)	62
	saturation parameter $\alpha$ and (c) time $\tau$ . The key to the graph:	02
	(scatted line) represents the Eq. (4.17) and (dotted line)	
	represents the numerical simulation.	
4.3	Plot of dimensionless concentration of product $v(\chi, \tau)$ versus	
	dimensionless thickness $\chi$ calculated using Eqn. (4.18) for	
	different values of (a) Thiele modulus $\phi$ , saturation	
	parameters (b) $\alpha$ (c) $\beta$ (d) $\gamma$ , (e) diffusion parameter $\xi$ and	63
	(f) time $\tau$ . The key to the graph: (scatted line) represents the	
	Eq. (4.18) and (dotted line) represents the numerical	
	simulation.	
4.4	Sensitive analysis of parameters: Percentage change in	64
	current.	04
4.5	Plot of steady state current versus thickness of the film $L$ .	65

Figure	FF*41	Page
No.	Title	no
4.6	Plot of dimensionless current $\psi( au)$ versus dimensionless time	
	$\tau$ calculated using Eqn. (4.19) for different values of (a)	<i>(5</i>
	Thiele modulus $\phi$ , saturation parameters (b) $\alpha$ (c) $\beta$ (d) $\gamma$ and	65
	(e) diffusion parameter $\xi$	
4.7	Estimation of kinetic parameter: pseudo first order rate	67
	constant $k$ and enzymatic rate $k_{cat}e_T$ using Eqn. (4.37).	07
5.1	The biosensor sensitivity using eqn. (5.22) for fixed values of	
	$D_s = D_p = 300 \ \mu m^2/s, V_{max} = 1 \ \mu M/s, d = 100 \ \mu m.$ (a).	79
	$k_s = 10 \ \mu\text{M}$ and various values of $k_m \mu\text{M}$ . (b). $k_m = 100 \mu\text{M}$	19
	and various values of $k_s \mu M$ .	
5.2	The biosensor sensitivity using eqn. (5.22) for fixed values of	
	$k_s = 10 \mu M, k_m = 100 \ \mu M.$ (a). $D_s = D_p = 300 \ \mu m^2/s,$	
	$d = 100 \mu m$ and various values of $V_{max} \mu M/s$ . (b). $V_{max} =$	70
	$1 \mu M/s$ , $d = 100 \mu m$ and various values of $D_s = D_p \mu m^2/s$ .	79
	(c). $D_s = D_p = 300 \ \mu m^2/s$ , $V_{max} = 1 \ \mu M/s$ and various	
	values of $d \mu m$ .	
5.3	The biosensor resistance using eqn. (5.23) for fixed values of	
	$D_s = D_p = 300 \ \mu m^2/s, V_{max} = 1 \ \mu M/s.$	
	(a). $k_s = 10  \mu M$ , $s^* = 10  \mu M$ and various values of $k_m  \mu M$ .	80
	(b). $k_m = 100 \ \mu\text{M}$ , $s^* = 30 \ \mu\text{M}$ and various values of $k_s \ \mu\text{M}$ .	
5.4	The biosensor resistance using eqn. (5.23) for fixed values of	
	$k_s=10~\mu M, k_m=100~\mu M.$ (a). $D_s=D_p=300~\mu m^2/$	
	$s, s^* = 10 \mu\text{M}$ and various values of $V_{max}\mu\text{M}/s$ .	01
	(b). $V_{max} = 1 \mu M/s$ , $s^* = 10 \mu M$ and various values of	81
	$D_s = D_p  \mu m^2/s$ . (c). $D_s = D_p = 300  \mu m^2/s$ , $V_{max} =$	
	$1 \mu M/s$ and various values of $s^* \mu M$ .	

# NOMENCLATURE AND UNITS

<b>Symbols</b>	Meaning	Unit	
$\boldsymbol{B_b}$	Bulk concentration of species B	mol/cm <sup>3</sup>	
A	Concentration of species A	mol/cm <sup>3</sup>	
B	Concentration of species B	mol/cm <sup>3</sup>	
C	Concentration of species C	mol/cm <sup>3</sup>	
D	Diffusion coefficient	$cm^2/s$	
	Distance from the electrode surface		
x	(Eqn.(2))	cm	
δ	Diffusion layer thickness	cm	
$k_r, k_f$	Reaction-rate constants	cm/s	
$N_{Ao}$	Known rate constant	cm/s	
$a = \frac{A}{B_b}, b = \frac{B}{B_b}$	Dimensionless concentration of the		
	species A, B and C	None	
$S = \frac{C}{B_b}$			
7	Dimensionless distance from the	None	
z.	electrode surface	None	
ε	Dimensionless relative rates of	None	
ε	diffusion and reaction	None	
$K^*$	Dimensionless homogeneous	None	
Λ	equilibrium constant	None	
	Dimensionless rate of injection of A		
$\mu$	relative to the limiting flux of B	None	
	toward the electrode		

Symbols	Meanings	Units	
<b>s</b> , b	Concentration of substrate, p	roduct	M
x	Distance from the electrode		cm
t	Time		S
$D_S, D_{\boldsymbol{B}}$	Diffusion coefficient for subs	strate, product	$cm^2s^{-1}$
$k_{cat}$	Catalytic reaction rate consta	nt	$s^{-1}$
$e_T$	Total enzyme concentration		M
$K_{M}$	Michaelis-Menten rate consta	ant	M
$\kappa_s, \kappa_b$	Partition coefficient for subst	trate, product	None
$s_{\infty}$ , $b_{\infty}$	Initial concentration of substr	rate, product	M
k	Pseudo first order rate consta	int	$s^{-1}$
L	Thickness of the polymer file	m	cm
F	Faraday's constant		$(96\ 487C\ mol^{-1})$
A	Surface area of the electrode	surface	(cm <sup>2</sup> )
$j_b$	Flux of hydrogen peroxide a	t the electrode surface	$(\text{mol cm}^{-2} \text{ s}^{-1})$
n	Stoichiometric charge transf	er coefficient	$(eq mol^{-1})$
I Current	$(A cm^{-2})$		
u,v	Dimensionless concentration	of substrate, product	(None)

# Greek symbols

 $\chi$  Dimensionless distance (None)

 $\tau$  Dimensionless time (None)

 $\xi$  Ratio of diffusion coefficient (None)

 $\phi$  Thiele modulus (None)

 $\alpha, \beta, \gamma$  Saturation parameters (None)

 $\psi$  Dimensionless current (None)

 $\psi_{ss}$  Dimensionless steady- state Current (None)

# Grouping parameter

 $A = \frac{\phi}{1+\alpha}$  Dimensionless parameter (None)

## Subscripts

S Substrate

B Hydrogen peroxide

 $\infty$  Bulk

ss Steady state

Symbol	Meaning	Unit	Experimental
			values
S	Concentration of substrate	$\mu M$	
p	Concentration of product	$\mu M$	
$s^*$	Concentration of substrate at $x = d$	$\mu M$	10-100
$k_m$	Michaelis-menten constant	$\mu M$	100
$k_s$	Inhibition constant	$\mu M$	10
$V_{max}$	Maximal enzymatic rate	$\mu M/s$	1-1000
d	Thickness of the enzyme layer	$\mu m$	10-100
F	Faraday constant	C/mol	96485
$D_s$	Diffusion coefficient of the substrate	$\mu m^2/s$	300
$D_p$	Diffusion coefficient of the product	$\mu m^2/s$	300
I	Current density of the biosensor	$\mu A/cm^2$	
x	Distance	cm	
S	Dimensionless concentration of	None	
	substrate		
P	Dimensionless concentration of product	None	
χ	Dimensionless distance	None	
$\phi_s^2$	Substrate reaction diffusion parameter	None	0.5-300
${\phi_p}^2$	Product reaction diffusion parameter	None	0.5-300
α	Saturation parameter	None	0.1-1
β	Saturation parameter	None	0.1-10
$B_S$	Biosensor sensitivity	None	
$B_R$	Biosensor resistance.	None	
$\psi$	Dimensionless current	None	
$n_e$	Number of electrons involved in charge	None	
	transfer at the electrode surface		

# CHAPTER 1 INTRODUCTION

## **CHAPTER-1**

#### Introduction

#### 1.1 Mathematical modeling

Models are descriptions of our assumptions about how the universe operates. We transfer those views into mathematical language in mathematical modeling. This has many advantages [1].

- Mathematics is a very precise language. It helps us to formulate ideas and identify underlying assumptions.
- Mathematics is a concise language, with well-defined rules for manipulations.
- All the results that mathematicians have proved over hundreds of years area tour disposal.
- Computers can be used to perform numerical calculations.
- Developing scientific understanding through quantitative expression of current knowledge of a system.
- Testing the effect of changes in a system.

#### 1.2 Models based on nonlinear differential equations

Differential equations play an important role in modeling virtually every physical, technical, or biological process. Many fundamental laws of physics and chemistry can beformulated as differential equations. A set of differential equations may be called as a model for a system. In all mathematical sciences the differential equations are used to model the behaviour of complex systems. The mathematical theory of differential equations is first developed, together with the sciences [1], where the equations had originated and where the results found application.

For nonlinear differential equation models in biology, chemical sciences, and otherareas, a key preliminary step in the analysis of a model is to introduce dimensionless variablesin order to extract dimensionless parameters that characterize

the behavior of the system. The central importance of identifying dimension less parameters in a model was emphasized by Lee Segel. When some of these dimensionless parameters take on extreme values, the original model can often be reduced to a simpler model that is easier to analyze. In the 1960's and early 1970's there was an intense focus on developing asymptotic methods to simplify the differential equation models in the limit of extreme values of dimensionless parameters.

We give a very brief historical survey of the applications of asymptotic and analytical methodologies for the analysis of spatio-temporal patterns in reaction-diffusion (RD) and related systems. Although far from complete, the bibliography is hopefully representative of some of the advances in this area over the past forty years. A two-component RD system with general reaction kinetics S (substrate) and P(product) has the form

$$S_t = D_S \nabla^2 S + f(S, P, r, t)$$

$$\tag{1.1}$$

$$P_t = D_P \nabla^2 P + g(S, P, r, t) \tag{1.2}$$

where  $\nabla^2$  is the Laplacian operator,  $D_S$  and  $D_p$  are the diffusion coefficients of the substrateSandproduct P.r is the dimensionless radial co-ordinate of the particle. The first term on the right-hand side of the above equation accounts for active species (substrate product) diffusion whereas second term the f(S, P, r, t) and g(S, P, r, t) homogeneous reaction term. In the subsequent chapters of this thesis, the system represented by the above nonlinear equation is considered and solved using various asymptotic methods.

## 1.3 Asymptotic approximation

The idea behind asymptotic is simple: break the solution into more manageable pieces, each piece helping to produce a better and better approximation. So the first piece describes the system in some idealized state. To this, we may add a second piece representing a small perturbation to the initial state. Each subsequent piece, usually allow for better accuracy, with each piece representing smaller and smaller perturbations.

 $y = y_0$ (First, idealized approximation)

 $+\varepsilon y_1$  (Add small perturbation)

 $+\varepsilon^2 y_2$  (Even smaller perturbation)

+....

Here  $y_i$ 's are  $i^{th}$  approximation of the solution y and represents a small perturbation. These series are called asymptotic approximations because they are expected exact in the asymptotic limit as tends to zero. One or two terms in the iterations provide a satisfactory approximation to reality.

Many of the functions that arise from everyday problems cannot easily be evaluated exactly, particularly those defined in terms of integrals or nonlinear differential equations. In these situations we usually have two options. We can use computers to seek complicated numerical solutions or we can look to construct an analytical approximation to the solution asymptotic [2] expansions. Asymptotic methods have particular importance in manyareasof applied mathematics.

With the rapid development of nonlinear science, the reappears an ever-increasing interest of scientists and engineers in the analytical asymptotic techniques for nonlinear problems. Though it is very easy for us now to find the solutions of linear systems by means of computer, it is, however, still very difficult to solve nonlinear problems either numerically or theoretically.

#### 1.4 Some analytical asymptotic methods

Recently, considerable attention has been paid to the analytical solutions for non-linearequations without possible small parameters. Traditional perturbation methods have many shortcomings, and

they are not valid for strongly nonlinear equations. To overcome the short comings, many new techniques have appeared in open literature. The re-exist some alternative analytical asymptotic approaches [3], such as the weighted linearization method, Adomian decomposition method, variational iteration method, tanh-method and so on. Just recently, some new perturbation methods such as artificial parameter method, Homotopy perturbation method, parameterized perturbation method and

Homotopy analysis method which do not depend on the small parameter assumption are proposed. In this thesis, variation alliteration method [4], Homotopy perturbation method [5], Homotopy analysis method [6] and Adomian decomposition method [7] are used to solve the system of non-linear equations.

#### 1.5 Various nonlinear equations in chemical sciences

# 1.5.1 Homotopy perturbation method and variational iteration method for solving the nonlinear equations with variable coefficients in applied sciences

#### 1.5.1.1 The Duffing equation

The Duffing equation (or Duffing oscillator) is a nonlinear differential equation of second-order that is used to develop driven and damped oscillators. This equation was solved using the Taylor matrix method by Sezer et al. [8]. Najafi et al. [9] applied the Adomian decomposition method (ADM) to solve the typical oscillation. Geng [10] solved these equations by an improved variational iteration method involving both integral and non-integral terms. The Duffing equation can also describe the motion of a cubic oscillator, which is defined as oscillations of a point mass on a nonlinear spring.

In this thesis, Adomian composition method (ADM) is applied to typical oscillation equations (Duffing and Van der Pol equations).

$$\frac{d^2y(x)}{dx^2} + y(x) + \varepsilon(y(x))^3 = 0$$
 (1.3)

Here, *y* is the deviation of the point mass from the equilibrium and *x* is dimensionless time. The initial conditions are as follows:

$$x = 0, y(0) = a, and \frac{dy}{dx}\Big|_{x=0} = 0$$
 (1.4)

#### 1.5.1.2 The Riccati equation

The Riccati equation is a well-known nonlinear differential equation of order one, that is commonly used in theoretical physics and applied mathematics, such as conformal mapping theory and algebraic geometry. Riccati differential equation is useful in certain financial models [11]. Piriadarshani et al. [12] applied differential transform method to solve various kinds of Riccati differential equation. Wannes et al.

[13] introduced the generalized Riccati Wick differential equation. Duan et al. [14] proposed the Riccati equation's properties with constant coefficients.

The general form of Riccati differential equation is defined by:

$$\frac{dy(t)}{dt} = a(t)y(t) + b(t)(y(t))^{2} + c(t)$$
(1.5)

where a(t), b(t) and c(t) are continuous functions of t. The initial condition is

$$t = 0, u(0) = \beta \tag{1.6}$$

## 1.5.1.3 FitzHugh -Nagumo equation

The FitzHugh –Nagumo equation occurs in solid-state physics, astrophysics, fluid mechanics, bursting oscillations, chemical chemistry, chemical kinematics, geochemistry, exciting electronic circuit theory, chaos, bifurcation, plasma physics, biology and population genetics. Via the variational principle, Khan [15] proposed a novel solitary two-type solution for this equation. Schiesser [16] used an algorithm for the numerical solution of the FitzHugh –Nagumo equation. Wallisch [17] generated travelling waves solution to the FitzHugh –Nagumo equation for one and two dimensions. Consider the FitzHugh –Nagumo equation

$$\frac{du}{dt} = ku(t)(1 - u(t))(2 - u(t)) \tag{1.7}$$

with initial condition,

$$t = 0, u(0) = \frac{1}{2} \tag{1.8}$$

#### 1.5.1.4 The Thomas-Fermi equation

The effective nuclear charge of heavy atoms is modeled using this problem [18]. The effective potentials and charge densities of atoms with several electrons can also be calculated using this model. To solve this problem, Pikulin [19] developed high efficiency computational algorithms. Thomas—Fermi equation, Zahoor et al. [20] developed a new bio-inspired computing method. For neutral atoms in a semi-infinite space, Jovanovic et al. [21] proposed an effective spectral methods solver. Xu et al. [22] used homotopy analysis method (HAM) to solve this equation. He [23] used the

variational approach to solve the equation. The Thomas–Fermi equation can be written as follows:

$$\frac{d^2u}{dt^2} = \frac{(u(t))^{3/2}}{\sqrt{t}} \tag{1.9}$$

with initial and boundary conditions

$$t = 0, u(0) = L \text{ and } t \to \infty, u(t) = 0$$
 (1.10)

Transform the Eq. (1.9) by u(t) = 1 + y(t), we get

$$\frac{d^2y(t)}{dt^2} = \frac{(1+y(t))^{3/2}}{\sqrt{t}} \tag{1.11}$$

$$t = 0, y(0) = L - 1 \text{ and let } \frac{dy}{dt}\Big|_{t=0} = M$$
 ,  $t \to \infty, y(t) = 0$  (1.12)

In this thesis, the above nonlinear differential equations with variable coefficients are adopted to solve using a homotopy perturbation method and a variational iteration method. The results obtained by these methods are very useful and convenient, as shown by comparing their results.

# 1.5.2 Analytical solution of non linear problems in homogeneous reactions occur in the mass-transfer boundary layer: Homotopy perturbation method

Consider the reversible homogeneous reaction

$$A + B \Leftrightarrow_{k_n}^{k_f} C \tag{1.13}$$

A is formed at a known rate  $N_{Ao}$  at an electrode surface, and B is present in the bulk solution. The concentrations of A and C in the bulk solution are negligible, and the fluxes of B and C at the electrode surface are also zero. The homogeneous reaction forms the species C and diffuses into the bulk. We assume the steady-state and ignore migration and convection in the diffusion layer [24]. In this case, the system of nonlinear one-dimensional reaction-diffusion equations becomes as follows 24]:

$$D\frac{d^{2}A(x)}{dx^{2}} = -k_{r}C(x) + k_{f}A(x)B(x)$$
(1.14)

$$D\frac{d^{2}B(x)}{dx^{2}} = -k_{r}C(x) + k_{f}A(x)B(x)$$
(1.15)

$$D\frac{d^{2}C(x)}{dx^{2}} = k_{r}C(x) - k_{f}A(x)B(x)$$
(1.16)

The k coefficients denote the forward and reverse reaction rate constants, and A, B, and C represent the species concentrations. Both diffusion coefficients are assumed to be equal to a constant D for the sake of consistency. The boundary conditions are

$$D\frac{dA}{dx} = -N_{Ao}; \frac{dB}{dx} = \frac{dC}{dx} = 0 \text{ at } x = 0$$
 (1.17)

$$A = 0; B = B_b; C = 0 \text{at} x = \delta$$

$$\tag{1.18}$$

In this thesis, an analytical expression has effectively derived the concentration in the rotating disc electrode controlled by migration and convection in the diffusion the steady-state nonlinear reaction-diffusion equations are solved analytically by a new approach of the homotopy perturbation method. There is a very good agreement between the analytical and the numerical solutions for all values of rate constant.

# 1.5.3 Analytical expressions for the concentration and current in the reduction of hydrogen peroxide at a metal-dispersed conducting polymer film

Reaction's scheme occurring within the polymer film and in the bulk solution can be written as follows [25]:

$$S + E_1 \underset{k_{-1}}{\overset{k_1}{\leftrightarrow}} E_1 S \xrightarrow{k_{cat}} P + E_2, E_2 + A \xrightarrow{k_e} E_1 + B, \qquad B + 2e^{-} \xrightarrow{k} C$$
 (1.19)

Eqn. (1.19) represents the oxidation of substrate (Glucose) S to product P(Hydrogen peroxide). Here  $E_1$  and  $E_2$  are the oxidized and reduced forms of the enzyme (oxidase) respectively. The reduction-oxidation process of the enzyme during the reduction of oxygen (A) to hydrogen peroxide (B) is shown in Eqn. (1.19). And the hydrogen peroxide which in turn reacts with microparticle in the presence of a pseudo first order rate constant k to produce water (C). Using Michaelis-Menten rate expression, the mass balance one dimensional equations for substrate and product within the polymer film can be written as follows [25]:

$$\frac{\partial s(x,t)}{\partial t} = D_S \frac{\partial^2 s(x,t)}{\partial x^2} - \frac{k_{cat} e_T s(x,t)}{K_M + s(x,t)}$$
(1.20)

$$\frac{\partial b(x,t)}{\partial t} = D_B \frac{\partial^2 b(x,t)}{\partial x^2} - kb(x,t) + \frac{k_{cat}e_T s(x,t)}{K_M + s(x,t)}$$
(1.21)

where s(x,t) and b(x,t) are the concentrations of substrate and product respectively.  $D_S$  and  $D_B$  are the diffusion coefficients,  $k_{cat}$  is the catalytic reaction rate constant and  $K_M = (k_{cat} + k_{-1})/k_1$  is the Michaelis-Menten rate constant. The initial and boundary conditions for the above equations are given by

$$t = 0, 0 < x < L: s = k_s s_{\infty}, b = 0 \tag{1.22}$$

$$t > 0, x = 0: \frac{\partial s}{\partial x} = 0, \frac{\partial b}{\partial x} = 0 \tag{1.23}$$

$$t > 0, x = L: s = \kappa_s s_{\infty} b = \kappa_h b_{\infty} \tag{1.24}$$

Here  $s_{\infty}$  and  $b_{\infty}$  is the concentration of substrate and product in the bulk solution.  $k_s$  and  $k_b$  is the reaction rate constant for substrate and product respectively. L is the thickness of the polymer film. The current I of the product b at the electrode surface is given by

$$I = -nFAj_b = -nFAD_B(db/dx)_{x=L}$$
(1.25)

where  $j_b$  is the flux of the hydrogen peroxide at the electrode surface. A simple mathematical analysis of reaction and diffusion of glucose and hydrogen peroxide within the conducting film containing metal microparticles have been presented. Using a new approach to the Homotopy perturbation method, an approximate analytical expression for the concentration of substrate and product are obtained. Approximate analytical expressions for the steady and non-steady state current response produced during the reduction of  $H_2O_2$  to water at the electrode surface are derived.

# 1.5.4 Sensitivity and resistance of amperometric biosensors in substrate inhibition processes

In the enzyme reaction,

$$E + S \leftrightarrow ES \to E + P \tag{1.26}$$

the substrate (S) binds to the enzyme (E) in order to form an enzyme-substrate complex ES. The substrate is converted to product (P) while it is part of this complex. The rate of the product's appearance depends on its substrate concentration. For example, the

simplest scheme of non-Michaelis-Menten kinetics may have been obtained by adding to the Michaelis-Menten scheme (Equation (26)), a stage of enzyme-substrate complex (ES) interaction with another substrate molecule (S) (Equation (1.26)) after the non-active complex (ESS) is generated as follows [26]:

$$ES + S \leftrightarrow ESS$$
 (1.27)

The steady-state nonlinear differential equations for the substrate inhibition are[10]:

$$D_{s} \frac{d^{2}s(x)}{dx^{2}} - \frac{V_{max}s(x)}{k_{m} + s(x) + \frac{(s(x))^{2}}{k_{s}}} = 0$$
(1.28)

$$D_p \frac{d^2 p(x)}{dx^2} + \frac{V_{max} s(x)}{k_m + s(x) + \frac{(s(x))^2}{k_s}} = 0$$
(1.29)

where  $D_s$ ,  $D_p$  are the diffusion coefficients of the substrate and product in the enzyme layer. s(x) and p(x) are the concentration of substrate and product in the enzyme layer.  $V_{max}$  is the maximal enzymatic rate,  $k_m$  denotes the Michaelis-Menten constant,  $k_s$  inhibition constant and d is the thickness of the enzyme layer. The corresponding boundary conditions are [26]

$$\frac{ds(x)}{dx} = 0, p(x) = 0 \text{ when } x = 0, s(x) = s^*, p(x) = 0 \text{ when } x = d$$
 (1.30)

where  $s^*$  is the concentration of substrate at x = d and d is thickness of the enzyme layer. The modeling of the amperometric biosensor with the substrate inhibition reveals the complex kinetics of the biosensor response. At low substrate concentration, the kinetics looks like a simple substrate diffusion. When inhibition constant is large  $(k_s \to \infty)$ , the reaction kinetics is Michaelis-Menden model. The steady-state current I of the biosensor is expressed as follows:

$$I = n_e F D_p \frac{dp(x)}{dx} \Big|_{x=0} \tag{1.31}$$

The mathematical model of the amperometric biosensor can be successfully used to investigate the biosensor's sensitivity and resistance. Simple and closed-form the approximate analytical expression for the sensitivity and resistance are obtained for substrate inhibition kinetics

#### 1.6 Objective and scope of the present investigation

The objectives of the present investigation are as follows:

- To derive an approximate analytical solution of nonlinear equations with variable coefficients in applied sciences using Homotopy perturbation method and variational iteration method.
- To derive the analytical solution of nonlinear problems in homogeneous reactions occur in the mass-transfer boundary layer using homotopy perturbation method.
- To find the analytical expressions for the concentration and current in the reduction of hydrogen peroxide at a metal-dispersed conducting polymer film using Taylors series and new homotopy perturbation.
- To present the sensitivity and resistance of amperometric biosensors in substrate inhibition processes using Taylors series and new homotopy pertuberation method.

## 1.7 Organization of the thesis

This thesis presents the development to mathematical models using various asymptotic methods. Variational iteration method, homotopy perturbation method, and the Adomian decomposition method are used to predict the theoretical results on solving the system of steady and non-steady-state nonlinear differential equations. Numerical simulations (Scilab program) is also obtained and compared to show the efficiency of the above methods applied.

**Chapter one** gives a short introduction to mathematical models, their applications in differential equations and some asymptotic methods.

**Chapter two** presents application of HPM and VIM which is used to solve a broad range of nonlinear equations, especially in engineering as well as physical

problems. Both methods are extremely useful and reliable, as shown by the examples in this chapter.

Chapter three focuses mathematical models for mass transfer accompanied by a reversible homogeneous chemical reaction. This model is based on a system of nonlinear equations containing a nonlinear term related to reversible homogeneous reactions. The concentration of species is obtained by solving the nonlinear equations using the homotopy perturbation method. Our approximate analytical results are also compared with the simulation result. A satisfactory agreement is observed between our analytical and simulation results.

Chapter four describes s mathematical model describing the reduction of Hydrogen peroxide (H<sub>2</sub>O<sub>2</sub>) to water in a metal dispersed conducting polymer film. The model is based on a system of reaction-diffusion equations containing a nonlinear term related to Michaelis-Menten kinetics of the enzymatic reaction. The approximate analytical expressions corresponding to the concentration of substrate and product for steady and non-steady state conditions have been obtained using a new approach to homotopy perturbation method (HPM). The influence of initial substrate concentration, the thickness of the film as well as the diffusion layer and kinetic parameters on the current response were investigated. A graphical procedure for estimating the kinetic parameters from the expression of the current response is also proposed.

Chapter five discusses a theoretical model of a sensitivity and resistance of amperometry biosensors with substrate inhibition kinetics. This model is based on the system of non-stationary diffusion equations containing a nonlinear term related to non-Michaelis-Menten kinetics of the enzymatic reaction. This chapter presents the approximate analytical expression of sensitivity and resistance of biosensor for small values of reaction diffusion parameters. The effect various parameters such as thickness of enzyme layer, bulk substrate concentration, Michaelis-Menten and saturation constant on sensitivity and resistance of biosensor are discussed.

**Chapter six** is the overall conclusion and future enhancements of the thesis.

#### **CHAPTER 2**

# HOMOTOPY PERTURBATION METHOD AND VARIATIONAL ITERATION METHOD FOR SOLVING THE NONLINEAR EQUATIONS WITH VARIABLE COEFFICIENTS IN APPLIED SCIENCES

#### **CHAPTER-2**

# Homotopy Perturbation Method and Variational Iteration Method for Solving the Nonlinear Equations with Variable Coefficients in Applied Sciences

#### 2.1 Introduction

The ordinary differential equations (ODEs) with variable coefficients can be used in a wide range of applications. Euler equations, Bessel equations, Legendre equations, and Laguerre equations are examples of these equations. Many nonlinear equations with variable coefficients, like Duffing equation [1-3], Riccati equation [4-7], FitzHugh –Nagumo equation [8-10], and Thomas-Fermi equation [11-16], are very helpful and applicable in physical, chemical and engineering sciences. Since solving such equations necessitates several nonphysical hypotheses, specific approximate methods to solve nonlinear differential equations have recently been established. In engineering, applied mathematics, physical, chemical, and biological sciences, linear and nonlinear ODEs with variable coefficients play an important role. The aim of the research was to come up with reliable methods for solving a broad range of integral equations, linear and nonlinear differential equations, and without making any tangible assumptions or discretizing the variables. The emergence of modern, efficient techniques to manage linear and nonlinear equations has exceeded most traditional methods. Newly developed techniques include the homotopy perturbation method, Adomian decomposition method and variational iteration method.

Already Wazwaz [17] solved the scientific models like the Riccati equation, the hybrid selection model, the Kidder equation, the Thomas-Fermi equation using the variational iteration method (VIM). Ganji et al. [18] used homotopy perturbation methods and variational iteration to solve different nonlinear equations. In this chapter, the homotopy perturbation method (HPM) [19-27] and the variational iteration method (VIM) [28-31] are applied to solve certain nonlinear equations. These nonlinear problems are the application of several physical and engineering sciences [32-36]. Also, all the analytical results converge to exact solutions.

#### 2.2 Homotopy perturbation method (HPM)

One of the asymptotic approaches to solving linear and nonlinear ordinary/partial differential equations is the homotopy perturbation method (HPM). This method was proposed by He in 1999 [37] which is also applied to solve a system of equations which is linear and nonlinear. Computational parameters were used to create this technique [38-40]. Almost all traditional perturbation methods make use of the small parameter assumption. Most nonlinear problems, on the other hand, do not have small parameters and determining small parameters appears to have been a one-of-a-kind art that requires advanced techniques.

Such parameters are so sensitive that even minor variations in them can greatly impact the result. The proper selection of such small parameters yields optimal results. A poor choice of small parameters, on the other hand, may have serious consequences. To eradicate the small parameter assumption, Liu [38] suggested an artificial parameter method and Liao [41,42] contributed to the homotopy analysis method. He [43] proposed the new perturbation technique to solve the nonlinear problem. Rajendran et al. [19-27] solved many nonlinear differential equations using the homotopy perturbation method.

#### 2.3 Variational iteration method (VIM)

The variational iteration method (VIM) is one of the asymptotic methods used to solve nonlinear ordinary and partial differential equations. He [44,45] formulated this approach and successfully applied it to solve ODEs and PDEs. Many researchers used this method to solve fractional, homogeneous, nonhomogeneous, linear and nonlinear differential equations. VIM can work in both bounded and unbounded domains. If an exact solution to the differential equations exists, this approach can be used to find successive convergent approximations. Wazwaz [46] solved the Volterra integral and integro-differential equations, both linear and nonlinear using this method.

#### 2.4 Scientific applications

The Duffing equation [1-3], Riccati equation [4-7], FitzHugh –Nagumo equation [8-10], and Thomas-Fermi equation [11-16] are the four extremely well nonlinear equations covered in this section.

#### 2.4.1. The Duffing equation

The Duffing equation (or Duffing oscillator) is a nonlinear differential equation of second order that is used to develop driven and damped oscillators. This equation can also be used to represent a dynamic system that exhibits chaotic behavior. The frequency response of the jump resonance phenomenon which is a form of frequency hysteresis, is also seen in the Duffing system. This equation was solved using the Taylor matrix method by Sezer et al. [1]. Najafi et al. [2] applied the Adomian decomposition method (ADM) to solve the typical oscillation. Geng [3] solved these equations involving both integral and non-integral terms by an improved variational iteration method. The following equation can be used to describe the motion of a cubic oscillator, which is described as oscillations of a point mass on a nonlinear spring.

In this chapter, Adomian Decomposition Method (ADM) is applied to typical oscillation equations (Duffing and Van der Pol equations).

$$\frac{d^2y(x)}{dx^2} + y(x) + \varepsilon(y(x))^3 = 0$$
 (2.1)

Here, y is the deviation of the point mass from the equilibrium and x is dimensionless time. The initial conditions are as follows:

At 
$$x = 0$$
,  $y(0) = a$  and  $\frac{dy}{dx}\Big|_{x=0} = 0$  (2.2)

#### 2.4.1.1. The analytical solution of Duffing equation model using HPM

$$(1-p)\left(\frac{d^2y(x)}{dx^2}\right) + p\left(\frac{d^2y(x)}{dx^2} + y(x) + \varepsilon(y(x))^3\right) = 0$$
 (2.3)

The approximate solution of (2.1) is

$$y(x) = y_0 + y_1 p + y_2 p^2 + \dots$$
 (2.4)

The following equations with corresponding boundary conditions was obtained by substituting Eq. (2.4) in Eq. (2.3) and equating the like coefficients of powers of p.

$$\frac{d^2y_0}{dx^2} = 0, y_0(0) = a, y'_0(0) = 0$$
(2.5)

$$\frac{d^2y_1}{dx^2} + y_0(x) + \varepsilon(y_0(x))^3 = 0, y_1(0) = 0, y_1'(0) = 0$$
(2.6)

$$\frac{d^2y_2}{dx^2} + y_1(x) + 3\varepsilon(y_0(x))^2 y_1(x) = 0, y_2(0) = 0, y_2'(0) = 0$$
(2.7)

$$\frac{d^2y_3}{dx^2} + y_2(x) + 3\varepsilon(y_0(x)(y_1(x))^2 + (y_0(x))^2y_2(x)) = 0, y_3(0) = 0, y_3'(0) = 0$$
(2.8)

On solving the Eqs. (2.5-2.8), the following results are obtained.

$$y_0(x) = a (2.9)$$

$$y_1(x) = -a(1 + \varepsilon a^2) \frac{x^2}{2}$$
 (2.10)

$$y_2(x) = a(1 + 4\varepsilon a^2 + 3\varepsilon^2 a^4) \frac{x^4}{24}$$
 (2.11)

$$y_3(x) = -a(1 + 25\varepsilon a^2 + 51\varepsilon^2 a^4 + 27\varepsilon^3 a^6) \frac{x^6}{720}$$
 (2.12)

Therefore, the approximate analytical solution of Eq. (2.1) is

$$y(x) = a\left(1 - (1 + \varepsilon a^2)\frac{x^2}{2} + (1 + 4\varepsilon a^2 + 3\varepsilon^2 a^4)\frac{x^4}{24} - (1 + 25\varepsilon a^2 + 51\varepsilon^2 a^4 + 27\varepsilon^3 a^6)\frac{x^6}{720} + \dots\right)$$
(2.13)

If  $\varepsilon \to 0$ , then the above approximate solution converges to  $a \cos(x)$ .

## 2.4.1.2. The analytical solution of Duffing equation using Variational iteration method

The variational iteration formula for Eq. (2.4.1.1) is given as

$$y_{n+1}(x) = y_n(x) + \int_0^x \lambda(\alpha)(y_n''(\alpha) + y_n(\alpha) + \varepsilon(y_n(\alpha))^3)d\alpha, n \ge 0$$
 (2.14)

Since Eq. (2.1) is a differential equation of order one, so the Lagrange multiplier,  $\lambda = \alpha - x$ . Hence Eq. (2.14) becomes as follows:

$$y_{n+1}(x) = y_n(x) + \int_0^x (\alpha - x)(y_n''(\alpha) + y_n(\alpha) + \varepsilon(y_n(\alpha))^3) d\alpha$$
 (2.15)

Let  $y_0(x) = a$ . The successive approximations become as follows:

$$y_{1}(x) = y_{0}(x) + \int_{0}^{x} (\alpha - x)(y_{0}''(\alpha) + y_{0}(\alpha) + \varepsilon(y_{0}(\alpha))^{3})d\alpha$$
$$= a\left(1 - (1 + \varepsilon\alpha^{2})\frac{x^{2}}{2}\right)$$
(2.16)

$$y_2(x) = y_1(x) + \int_0^x (\alpha - x)(y_1''(\alpha) + y_1(\alpha) + \varepsilon(y_1(\alpha))^3) d\alpha$$
  
=  $a - a(1 + \varepsilon a^2) \frac{x^2}{2} + a(1 + 4\varepsilon a^2 + 3\varepsilon^2 a^4) \frac{x^4}{24} + \dots$  (2.17)

Therefore,

$$y_n(x) \approx a \left( 1 - (1 + \varepsilon a^2) \frac{x^2}{2} + (1 + 4\varepsilon a^2 + 3\varepsilon^2 a^4) \frac{x^4}{24} - (1 + 25\varepsilon a^2 + 51\varepsilon^2 a^4 + 27\varepsilon^3 a^6) \frac{x^6}{720} + \dots \right)$$
(2.18)

Eq. (2.13) and Eq. (2.18) are same.

#### 2.4.2. The Riccati equation

The Riccati equation is a well-known nonlinear differential equation of order one, that is commonly used in theoretical physics and applied mathematics, such as conformal mapping theory and algebraic geometry. Riccati differential equation is useful in certain financial models [4]. Piriadarshani et al. [5] applied differential transform method to solve various kinds of Riccati differential equation. Wannes et al. [6] introduced the generalized Riccati Wick differential equation. Duan et al. [7] proposed the Riccati equation's properties with constant coefficients.

The general form of Riccati differential equation is defined by:

$$\frac{dy(t)}{dt} = a(t)y(t) + b(t)(y(t))^{2} + c(t)$$
(2.19)

where a(t), b(t) and c(t) are continuous functions of t.

The initial condition is

$$t = 0, u(0) = \beta \tag{2.20}$$

#### 2.4.2.1. The analytical solution of Riccati equation model using HPM

The homotopy for the Riccati Eq. (2.19) is as follows:

$$(1-p)\left(\frac{dy(t)}{dt} - c(t)\right) + p\left(\frac{dy(t)}{dt} - (a(t)y(t) + b(t)(y(t))^2 + c(t))\right) = 0 \quad (2.21)$$

The approximate solution of Eq.(2.19) is

$$y(t) = y_0 + y_1 p + y_2 p^2 + \dots$$
 (2.22)

The following equations with corresponding boundary conditions was obtained by substituting Eq. (2.21) in Eq. (2.22) and equating the like coefficients of powers of p.

$$\frac{dy_0}{dt} - c(t) = 0, y_0(0) = \beta \tag{2.23}$$

$$\frac{dy_1}{dt} - b(t)(y_0(t))^2 - a(t)y_0(t) = 0, y_1(0) = 0$$
(2.24)

$$\frac{dy_2}{dt} - 2b(t)y_0(t)y_1(t) - a(t)y_1(t) - c(t) = 0, y_2(0) = 0$$
 (2.25)

Case (i): Now take the coefficients as 
$$a(t) = 1$$
,  $b(t) = -1$ ,  $c(t) = 2$  (2.26)

Riccati equation becomes

$$\frac{dy}{dt} = -(y(t))^2 + y(t) + 2 \tag{2.27}$$

The boundary condition is

At 
$$t = 0, y(0) = 1$$
 (2.28)

Now we construct the homotopy for the Eq. (2.27) as follows:

$$(1-p)\left(\frac{dy(t)}{dt} - 2\right) + p\left(\frac{dy(t)}{dt} + (y(t))^2 - y(t) - 2\right) = 0$$
(2.29)

The approximate solution of Eq.(2.27) is

$$y(x) = y_0 + y_1 p + y_2 p^2 + \dots$$
 (2.30)

The following equations with corresponding boundary conditions was obtained by substituting Eq. (2.30) in Eq. (2.29) and equating the like coefficients of powers of p.

$$\frac{dy_0}{dt} - 2 = 0, y_0(0) = 1 (2.31)$$

$$\frac{dy_1}{dt} + (y_0(t))^2 - y_0(t) = 0, y_1(0) = 0$$
 (2.32)

$$\frac{dy_2}{dt} + 2y_0(t)y_1(t) - y_1(t) = 0, y_2(0) = 0 (2.33)$$

$$\frac{dy_3}{dt} - y_2(t) + (y_1(t))^2 + 2y_0(t)y_2(t) = 0, y_3(0) = 0$$
 (2.34)

$$\frac{dy_4}{dt} - y_3(t) + 2y_0(t)y_3(t) = 0, y_4(0) = 0 (2.35)$$

On solving the Eqs. (2.31-2.35), we get

$$y_0(t) = 1 + 2t (2.36)$$

$$y_1(t) = -t^2 - \frac{4}{3}t^3 (2.37)$$

$$y_2(t) = \frac{1}{3}t^3 + \frac{4}{3}t^4 + \frac{16}{15}t^5 \tag{2.38}$$

$$y_3(t) = -\frac{1}{12}t^4 - \frac{11}{15}t^5 - \frac{68}{45}t^6 - \frac{272}{315}t^7$$
 (2.39)

$$y_4(t) = \frac{1}{60}t^5 + \frac{8}{45}t^6 + \frac{40}{63}t^7 + \frac{272}{315}t^8 + \frac{1088}{2835}t^9$$
 (2.40)

Therefore, the approximate analytical solution of Eq. (2.27) is

$$y(t) = 1 + 2t - t^2 - t^3 + \frac{5}{4}t^4 + \frac{7}{20}t^5 + \dots$$
 (2.41)

## 2.4.2.2. The analytical solution of Riccati equation model using Variational iteration method

The variational iteration formula for Eq. (2.27) is given as

$$y_{n+1}(t) = y_n(t) + \int_0^t \lambda(\alpha)(y_n'(\alpha) + (y_n(\alpha))^2 - y_n(\alpha) - 2)d\alpha, n \ge 0$$
 (2.42)

Since Eq. (2.27) is a differential equation of order one, so the Lagrange multiplier,  $\lambda = -1$ . Hence Eq. (2.42) becomes as follows:

$$y_{n+1}(t) = y_n(t) - \int_0^t (y_n'(\alpha) + (y_n(\alpha))^2 - y_n(\alpha) - 2) d\alpha, n \ge 0$$
 (2.43)

Let  $y_0(t) = 1$ . The successive approximations are as follows:

$$y_1(t) = y_0(t) - \int_0^t (y_0'(\alpha) + (y_0(\alpha))^2 - y_0(\alpha) - 2)d\alpha = 1 + 2t$$
 (2.44)

$$y_2(t) = y_1(t) - \int_0^t \left( y_1'(\alpha) + \left( y_1(\alpha) \right)^2 - y_1(\alpha) - 2 \right) d\alpha = 1 + 2t - t^2 - \frac{4}{3}t^3$$

$$= 1 + 2t - t^2 - \frac{4}{3}t^3$$
(2.45)

$$y_3(t) = y_2(t) - \int_0^t (y_2'(\alpha) + (y_2(\alpha))^2 - y_2(\alpha) - 2) d\alpha$$
  
= 1 + 2t - t^2 - t^3 + \frac{4}{3}t^4 + \frac{13}{15}t^5 - \frac{4}{9}t^6 - \frac{16}{63}t^7 \qquad (2.46)

$$y_4(t) = y_3(t) - \int_0^t (y_3'(\alpha) + (y_3(\alpha))^2 - y_3(\alpha) - 2)d\alpha$$

$$= 1 + 2t - t^2 - t^3 + \frac{5}{4}t^4 + \frac{1}{3}t^5 - \frac{41}{30}t^6 - \frac{61}{315}t^7 + \frac{1013}{1260}t^8 + \frac{26}{2835}t^9$$

$$- \frac{584}{1575}t^{10}$$

$$- \frac{349}{51975}t^{11} + \frac{38}{315}t^{12} + \frac{688}{36855}t^{13} - \frac{64}{3969}t^{14} - \frac{256}{59535}t^{15}(2.4.2.28)$$

Therefore,

$$y_n(t) \approx 1 + 2t - t^2 - t^3 + \frac{5}{4}t^4 + \frac{7}{20}t^5 + \dots$$
 (2.48)

Case (ii) Now assume that 
$$a(t) = -2t$$
,  $b(t) = 1$ ,  $c(t) = t^2 + 1$  and  $\beta = \frac{1}{2}$ 

Then, the equation of Riccati becomes

$$\frac{dy}{dt} = (y(t))^2 - 2ty(t) + t^2 + 1 \tag{2.49}$$

with initial condition,

At 
$$t = 0, y(0) = \frac{1}{2}$$
 (2.50)

Now we construct the homotopy for the Eq. (2.49) as follows:

$$(1-p)\left(\frac{dy(t)}{dt} - c(t)\right) + p\left(\frac{dy(t)}{dt} - (a(t)y(t) + b(t)(y(t))^2 + c(t))\right) = 0$$
 (2.51)

The approximate solution of Eq. (2.49) is

$$y(x) = y_0 + y_1 p + y_2 p^2 + \dots (2.52)$$

The following equations with corresponding boundary conditions was obtained by substituting Eq. (2.52) in Eq. (2.51) and equating the like coefficients of powers of p.

$$\frac{dy_0}{dt} - t^2 - 1 = 0, y_0(0) = \frac{1}{2}$$
 (2.53)

$$\frac{dy_1}{dt} - (y_0(t))^2 + 2ty_0(t) = 0, y_1(0) = 0$$
(2.54)

$$\frac{dy_2}{dt} - 2y_0(t)y_1(t) + 2ty_1(t) = 0, y_2(0) = 0 {(2.55)}$$

$$\frac{dy_3}{dt} - (y_1(t))^2 - 2y_0(t)y_2(t) + 2ty_2(t) = 0, y_3(0) = 0$$
 (2.56)

On solving the Eqs. (2.53 - 2.56), we get

$$y_0(t) = \frac{1}{2} + t + \frac{t^3}{3} \tag{2.57}$$

$$y_1(t) = \frac{1}{4}t - \frac{1}{3}t^3 + \frac{1}{12}t^4 + \frac{1}{63}t^7$$
 (2.58)

$$y_2(t) = \frac{1}{8}t^2 - \frac{1}{12}t^4 + \frac{1}{20}t^5 - \frac{2}{63}t^7 + \frac{1}{112}t^8 + \frac{2}{2079}t^{11}$$
 (2.59)

$$y_3(t) = \frac{1}{16}t^3 - \frac{1}{20}t^5 + \frac{7}{240}t^6 + \frac{1}{63}t^7 - \frac{1}{56}t^8 + \frac{2}{315}t^9 - \frac{2}{693}t^{11} + \frac{53}{66528}t^{12} + \frac{13}{218295}t^{15}$$
(2.60)

Therefore, the approximate analytical solution of Eq. (2.49) is

$$y(t) = \frac{1}{2} + \frac{5}{4}t + \frac{1}{8}t^2 + \frac{1}{16}t^3 + \frac{1}{32}t^4 + \frac{1}{64}t^5 + \dots$$
 (2.61)

which is converges to the exact solution

$$y(t) = t + \frac{1}{2-t}, |t| < 2$$
 (2.62)

and this is the same solution acquired with VIM by Wazwaz [17].

#### 2.4.3. FitzHugh –Nagumo equation

The FitzHugh –Nagumo equation occurs in solid-state physics, astrophysics, fluid mechanics, bursting oscillations, chemical chemistry, chemical kinematics, geochemistry, exciting electronic circuit theory, chaos, bifurcation, plasma physics, biology and population genetics. Via the variational principle, Khan [8] proposed a novel solitary two-type solution for this equation. Schiesser [9] used an algorithm for the numerical solution of the FitzHugh–Nagumo equation. Wallisch [10] generated travelling waves solution to the FitzHugh-Nagumo equation for one and two dimensions.

Consider the FitzHugh -Nagumo equation

$$\frac{du}{dt} = ku(t)(1 - u(t))(2 - u(t)) \tag{2.63}$$

with initial condition,

At 
$$t = 0, u(0) = \frac{1}{2}$$
 (2.64)

#### 2.4.3.1. The analytical expression of the FitzHugh –Nagumo equation using HPM

By the basic concept of HPM,

$$(1-p)\left(\frac{du}{dt}\right) + p\left(\frac{du}{dt} - 2ku(t) + 3ku(t)^2 - ku(t)^3\right) = 0$$
 (2.65)

The approximate solution of 
$$u(t)$$
 is  $u_0 + u_1 p + u_2 p^2 + \dots$  (2.66)

The following equations with corresponding boundary conditions was obtained by substituting Eq. (2.66) in Eq. (2.65) and equating the like coefficients of powers of p.

$$\frac{du_0}{dt} = 0, u_0(0) = \frac{1}{2} \tag{2.67}$$

$$\frac{du_1}{dt} - 2ku_0(t) + 3k(u_0(t))^2 - k(u_0(t))^3 = 0, u_1(0) = 0$$
(2.68)

$$\frac{du_2}{dt} - 2ku_1(t) + 6ku_0(t)u_1(t) - 3k(u_0(t))^2u_1(t) = 0, u_2(0) = 0$$
 (2.69)

$$\frac{du_3}{dt} - 2ku_2(t) + 3k((u_1(t))^2 + 2u_0(t)u_2(t)) - k\left(3u_0(t)(u_1(t))^2 + 3(u_0(t))^2u_2(t)\right) = 0, u_3(0) = 0$$
(2.70)

Solving Eqs.(2.67 - 2.70), we get

$$u_0(t) = \frac{1}{2} \tag{2.71}$$

$$u_1(t) = \frac{3}{8}kt (2.72)$$

$$u_2(t) = -\frac{3}{64}(kt)^2 \tag{2.73}$$

$$u_3(t) = -\frac{17}{256}(kt)^3 \tag{2.74}$$

Therefore, the approximate solution of Eq. (2.63) is

$$u(t) = \frac{1}{2} + \frac{3}{8}kt - \frac{3}{64}(kt)^2 - \frac{17}{256}(kt)^3 + \dots$$
 (2.75)

This expansion of u(t) leads to the exact solution

$$u(t) = 1 - (1 + 3\exp(3kt))^{-1/2}$$
(2.76)

which the same solution of obtained by Wazwaz [17] using VIM.

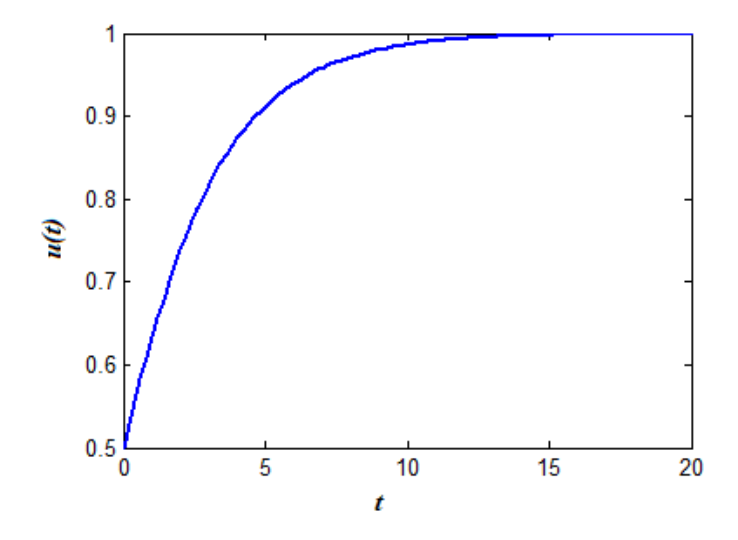


**Figure 2.1:** Comparison The exact solution of FitzHugh –Nagumo equation u(t) (Eq. (2.4.3.14)), versus with numeric solution.

The exact solution of FitzHugh –Nagumo equation u(t) (Eq. (2.4.3.14)), is compared with numerical solution in Fig. 1 and satisfactory agreement is noted.

#### 2.4.4. The Thomas-Fermi equation

The effective nuclear charge of heavy atoms is modeled using this problem [11]. The effective potentials and charge densities of atoms with several electrons can also be calculated using this model. To solve this problem, Pikulin [12] developed high efficiency computational algorithms. To evaluate the nonlinear singular Thomas–Fermi equation, Zahoor et al. [13] developed a new bio-inspired computing method. For neutral atoms in a semi-infinite space, Jovanovic et al. [14] proposed an effective spectral methods solver. Xu et al. [15] used homotopy analysis method (HAM) to solve this equation. He [16] used the variational approach to solve the equation. The Thomas–Fermi equation can be written as follows:

$$\frac{d^2u}{dt^2} = \frac{(u(t))^{3/2}}{\sqrt{t}} \tag{2.77}$$

with initial and boundary conditions

At 
$$t = 0$$
,  $u(0) = L$  and (2.78)

At 
$$t \to \infty$$
,  $u(t) = 0$  (2.79)

Transform the Eq. (2.77) by u(t) = 1 + y(t), we get

$$\frac{d^2y(t)}{dt^2} = \frac{(1+y(t))^{3/2}}{\sqrt{t}} \tag{2.80}$$

At 
$$t = 0$$
,  $y(0) = L - 1$  and let  $\frac{dy}{dt}\Big|_{t=0} = M$  (2.81)

At 
$$t \to \infty$$
,  $y(t) = 0$  (2.82)

Since, 
$$(1+y(t))^{3/2} \approx 1 + \frac{3}{2}y(t) + \frac{3}{8}(y(t))^2 - \frac{1}{16}(y(t))^3$$
 (2.83)

Therefore, Eq. (2.80) becomes

$$\frac{d^2y(t)}{dt^2} = \frac{1 + \frac{3}{2}y(t) + \frac{3}{8}(y(t))^2 - \frac{1}{16}(y(t))^3}{\sqrt{t}}$$
(2.84)

#### 2.4.4.1. The analytical solution of the Thomas-Fermi equation using HPM

By the basic concept of HPM,

$$(1-p)\left(\frac{d^2y(t)}{dt^2}\right) + p\left(\frac{d^2y(t)}{dt^2} - \frac{1}{\sqrt{t}}\left(1 + \frac{3}{2}y(t) + \frac{3}{8}(y(t))^2 - \frac{1}{16}(y(t))^3\right)\right) = 0 \quad (2.85)$$

The approximate solution of the Eq. (2.85) is

$$y(t) = y_0 + y_1 p + y_2 p^2 + \dots$$
 (2.86)

The following equations with corresponding boundary conditions was obtained by substituting Eq. (2.86) in Eq. (2.85) and equating the like coefficients of powers of p.

$$\frac{d^2 y_0(t)}{dt^2} = 0, y_0(0) = L - 1, y_0'(0) = M$$
(2.87)

$$\frac{d^2y_1(t)}{dt^2} - \frac{1}{\sqrt{t}} \left( 1 + \frac{3}{2}y_0(t) + \frac{3}{8}(y_0(t))^2 - \frac{1}{16}(y_0(t))^3 \right) = 0, y_1(0) = 0, y_1'(0) = 0$$
 (2.88)

$$\frac{d^2 y_2(t)}{dt^2} - \frac{1}{\sqrt{t}} \left( \frac{3}{2} y_1(t) + \frac{3}{4} y_0(t) y_1(t) - \frac{3}{16} (y_0(t))^2 y_1(t) \right) = 0, y_2(0) = 0, y_2'(0) = 0$$
(2.89)

$$\frac{d^2y_3(t)}{dt^2} - \frac{1}{\sqrt{t}} \left( \frac{3}{2} y_2(t) + \frac{3}{8} ((y_1(t))^2 + 2y_0(t) y_2(t)) - \frac{3}{16} \left( (y_0(t))^2 y_2(t) + (y_1(t))^2 y_0(t) \right) \right) = 0,$$

$$y_3(0) = 0, y_3'(0)$$
 (2.90)

Solving Eqs. (2.87 - 2.90), we get

$$y_0(t) = L - 1 + M_t$$
 (2.91)

$$y_1(t) = (9L(L+1) - 1 - L^3) \frac{1}{12} t^{3/2} + (3 + 6L - L^2) \frac{M}{20} t^{5/2}$$
$$+ (9 - 3L) \frac{M^2}{140} t^{7/2} - \frac{M^3}{252} t^{9/2}$$
(2.92)

$$y_{2}(t) = \left(\frac{(7L - 5L^{4} - 1)}{128} + \frac{41L^{2}}{192} + \frac{L^{5}}{384} + \frac{7L^{3}}{64}\right)t^{3} + \left(-\frac{13L^{3}}{320} + \frac{9L^{2}}{128} + \frac{13L^{4}}{3840} + \frac{97L}{960} - \frac{1}{1280}\right)Mt^{4} + \left(\frac{(43L^{3} - 387L^{2} + 247)}{22400} + \frac{9L}{896}\right)M^{2}t^{5} + \left(\frac{61L^{2}}{100800} - \frac{61L}{16800} + \frac{47}{33600}\right)M^{3}t^{6} + \left(\frac{37L}{282240} - \frac{37}{94080}\right)M^{4}t^{7} + \left(\frac{1}{75264}\right)M^{5}t^{8}$$

$$(2.93)$$

Therefore, the approximate solution of Eq. (2.94) is

$$\begin{split} y(t) &= L - 1 + Mt + \left(\frac{(7L - 5L^4 - 1)}{128} + \frac{41L^2}{192} + \frac{L^5}{384} + \frac{7L^3}{64}\right)t^3 \\ &\quad + \left(-\frac{13L^3}{320} + \frac{9L^2}{128} + \frac{13L^4}{3840} + \frac{97L}{960} - \frac{1}{1280}\right)Mt^4 \\ &\quad + \left(\frac{(43L^3 - 387L^2 + 247)}{22400} + \frac{9L}{896}\right)M^2t^5 + \left(\frac{61L^2}{100800} - \frac{61L}{16800} + \frac{47}{33600}\right)M^3t^6 \\ &\quad + \left(\frac{37L}{282240} - \frac{37}{94080}\right)M^4t^7 \end{split}$$

$$+\left(\frac{1}{75264}\right)M^{5}t^{8} + (9L(L+1) - 1 - L^{3})\frac{1}{12}t^{3/2} + (3 + 6L - L^{2})\frac{M}{20}t^{5/2} + (9L(L+1) - 1 - L^{3})\frac{M^{2}}{140}t^{7/2}$$

$$+\left(-\frac{M^{3}}{252} - \frac{1}{32256} - \frac{11L^{7}}{96768} - \frac{305L}{96768} + \frac{575L^{4}}{96768} + \frac{1741L^{3}}{32256} - \frac{7L^{5}}{512} - \frac{103L^{2}}{3584} + \frac{11L^{6}}{4608}\right)t^{9/2} + \dots$$

$$(2.94)$$

Let  $t = x^2$ . Then

$$u(x) = 1 + y(x)$$

$$= L + Mx^{2} + (9L(L+1) - 1 - L^{3}) \frac{1}{12}x^{3} + (3 + 6L - L^{2}) \frac{M}{20}x^{5}$$

$$+ \left(\frac{(7L - 5L^{4} - 1)}{128} + \frac{41L^{2}}{192} + \frac{L^{5}}{384} + \frac{7L^{3}}{64}\right)x^{6}$$

$$+ (9 - 3L) \frac{M^{2}}{140}x^{7} + \left(-\frac{13L^{3}}{320} + \frac{9L^{2}}{128} + \frac{13L^{4}}{3840} + \frac{97L}{960} - \frac{1}{1280}\right)Mx^{8} +$$

$$\left(-\frac{M^{3}}{252} - \frac{1}{32256} - \frac{11L^{7}}{96768} - \frac{305L}{96768} + \frac{575L^{4}}{96768}\right)x^{9} + \dots$$

$$\left(2.95\right)$$

For L=1 we get the same solution obtained by Wazwaz [17] using VIM. Padé approximant method is used to find the unknown M. Consider the [2/2] approximant as follows:

$$u(x) = \frac{a_0 + a_1 x + a_2 x^2}{1 + b_1 x + b_2 x^2}$$
 (2.96)

Let 
$$u(x) = u_0 + u_1 x + u_2 x^2 + u_3 x^3 + u_4 x^4 + u_5 x^5 + u_6 x^6 + u_7 x^7 + u_8 x^8 + \dots$$
(2.97)

From Eq. (2.96) and Eq. (2.97) we get,

$$(u_0 + u_1 x + u_2 x^2 + u_3 x^3 + u_4 x^4 + u_5 x^5 + u_6 x^6 + u_7 x^7 + u_8 x^8 + \dots)(1 + b_1 x + b_2 x^2) = a_0 + a_1 x + a_2 x^2$$
(2.98)

Equating the coefficients of  $x^0$ , x,  $x^2$ , we get

$$u_0 = a_0 \tag{2.99}$$

$$u_1 + u_0 b_1 = a_1 \tag{2.100}$$

$$u_2 + u_1 b_1 + u_0 b_2 = a_2 (2.101)$$

$$u_3 + u_2 b_1 + u_1 b_2 = 0 (2.102)$$

$$u_4 + u_3 b_1 + u_2 b_2 = 0 (2.103)$$

Solving Eq. (2.102) and Eq. (2.103), we get

$$b_1 = \frac{u_2 u_3 - u_4 u_1}{u_1 u_3 - u_2^2}, b_2 = \frac{u_2 u_4 - u_3^2}{u_1 u_3 - u_2^2}$$
(2.104)

From Eq. (2.95),

$$u_0 = L, u_1 = 0, u_2 = M, u_3 = (9L(L+1) - 1 - L^3) \frac{1}{12}, u_4 = 0, u_5$$

$$= (3 + 6L - L^2) \frac{M}{20},$$

$$u_6 = \frac{(7L - 5L^4 - 1)}{128} + \frac{41L^2}{192} + \frac{L^5}{384} + \frac{7L^3}{64}, u_7 = (9 - 3L) \frac{M^2}{140}, u_8$$

$$= \left( -\frac{13L^3}{320} + \frac{9L^2}{128} + \frac{13L^4}{3840} + \frac{97L}{960} - \frac{1}{1280} \right) M, \dots$$

Therefore, 
$$b_1 = \frac{L^3 - 9L(L+1) + 1}{12M}$$
,  $b_2 = \frac{\left(L^3 - 9L(L+1) + 1\right)^2}{144M^2}$ ,  $a_1 = \frac{L^4 - 9L^2(L+1) + L}{12M}$ , 
$$a_2 = \frac{L^7 - 2L^2(9L^4 - 82L^2 + 9) + 63L^3(1 + L^2)}{144M^2} + M \tag{2.105}$$

Using the boundary condition  $\lim_{n\to\infty} u(t) = 0$  in Eq.(2.96), we get the unknown M.

**Table 2.1.** The values of u'(0) = M for various Padé approximant

S.No	Padé approximant		u'(0)=M	
5.110	т исе ирргожинии	L=1	L=2	L=3
1.	[2/2]	-1.2114	-3.0411	-5.1087
2.	[4/4]	-1.5505	-3.9193	-6.6607
3.	[7/7]	-1.5874	-3.9948	-6.7751
4.	[8/8]	-1.5874	-3.9948	-6.7773
5.	[10/10]	-1.5874	-3.9948	-6.7773

Table 2.1 represents the initial slopes u'(0) = M for various Padé approximant and for different values of L.

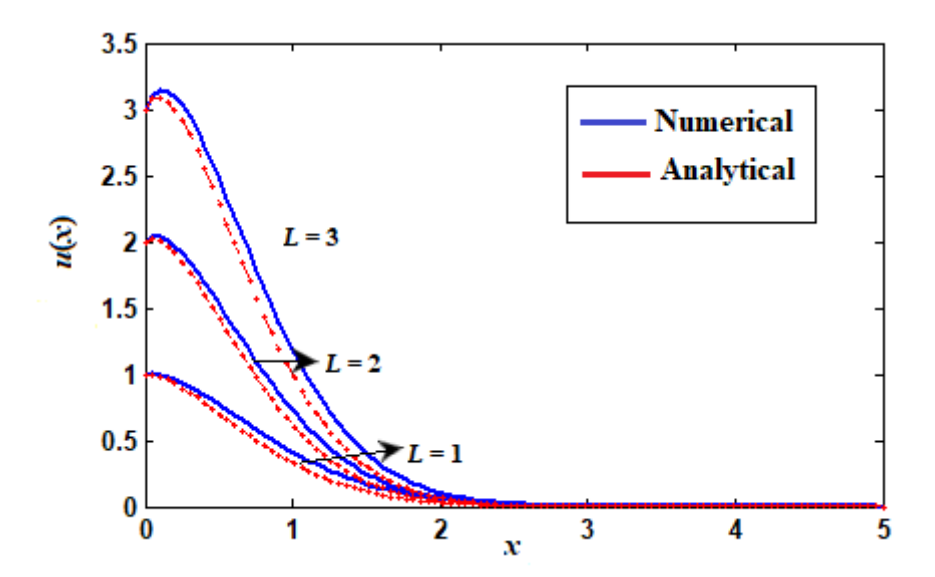


**Figure 2.2** Comparison of Padé approximant [11/11] solution of Thomas-Fermi equation with numerical solution for different initial condition.

The approximate analytical solution of Thomas-Fermi equation u(x) is compared with numerical solution for various values of L in Fig. 2.2 and satisfactory agreement is noted.

#### 2.5. Conclusions

In this chapter, the authors demonstrate that HPM and VIM are the two methods that can solve a broad range of nonlinear equations, especially in engineering as well as physical problems. Both methods are extremely useful and reliable, as shown by the examples in this article. Small parameters are not needed in VIM or HPM, and traditional perturbation methods' drawbacks and non-physical assumptions are eliminated. Additionally, when computing Adomian polynomials, VIM and HPM will solve the problems that arise. Both approaches are effective techniques for solving nonlinear equations in a number of fields and do not need linearization.

#### **CHAPTER 3**

# ANALYTICAL SOLUTION OF NON LINEAR PROBLEMS IN HOMOGENEOUS REACTIONS OCCUR IN THE MASSTRANSFER BOUNDARY LAYER: HOMOTOPY PERTURBATION

**METHOD** 

#### **CHAPTER-3**

## Analytical Solution of Non Linear Problems in Homogeneous Reactions Occur in the Mass-Transfer Boundary Layer: Homotopy Perturbation Method

#### 3.1. Introduction

Many electrode processes with homogeneous reactions that occur continuously in the mass-transfer boundary layer. These reactions involve splitting or forming in the process of deposition or degradation of metal-linking complexes, the interaction and dissociation of ions and redox soluble mediators. Quantitative studies of electrode-kinetics experiments as well as simulation of electrochemical reactor processes require the description of species concentrations at the electrode surface. Homogeneous reactions can strongly affect the concentration of species.

The computation of concentration profiles near electrodes in the solution is based on the species conservation equation.

$$\frac{\partial c_i}{\partial t} = -\nabla \cdot N_i + R_i \tag{3.1}$$

where  $c_i$  is the molar concentration of species i, and  $R_i$  is the net rate of production of i locally by homogeneous reactions. The molar flux  $N_i$  and the rate of production of  $M_i^{z_i}$  usually represented by

$$N_i = -D_i \nabla c_i - z_i c_i D_i \frac{F}{RT} \nabla \varphi + c_i v \text{ and } R_i = v_i \left[ k_r \prod_j c_j^{v_j} - k_f \prod_i c_i^{v_i} \right]$$
(3.2)

This describes species transport through diffusion and convection and ion migration in an electric field [1]. When charged species are involved, equations 1-2 must be written for each species in solution and combined with the electroneutrality state  $\sum_i z_i c_i = 0$ , and  $\varphi$  must be determined. Implementation of appropriate boundary conditions on the electrode surface and in the bulk solution is needed for their solution. This kind of nonlinear problems occurs in many relevant situations, such as cyclic voltammetry, chronopotentiometry, rotating disk and ring-disk electrodes, and various

boundary-layer flows with multiple geometries, system chemistries, flow and boundary conditions [2]-[6].

Recently Chapman et al [7] discuss the mass transfer at the electrodes for the homogeneous and fast reversible reaction. More recently the empirical expression of species concentration using the Taylor series method and hyperbolic function method was obtained by Mary et al. [8]. In this chapter, we present a simple and effective homotopy perturbation approach for solving the nonlinear differential equation in the sense of mass transfer at the electrodes with reversible homogeneous reactions. An approximate analytical expression for the concentration of species in the homogeneous electrochemical reaction is obtained for various parameter values.

#### 3.2. Mathematical formulation of the problem

Consider the reversible homogeneous reaction

$$A + B \Leftrightarrow_{k_r}^{k_f} C \tag{3.3}$$

A is formed at a known rate  $N_{\text{Ao}}$  at an electrode surface, and B is present in the bulk solution.

The concentrations of A and C in the bulk solution are negligible, and the fluxes of B and C at the electrode surface are also zero. The homogeneous reaction forms the species C and diffuses into the bulk. For measuring concentration profiles, Eqs. (3.1) and (3.2) may be combined for each component. We assume the steady-state and ignore migration and convection in the diffusion layer [7]. In this case, the system of nonlinear one-dimensional reaction-diffusion equations becomes as follows [7]:

$$D\frac{d^{2}A(x)}{dx^{2}} = -k_{r}C(x) + k_{f}A(x)B(x)$$
(3.4)

$$D\frac{d^{2}B(x)}{dx^{2}} = -k_{r}C(x) + k_{f}A(x)B(x)$$
(3.5)

$$D\frac{d^{2}C(x)}{dx^{2}} = k_{r}C(x) - k_{f}A(x)B(x)$$
(3.6)

The k coefficients denote the forward and reverse reaction rate constants, and A, B, and C represent the species concentrations. Both diffusion coefficients are

assumed to be equal to a constant D for the sake of consistency. The boundary conditions are

$$D\frac{dA}{dx} = -N_{Ao}; \frac{dB}{dx} = \frac{dC}{dx} = 0 \text{ at } x = 0$$
(3.7)

$$A = 0; B = B_b; C = 0 \text{ at } x = \delta$$
 (3.8)

By introducing the following dimensionless variables

$$a = \left[\frac{A}{B_b}\right], b = \left[\frac{B}{B_b}\right], S = \left[\frac{C}{B_b}\right], z = \left[\frac{x}{\delta}\right],$$

$$\varepsilon = \left[\frac{D}{\delta^2 k_f B_b}\right]^{\frac{1}{2}}, K^* = \left[\frac{k_f B_b}{k_r}\right], \mu = \left[\frac{N_{AO}\delta}{DB_b}\right]$$
(3.9)

Eqns. (3.4)-(3.6) becomes in dimensionless form as follows:

$$\varepsilon^2 \frac{d^2 a(z)}{dz^2} = a(z)b(z) - \frac{S(z)}{K^*}$$
(3.10)

$$\varepsilon^2 \frac{d^2 b(z)}{dz^2} = a(z)b(z) - \frac{S(z)}{K^*}$$
(3.11)

$$\varepsilon^2 \frac{d^2 S(z)}{dz^2} = \frac{S(z)}{K^*} - \alpha(z)b(z) \tag{3.12}$$

The corresponding dimensionless boundary conditions are,

$$a'(z=0) = \mu, b'(z=0) = 0, S'(z=0) = 0$$
 (3.13)

$$a(z = 1) = 0, b(z = 1) = 1, S(z = 1) = 0$$
 (3.14)

where  $\varepsilon$  is the relative rates of diffusion and reaction.  $K^*$  is the homogeneous equilibrium constant.  $\mu$  is the rate of injection of A relative to the limiting flux of B toward the electrode.

### 3.3 Analytical expression of the concentration using homotopyperturbation method

The nonlinear equations (3.10 - 3.12), in recent years, numerous methods have been developed to derive analytical or semi-analytical solutions regardless of how strong the nonlinearity maybe. Homotopy analysis method [9,10], variational iteration method [11,12], Adomian decomposition method [13] and Green's function iterative

method [14,15] are used to solve the nonlinear equations. Due to its simpleimplementation and high accuracy, the homotopy perturbation method (HPM) [16-20], Residual method [21], Padé approximants method [22], Akbari Ganji's method (AGM) [23] and Taylor series method [24], the new approach of homotopy perturbation method (NHPM) [25,26] has received great deal of attention.

By solving equations (3.10)-(3.12) using the homotopy perturbation approach (details in Appendix A), the following approximate analytical representation of ionic concentration is obtained .

$$a(z) = \mu(z-1) + \frac{\mu}{120K^*\varepsilon^4} [(z-1)(z^2 - 2z - 4)^2 + 20K^*\varepsilon^2(z^3 - 3z^2 + 2)]$$
(3.15)

$$b(z) = 1 + \frac{\mu}{120K^*\varepsilon^4} [(z-1)(z^2 - 2z - 4)^2 + 20K^*\varepsilon^2(z^3 - 3z^2 + 2)]$$
 (3.16)

$$S(z) = 1 - b(z)$$
 (3.17)

#### 3.4. Previous analytical results

Chapman [7] derived approximate distributions of concentration. Consider the case of small  $\epsilon$ , that is, the case where the homogeneous rate constant  $k_f$  is large enough to make  $\epsilon$  small. If the first terms is neglected, the following solutions are obtained from a quadratic algebraic equation for S.

$$S(z) = \frac{1}{2} \left[ \left( \mu(1-z) + 1 + \frac{1}{K^*} \right) - \left( \left( \mu(1-z) + 1 + \frac{1}{K^*} \right)^2 - 4\mu(1-z) \right)^{1/2} \right]$$
(3.18)

$$a(z) = \mu(1-z) - S(z) \tag{3.19}$$

$$b(z) = 1 - S(z) (3.20)$$

Recently, Mary et al. [8] used Taylor's series method (TSM) to obtain the analytical representation of species concentration as follows:

$$a(z) = b(z) + \mu z - \mu - 1 \tag{3.21}$$

$$b(z) = m + \frac{\alpha z^2}{2\varepsilon^2} + \frac{(m\mu)z^3}{\varepsilon^2 3!} + \frac{\alpha\beta z^4}{\varepsilon^4 4!} + \frac{1}{\varepsilon^4} [\beta\mu m + 3\alpha\mu] \frac{z^5}{5!} + \frac{1}{\varepsilon^6} [\alpha\beta^2 + 6\alpha^2 + 4\varepsilon^2 m\mu^2] \frac{z^6}{6!}$$

$$(3.22)$$

$$S(z) = 1 - b(z) (3.23)$$

where 
$$\alpha = m(m - \mu - 1) + \frac{m-1}{K^*}\beta = 2m - \mu - 1 + \frac{1}{K^*}$$
 (3.24)

The value of m is obtained by solving the following equation.

$$m + \frac{\alpha}{2\varepsilon^2} + \frac{m\mu}{\varepsilon^2 3!} + \frac{\alpha\beta}{\varepsilon^4 4!} + \frac{1}{\varepsilon^4} [\mu\beta m + 3\mu\alpha] \frac{1}{5!} + \frac{1}{\varepsilon^6} [\alpha\beta^2 + 6\alpha^2 + 4\varepsilon^2 m\mu^2] \frac{1}{6!} - 1 = 0 \quad (3.25)$$

But in this method, it is very difficult to find the constant m. Our analytical results (Eqs. 3.15 - 3.17) are easily computable when compared with Taylor's series solution (Eqs.3.21-3.23).

#### 3.5 Numerical simulation and discussion

The differential Eqs. (3.10 - 3.12) with the corresponding boundary conditions has also been solved numerically using SCILAB/MATLAB program (Appendix-B). The numerical solution is compared with our analytical results (HPM method) and previously available results (Taylor's series method) in Tables 3.1–3.3. There is no much difference in average error percentage between HPM and TSM. But we can easily calculate the concentration for all values of the parameter in HPM.

Also, a comparison between the analytical and numerical results are shown in Figures 3.1.The maximum error between analytical (HPM) and the numerical result is 1.35%. It is evident from Tables 3.1-3.12 and Fig. 3.1 that our results are very close to the exact simulation results.

The concentration of species depends upon the parameter relative rates of diffusion and reaction  $(\varepsilon)$ , rate of injection of A relative to the limiting flux of B toward the electrode  $(\mu)$  and homogeneous equilibrium constant  $(K^*)$ . Figure 1, shows the concentration of species a(z),b(z) and S(z) for various values of relative rates of diffusion and reaction and the homogeneous equilibrium constant.

From this fig.3.1, it is observed that an increase in equilibrium constant leads to increase in a(z) and b(z) and decreases in S(z). From this fig.3.2, it is noted that an increase in rate of injection leads to decrease in a(z), b(z) and S(z).

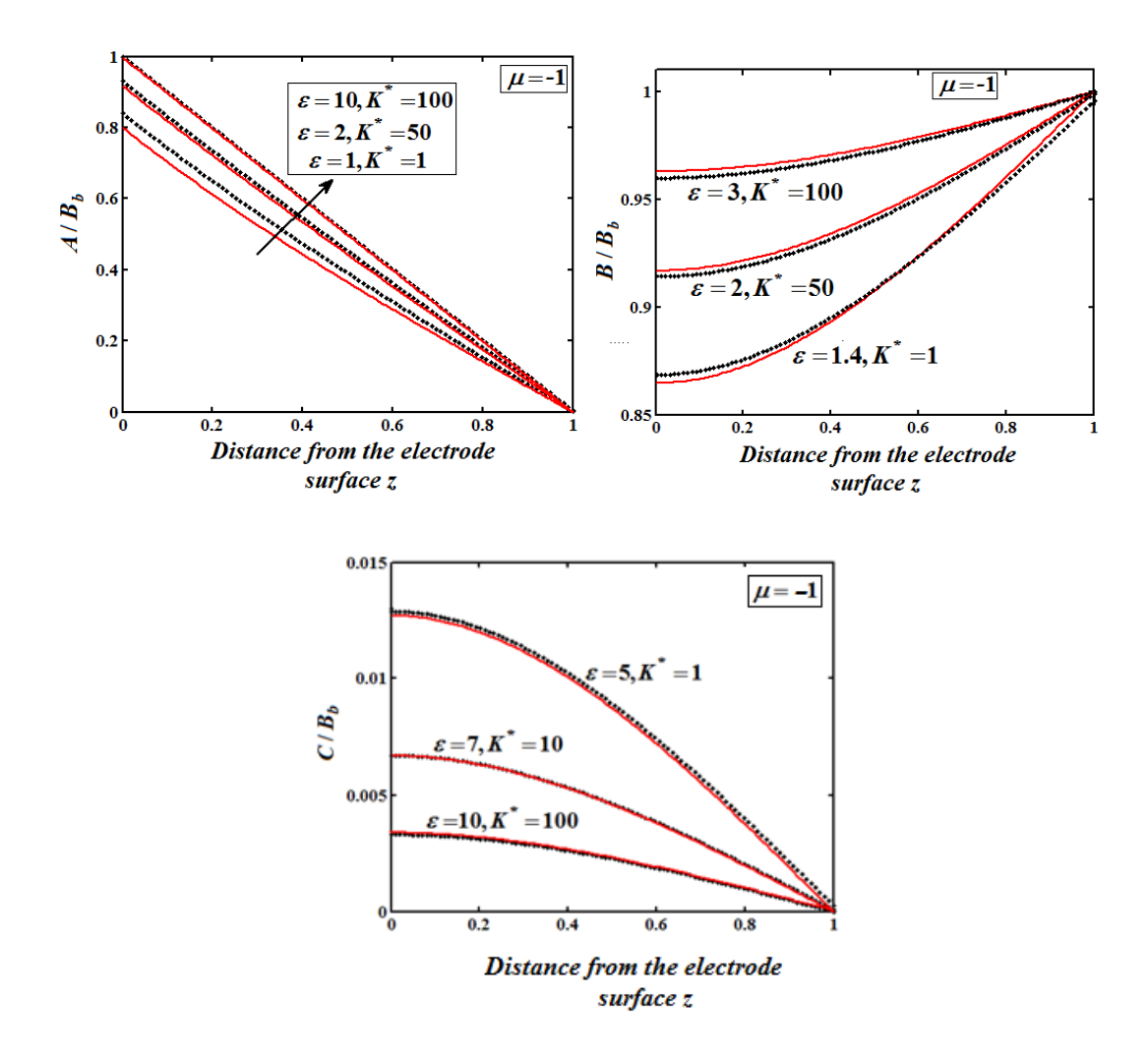


**Figure 3.1.** Comparison of concentrations a(z), b(z) and S(z) (Eqns. (3.15)-(3.17)) with simulation results for various values of parameters  $\varepsilon$ ,  $K^*$  and  $\mu$ .

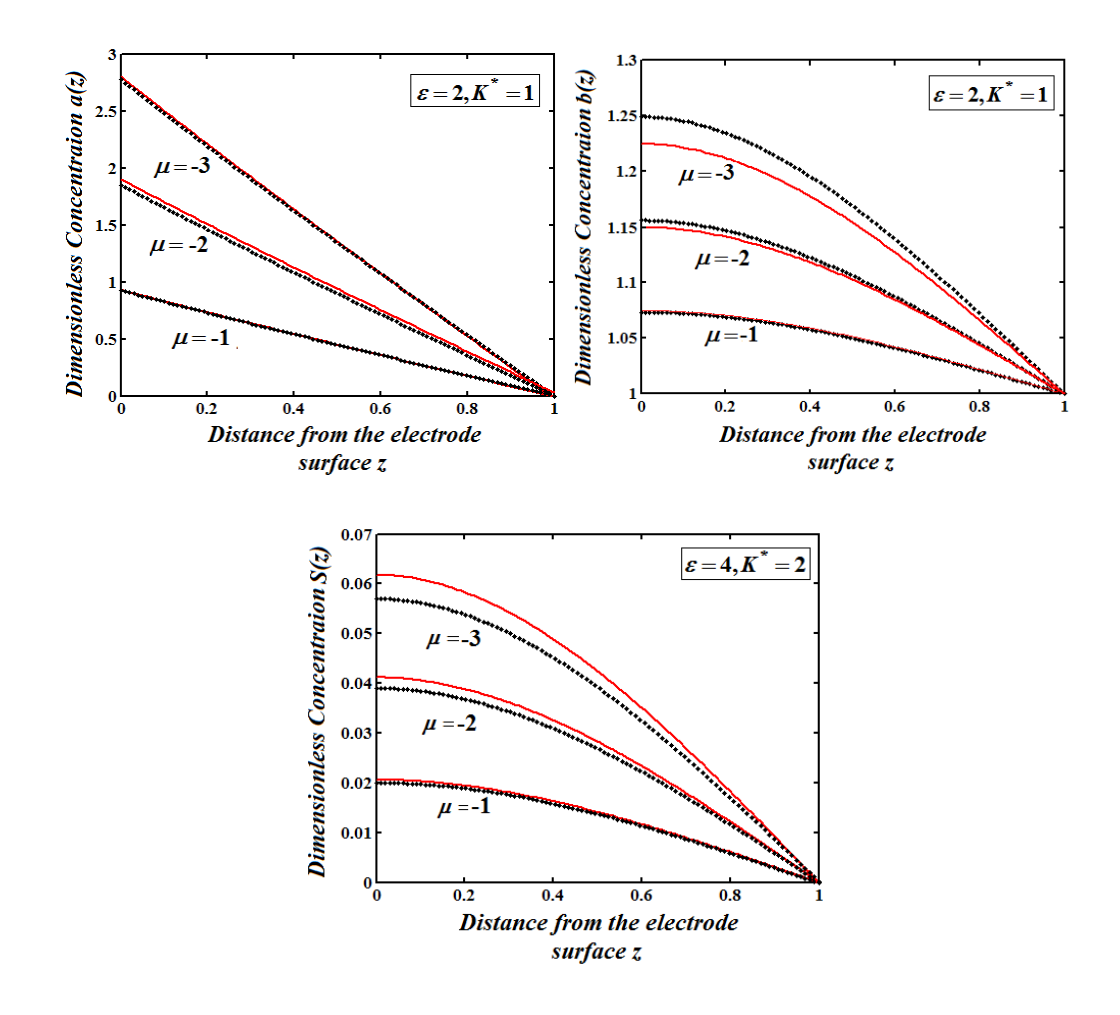


**Figure 3.2.** Comparison of concentrations a(z), b(z) and S(z) (Eqns. (3.15)-(3.17)) with simulation results for various values of parameters  $\varepsilon$ ,  $K^*$  and  $\mu$ 

#### 3.6 Conclusions

An analytical expression has effectively derived the concentration in the rotating disc electrode controlled by migration and convection in the diffusion layer. In this study, the model is applied to a one-dimensional case of a rotating disc electrode. The steady-state nonlinear reaction-diffusion equations are solved analytically by a new approach of the homotopy perturbation method. There is a very good agreement between the analytical and the numerical solutions for all values of rate constant.

**Table 3.1.** Comparison of numerical solution of concentration of species a(z) with the analytical solutions by Homotopy perturbation method and Taylor series method for  $K^* = 1$ ,  $\mu = -3$  and for different values  $\varepsilon$ .

			$\varepsilon = 0.7$				8	$\epsilon = 0.8$					$\varepsilon = 0.9$		
Z	Num	Our HPM Eq.(3.15)	Error % of HPM	TSM Eq.(3.21)	Error % of TSM	Num	Our HPM Eq.(3.15)	Error % of HPM	TSM Eq.(3. 21)	Error % of TSM	Num	Our HPM Eq.(3.15)	Error % of HPM	TSM Eq.(3.21)	Error % of TSM
0	2.500	2.494	0.24	2.483	0.70	2.538	2.527	0.44	2.483	0.56	2.573	2.568	0.21	2.563	0.40
0.2	1.922	1.920	0.11	1.907	0.79	1.957	1.949	0.42	1.907	0.48	1.991	1.997	0.31	1.985	0.28
0.4	1.390	1.380	0.70	1.371	1.38	1.420	1.415	0.37	1.371	0.69	1.449	1.436	0.90	1.445	0.26
0.6	0.894	0.889	0.53	0.867	3.08	0.917	0.909	0.82	0.867	1.41	0.938	0.929	0.95	0.935	0.39
0.8	0.427	0.424	0.88	0.399	6.53	0.440	0.436	0.84	0.399	2.39	0.451	0.444	1.51	0.451	0.04
1	0.000	0.000	0.00	0.000	0.00	0.000	0.000	0.00	0.000	0.00	0.000	0.000	0.00	0.000	0.00
	Average	% error	0.41		2.08			0.48		0.92			0.65		0.23

**Table 3.2.** Comparison of numerical solution of concentration of species b(z) with the analytical solutions by Homotopy perturbation method and Taylor series method for  $K^* = 1$ ,  $\mu = -3$  and for different values  $\varepsilon$ .

			$\varepsilon = 1$					$\varepsilon = 1.5$					$\varepsilon = 2$		
Z		Our	Error	TSM	Error		Our HPM	Error %	TSMEq.(3	Error		Our	Error	TSM	Error
	Num	HPM	% of	Eq.(3.22)	% of	Num	Eq.(3.16)	of HPM	.22)	% of	Num	HPM	% of	Eq.(3.22)	% of
		Eq.(3.16)	HPM	1.4.	TSM		1.()		,	TSM		Eq.(3.16)	HPM	1.(-, )	TSM
0	0.607	0.603	0.68	0.599	1.30	0.740	0.737	0.34	0.737	0.35	0.821	0.816	0.62	0.822	0.10
0.2	0.629	0.624	0.80	0.614	1.41	0.754	0.747	0.91	0.752	0.32	0.832	0.827	0.64	0.832	0.10
0.4	0.690	0.687	0.42	0.658	1.98	0.794	0.789	0.68	0.791	0.42	0.859	0.855	0.54	0.858	0.16
0.6	0.776	0.778	0.15	0.735	2.04	0.853	0.849	0.47	0.848	0.53	0.900	0.896	0.41	0.898	0.22
0.8	0.883	0.885	0.25	0.847	1.65	0.925	0.921	0.39	0.919	0.58	0.949	0.946	0.33	0.947	0.28
1	1.000	1.000	0.00	1.000	0.00	1.000	1.000	0.00	1.000	0.00	1.000	1.000	0.00	1.000	0.00
A	Average 9	% error	0.38		1.40			0.46		0.37			0.43		0.14

**Table 3.3.** Comparison of numerical solution of concentration of species S(z) with the analytical solutions by Homotopy perturbation method and Taylor series method for  $\varepsilon = 2$ ,  $\mu = -1$  and for different values  $K^*$ .

			$K^* = 0.1$					$K^* = 0.2$	2				$K^*=0.$	5	
Z	Num	Our HPM Eq.(3.1	Error % of HPM	TSM Eq.(3.23)	Error % of TSM	Num	Our HPM Eq. (3.17)	Error % of HPM	TSM Eq.(3.23)	Error % of TSM	Num	Our HPM Eq.(3.17)	Error % of HPM	TSM Eq. (3.23)	Error % of TSM
0	0.039	0.038	0.78	0.039	0.52	0.050	0.050	0.20	0.050	0.26	0.061	0.061	0.49	0.061	0.26
0.2	0.036	0.036	0.84	0.036	0.55	0.047	0.047	0.04	0.047	0.43	0.057	0.058	0.35	0.058	0.35
0.4	0.030	0.030	0.34	0.030	2.02	0.039	0.039	0.93	0.039	0.77	0.048	0.048	0.42	0.048	0.63
0.6	0.021	0.021	0.42	0.022	2.37	0.028	0.027	0.91	0.028	1.81	0.034	0.034	0.58	0.035	1.47
0.8	0.011	0.011	0.46	0.011	3.67	0.014	0.014	0.14	0.015	5.00	0.017	0.017	0.58	0.018	4.65
1	0.000	0.000	0.00	0.000	0.00	0.000	0.000	0.00	0.000	0.00	0.000	0.000	0.00	0.000	0.00
Α	verage %	error	0.47		1.52			0.37		1.38			0.40		1.23

**Table 3.4.** Comparison of our analytical expression of concentration of species a with the numerical result for various values of the parameter  $\mu$  and some fixed values parameter  $\epsilon = 2$ ,  $\mu = -1$  using Eqn. (3.15).

		$K^* = 1$			$K^* = 10$		$K^* = 1000$			
Z				Numerica				Our		
2	Numerical	Our	% of	1	Our	% of	Numerical	Eq.(3.15	% of	
	Result	Eq.(3.15)	deviation	Result	Eq.(3.15)	deviation	Result	)	deviation	
0	0.934	0.925	0.98	0.929	0.918	1.26	0.929	0.917	1.28	
0.2	0.736	0.729	0.92	0.731	0.722	1.24	0.731	0.721	1.28	
0.4	0.544	0.541	0.64	0.540	0.535	1.03	0.540	0.534	1.06	
0.6	0.357	0.358	0.09	0.354	0.353	0.29	0.354	0.353	0.35	
0.8	0.173	0.178	2.66	0.172	0.176	2.21	0.172	0.175	2.18	
1	0.000	0.000	0.00	0.000	0.000	0.00	0.000	0.000	0.00	
	Average perc	entage error:	0.88	Average pe	rcentage erro	or: 1.00	Average percentage error: 1.02			

**Table 3.5.** Comparison of our analytical expression of concentration of species b with the numerical result for various values of the parameter  $\mu$  and some fixed values parameter  $\epsilon = 2$ ,  $\mu = -1$  using Eqn. (3.16).

		$K^* = 1$			$K^* = 10$			$K^* = 1000$	
Z	Numerical	Our	% of	Numerical	Our	% of	Numerical	Our	% of
	Result	Eq.(3.16)	deviation	Result	Eq.(3.16)	deviation	Result	eq.(3.16)	deviation
0	0.934	0.925	0.99	0.929	0.918	1.26	0.929	0.917	1.28
0.2	0.938	0.929	0.93	0.933	0.922	1.19	0.933	0.921	1.22
0.4	0.948	0.941	0.79	0.944	0.935	1.01	0.944	0.934	1.03
0.6	0.963	0.958	0.59	0.960	0.953	0.75	0.960	0.953	0.76
0.8	0.981	0.978	0.35	0.980	0.976	0.43	0.980	0.975	0.45
1	1.000	1.000	0.00	1.000	1.000	0.00	1.000	1.000	0.00
	Average per	centage error	: 0.61	Average per	centage error	: 0.77	Average percentage error: 0.79		

**Table 3.6.** Comparison of our analytical expression of concentration of species S with the numerical result for various values of the parameter  $\mu$  and some fixed values parameter  $\varepsilon = 4$ ,  $\mu = -1$  using Eqn. (3.17).

		$K^* = 1$			$K^* = 10$			$K^* = 1000$	
Z	Numerical	Our	% of	Numerical	Our	% of	Numerical	Our	% of
	Result	Eq.(3.17)	deviation	Result	Eq.(3.17)	deviation	Result	Eq.(3.17)	deviation
0	0.020	0.019	0.89	0.020	0.020	0.73	0.020	0.020	0.23
0.2	0.018	0.018	0.79	0.019	0.019	0.64	0.019	0.019	0.65
0.4	0.015	0.015	0.51	0.015	0.016	3.19	0.016	0.016	0.29
0.6	0.011	0.011	0.25	0.011	0.011	0.45	0.011	0.011	0.44
0.8	0.006	0.006	2.91	0.006	0.006	3.09	0.006	0.006	3.11
1	0.000	0.000	0.00	0.000	0.000	0.00	0.000 0.000 0.00		
	Average per	rcentage erro	or: 0.89	Average per	rcentage erro	or: 1.35	Average percentage error :0.79		

**Table 3.7.** Comparison of our analytical expression of concentration of species a with the numerical result for various values of the parameter  $\mu$  and some fixed values parameter  $\epsilon = 2$ ,  $K^* = 1$  using Eqn. (3.15).

		$\mu = -1$			$\mu = -1.5$			$\mu = -2$	
Z	Numerical	Our	% of	Numerical	Our	% of	Numerical	Our	% of
	Result	Eq.(3.15)	deviation	Result	Eq.(3.15)	deviation	Result	Eq.(3.15)	deviation
0	0.934	0.925	0.98	1.388	1.404	1.18	1.875	1.850	1.33
0.2	0.736	0.729	0.92	1.094	1.106	1.10	1.478	1.459	1.32
0.4	0.544	0.541	0.64	0.811	0.818	0.88	1.094	1.082	1.15
0.6	0.357	0.358	0.10	0.536	0.537	0.15	0.718	0.715	0.38
0.8	0.173	0.178	2.65	0.267	0.261	2.40	0.348	0.356	2.18
1	0.000	0.000	0.00	0.000	0.000	0.00	0.000	0.000	0.00
	Average per	centage error	: 0.88	Average per	rcentage erro	or: 0.95	Average percentage error: 1.06		

**Table 3.8.** Comparison of our analytical expression of concentration of species a with the numerical result for various values of the parameter  $\varepsilon$  and some fixed values parameter  $\mu = -1$ ,  $K^* = 4$ , using Eqn. (3.15).

		$\varepsilon = 2$			$\varepsilon = 5$			$\varepsilon = 8$		
Z	Numerical	Our	% of	Numerical	Our	% of	Numerical	Our	% of	
	Result	Eq.(3.15)	deviation	Result	Eq.(3.15)	deviation	Result	Eq.(3.15)	deviation	
0	0.930	0.919	1.22	0.987	0.987	0.04	0.995	0.995	0.01	
0.2	0.732	0.723	1.20	0.786	0.788	0.21	0.793	0.795	0.25	
0.4	0.541	0.536	0.96	0.586	0.590	0.63	0.592	0.596	0.67	
0.6	0.355	0.354	0.26	0.387	0.393	1.49	0.391	0.397	1.52	
0.8	0.172	0.176	2.31	0.188	0.196	4.18	0.191	0.199	4.18	
1	0.000	0.000	0.00	0.000	0.000	0.00	0.000 0.000 0.00			
	Average per	rcentage erro	or: 0.99	Average pe	ercentage err	or: 1.09	Average percentage error: 1.11			

**Table 3.9.** Comparison of our analytical expression of concentration of species b with the numerical result for various values of the parameter  $\mu$  and some fixed values parameter  $\epsilon = 2$ ,  $K^* = 10$  using Eqn. (3.16).

		$\mu = -1$			$\mu = -1.5$			$\mu = -2$		
Z	Numerical	Our	% of	Numerical	Our	% of	Numerical	Our	% of	
	Result	Eq.(3.16)	deviation	Result	Eq.(3.16)	deviation	Result	Eq.(3.16)	deviation	
0	0.9272	0.9173	1.07	0.8967	0.8873	1.05	0.8661	0.8497	1.92	
0.2	0.9329	0.9219	1.17	0.9021	0.8936	0.94	0.8737	0.8582	1.81	
0.4	0.9435	0.9345	0.95	0.9186	0.9108	0.85	0.8943	0.8810	1.51	
0.6	0.9594	0.9530	0.66	0.9420	0.9360	0.64	0.9212	0.9147	0.71	
0.8	0.9798	0.9755	0.44	0.9705	0.9667	0.40	0.9617	0.9555	0.65	
1	1.0000	1.0000	0.00	1.000	1.000	0.00	1.0000 1.0000 0.00			
	Average per	rcentage erro	or: 0.72	Average per	rcentage erro	or: 0.65	Average percentage error: 1.10			

**Table 3.10.** Comparison of our analytical expression of concentration of species b with the numerical result for various values of the parameter  $\varepsilon$  and some fixed values parameter  $\mu = -2$ ,  $K^* = 50$  using Eqn. (3.16).

		$\varepsilon = 1$			$\varepsilon = 4$			$\varepsilon = 7$	
Z	Numerical	Our	% of	Numerical	Our	% of	Numerical	Our	% of
	Result	Eq.(3.16)	deviation	Result	Eq.(3.16)	deviation	Result	Eq.(3.16)	deviation
0	0.8652	0.8437	2.55	0.9607	0.9456	1.60	0.9867	0.9815	0.53
0.2	0.8729	0.8530	2.33	0.9630	0.9487	1.51	0.9874	0.9825	0.50
0.4	0.8936	0.8783	1.75	0.9690	0.9569	1.26	0.9895	0.9853	0.42
0.6	0.9242	0.9155	0.95	0.9780	0.9691	0.92	0.9925	0.9895	0.30
0.8	0.9614	0.9608	0.07	0.9888	0.9839	0.50	0.9960	0.9945	0.15
1	1.0000	1.0000	0.00	1.0000	1.0000	0.00	1.0000	1.0000	0.00
	Average per	centage erro	or: 1.27	Average pe	ercentage err	or : 0.96	Average percentage error: 0.32		

**Table 3. 11.** Comparison of our analytical expression of concentration of species S with the numerical result for various values of the parameter  $\varepsilon$  and some fixed values parameter  $\varepsilon = 4$ ,  $K^* = 100$  using Eqn. (3.17).

		$\mu = -1$			$\mu = -1.5$			$\mu = -2$		
Z	Numerical	Our	% of	Numerical	Our	% of	Numerical	Our	% of	
	Result	Eq.(3.17)	deviation	Result	Eq.(3.17)	deviation	Result	Eq.(3.17)	deviation	
0	0.0200	0.0198	0.71	0.0297	0.0294	0.93	0.0393	0.0388	1.14	
0.2	0.0189	0.0187	1.21	0.0280	0.0278	0.83	0.0370	0.0367	1.06	
0.4	0.0157	0.0157	0.31	0.0234	0.0233	0.54	0.0310	0.0307	0.76	
0.6	0.0115	0.0112	1.81	0.0167	0.0167	0.23	0.0220	0.0220	0.03	
0.8	0.0057	0.0059	3.00	0.0085	0.0087	2.80	0.0112	0.0115	2.54	
1	0.0000	0.0000	0.00	0.0000	0.0000	0.00	0.0000 0.0000 0.00			
	Average per	rcentage erro	or: 1.17	Average per	rcentage erro	or: 0.89	Average percentage error: 0.92			

**Table 3.12.** Comparison of our analytical expression of concentration of species S with the numerical result for various values of the parameter  $\varepsilon$  and some fixed values parameter  $\mu$  = -2,  $K^*$  = 500 using Eqn. (3.17).

	$\varepsilon = 5$			$\varepsilon = 7$			$\varepsilon = 10$		
Z	Numerical	Our	% of	Numerical	Our	% of	Numerical	Our	% of
	Result	Eq.(3.17)	deviation	Result	Eq.(3.17)	deviation	Result	Eq.(3.17)	deviation
0	0.0257	0.0255	0.63	0.0133	0.0133	0.27	0.0066	0.0066	0.09
0.2	0.0242	0.0241	0.51	0.0126	0.0126	0.17	0.0062	0.0062	0.59
0.4	0.0202	0.0202	0.17	0.0105	0.0105	0.24	0.0051	0.0052	1.61
0.6	0.0144	0.0145	0.63	0.0075	0.0076	1.03	0.0037	0.0037	1.87
0.8	0.0073	0.0075	3.18	0.0038	0.0039	3.60	0.0019	0.0020	2.75
1	0.0000	0.0000	0.00	0.0000	0.0000	0.00	0.0000	0.0000	0.00
	Average pro	centageeror:	0.85	Average percentage error: 0.88			Average percentage error: 1.15		

#### **APPENDIX 3.A:**

#### Analytical expression of the concentration using homotopy perturbation method

We construct the homotopy for the equations (3.10)-(3.12) as follows

$$(1-p)\left[\frac{d^2a}{dz^2}\right] + p\left[\frac{d^2a}{dz^2} - \frac{ab}{\varepsilon^2} + \frac{s}{K^*\varepsilon^2}\right] = 0$$
(3.A1)

$$(1-p)\left[\frac{d^2b}{dz^2}\right] + p\left[\frac{d^2b}{dz^2} - \frac{ab}{\varepsilon^2} + \frac{S}{K^*\varepsilon^2}\right] = 0$$
(3.A2)

$$(1-p)\left[\frac{d^2S}{dz^2} + \frac{ab}{\varepsilon^2}\right] + p\left[\frac{d^2S}{dz^2} + \frac{ab}{\varepsilon^2} - \frac{S}{K^*\varepsilon^2}\right] = 0$$
(3.A3)

where  $p \in [0,1]$  is an embedding parameter. Using Maclaurin series

$$a(z) = a(0) + za'(0) + z^2 \frac{a''(0)}{2!} + ...,$$
 (3.A4)

Now, assume that the solutions of Eqs. (3.A1) - (3.A3) is

$$a = a_0 + p \rightleftharpoons a_1 + p^2 a_2 + \cdots$$
 (3.A5)

$$b = b_0 + p \rightleftharpoons b_1 + p^2 b_2 + \cdots$$
 and

$$S = S_0 + p \rightleftharpoons S_1 + p^2 S_2 + \cdots$$

Substituting Eq. (3.A5) into Eqs. (3.A1)-(3.A3) and equating the like coefficients of 'p' on both sides lead to the following linear differential equations:

$$p^0: \frac{d^2 a_0}{dz^2} = 0 ag{3.A6}$$

$$p^0: \frac{d^2b_0}{dz^2} = 0 ag{3.A7}$$

$$p^0: \frac{d^2S_0}{dz^2} + \frac{a_0b_0}{\varepsilon^2} = 0 \tag{3.A8}$$

Solving Eqs. (3.A6)-(3.A8) Subject to boundary conditions:

$$a'_0(z=0) = \mu, b'_0(z=0) = 0, S'_0(z=0) = 0$$
 (3.A9)

$$a_0(z=1) = 0, b_0(z=1) = 1, S_0(z=1) = 0$$
 (3.A10)

$$p^{1}: \frac{d^{2}a_{1}}{dz^{2}} - \frac{a_{0}b_{0}}{\varepsilon^{2}} + \frac{S_{0}}{K^{*}\varepsilon^{2}} = 0.$$
(3.A11)

$$p^{1}: \frac{d^{2}b_{1}}{dz^{2}} - \frac{a_{0}b_{0}}{\varepsilon^{2}} + \frac{S_{0}}{K^{*}\varepsilon^{2}} = 0.$$
(3.A12)

Solving Eqs. (3.A9) and (3.A10), subject to boundary conditions:

$$a'_1(z=0) = \mu, b'_1(z=0) = 0$$
 (3.A13)

$$a_1(z=1) = 0, b_1(z=1) = 1$$
 (3.A14)

The solution of the Eqns. (3.A6) to (3.A8) are given by

$$a_0(z) = \mu(z-1)$$
 (3.A15)

$$b_0(z) = 1$$
 (3.A16)

$$S_0(z) = \frac{\mu(2+z^3-3z^2)}{6\varepsilon^2}$$
 (3.A17)

and the solution of the Eqns. (3.A11) to (3.A12) are given by

$$a_1(z) = \frac{\mu}{120K^*\varepsilon^4} \left( (z-1)(z^2 - 2z - 4)^2 + 20K^*\varepsilon^2 (z^3 - 3z^2 + 2) \right)$$
 (3.A18)

$$b_1(z) = \frac{\mu}{120K^*\varepsilon^4} \left( (z-1)(z^2 - 2z - 4)^2 + 20K^*\varepsilon^2 (z^3 - 3z^2 + 2) \right)$$
 (3.A19)

With the use of these two iterations only, we obtain an approximate solution for the ionic concentration given by:

$$a(z) = a_0(z) + a_1(z) b(z) = b_0(z) + \rightleftharpoons b_1(z)$$
 (3.A20)

#### **APPENDIX 3.B:**

Matlab program for the numerical solution of nonlinear differential equations (3.10)-(3.12)

```
function sol=ex6
ex6init=bvpinit(linspace(0,1),[0 1 1 0 0 0]);
sol = bvp4c(@ex6ode, @ex6bc, ex6init)
end
functiondydx=ex6ode(x,y)
dydx=[y(2)
(1/(2)^2)^*(y(1)^*y(3)-((y(5))/(3)))
y(4)
(1/(2)^2)^*(y(1)^*y(3)-((y(5))/(3)))
y(6)
(1/(2)^2)*(((y(5))/(3)))-y(1)*y(3)];
end
Function res=ex6bc(ya,yb)
res=[ya(1)-0]
yb(2)-1
ya(3)-1
yb(4)-0
ya(5)-0
yb(6)-0];
end
```

## **CHAPTER 4**

# ANALYTICAL EXPRESSIONS FOR THE CONCENTRATION AND CURRENT IN THE REDUCTION OF HYDROGEN PEROXIDE AT A METAL-DISPERSED CONDUCTING POLYMER FILM

## **CHAPTER-4**

## Analytical Expressions for the Concentration and Current in the Reduction of Hydrogen Peroxide at a Metal-Dispersed Conducting Polymer Film

## 4.1 Introduction

Enzyme-based fuel cells can produce higher energy than conventional batteries utilizing significantly all the naturally good materials. Enzymatic biofuel cells rely on the oxidation of substrates such as hydrogen or glucose and reduction of oxygen to harvest energy from complex media. In particular, glucose biofuel cells (BFCs) represent a promising alternative to supply energy from living organisms to implanted electronic devices. Oxidase enzymes are widely used in energy devices (biosensor, enzymatic biofuel cell, bioreactor, etc.). In glucose oxidation-reduction process, oxygen is diminished to water (H<sub>2</sub>O) or hydrogen peroxide (H<sub>2</sub>O<sub>2</sub>). Glucose oxidase is found in nectar and goes about as a common additive. Enzymatic glucose biosensors [1] utilize an electrode rather than oxygen to take up the electrons required to oxidize glucose and produce current in the extent to glucose fixation. Glucose oxidase is broadly used for the determination of free glucose in body liquids (diagnostics), in crude botanic material, and the nourishment business. Toghill and Compton [2] discussed non-enzymatic glucose sensors. It likewise has numerous applications in biotechnologies, commonly protein tests for natural chemistry incorporating biosensors in nanotechnologies [3]. Besides, glucose oxidase has damage the cancer tissue and cells as a result of hydrogen peroxide formation.

In recent times, many kinds of literature focused on glucose/hydrogen peroxide biofuel cell. Pizzariello et al. [4] developed a glucose/hydrogen peroxide biofuel cell using a composite bulk modified bioelectrode based on a solid binding matrix. Choudhury et al. [5] discussed the effect of hydrogen peroxide as an oxidant in an alkaline direct borohydride fuel cell. Bessette et al. [6] reported the performance of the microfiber carbon electrode in magnesium—hydrogen peroxide semi-fuel cell under optimum conditions and at a reduced concentration of H<sub>2</sub>O<sub>2</sub>. Prof et al. [7] developed a three-phase H<sub>2</sub>/O<sub>2</sub> fuel cell for the production of a concentrated aqueous solution of H<sub>2</sub>O<sub>2</sub> in an electrochemical reduction of O<sub>2</sub>.

Yang et al. [8] investigated the influence of H<sub>2</sub>O<sub>2</sub> concentration in the performance of magnesium-hydrogen peroxide fuel cell with palladium-silver deposited cathode and silver-nickel deposited electrode. Han et al. [9] developed a hydrogen peroxide fuel cell with TiO2 nanotube photoanode to increase the performance of the cell by make use of light and biomass. Also, Kjeang et al. [10] demonstrated a microfluidic fuel cell incorporating hydrogen peroxide as oxidant. Adams et al. [11] reported an electrochemical reduction of hydrogen peroxide using highly active palladium platinum catalysts. Bankar et al. [12] reviewed the production, characterization, and applications of glucose oxidase. Do et al. [13] developed a mathematical model which describes the bioelectrochemical reduction of hydrogen peroxide with direct electron transfer mechanism. Benfeitas et al. [14] investigated hydrogen peroxide metabolism in human erythrocytes. The first example of glucose or hydrogen peroxide-based biofuel cell functioning under physiological conditions was reported in Agnes et al. [15]. An et al. [16] developed and tested the performance of an alkaline direct ethanol fuel cell with hydrogen peroxide as oxidant. Also studied a onedimensional mathematical model of the mixed potential in hydrogen peroxide fuel cell [17].

Somasundaram et al. [18] developed a kinetic model for the reduction of hydrogen peroxide to water in a metal-dispersed conducting polymer film. This model is based on a system of the nonlinear reaction-diffusion equation. Somasundaram et al. [18] obtained the steady-state concentration and current for limiting cases (low and high substrate concentration) only. In solving reaction-diffusion problems, there are mainly three types of methods: experimental, analytical, and numerical. Experiments are expensive, time-consuming, and usually, do not allow much flexibility in parameter variation. Numerical methods are popular for its computing capabilities, although it provides only a long list of numbers, not an equation. Analytical methods are the most difficult ones, providing solutions with parameters. In this chapter, we will consider the last two techniques to solve the coupled nonlinear reaction-diffusion equation describing the reduction of hydrogen peroxide to water. The purpose of this chapter is to derive the analytical expressions for the concentration of glucose (substrate), hydrogen peroxide (product) and current for non-steady state condition.

## 4.2 Mathematical formulation

Fig.4.1 represents the schematic diagram for the reduction of hydrogen peroxide to water. The reactions scheme occurring within the polymer film and in the bulk solution can be written as follows [18]:

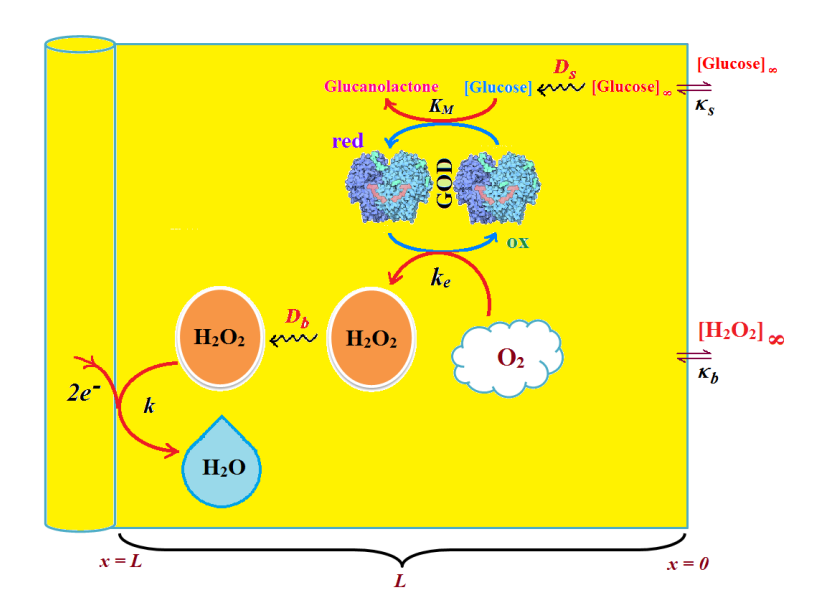


**Figure 4.1.** Schematic diagram for the reduction of hydrogen peroxide to water.

$$S + E_1 \underset{k=1}{\overset{k_1}{\leftrightarrow}} E_1 S \xrightarrow{k_{cat}} P + E_2 \tag{4.1}$$

$$E_2 + A \xrightarrow{k_e} E_1 + B \tag{4.2}$$

$$B + 2e^{-\frac{k}{2}}C \tag{4.3}$$

Eqn. (4.1) represents the oxidation of substrate (Glucose) S to product P (Hydrogen peroxide). Here  $E_1$  and  $E_2$  are the oxidized and reduced forms of the enzyme (oxidase) respectively. The reduction-oxidation process of the enzyme during the reduction of oxygen (A) to hydrogen peroxide (B) is shown in Eqn. (4.2). And the hydrogen peroxide which in turn reacts with microparticle in the presence of a pseudo first order rate constant k to produce water (C). Using Michaelis-Menten rate expression, the mass balance one dimensional equations for substrate and product within the polymer film can be written as follows [18]:

$$\frac{\partial s(x,t)}{\partial t} = D_S \frac{\partial^2 s(x,t)}{\partial x^2} - \frac{k_{cat} e_T s(x,t)}{K_M + s(x,t)} \tag{4.4}$$

$$\frac{\partial b(x,t)}{\partial t} = D_B \frac{\partial^2 b(x,t)}{\partial x^2} - kb(x,t) + \frac{k_{cat}e_T s(x,t)}{K_M + s(x,t)}$$
(4.5)

where s(x,t) and b(x,t) are the concentrations of substrate and product respectively.  $D_S$  and  $D_B$  are the diffusion coefficients,  $k_{cat}$  is the catalytic reaction rate constant and  $K_M = (k_{cat} + k_{-1})/k_1$  is the Michaelis-Menten rate constant. The initial and boundary conditions for the above equations are given by

$$t = 0.0 < x < L: s = k_s s_{\infty} b = 0 \tag{4.6}$$

$$t > 0, x = 0: \frac{\partial s}{\partial x} = 0, \frac{\partial b}{\partial x} = 0 \tag{4.7}$$

$$t > 0, x = L: s = \kappa_s s_{\infty} b = \kappa_h b_{\infty} \tag{4.8}$$

Here  $s_{\infty}$  and  $b_{\infty}$  is the concentration of substrate and product in the bulk solution.  $k_s$  and  $k_b$  is the reaction rate constant for substrate and product respectively. L is the thickness of the polymer film. The current I of the product b at the electrode surface is given by

$$I = -nFAjb = -nFADB \left(\frac{db}{dx}\right)_{x=L} \tag{4.9}$$

where  $j_b$  is the flux of the hydrogen peroxide at the electrode surface. Eqns. (4.4) and (4.5) can be written in dimensionless form using the following dimensionless parameters.

$$u = \frac{s}{\kappa_S s_\infty}, v = \frac{b}{\kappa_b b_\infty}, \chi = \frac{x}{L}, \tau = \frac{D_S t}{L^2}, \xi = \frac{D_B}{D_S},$$

$$\alpha = \frac{\kappa_S s_\infty}{\kappa_M}, \beta = \frac{\kappa_b b_\infty}{\kappa_M}, \gamma = \frac{kL^2}{D_S}, \phi = \frac{k_{cat} e_T L^2}{D_S \kappa_M}$$
(14.10)

Using Eqn. (4.10), equations (4.4) and (4.5) reduce to the following non-dimensional form:

$$\frac{\partial u(\chi,\tau)}{\partial \tau} = \frac{\partial^2 u(\chi,\tau)}{\partial \chi^2} - \frac{\phi u(\chi,\tau)}{1 + \alpha u(\chi,\tau)} \tag{4.11}$$

$$\frac{\partial v(\chi,\tau)}{\partial \tau} = \xi \frac{\partial^2 v(\chi,\tau)}{\partial \chi^2} - \gamma v(\chi,\tau) + \frac{\alpha \phi u(\chi,\tau)}{\beta (1 + \alpha u(\chi,\tau))}$$
(4.12)

where  $u(\chi, \tau)$  and  $v(\chi, \tau)$  represents the dimensionless concentration of substrate and product respectively;  $\chi$  is a normalized distance;  $\tau$  is a dimensionless time;  $\xi$  is the

ratio of the diffusion coefficient.  $\alpha$ ,  $\beta$  and  $\gamma$  are the saturation parameters.  $\varphi$  is the Thiele modulus depends upon the enzyme concentration, diffusion coefficient of substrate  $D_s$  and the Michaelis-Menten constant  $K_m$ ; The corresponding dimensionless initial and boundary conditions for equations (4.11) and (4.12) are as follows:

$$\tau = 0.0 < \chi < 1: u = 1, v = 0 \tag{4.13}$$

$$\tau > 0, \chi = 0: \frac{\partial u}{\partial x} = 0, \frac{\partial v}{\partial x} = 0 \tag{4.14}$$

$$\tau > 0, \chi = 1: u = 1, v = 1$$
 (4.15)

The dimensionless current for hydrogen peroxide is

$$\psi = -\frac{IL}{nFAk_b b_{\infty} D_B} = -\left(\frac{\partial v}{\partial \chi}\right)_{\chi=1} \tag{4.16}$$

## 4.3 Analytical expression for the concentration of substrate and product for general case under non-steady condition

Nonlinear phenomena play a vital role in various zones of the sciences and engineering. Because of the expanding enthusiasm towards finding exact solutions for those problems, a variety of analytical methods are proposed. Recently Adomian decomposition method [19], homotopy analysis method [20], variational iteration method [21], homotopy perturbation method [22,23], are used to solve the nonlinear problems. Among such methods, a new approach of homotopy perturbation method is applied to solve the nonlinear differential equations Eqns. (4.11) and (4.12). The focal point of this method is that it resulted in a simple approximate solution in the zeroth iteration itself [24]. This technique is appropriate for problems where transient effects, reaction-diffusion phenomena, and nonlinearity play an important role. The analytical expressions of concentrations of substrate and product can be obtained method as follows(Appendix-A):

$$u(\chi,\tau) = \frac{\cosh(\sqrt{A}\chi)}{\cosh(\sqrt{A})} + \frac{16A}{\pi} \sum_{n=0}^{\infty} \frac{(-1)^n \cos[(2n+1)\pi\chi/2]e^{-[(2n+1)^2\pi^2 + 4A]^{\frac{\tau}{4}}}}{(2n+1)[(2n+1)^2\pi^2 + 4A]}$$
(4.17)

$$v(\chi,\tau) = \frac{\cosh(\sqrt{\gamma/\xi}\chi)}{\cosh(\sqrt{\gamma/\xi})} + \frac{\alpha A}{\beta(\xi A - \gamma)} \left( \frac{\cosh(\sqrt{\gamma/\xi}\chi)}{\cosh(\sqrt{\gamma/\xi})} - \frac{\cosh(\sqrt{A}\chi)}{\cosh(\sqrt{A}\chi)} \right)$$

$$- \sum_{n=0}^{\infty} \mu_{An}(\tau)(-1)^n \cos[(2n+1)\pi\chi/2]$$
(4.18)

Using Eqns. (4.16) and (4.18), the dimensionless current is given by

$$\psi(\tau) = -\sqrt{\gamma/\xi} \tanh(\sqrt{\gamma/\xi}) - \frac{\alpha A[\sqrt{\gamma/\xi} \tanh(\sqrt{\gamma/\xi}) - \sqrt{A} \tanh(\sqrt{A})]}{\beta(\xi A - \gamma)} + \frac{\pi}{2} \sum_{n=0}^{\infty} \mu_{An}(\tau) (2n+1)$$

$$(4.19)$$

where 
$$A = \phi/(1+\alpha)$$
 (4.20)

$$\mu_{An}(\tau) = \frac{4\pi\xi(2n+1)e^{-[(2n+1)^2\pi^2\xi+4\gamma]\frac{\tau}{4}}}{[(2n+1)^2\pi^2\xi+4\gamma]} - \frac{64\alpha A^2e^{-[(2n+1)^2\pi^2+4A]\frac{\tau}{4}}}{\pi\xi\beta(2n+1)[(2n+1)^2\pi^2+4A][(2n+1)^2\pi^2(\xi-1)-4(A-\gamma)]} + \frac{64\pi\alpha A^2(2n+1)e^{-[(2n+1)^2\pi^2\xi+4\gamma]\frac{\tau}{4}}}{\beta[(2n+1)^2\pi^2\xi+4\gamma][(2n+1)^2\pi^2\xi-4(A-\gamma)][(2n+1)^2\pi^2(\xi-1)-4(A-\gamma)]}$$

when  $\tau \to \infty$ , the equation (4.19) becomes

$$\psi_{ss} = -\sqrt{\gamma/\xi} \tanh(\sqrt{\gamma/\xi}) - \frac{\alpha A[\sqrt{\gamma/\xi} \tanh(\sqrt{\gamma/\xi}) - \sqrt{A} \tanh(\sqrt{A})]}{\beta(\xi A - \gamma)}$$
(4.22)

The above equation (Eqn. (4.22)) represents the new analytical expression of steady state current.

## 4.3.1 Limiting case

The consequences for the limiting situations of zero order kinetics ( $S >> K_M$ ) and first order kinetics ( $S << K_M$ ) arising from Eqns. (4.4) and (4.5) or (4.11) and (4.12) are reported below.

## 4.3.1.1 Case 1: Saturated (zero-order) catalytic kinetics (High substrate)

In this case, the situation where the substrate concentration S is greater than the Michaelis-Menten constant  $K_M$  is considered. When  $S >> K_M$  or  $\alpha u >> 1$ , the nonlinear Eqns. (4.11) and (4.12) reduces to the following dimensionless linear form:

$$\frac{\partial u(\chi,\tau)}{\partial \tau} = \frac{\partial^2 u(\chi,\tau)}{\partial \chi^2} - \frac{\phi}{\alpha} \tag{4.23}$$

$$\frac{\partial v(\chi,\tau)}{\partial \tau} = \xi \frac{\partial^2 v(\chi,\tau)}{\partial \chi^2} - \gamma v(\chi,\tau) + \frac{\phi}{\beta}$$
(4.24)

Solving the above Eqns. (4.23) and (4.24), the concentration of substrate and product can be obtained as follows:

$$u(\chi,\tau) = 1 + \frac{\phi}{2\alpha}(\chi^2 - 1) + \frac{16\phi}{\pi^3\alpha} \sum_{n=0}^{\infty} \frac{(-1)^n \cos[(2n-1)\pi\chi/2]e^{-[(2n-1)^2\pi^2]_4^{\frac{\tau}{4}}}}{(2n-1)^3}$$
(4.25)

$$v(\chi,\tau) = \frac{\cosh(\sqrt{\gamma/\xi}\chi)}{\cosh(\sqrt{\gamma/\xi})} + \frac{\phi}{\beta\gamma} \left( 1 - \frac{\cosh(\sqrt{\gamma/\xi}\chi)}{\cosh(\sqrt{\gamma/\xi})} \right)$$

$$- \frac{4}{\pi} \sum_{n=0}^{\infty} \left\{ \frac{[\pi^2 (2n+1)^2 \xi - 4] e^{-[(2n+1)^2 \pi^2 \xi + 4\gamma]^{\frac{\tau}{4}}}}{(2n+1)[(2n+1)^2 \pi^2 \xi + 4\gamma]} \right\} (-1)^n \cos[(2n+1)\pi\chi/2]$$

$$+ 1)\pi\chi/2]$$

The expression for the current in this case is given as

$$\psi(\tau) = -\left(1 + \frac{\varphi}{\beta\gamma}\right)\sqrt{\gamma/\xi} \tanh(\sqrt{\gamma/\xi}) + 2\sum_{n=0}^{\infty} \frac{\left[(2n+1)^2 \pi^2 \xi - 4\right] e^{-\left[(2n+1)^2 \pi^2 \xi + 4\gamma\right] \frac{t}{4}}}{(2n+1)\left[(2n+1)^2 \pi^2 \xi + 4\gamma\right]}$$
(4.27)

From the above equation, the steady state  $(\tau \to \infty)$  current can be obtained as follows:

$$\psi_{ss} = -\left(1 + \frac{\phi}{\beta \nu}\right) \sqrt{\gamma/\xi} \tanh(\sqrt{\gamma/\xi}) \tag{4.28}$$

## 4.3.1.2. Case 2: Unsaturated (first-order) catalytic kinetics (Low substrate)

The situation where the substrate concentration S is less than the rate constant  $K_M$  is considered. In this case  $S \ll K_M$  or  $\alpha u \ll 1$ , the Eqns. (4.11) and (4.12) reduces to the following form:

$$\frac{\partial u(\chi,\tau)}{\partial \tau} = \frac{\partial^2 u(\chi,\tau)}{\partial \chi^2} - \phi u(\chi,\tau) \tag{4.29}$$

$$\frac{\partial v(\chi,\tau)}{\partial \tau} = \xi \frac{\partial^2 v(\chi,\tau)}{\partial \chi^2} - \gamma v(\chi,\tau) + \frac{\phi \alpha u(\chi,\tau)}{\beta}$$
(4.30)

The solutions for Eqns. (4.29) and (4.30) are obtained as below:

$$u(\chi,\tau) = \frac{\cosh(\sqrt{\phi}\chi)}{\cosh(\sqrt{\phi})} + \frac{16\phi}{\pi} \sum_{n=0}^{\infty} \frac{(-1)^n \cos[(2n+1)\pi\chi/2]e^{-[(2n+1)^2\pi^2 + 4\phi]\frac{\tau}{4}}}{(2n+1)[(2n+1)^2\pi^2 + 4\phi]}$$

$$v(\chi,\tau) = \frac{\cosh(\sqrt{\gamma/\xi}\chi)}{\cosh(\sqrt{\gamma/\xi})} + \frac{\alpha\phi}{\beta(\xi\phi - \gamma)} \left(\frac{\cosh(\sqrt{\gamma/\xi}\chi)}{\cosh(\sqrt{\gamma/\xi})} - \frac{\cosh(\sqrt{\phi}\chi)}{\cosh(\sqrt{\phi})}\right) - \sum_{n=0}^{\infty} \mu_{\phi n}(\tau)(-1)^n \cos[(2n+1)\pi\chi/2]$$
(4.31)

The current expression for this case is given as

$$\psi(\tau) = -\sqrt{\gamma/\xi} \tanh(\sqrt{\gamma/\xi}) - \frac{\alpha\phi[\sqrt{\gamma/\xi} \tanh(\sqrt{\gamma/\xi}) - \sqrt{\phi} \tanh(\sqrt{\phi})]}{\beta(\xi\phi - \gamma)} + \frac{\pi}{2} \sum_{n=0}^{\infty} \mu_{\phi n}(\tau)(2n+1)$$
(4.33)

where

$$\mu_{\phi n}(\tau) = \frac{4\pi\xi(2n+1)e^{-[(2n+1)^2\pi^2\xi+4\gamma]\frac{\tau}{4}}}{[(2n+1)^2\pi^2\xi+4\gamma]} - \frac{64\alpha\phi^2e^{-[(2n+1)^2\pi^2+4\phi]\frac{\tau}{4}}}{\pi\xi\beta(2n+1)[(2n+1)^2\pi^2+4\phi][(2n+1)^2\pi^2(\xi-1)-4(\phi-\gamma)]} + \frac{64\pi\alpha\phi^2(2n+1)e^{-[(2n+1)^2\pi^2\xi+4\gamma]\frac{\tau}{4}}}{\beta[(2n+1)^2\pi^2\xi+4\gamma][(2n+1)^2\pi^2\xi-4(\phi-\gamma)][(2n+1)^2\pi^2(\xi-1)-4(\phi-\gamma)]}$$

When  $\tau \to \infty$  the equation (4.33) becomes

$$\psi_{ss} = -\sqrt{\gamma/\xi} \tanh(\sqrt{\gamma/\xi}) - \frac{\alpha\phi[\sqrt{\gamma/\xi}\tanh(\sqrt{\gamma/\xi}) - \sqrt{\phi}\tanh(\sqrt{\phi})]}{\beta(\xi\phi - \gamma)}$$
(4.35)

The analytical expression of concentration of substrate, product and current for steady and non-steady state condition when  $\xi = 1$  for all the limiting cases are given in Table 4.1 and Table 4.2.

**Table 4.1.** Summary of analytical expression of concentration of substrate, product and current for non-steady state condition when  $\xi=1$ 

	This work					
Conditions						
		[18]				
	$u(\chi,\tau) = \frac{\cosh(\sqrt{A}\chi)}{\cosh(\sqrt{A})}$					
	$+\frac{16A}{\pi}\sum_{n=0}^{\infty}\frac{(-1)^n\cos[(2n+1)\pi\chi/2]e^{-[(2n+1)^2\pi^2+4A]\frac{\tau}{4}}}{(2n+1)[(2n+1)^2\pi^2+4A]}$					
Non steady state	$v(\chi,\tau) = \frac{\cosh(\sqrt{\gamma}\chi)}{\cosh(\sqrt{\gamma})} + \frac{\alpha A}{\beta(A-\gamma)} \left( \frac{\cosh(\sqrt{\gamma}\chi)}{\cosh(\sqrt{\gamma})} - \frac{\cosh(\sqrt{A}\chi)}{\cosh(\sqrt{A}\chi)} \right)$					
(HPM)	$-\sum_{n=0}^{\infty}\mu_{An}(\tau)(-1)^{n}\cos[(2n+1)\pi\chi/2]$					
	$\psi(\tau) = -\sqrt{\gamma} \tanh(\sqrt{\gamma}) - \frac{\alpha A[\sqrt{\gamma} \tanh(\sqrt{\gamma}) - \sqrt{A} \tanh(\sqrt{A})]}{\beta(A - \gamma)}$					
	$+\frac{\pi}{2}\sum_{n=0}^{\infty}\mu_{An}(\tau)(2n+1)$					
	$u(\chi,\tau) = \frac{\cosh(\sqrt{\phi}\chi)}{\cosh(\sqrt{\phi})}$					
	$+\frac{16\phi}{\pi}\sum_{n=0}^{\infty}\frac{(-1)^n\cos[(2n+1)\pi\chi/2]e^{-[(2n+1)^2\pi^2+4\phi]\frac{\tau}{4}}}{(2n+1)[(2n+1)^2\pi^2+4\phi]}$					
	$v(\chi,\tau)$					
High substrate	$= \frac{\cosh(\sqrt{\gamma}\chi)}{\cosh(\sqrt{\gamma})} + \frac{\phi}{\beta\gamma} \left( 1 - \frac{\cosh(\sqrt{\gamma}\chi)}{\cosh(\sqrt{\gamma})} \right)$					
	$-\frac{4}{\pi}\sum_{n=0}^{\infty}\frac{(-1)^{n}[\pi^{2}(2n+1)^{2}-4]\cos[(2n+1)\pi\chi/2]}{(2n+1)[(2n+1)^{2}\pi^{2}+4\gamma]}e^{-[(2n+1)^{2}\pi^{2}+4\gamma]\frac{\tau}{4}}$					
	$\psi(\tau) = -\left(1 + \frac{\alpha}{\beta\gamma}\right)\sqrt{\gamma}\tanh(\sqrt{\gamma})$					
	$+2\sum_{n=0}^{\infty} \frac{[\pi^2(2n+1)^2-4]e^{-[(2n+1)^2\pi^2+4\gamma]_{\frac{\pi}{4}}^{\frac{\tau}{4}}}}{[(2n+1)^2\pi^2+4\gamma]}$					

$$u(\chi,\tau) = \frac{\cosh(\sqrt{\phi}\chi)}{\cosh(\sqrt{\phi})}$$

$$+ \frac{16\phi}{\pi} \sum_{n=0}^{\infty} \frac{(-1)^n \cos[(2n+1)\pi\chi/2]e^{-[(2n+1)^2\pi^2 + 4\phi]\frac{\tau}{4}}}{(2n+1)[(2n+1)^2\pi^2 + 4\phi]}$$

$$v(\chi,\tau) = \frac{\cosh(\sqrt{\gamma}\chi)}{\cosh(\sqrt{\gamma})} + \frac{\alpha\phi}{\beta(\phi-\gamma)} \left(\frac{\cosh(\sqrt{\gamma}\chi)}{\cosh(\sqrt{\gamma})} - \frac{\cosh(\sqrt{\phi}\chi)}{\cosh(\sqrt{\phi})}\right)$$
substrate
$$-\sum_{n=0}^{\infty} \mu_{\phi n}(\tau)(-1)^n \cos[(2n+1)\pi\chi/2]$$

$$\psi(\tau) = -\sqrt{\gamma} \tanh(\sqrt{\gamma}) - \frac{\alpha\phi[\sqrt{\gamma} \tanh(\sqrt{\gamma}) - \sqrt{\phi} \tanh(\sqrt{\phi})]}{\beta(\phi-\gamma)}$$

$$+ \frac{\pi}{2} \sum_{n=0}^{\infty} \mu_{\phi n}(\tau)(2n+1)$$

**Table 4.2.**Summary of analytical expression of concentration of substrate, product and current for steady state condition when  $\xi = 1$ .

Conditions	This work	Previous work [18]
	_	
	$u(\chi) = \frac{\cosh(\sqrt{A}\chi)}{\cosh(\sqrt{A})}$	
	14.5	
	$v(\chi) = \frac{\cosh(\sqrt{\gamma}\chi)}{\cosh(\sqrt{\gamma})}$	
Steady	$+\frac{\alpha A}{\beta(A-\gamma)}\left(\frac{\cosh(\sqrt{\gamma}\chi)}{\cosh(\sqrt{\gamma})}\right)$	
state (HPM)	$-rac{cosh(\sqrt{A}\chi)}{cosh(\sqrt{A})}$	
	$ \psi_{ss} $	
	$=-\sqrt{\gamma}\tanh(\sqrt{\gamma})$	
	$-\frac{\alpha A[\sqrt{\gamma} \tanh(\sqrt{\gamma}) - \sqrt{A} \tanh(\sqrt{A})]}{\beta(A-\gamma)}$	

	$u(\chi) = 1 + \frac{\phi}{2\alpha}(\chi^2 - 1)$	
	1( /=->	
	$v(\chi) = \frac{\cosh(\sqrt{\gamma}\chi)}{\cosh(\sqrt{\gamma})}$	
	$cosh(\sqrt{\gamma})$	
High	φ (.	
substrate	$+\frac{\phi}{\beta \gamma} \bigg( 1$	
Substrate	, , ,	
	$-rac{cosh(\sqrt{\gamma}\chi)}{cosh(\sqrt{\gamma})}$	
	$cosh(\sqrt{\gamma})$	
	$\psi_{ss} = -\left(1 + \frac{\alpha}{\beta \gamma}\right) \sqrt{\gamma} \tanh(\sqrt{\gamma})$	
	$(\beta \gamma) (\gamma \gamma \beta \gamma \beta \gamma \gamma \gamma \beta \gamma $	
	$cosh(\sqrt{\phi}\chi)$	$u(\chi) = \frac{\cosh(\sqrt{\phi}\chi)}{\cosh(\sqrt{\phi})}v(\chi)$
	$u(\chi) = \frac{\cosh(\sqrt{\phi}\chi)}{\cosh(\sqrt{\phi})}$	$u(\chi) = \frac{u(\chi)}{\cosh(\sqrt{\phi})} v(\chi)$
	( ) ,	$cosh(\sqrt{y}y)$
	$v(\chi)$	$=\frac{\cosh(\sqrt{\gamma}\chi)}{\cosh(\sqrt{\gamma})}$
	_	
	$=\frac{\cosh(\sqrt{\gamma}\chi)}{\cosh(\sqrt{\chi})}$	$+\frac{\alpha\phi}{\beta(\phi-\gamma)}\left(\frac{\cosh(\sqrt{\gamma}\chi)}{\cosh(\sqrt{\gamma}\chi)}\right)$
	( ) ( )	$\beta(\phi-\gamma)\setminus cosh(\sqrt{\gamma})$
	$+\frac{\alpha\phi}{\beta(\phi-\gamma)}\left(\frac{\cosh(\sqrt{\gamma}\chi)}{\cosh(\sqrt{\gamma}\chi)}\right)$	$cosh(\sqrt{\phi}\chi)$
	$\beta(\phi-\gamma) \setminus cosh(\sqrt{\gamma})$	$-\frac{\cosh(\sqrt{\phi}\chi)}{\cosh(\sqrt{\phi})}$
Low	$cosh(\sqrt{\phi}\gamma)$	σουπ( γ φ ) ,
substrate	$\left(-\frac{\cosh(\sqrt{\phi\chi})}{\cosh(\sqrt{\phi})}\right)$	$\psi_{ss}$
substrate	$(\sqrt{\psi})$	$= -\sqrt{\gamma} \tanh(\sqrt{\gamma})$
	$\psi_{ss}$	, , , , , , , , , , , , , , , , , , ,
		$-\frac{\alpha\phi[\sqrt{\gamma}\tanh(\sqrt{\gamma})-\sqrt{\phi}\tanh(\sqrt{\phi})]}{\beta(\phi-\gamma)}$
	$=-\sqrt{\gamma}\tanh(\sqrt{\gamma})$	$\beta(\phi-\gamma)$
	$-\frac{\alpha\phi[\sqrt{\gamma}\tanh(\sqrt{\gamma})-\sqrt{\phi}\tanh(\sqrt{\phi})]}{\beta(\phi-\gamma)}$	
	$\beta(\phi-\gamma)$	

## 4.4. Numerical simulation

To examine the accuracy of the solution obtained using the HPM method with a finite number of terms, the system of differential equations were solved numerically. Analytical solution of the equations (4.11) and (4.12) is a challenging problem which can be accomplished numerically with the help of Matlab software. The function pdex4 (Euler's method) in Matlab software [25], which is a function of solving the boundary value problems is used to solve Eqns. (4.11) and (4.12) numerically. Our results are compared with numerical results graphically in Fig. 4.2 and 4.3. The comparison confirmed that our obtained analytical results fitted very well with the numerical results. The maximum average relative error between the analytical and numerical result for substrate and product is 1.40% and 0.80% respectively (Refer Table 4.3 and 4.4).

**Table 4.3.** Comparison of our analytical result of dimensionless substrate  $u(\chi, \tau)$  with the numerical simulation for various value of  $\tau$  and  $\chi$  using Eqn. (4.17) when  $\phi = 1$  and  $\alpha = 0.5$ 

χ	$\tau = 0.1$			$\tau = 0.5$			$\tau = 1$			au = 100		
	Analytical Eqn. (4.17)	Numerical	% of deviation	Analytical Eqn. (4.17)	Numerical	% of deviation	Analytical Eqn. (4.17)	Numerical	% of deviation	Analytical Eqn. (4.17)	Numerical	% of deviation
0	0.9365	0.9358	0.07	0.7961	0.7885	0.96	0.7513	0.7373	1.89	0.7394	0.7221	2.39
0.2	0.9372	0.9366	0.06	0.8032	0.7959	0.91	0.7606	0.7472	1.79	0.7493	0.7327	2.26
0.4	0.9401	0.9397	0.04	0.8251	0.8187	0.78	0.7888	0.7773	1.47	0.7792	0.7650	1.85
0.6	0.9478	0.9475	0.03	0.8633	0.8585	0.55	0.8369	0.8284	1.02	0.8300	0.8194	1.29
0.8	0.9653	0.9652	0.01	0.9204	0.9178	0.28	0.9066	0.902	0.50	0.9029	0.8973	0.62
1	1.0001	1	0.01	1	1	0	1	1	0	1	1	0
	Average % of deviation 0.04		Average % of deviation 0.58		Average % of deviation 1.11			Average %	1.40			

**Table 4.4.** Comparison of our analytical result of dimensionless product  $v(\chi, \tau)$  with the numerical simulation for various values of  $\tau$  and  $\chi$  using Eqn. (4.18) when  $\phi = 0.1$ ,  $\alpha = 0.5$ ,  $\beta = 0.05$ ,  $\gamma = 0.01$  and  $\xi = 1$ 

χ	$\tau = 0.7$			au=1			$\tau = 2$			au = 10		
	Analytical Eqn. (4.18)	Numerical	% of deviation	Analytical Eqn. (4.18)	Numerical	% of deviation	Analytical Eqn. (4.18)	Numerical	% of deviation	Analytical Eqn. (4.18)	Numerical	% of deviation
0	1.0237	1.037	1.28	1.1783	1.185	0.56	1.3063	1.309	0.20	1.3179	1.321	0.23
0.2	1.0251	1.038	1.24	1.1725	1.179	0.55	1.2943	1.297	0.20	1.3053	1.308	0.20
0.4	1.0289	1.04	1.06	1.1543	1.160	0.49	1.2579	1.260	0.16	1.2673	1.270	0.21
0.6	1.0307	1.039	0.79	1.1218	1.126	0.37	1.1971	1.199	0.15	1.2039	1.206	0.17
0.8	1.0237	1.028	0.41	1.0717	1.074	0.21	1.1113	1.112	0.06	1.1149	1.116	0.09
1	0.9997	1	0.03	0.9998	1	0.02	0.9999	1	0.01	1	1	0
	Average % of deviation		0.80	Average % o	of deviation	0.36	Average %	of deviation	0.13	Average %	of deviation	0.15

## 4.5 Results and Discussion

Eqns. (4.17) to (4.19) represents the new analytical expressions for the dimensionless concentration of substrate, product and current respectively. Fig. 4.2 represent the dimensionless concentration of substrate  $u(\chi,\tau)$  versus dimensionless distance from the electrode  $\chi$  for different values of Thiele modulus  $\phi$ , saturation parameter  $\alpha$  and time  $\tau$ . Thiele modulus is the ratio of the reaction rate to the rate of diffusion. From Fig. 4.2(a), it is inferred that the concentration of substrate decreases when Thiele modulus  $\phi$  increases. When Thiele modulus  $\phi < 0.1$ , the diffusion resistance is insufficient to limit the rate of reaction and the concentration remains the same within the film. The concentration of substrate reaches zero inside the enzyme layer when the diffusion modulus i.e. Thiele module  $\phi \ge 100$  which is observed at high film thickness L or enzymatic rate  $k_{cat}e_T$  or for low reaction rate constant  $K_M$  or diffusion  $D_s$ . This is because when  $\varphi$  is large, a significant diffusion modulus prevents a constant concentration of substrate within the film and thus lowers the concentration. The influence of the saturation parameter  $\alpha$  can be analyzed from Fig. 4.2(b). It shows that, the concentration of substrate increases when the saturation parameter  $\alpha$  increases. This is because as the initial substrate concentration  $s_{\infty}$  increases obviously the concentration of substrate S increases. From Fig.4. 2(c), it is evident that the substrate concentration increases when time  $\tau$  decreases. For  $\tau \leq 0.01$ , the concentration remains the same.

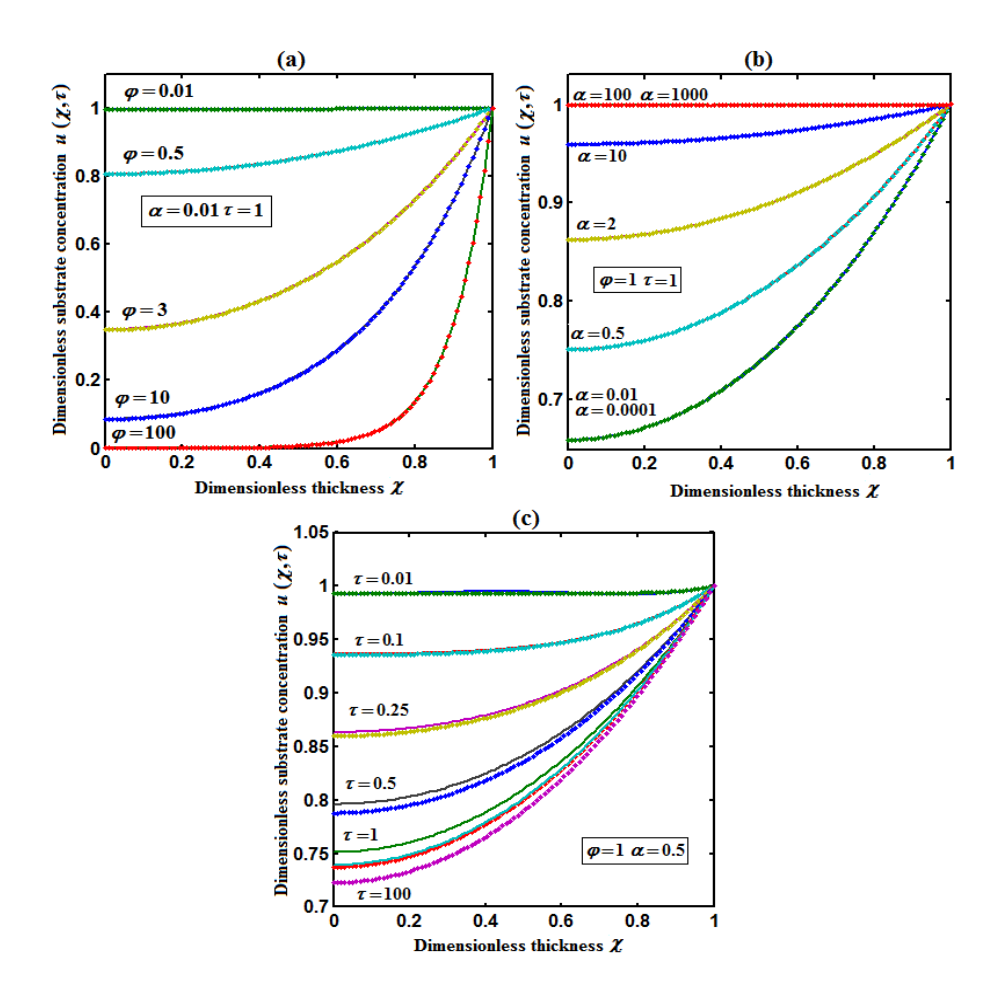
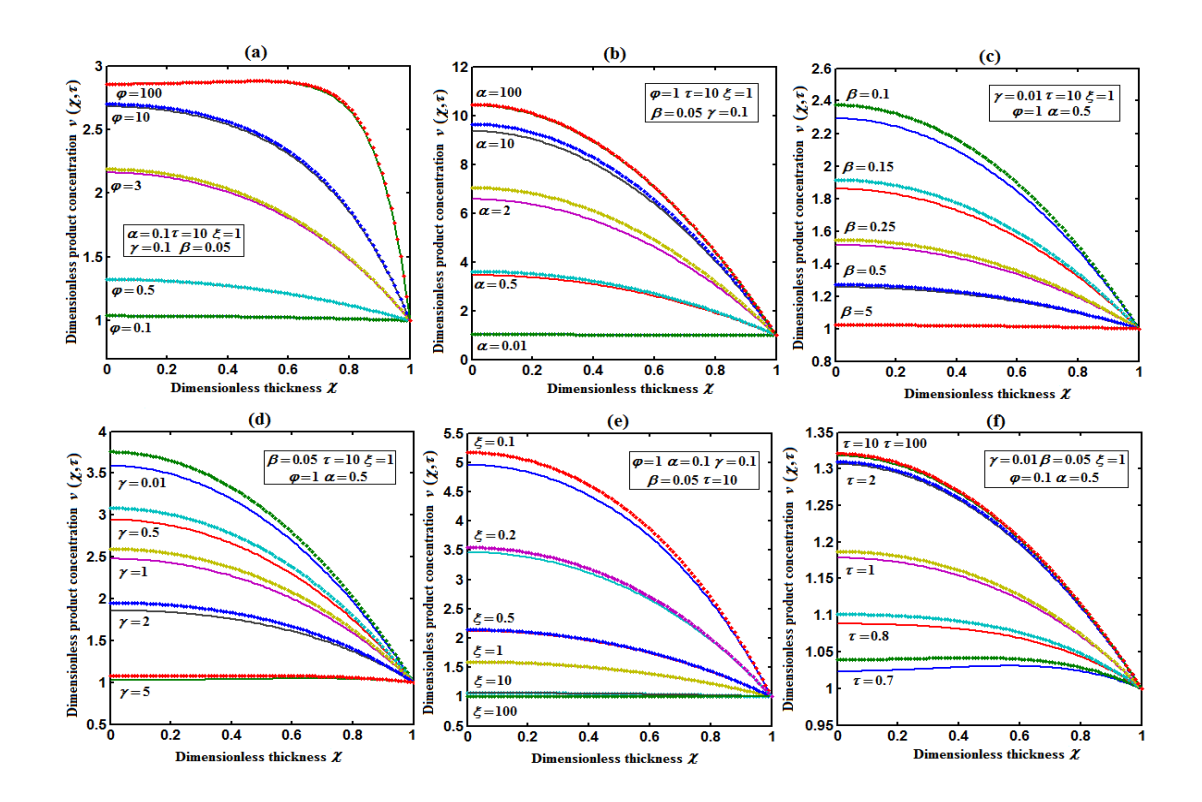


Figure 4.2. Plot of dimensionless concentration of substrate  $u(\chi, \tau)$  versus dimensionless thickness  $\chi$  calculated using Eqn. (4.17) for different values of (a) Thiele modulus  $\varphi$ , (b) saturation parameter  $\alpha$  and (c) time  $\tau$ . The key to the graph: (scatted line) represents the Eq. (4.17) and (dotted line) represents the numerical simulation.

The change in product concentration with respect to dimensionless distance from the electrode for various values of parameter is shown in Fig. 4.3(a) – (f) respectively. Fig. 4.3(a) illustrates that for high catalytic activity, the concentration of substrate increases. By increasing the initial concentration of substrate  $\alpha$  or high catalytic activity, the product concentration increases, shown in Fig. 4.3(a) and 4.3(b). From Fig. 4.3(c) and 4.3(d), it is observed that, the concentration of product increases when the saturation parameters  $\beta$  and  $\gamma$  decreases. Compared to other parameters, time  $\tau$  has less influence over product concentration. Higher product concentration is obtained for steady- state time.



**Figure 4.3.** Plot of dimensionless concentration of product  $v(\chi, \tau)$  versus dimensionless thickness  $\chi$  calculated using Eqn. (4.18) for different values of (a) Thiele modulus  $\phi$ , saturation parameters (b)  $\alpha$  (c)  $\beta$ (d)  $\gamma$ , (e) diffusion parameter  $\xi$  and (f) time  $\tau$ . The key to the graph: (scatted line) represents the Eq. (4.18) and (dotted line) represents the numerical simulation.

## 4.6 Differential sensitive analysis of kinetic parameters

Eqn. (4.19) represents the new approximate analytical expression for the nonsteady state current  $\psi$  in terms of the parameters  $\alpha$ ,  $\beta$ ,  $\gamma$ ,  $\psi$  and  $\xi$ . By differentiating the current partially with respect to these parameters, the impact of the parameters over current can be determined [26]. The percentage of change in current with respect to  $\gamma$ ,  $\beta$ ,  $\psi$ ,  $\xi$  and  $\alpha$  are 46 %, 35 %, 14%, 3% and 2 % respectively. From this, it is evident that parameter  $\gamma$  and  $\beta$  has more impact on current. These parameters are highly sensitive parameters. This implies that when the thickness of the film L or the concentration of product in the bulk  $b_{\infty}$  increases, the current increases. The parameter  $\psi$  is called as moderately sensitive parameter as it has 14% of influence over current. The remaining two parameters  $\xi$  (ratio of diffusion coefficient) and  $\alpha$  (saturation parameter) are less sensitive. The spread sheet analysis of these results is described in Figure. 4.4. These results are also confirmed in the Figures. 4.5, 4.6(a) - 6(e).

From Fig. 4.5, it is observed that the current initially increases with thickness and then decreases. After  $L \geq 2$ mm, the current reaches the steady state value. An interesting as well as effective information can be predicted from Fig. 4.6(a) – 4.6(e) regarding the influence of the kinetic parameters over current  $\psi(\tau)$  along time  $\tau$ . The current considerably depends on the fact either the enzymatic rate within the film or the electron transport outside the film. From Fig.4. 6(a), it is confirmed that the current increases when the Thiele module  $\psi$ increases. With increased initial concentration of substrate in bulk solution  $S_{\infty}$ , the corresponding current increases. This result is confirmed in Fig. 4.6(b). The influence of the saturation parameters  $\beta$  and  $\gamma$  on the current was shown in Fig. 4.6(c) and 4.6(d). Both parameters are inversely proportional to the current. Compared to  $\gamma$ ,  $\beta$  shows much deviation over current. From Fig. 4.6(e), it was found that the sharp decrease in the current with increasing ratio of diffusion coefficient  $\xi$ . And when  $\xi$  is small, the current decreases slowly. From this figure, it is observed that for high current, the diffusion coefficient of product should be less than the diffusion coefficient of substrate i. e.  $D_S < D_P$ .

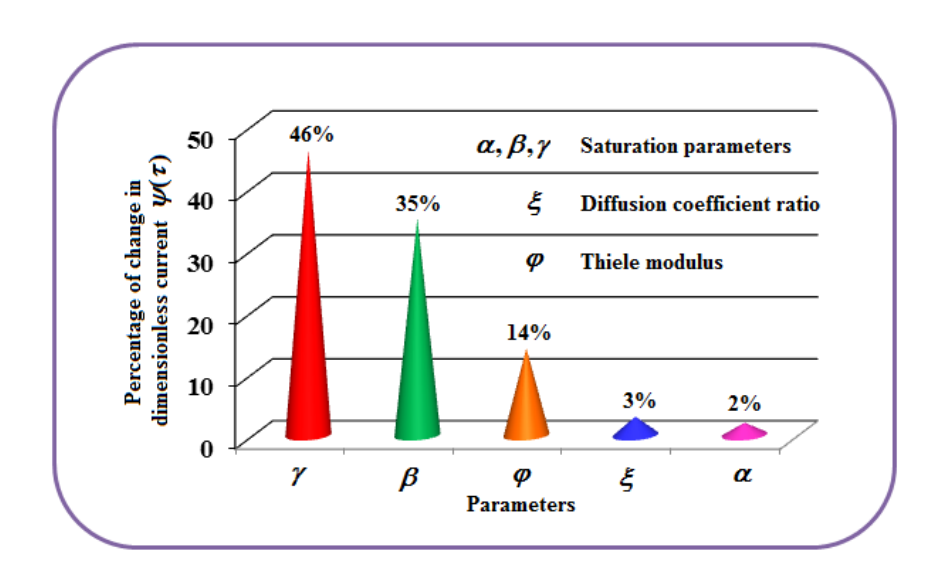
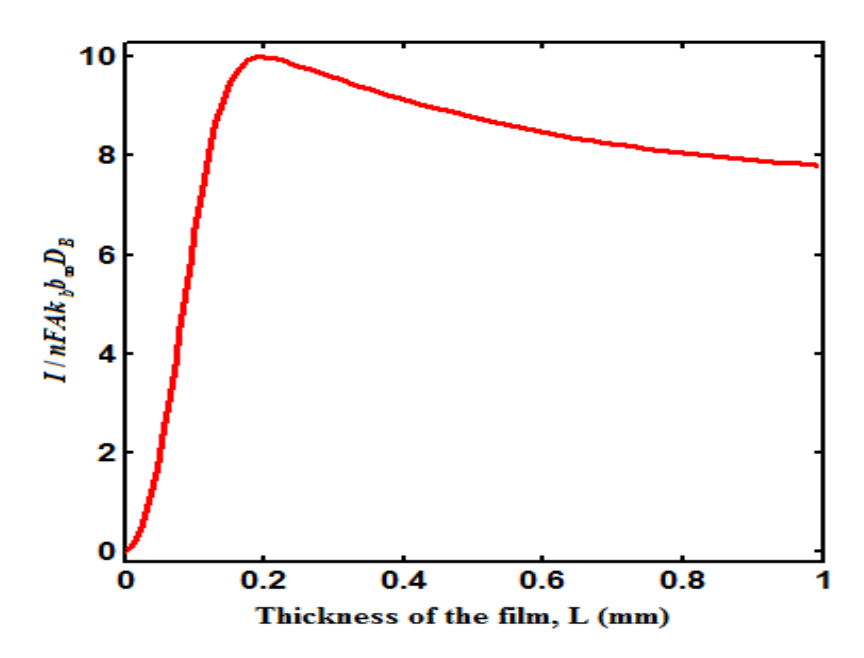


Figure 4.4. Sensitive analysis of parameters: Percentage change in current.



**Figure 4.5.** Plot of steady state current versus thickness of the film *L*.

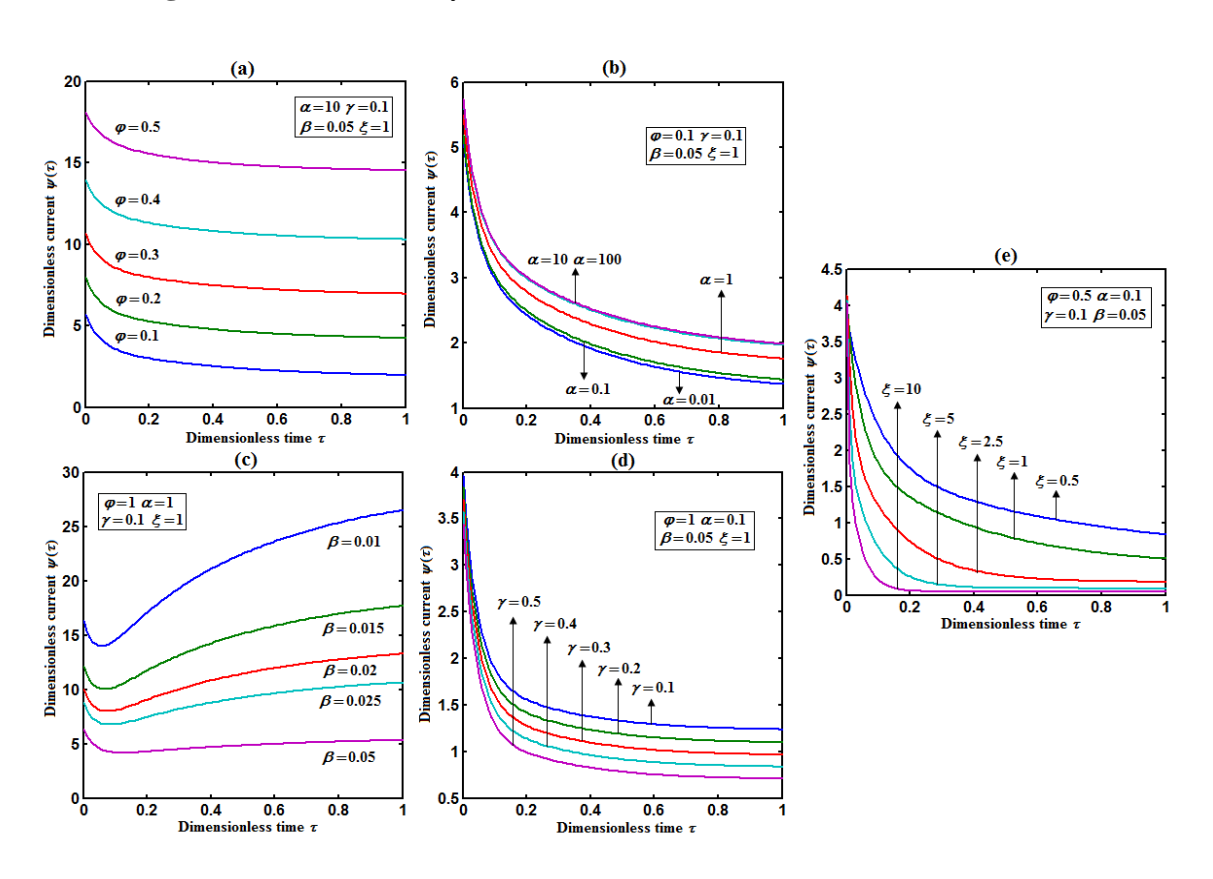


Figure 4.6. Plot of dimensionless current  $\psi(\tau)$  versus dimensionless time τ calculated using Eqn. (4.19) for different values of (a) Thiele modulus  $\psi$ , saturation parameters (b)α (c)β (d)γ and (e) diffusion parameter  $\xi$ .

## **4.7 Estimation of kinetic parameters** k, $k_{cat}e_T$ and $K_M$

Numerous enzyme kinetics papers are dedicated for estimating the kinetics parameters and distinguishing between reaction mechanisms [27-29]. Pseudo first order constant k, helps us to quantify the rate of the chemical reaction. The Michaelis-Menten rate constant  $K_M$ , determines the relationship between the steady-state concentrations rather the equilibrium concentrations. The maximum velocity of the enzyme depends upon the catalytic rate constant  $k_{cat}$  and the total enzyme concentration  $e_T$ . The parameter  $k_{cat}$  is a very useful parameter which employs for the breakdown of the enzyme substrate complex ES to product P when the enzyme is fully saturated with substrate. These kinetic parameters can be obtained from our analytical expression of current (Eqn. (4.28)). For small value of  $\gamma/\xi$ ,  $tanh(\sqrt{\gamma/\xi}) \approx \sqrt{\gamma/\xi}$ . Now Eqn. (4.28) reduces to following form:

$$\psi_{ss} = -\left(1 + \frac{\phi}{\beta \nu}\right) \frac{\gamma}{\xi} \tag{4.36}$$

Using Eqn. (4.10), the above equation can be rearranged as

$$\frac{I}{nFA\kappa_{h}b_{\infty}L} = k_{cat}e_{T}\left(\frac{1}{\kappa_{h}b_{\infty}}\right) + k \tag{4.37}$$

As in Fig.4. 7(a), plot of  $I/nFA\kappa_b b_\infty L$  versus  $1/\kappa_b b_\infty$  gives the slope =k, intercept  $=k_{cat}e_T$ . When the diffusion coefficient of substrate and product are equal i.e. $\xi=1$ , and  $\gamma$  is small, the current (Eqn.4. 22) becomes

$$\psi_{ss} = -\gamma - \frac{\alpha}{\beta} \left( \frac{\phi}{1+\alpha} \right) \tag{4.38}$$

By substituting the value of  $\psi_{ss}$ ,  $\gamma$ ,  $\alpha$ ,  $\beta$  and  $\psi$  from the Eqn. (4.10) and k,  $k_{cat}e_T$  from Eqn. (4.37), the parameter  $K_M$  can be obtained. Hence we can obtain pseudo first order rate constant k, enzymatic rate  $k_{cat}e_T$  and Michaelis-Menten rate constant  $K_M$  from Eqns. (4.22) and (4.28).

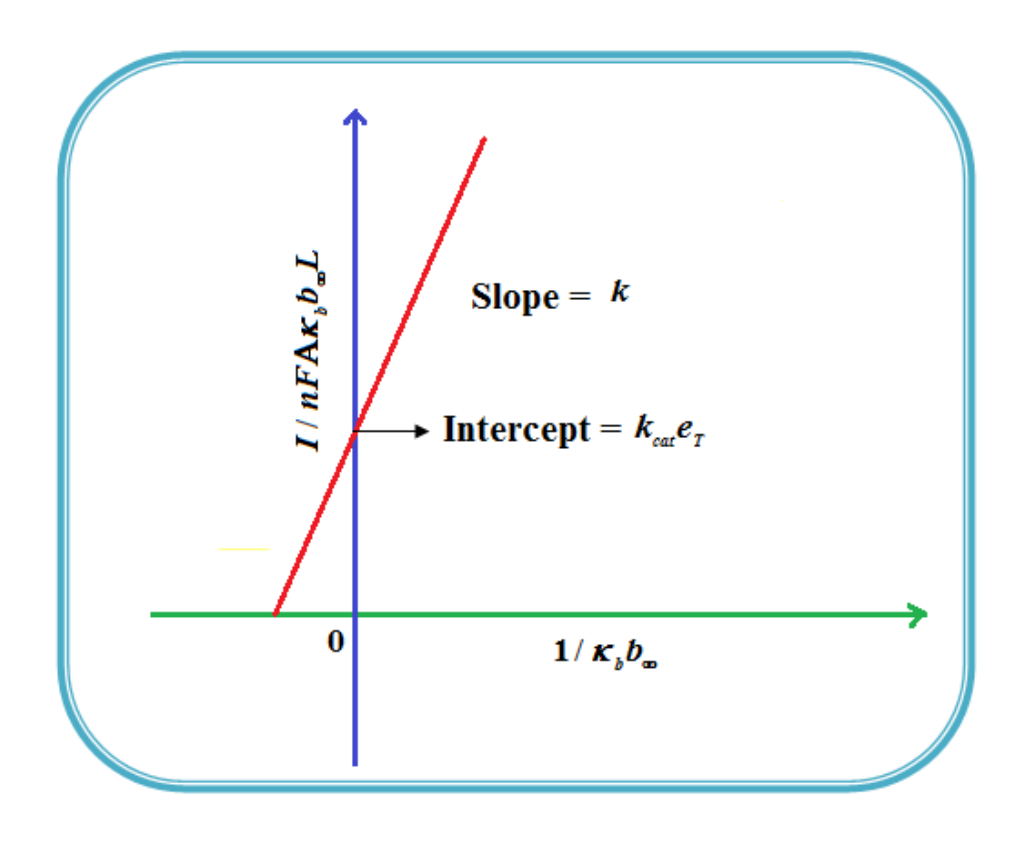


**Figure 4.7.** Estimation of kinetic parameter: pseudo first order rate constant k and enzymatic rate  $k_{cat}e_T$  using Eqn. (4.37).

## 4.8 Conclusions

A simple mathematical analysis of reaction and diffusion of glucose and hydrogen peroxide within the conducting film containing metal microparticles have been presented. Using a new approach to the Homotopy perturbation method, an approximate analytical expression for the concentration of substrate and product are obtained. Approximate analytical expressions for the steady and non-steady state current response produced during the reduction of  $H_2O_2$  to water at the electrode surface are derived. The differential sensitive analysis for the steady-state current response for the controllable parameters: the thickness of the film, bulk substrate, and product concentration and enzymatic rate are analyzed. Also, the estimation of kinetic parameters is reported graphically.

## Appendix 4.A: Approximate analytical solution of the nonlinear Eqn. 4.9 using anew approach to the Homotopy perturbation method.

In this Appendix, we have indicated how to determine the solution of Eqn. (4.9) using the boundary condition Eqns. (4.10) and (4.12). To solve Eqn. (4.9), the homotopy can be constructed

as follows:

$$(1-p)\left[\frac{\partial^{2}u(\chi,\tau)}{\partial\chi^{2}} - \frac{\phi u(\chi,\tau)}{1+\alpha u(\chi=1,\tau)} - \frac{\partial u(\chi,\tau)}{\partial\tau}\right] + p\left[\frac{\partial^{2}u(\chi,\tau)}{\partial\chi^{2}} - \frac{\phi u(\chi,\tau)}{1+\alpha u(\chi,\tau)} - \frac{\partial u(\chi,\tau)}{\partial\tau}\right] = 0$$

$$(4.A1)$$

or

$$(1-p)\left[\frac{\partial^{2}u(\chi,\tau)}{\partial\chi^{2}} - \frac{\phi u(\chi,\tau)}{1+\alpha} - \frac{\partial u(\chi,\tau)}{\partial\tau}\right] + p\left[\frac{\partial^{2}u(\chi,\tau)}{\partial\chi^{2}} - \frac{\phi u(\chi,\tau)}{1+\alpha u(\chi,\tau)} - \frac{\partial u(\chi,\tau)}{\partial\tau}\right] = 0$$

$$(4.A2)$$

The approximate solution of Eqn. (4.11) is

$$u = u_0 + pu_1 + p^2 u_2 + \dots (4.A3)$$

Substituting equation (4.A3) into equation (4.A2) and arranging the coefficients of powers p,

we get

$$p^{0}: \frac{d^{2}u_{0}(\chi,\tau)}{d\chi^{2}} - \frac{\varphi u_{0}(\chi,\tau)}{1+a} - \frac{\partial u_{0}(\chi,\tau)}{\partial \tau} = 0$$

$$(4.A4)$$

The initial and boundary conditions for the above Eqn. (4.A4) becomes

At 
$$\tau = 0, u_0 = 1$$
 (4.A6)

$$\chi = 0, \frac{\partial u_0}{\partial x} = 0 \tag{4.A7}$$

$$\chi = 1, u_0 = 1 \tag{4.A8}$$

The partial differential equation (4.A4) and the corresponding boundary conditions Eqn. (4.A6) - (4.A8) in the Laplace plane becomes as follows

$$\frac{d^2\bar{u}_0(\chi)}{d\chi^2} - \frac{\varphi\bar{u}_0(\chi)}{1+a} - s\bar{u}_0(\chi) + 1 = 0 \tag{4.A9}$$

The corresponding boundary conditions are

$$\chi = 0, \frac{\partial \bar{u}_0}{\partial \chi} = 0 \tag{4.A10}$$

$$\chi = 1, \bar{u}_0 = 1/s$$
 (4.A11)

where sis the Laplace variable and an over bar indicates a Laplace-transformed quantity.

Solving the Eq. (4.A9), and using the boundary conditions and (4.A10) and (4.A11) we can find the following results

$$\bar{u}_0(\chi) = \left[\frac{1}{s} - \frac{1}{A+s}\right] \frac{\cosh(\sqrt{A+s}\chi)}{\cosh(\sqrt{A+s})} + \frac{1}{A+s} \tag{4.A12}$$

Now, we indicate how Eqn. (4.A12) can be inverted using the complex inversion formula. If  $\overline{y}(s)$  represents the Laplace transform of a function  $y(\tau)$ , then according to the complex inversion formula we can state that

$$y(\tau) = \frac{1}{2\pi \int_{c-i\infty}^{c+i\infty} exp[s\tau]\overline{y}(s)ds} = \frac{1}{2\pi i} \oint_{c} exp[s\tau]\overline{y}(s)ds$$
 (4.A13)

where the integration in Eqn. (4.A13) is to be performed along a line s = c in the complexplane where s = x + iy. The real number c is chosen such that s = c lies to the right of all the singularities, but is otherwise assumed to be arbitrary. In practice, the integral is evaluated by considering the contour integral presented on the right-hand side of Eqn. (4.A13), which is then evaluated using the so-called Bromwich contour. The contour integral is then evaluated using the residue theorem which states for any analytic function F(z).

$$\oint_{\mathcal{C}} F(z)dz = 2\pi i \sum_{n} Re \, s \, [F(z)]_{z=z_0} \tag{4.A14}$$

where the residues are computed at the poles of the function F(z). Hence from Eqn. (4.A14),

we note that

$$y(\tau) = \sum_{n} \operatorname{Re} s \left[ \exp[s\tau] \overline{y}(s) \right]_{s=s_0}$$
(4.A15)

From the theory of complex variables we can show that the residue of a function F(z) at a simple pole at z = a is given by

$$Re\ s\ [F(z)]_{z=a} = \lim_{z \to a} \{(z-a)F(z)\}$$
 (4.A16)

Hence, in order to invert Eqn. (4.A12), we need to evaluate

$$Re \ s \left[ \frac{\cosh(\sqrt{A+s}\chi)}{s \cosh(\sqrt{A+s})} \right] - Re \ s \left[ \frac{\cosh(\sqrt{A+s}\chi)}{(A+s) \cosh(\sqrt{A+s})} \right]$$
(4.A17)

The poles are obtained from  $s \cosh(\sqrt{A+s}) = 0$  and  $(A+s) \cosh(\sqrt{A+s}) = 0$ . Hence there is a simple pole at s=0, s=-A and there are infinitely many poles given by the solution of the equation  $\cosh(\sqrt{A+s}) = 0$  and so  $s_n = \frac{-\pi^2(2n+1)^2}{4} - A$  where n=0,1,2, .Hence we note that

$$Re \ s \left[ \frac{\cosh(\sqrt{A+s}\chi)}{s \cosh(\sqrt{A+s}\chi)} \right] = Re \ s \left[ \frac{\cosh(\sqrt{A+s}\chi)}{s \cosh(\sqrt{A+s}\chi)} \right]_{s=0} + Re \ s \left[ \frac{\cosh(\sqrt{A+s}\chi)}{s \cosh(\sqrt{A+s}\chi)} \right]_{s=s_n} - Re \ s \left[ \frac{\cosh(\sqrt{A+s}\chi)}{(A+s) \cosh(\sqrt{A+s}\chi)} \right]_{s=s_n}$$

$$(4.A18)$$

The residue at s = 0in Eq. (4.A18) is given by

$$Re \ s \left[ \frac{\cosh(\sqrt{A+s}\chi)}{s \cosh(\sqrt{A+s})} \right]_{s=0} = \lim_{s \to 0} \left[ \frac{(s-0)e^{st} \cosh(\sqrt{A+s}\chi)}{s \cosh(\sqrt{A+s})} \right] = \frac{\cosh(\sqrt{A}\chi)}{\cosh(\sqrt{A})}$$

$$(4.A19)$$

The residue at  $s = s_n$  in Eq. (4.A18) becomes

$$Re\ s\left[\frac{cosh(\sqrt{A+s}\chi)}{s\ cosh(\sqrt{A+s})}\right]_{s=s_n} = \lim_{s\to s_n} \left[\frac{e^{st}\ cosh(\sqrt{A+s}\chi)}{s\ cosh(\sqrt{A+s})}\right] = \lim_{s\to s_n} \left[\frac{e^{st}\ cosh(\sqrt{A+s}\chi)}{s\frac{d}{ds}\ cosh(\sqrt{A+s}\chi)}\right]$$

$$= -4\pi \sum_{n=0}^{\infty} \frac{(-1)^n (2n+1) \cos[(2n+1)\pi \chi/2] e^{-[(2n+1)^2 \pi^2 + 4A] \frac{t}{4}}}{(2n+1)^2 \pi^2 + 4A}$$
(4.A20)

The residue at s = -Ain Eq. (4.A18) is given by

$$Re \ s \left[ \frac{\cosh(\sqrt{A+s}\chi)}{s \cosh(\sqrt{A+s})} \right]_{s=-4} = \lim_{s \to -A} \left[ \frac{(s+A)e^{-At} \cosh(\sqrt{A+s}\chi)}{(s+A) \cosh(\sqrt{A+s})} \right] = e^{-At}$$
 (4.A21)

The fourth residue at  $s = s_n$  in Eq. (4.A18) becomes

$$Re \ S \left[ \frac{\cosh(\sqrt{A+s}\chi)}{(A+s)\cosh(\sqrt{A+s})} \right]_{S=S_n} = \lim_{S \to S_n} \left[ \frac{e^{st} \cosh(\sqrt{A+s}\chi)}{(A+s)\cosh(\sqrt{A+s})} \right] = \lim_{S \to S_n} \left[ \frac{e^{st} \cosh(\sqrt{A+s}\chi)}{(A+s)\frac{d}{ds}\cosh(\sqrt{A+s}\chi)} \right]$$

$$= -\frac{4}{\pi} \sum_{n=0}^{\infty} \frac{(-1)^n \cos[(2n+1)\pi\chi/2] e^{-[(2n+1)^2\pi^2 + 4\phi]\frac{\tau}{4}}}{(2n+1)}$$
(4.A22)

From Eqns. (4.A12) - (4.A22) we get Eqn. (4.17) in the text. Similarly, we can solve Eqn.(4.12) by using complex inversion formula.

## CHAPTER 5 SENSITIVITY AND RESISTANCE OF AMPEROMETRIC BIOSENSORS IN SUBSTRATE INHIBITION PROCESSES

## **CHAPTER 5**

## Sensitivity and Resistance of Amperometric Biosensors in Substrate Inhibition Processes

### 5.1 Introduction

Biosensors are approximate analytical devices that tightly combine biorecognition elements and physical transducer for the detection of the target compounds. An amperometric biosensor is a tool used in a solution to measure the concentration of a specific particular chemical or biochemical substances [1–4]. In biosensor, many enzymes are inhibited by their substrates. In the literature, the theoretical model has been widely applied as an essential tool to study and optimize the approximate analytical characteristics of biosensors. Practical biosensors contain a multilayer enzyme membrane; Exploratory monolayer membrane-containing biosensors are widely used to study the biochemical behavior of biosensors. The inhibition of substrates is often considered abiochemical oddity and experimental annoyance. This model is based on the system of non-stationary diffusion equations containing a nonlinear term related to non-Michaelis-Menten kinetics of the enzyme reaction [3].

The biosensor model with a substrate and product inhibition was constructed to reduce the number of biosensor properties. Manimozhi et al. [5] found the solution of steady-state substrate concentration in the case of substrate inhibition using the Homotopy perturbation method (HPM) and variational iteration method (VIM). Already the approximate analytical expression for steady-state concentrations of substrate and product with substrate inhibition using the Adomian decomposition method was discussed by Anitha et al. [6].

A carbon nanotube based biosensor was mathematically modelled by Lyons [7,8]. The one-dimensional steady-state boundary value problem describing the transport and the kinetics of the substrate and the mediator in the two compartment domain was solved approximate analytically. Baronas et al. [9]proposed the mathematical model for the mediated biosensor with the CNT electrode deposited on the perforated membrane. In this chapter, for small values of reaction/diffusion

parameters, we have derived an approximate analytical expression of sensitivity and resistance of biosensor.

## 5.2 Mathematical formulation of the problems

In the enzyme reaction,

$$E + S \leftrightarrow ES \rightarrow E + P$$
 (5.1)

the substrate (S) binds to the enzyme (E) in order to form an enzyme-substrate complex ES. The substrate is converted to product (P) while it is part of this complex. The rate of the product's appearance depends on its substrate concentration.

For example, the simplest scheme of non-Michaelis-Menten kinetics may have been obtained by adding to the Michaelis-Menten scheme (Equation (5.1)), a stage of enzyme-substrate complex (ES) interaction with another substrate molecule (S) (Equation (5.2)) after the non-active complex (ESS) is generated as follows[10]:

$$ES + S \leftrightarrow ESS$$
 (5.2)

The steady-state nonlinear differential equations for the substrate inhibition are[10]:

$$D_{s} \frac{d^{2}s(x)}{dx^{2}} - \frac{V_{max} s(x)}{k_{m} + s(x) + \frac{(s(x))^{2}}{k_{s}}} = 0$$
(5.3)

$$D_p \frac{d^2 p(x)}{dx^2} + \frac{V_{max} s(x)}{k_m + s(x) + \frac{(s(x))^2}{k_s}} = 0$$
(5.4)

where  $D_s$ ,  $D_p$  are the diffusion coefficients of the substrate and product in the enzyme layer. s(x) and p(x) are the concentration of substrate and product in the enzyme layer.  $V_{max}$  is the maximal enzymatic rate,  $k_m$  denotes the Michaelis-Menten constant,  $k_s$  inhibition constant and d is the thickness of the enzyme layer. The corresponding boundary conditions are [10]

$$\frac{ds(x)}{dx} = 0, p(x) = 0 \text{ when } x = 0$$
 (5.5)

where  $s^*$  is the concentration of substrate at x = d and d is thickness of the enzyme layer. The modeling of the amperometric biosensor with the substrate inhibition reveals the complex kinetics of the biosensor response. At low substrate concentration, the

kinetics looks like a simple substrate diffusion. When inhibition constant is large  $(k_s \to \infty)$ , the reaction kinetics is Michaelis-Menden model.

The steady-state current *I* of the biosensor is expressed as follows:

$$I = n_e F D_p \left. \frac{dp(x)}{dx} \right|_{x=0} \tag{5.7}$$

we introduce the set of dimensionless variables as follows:

$$S(\chi) = \frac{s(x)}{s^*}, P(\chi) = \frac{p(x)}{s^*}, \chi = \frac{x}{d}, \phi_s^2 = \frac{V_{max}d^2}{D_s k_m}, \phi_p^2 = \frac{V_{max}d^2}{D_p k_m}, \alpha = \frac{s^*}{k_m}, \beta = \frac{(s^*)^2}{k_m k_s}$$
(5.8)

where  $S(\chi)$  and  $P(\chi)$  indicate the dimensionless concentration of substrate and product respectively.  $\phi_s^2$  and  $\phi_p^2$  denote the corresponding reaction diffusion parameters.  $\chi$  represents the dimensionless distance.  $\alpha$  and  $\beta$  represents the saturation parameters. The governing nonlinear reaction/diffusion equations (5.3) and (5.4) are expressed in the following non-dimensionless form.

$$\frac{d^2 S(\chi)}{d\chi^2} - \frac{\phi_S^2 S(\chi)}{1 + \alpha S(\chi) + \beta (S(\chi))^2} = 0$$
 (5.9)

$$\frac{d^2 P(\chi)}{d\chi^2} + \frac{\phi_p^2 S(\chi)}{1 + \alpha S(\chi) + \beta (S(\chi))^2} = 0$$
 (5.10)

The boundary conditions are given by:

$$\frac{\mathrm{d}s}{\mathrm{d}\chi} = 0, P = 0 \text{ when } \chi = 0 \tag{5.11}$$

$$S = 1, P = 0 \text{ when } \chi = 1$$
 (5.12)

The dimensionless current is reduced to

$$\psi = \frac{I}{n_e F D_P} \left[ \frac{d}{s^*} \right] = \frac{dP}{d\chi} \Big|_{\chi=0}$$
 (5.13)

## 5.3 Approximate analytical expression of concentration of substrate and product

## 5.3.1 Approximate solution using Taylor series method

Equations (5.9)-(5.10) are representing the system of nonlinear equations. It is very difficult to find the exact solution of these nonlinear equations. Solving systems of nonlinear equations is perhaps one of the most difficult problems, especially in a diverse range of science and engineering applications. Recently so many approximate analytical methods [11] are used to solve the nonlinear equations—such as homotopy perturbation method [12–16],residual method [17], Taylor series method [18–21], AGM method [22–24], new approximate analytical method [25–27]. The concentration of substrate and product are obtained by solving the nonlinear equations (9)-(10) using Taylor series method [28–30] (see Appendix A) as follows:

$$S(\chi) \approx 1 + S'(1)(\chi - 1) + \frac{1}{2} \frac{\phi_s^2(\chi - 1)^2}{1 + \alpha + \beta} + \frac{\phi_s^2 S'(1)(\chi - 1)^3}{1 + \alpha + \beta} \left(1 - \frac{\alpha + 2\beta}{1 + \alpha + \beta}\right)$$
 (5.14)

$$P(\chi) \approx P'(1)(x-1) - \frac{1}{2} \frac{\phi_P^2(x-1)^2}{1+\alpha+\beta} - \frac{\phi_P^2 S'(1)(x-1)^3}{1+\alpha+\beta} \left(1 - \frac{\alpha+2\beta}{1+\alpha+\beta}\right)$$
 (5.15)

Where

$$S'(1) = \frac{2\phi_s^2(1+\alpha+\beta)}{2(1+2\alpha+2\beta)+2(\alpha+\beta)^2+\phi_s^2(1-\beta)}; \ P'(1) = \frac{\phi_p^2(3+3\alpha+3\beta-l+\beta l)}{6(1+\alpha+\beta)^2}$$
 (5.16)

## 5.3.2 Approximate solution using new homotopy perturbation method

With the rapid development of nonlinear science, there appears an ever-increasing interest of scientists and engineers in the approximate analytical asymptotic techniques for nonlinear problems [31]. It is very difficult to solve nonlinear problems either numerically or theoretically. Perturbation methods provide the most versatile tools available in nonlinear analysis of engineering problems, and they are constantly being developed and applied to ever more complex problems. Homotopy perturbation method was first proposed by the He[32]. Recently, a new approach to HPM is presented to solve the nonlinear problem and this gives a simple approximate solution in the zeroth iteration [33]. By using this new homotopy perturbation[34–36] (Appendix B), the concentrations of substrate and products can be obtained as follows:

$$S(\chi) \approx \frac{\cosh(m\chi)}{\cosh(m)}$$
 (5.17)

$$P(\chi) \approx \frac{\phi_p^2}{\phi_s^2} \left( \chi + \frac{1 - \chi - \cosh(m\chi)}{\cosh(m)} \right)$$
 (5.18)

where 
$$m = \frac{\phi_s}{\sqrt{1+\alpha+\beta}} = \sqrt{\frac{V_{max}d^2}{D_s(k_m + s^* + \frac{(s^*)^2}{k_s})}}$$
 (5.19)

The dimensionless current is

$$\psi = \frac{I}{n_e F D_P} \left[ \frac{d}{s^*} \right] = \frac{dP(\chi)}{d\chi} \Big|_{\chi = 0} = \frac{\phi_p^2}{\phi_s^2} \left( 1 - \frac{1}{\cosh(m)} \right) = \frac{D_S}{D_P} \left( 1 - \frac{1}{\cosh(m)} \right)$$
 (5.20)

The value of steady-state current (I) is

$$\frac{I}{n_e F} = \frac{D_s s^*}{d} \left( 1 - \operatorname{sech} \left( \sqrt{\frac{V_{max} d^2}{D_s \left( k_m + s^* + \frac{(s^*)^2}{k_s} \right)}} \right) \right)$$
 (5.21)

The result obtained using newhomotopy perturbation method is equivalent to approximate analytical expression derived by hyperbolic function method [38].

## 5.3.3 Sensitivity of biosensor

The sensitivity is one of the most important characteristic of biosensors. The sensitivity  $B_S$  of a biosensor can be expressed as a gradient of the maximal biosensor current density with respect to the substrate concentration  $s^*[10]$ . The dimensionless sensitivity for the substrate concentration  $s^*$  is given by

$$B_S(s^*) = \frac{s^*}{I(s^*)} \frac{\mathrm{d}I(s^*)}{\mathrm{d}s^*} = 1 + \left(\frac{1}{2} + \frac{s^*}{k_S}\right) \frac{s^*}{\left(k_m + s^* + \frac{(s^*)^2}{k_S}\right)} \frac{m \tanh(m)}{1 - \cosh(m)}$$
(5.22)

where  $B_S$  stands for the dimensionless sensitivity of the amperometric biosensor and  $I(s^*)$  is the density of the steady-state biosensor current calculated at the substrate concentration  $s^*$ . From the eqn.(5.22), it is conformed that the sensitivity  $B_S$  varies between -1 and 1.

## 5.3.4 Resitance of biosensor

The resistance of the membrane-based biosensors to changes of the membrane thickness is introduced. The normalized dimensionless resistance  $B_R$  of the biosensor is expressed as the gradient of the steady-state biosensor current with respect to the enzyme layer thickness d[10],

$$B_R(d) = \frac{d}{I(d)} \frac{dI(d)}{dd} = \frac{m \tanh(m)}{\cosh(m) - 1} - 1$$
 (5.23)

where  $B_R$  stands for the dimensionless sensitivity of the amperometric biosensor and I(d) is the steady-state biosensor current calculated at the thickness of the enzyme layer d. The resistance  $B_R$  varies between -1 and 1. The inverse of resistance is referred to as conductance, and such detection is referred to as conductometric electrochemical biosensor or simply conductometric biosensor [10]. The relationship between sensitivity and resistance are obtained from the equations (5.22 & 5.23) as follows:

$$B_S(s^*) = 1 + \left(\frac{1}{2} + \frac{s^*}{k_S}\right) \frac{s^*}{\left(k_m + s^* + \frac{(s^*)^2}{k_S}\right)} (B_R(d) + 1)$$
 (5.24)

## 5.3.5 Thickness of the membrane

Using (5.18) we find approximate analytically the membrane thickness d, at which the steady-state current I gains the maximum at given parameters  $V_{max}$ ,  $D_s$ ,  $k_m$ ,  $k_s$  and  $s^*$ . We can rewrite the equation (5.18) as follows:

$$\frac{I(d)}{n_o F} = \frac{D_S s^*}{d} (1 - \text{sech}(m))$$
 (5.25)

We calculate a derivative of I(d) with the respect to the thickness d.

$$\frac{\partial I(d)}{\partial d} = n_e F D_s s^* \frac{1}{d^2} [(1 + m \tanh(m)) \operatorname{sech}(m) - 1]$$
 (5.26)

And we're looking for d, where the derivative gets zero.

$$(1 + m \tanh(m))$$
sech  $(m) - 1 = -\cosh^2(m) + \cosh(m) + m \sinh(m) = 0$  (5.27)

Equation (5.24) was solved numerically. A single solution  $m = m_{max} = 1.5055$  was obtained. Consequentially, I gains the maximum at the membrane thickness d, where

$$d_{max} = m_{max} \sqrt{\frac{D_s \left(k_m + s^* + \frac{(s^*)^2}{k_s}\right)}{V_{max}}} = 285.65 \mu m$$
 (5.28)

at the values  $k_s=10~\mu M$ ,  $k_m=100~\mu M$ ,  $D_s=D_p=300~\mu m^2/s$ ,  $s^*=10~\mu M$  and  $V_{max}=1~\mu M/s$  (values used in Fig. 5.4a).

## 5.4. Result and Discussion

Equations (5.14)-(5.19) are the simple and closed-form of approximate analytical expressions of sensitivity and resistance of amperometry biosensor with substrate inhabitation kinetics for the for different values of parameters such as substrate reaction-diffusion parameter ( $\phi_s^2$ ), product reaction-diffusion parameter ( $\phi_p^2$ ), thickness of membrane, diffusion coefficients and saturation parameters ( $\alpha$  and  $\beta$ ), respectively.

The error percentage between numerical and the approximate solution obtained by the Taylor series method and hyperbolic function method is less than 3.72% for small values of reaction-diffusion parameters (Tables 5.1 and 5.2). Here the analytical results are obtained using three terms for the Taylor series and zeroth-order iteration for NHPM. The approximation accuracy should be increased by increasing high order terms in the Taylor series and iteration in NHPM.

## 5.4.1 Sensitivity

The sensitivity is also one of the most important characteristics of the biosensors[10]. The biosensor sensitivity can be expressed as the gradient of the steady-state current with respect to the substrate concentration. Since the biosensor current as well as the substrate concentration varies even in orders of magnitude, especially when comparing different sensors, another useful parameter to consider is a dimensionless sensitivity.

The biosensor sensitivity for different values of the parameter are displays in the Figs. 5.1(a-b) and 5. 2(a-c). It is notice that a decrease in all parameter leads to decrease in sensitivity. When  $s^* \approx 10^3 \mu M$  the sensitivity reaches the minimum value -1.Due to the substrateinhibition, the sensitivity differentiably only at intermediate concentrations of the substratei.e 1  $\mu M < s^* < 100 \mu M$ .

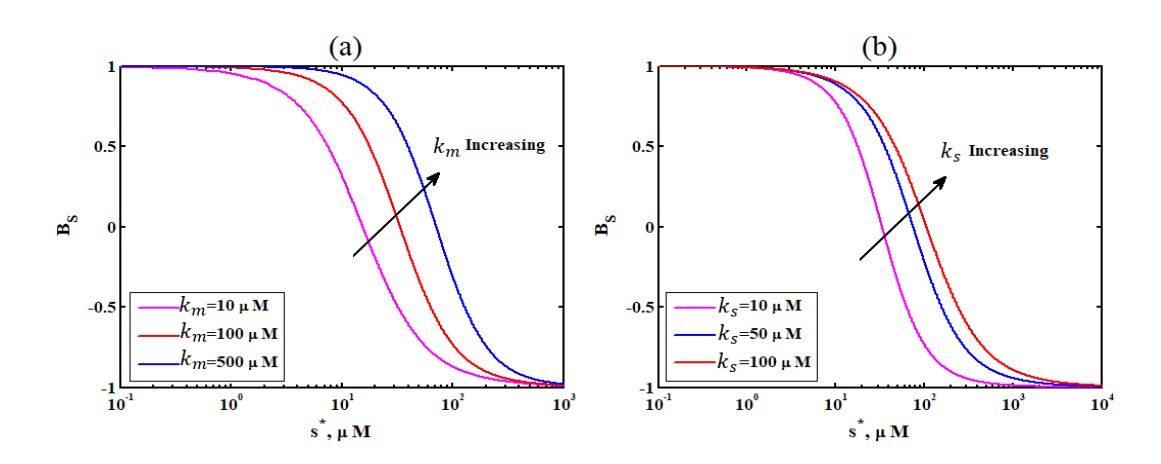


**Figure 5.1.** The biosensor sensitivity using eqn. (5.22) for fixed values of  $D_s = D_p = 300 \ \mu m^2/s$ ,  $V_{max} = 1 \ \mu M/s$ ,  $d = 100 \ \mu m$ . (a).  $k_s = 10 \ \mu M$  and various values of  $k_m \mu M$ . (b). $k_m = 100 \mu M$  and various values of  $k_s \mu M$ .

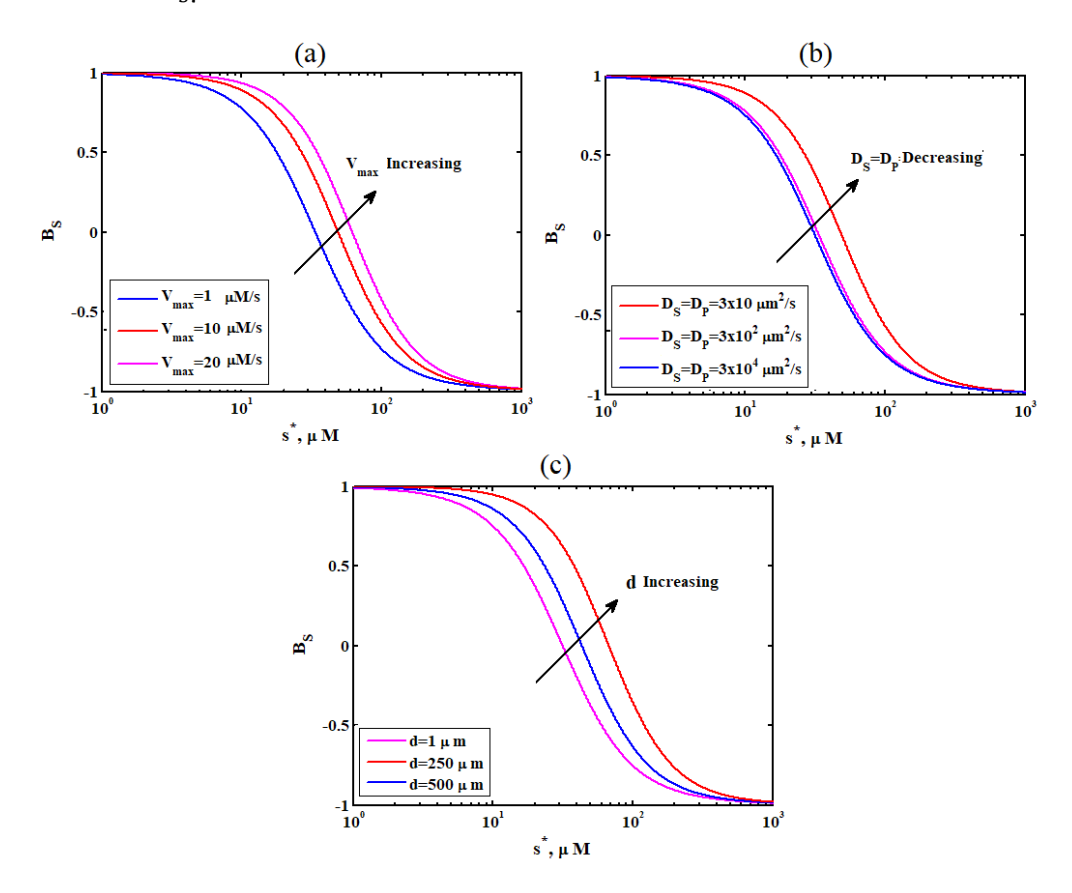


**Figure 5.2.** The biosensor sensitivity using eqn. (5.22) for fixed values of  $k_s = 10 \mu M$ ,  $k_m = 100 \mu M$ . (a).  $D_s = D_p = 300 \mu m^2/s$ ,  $d = 100 \mu m$  and various values of  $V_{max}\mu M/s$ . (b). $V_{max} = 1 \mu M/s$ ,  $d = 100 \mu m$  and various values of  $D_s = D_p \mu m^2/s$ . (c). $D_s = D_p = 300 \mu m^2/s$ ,  $V_{max} = 1 \mu M/s$  and various values of  $d \mu m$ .

## **5.4.2** Resistance

Figures 5.3-5.4 illustrate the biosensor resistance  $B_R$  versus the membrane thickness d for different values of theparameter. One can see from the figures that the shape of all the curves of the normalized resistance is very similar. The results show that the effect of increasing values of the membrane thickness d, results in a deceasing resistivity. It means that the maximal as well as minimal biosensor resistance  $B_R$  is directly proportional to  $\phi_s^2 (= V_{max} d^2/D_s k_m)$ .

Since I is a non-monotonous function of d, the  $B_R$  varies between -1 and 1. The cases when  $B_R$  is close to -1 or 1 correspond to the biosensors the response of which is very sensitive to changes in the thickness d of the enzyme membrane. The noticeable change in the behavior of the biosensor resistance at the moderate substrate concentrations due to the transition from the kinetic-limited to the diffusion-controlled mode of the biosensor action.

As one can see in Figures 4.3 and 4.4 an increase in the electrochemical reaction rate constant  $k_m$ , substrate concentration  $s^*$  or decrease in  $k_s$  and  $V_{max}$  proportionally shifts the curve representing the resistance  $B_R$  to the right. Thus, an increase in the diffusion coefficient proportionally prolongs the linear part of the biosensor resistance calibration curve.

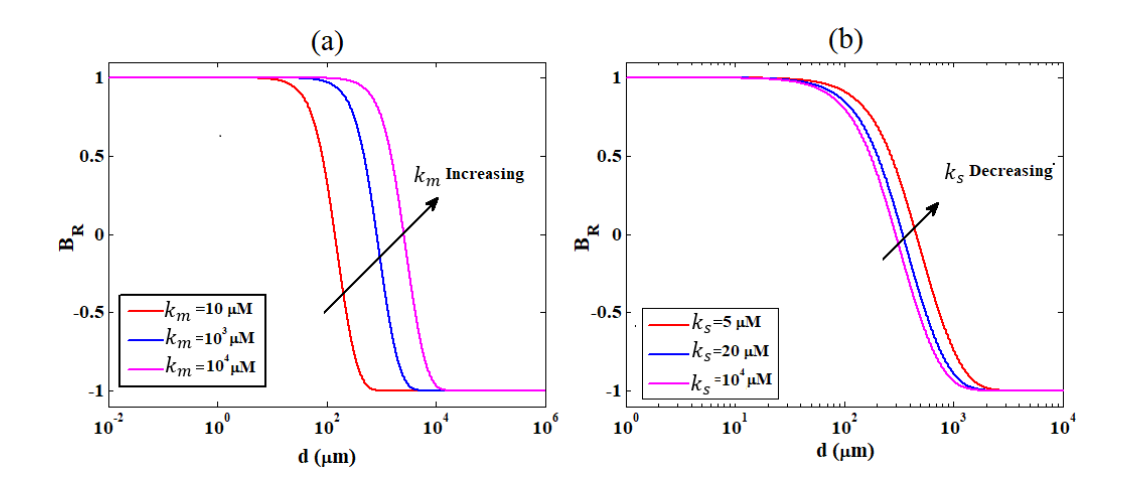


**Figure 5.3.** The biosensor resistance using eqn. (5.23) for fixed values of  $D_s = D_p = 300 \ \mu m^2/s$ ,  $V_{max} = 1 \ \mu M/s$ .(a). $k_s = 10 \ \mu M$ ,  $s^* = 10 \ \mu M$  and various values of  $k_m \ \mu M$ . (b). $k_m = 100 \ \mu M$ ,  $s^* = 30 \ \mu M$  and various values of  $k_s \ \mu M$ .

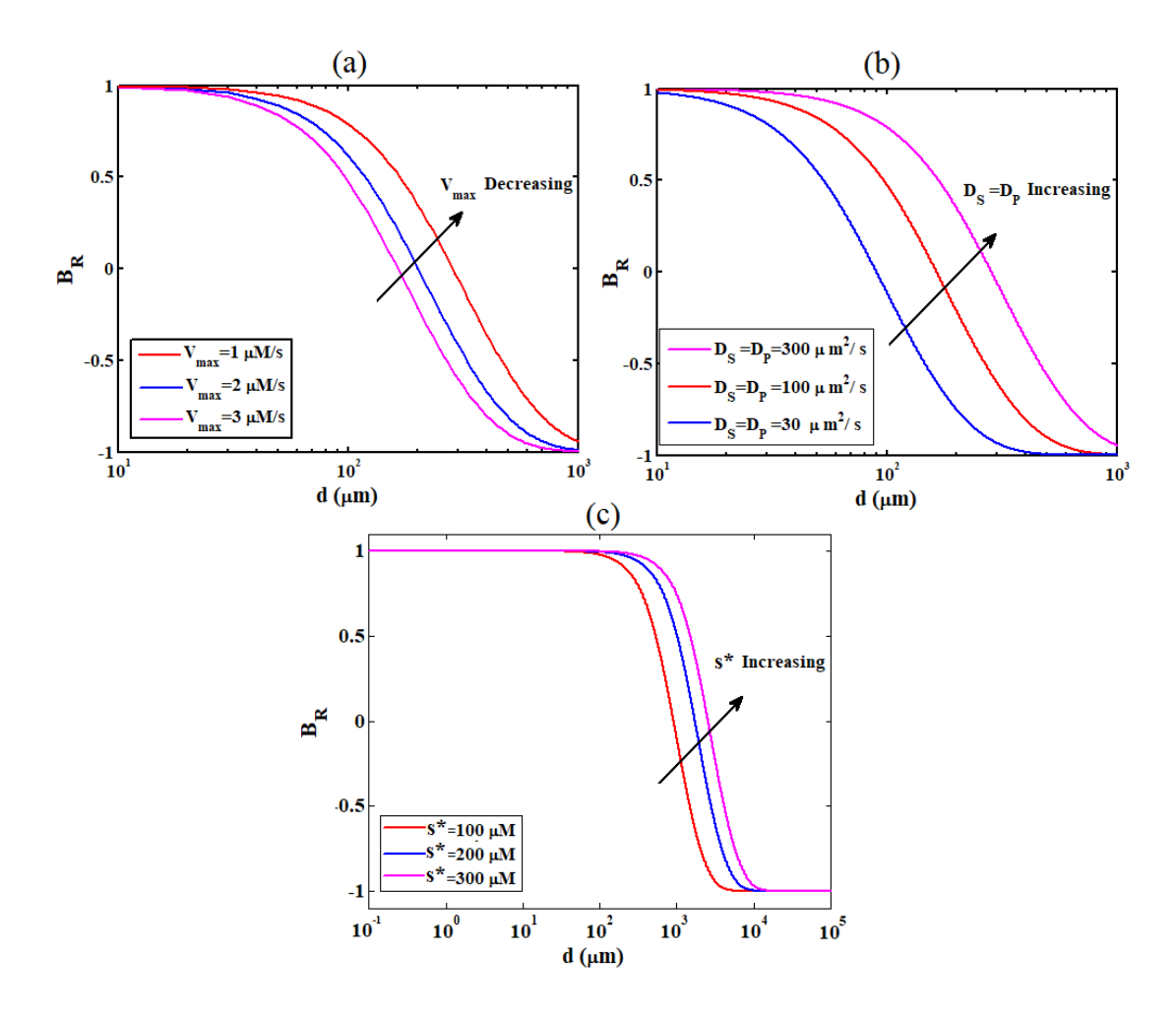


**Figure 5.4.** The biosensor resistance using eqn. (5.23) for fixed values of  $k_s = 10 \ \mu M, k_m = 100 \ \mu M$ . (a).  $D_s = D_p = 300 \ \mu m^2/s, s^* = 10 \ \mu M$  and various values of  $V_{max} \mu M/s$ .(b). $V_{max} = 1 \ \mu M/s, s^* = 10 \ \mu M$  and various values of  $D_s = D_p \ \mu m^2/s$ . (c).  $D_s = D_p = 300 \ \mu m^2/s, V_{max} = 1 \ \mu M/s$  and various values of  $s^* \mu M$ .

#### 5.5 Conclusions

The mathematical model of the amperometric biosensor can be successfully used to investigate the biosensor's sensitivity and resistance. Simple and closed-form the approximate analytical expression for the sensitivity and resistance are obtained for substrate inhibition kinetics. The current function I gain the maximum at the membrane thickness  $d_{max} = 1.5055 \sqrt{D_s \left(k_m + s^* + \frac{(s^*)^2}{k_s}\right)/V_{max}}$ . The effect of thickness of the membrane, concentration of substrate at x = d, diffusion coefficient, Michaelis-Menten constant, inhibition constant on sensitivity and resistance are discussed. The biosensor

sensitivity and the linear range of the calibration curve can be increased when substrate concentration  $s^* < 1 \,\mu M$  or  $s^* > 10^3 \,\mu M$  and all values of other parameters.

Enzyme concentration can significantly reduce biosensor resistance. By decreasing the concentration of the substrate, biosensor resistance may also be greatly reduced (Fig-4). When the biosensor operates in the diffusion-limiting mode instead of in the enzyme reaction-controlled mode, the linear portion of the calibration curve is longer.

**Table 5.1:** Comparison of numerical solution of concentration of substrate with the analytical solutions obtained by hyperbolic function method and Taylor series method for  $\alpha = 0.1$ ,  $\beta = 0.1$  and for different values of  $\phi_s^2$ .

		$\phi_s^2$ =	= 0.5, m = 0	0.65			$\phi_s^2$	$x^2 = 1, m = 0$	).9	
χ	NUM	NHPM Eq. (5.17)	TSM Eq. (5.14)	Error % for NHP M	Error % for TSM	NUM	NHPM Eq. (5.17)	TSM Eq. (5.14)	Error % for NHP M	Error % for TSM
0	0.8170	0.8226	0.8292	0.68	1.49	0.6768	0.6914	0.7156	2.15	5.73
0.25	0.8281	0.8333	0.8390	0.6	1.31	0.6959	0.7094	0.7303	1.94	4.94
0.5	0.8618	0.8658	0.8696	0.46	0.90	0.7540	0.7646	0.7784	1.41	3.24
0.75	0.9187	0.9209	0.9226	0.23	0.42	0.8539	0.8598	0.8663	0.69	1.44
1	1.0000	1.0000	1.0000	0.00	0.00	1.0000	1.0000	1.0000	0.00	0.00
	A	verage Erro	or %	0.40	0.82	A	verage Erro	or %	1.24	3.07

**Table 5.2:** Comparison of numerical solution of concentration of product with the analytical solution obtained by hyperbolic function method and Taylor series method for  $\alpha = 0.1$ ,  $\beta = 0.1$ ,  $\phi_s^2 = 1$  and for different values of  $\phi_p^2$ .

		$\phi_p^{-2}$	= 0.5, m =	= 0.9			$\phi_{l}$	$p^2 = 1, m =$	0.9	
24		NHPM	TSM	Error	Error		NHPM	TSM	Error %	E 0/
χ	NUM	Eq.	Eq.	% for	% for	NUM	Eq.	Eq.	for	Error %
		(5.18)	(5.15)	NHPM	TSM		(5.18)	(5.15)	NHPM	for TSM
0	0.0000	0.0000	0.0000	0.00	0.00	0.0000	0.0000	0.0000	0.00	0.00
0.25	0.0309	0.0295	0.0282	4.41	8.69	0.0617	0.0591	0.0564	4.25	8.55
0.5	0.0422	0.0405	0.0397	3.97	5.96	0.0844	0.0810	0.0794	3.97	5.96
0.75	0.0327	0.0315	0.0313	3.65	4.24	0.0653	0.0630	0.0626	3.50	4.0
1	0.0000	0.0000	0.0000	0.00	0.00	0.0000	0.0000	0.0000	0.00	0.000
	Average Error %			2.40	3.78	Average Error % 2.			2.34	3.72

Here Num denotes numerical solution, NHPM-new homotopy perturbation method, TSM-Taylor series method.

#### **APPENDIX 5.A:**

## Analytical solution of nonlinear equation (Eq.5.11 and Eq.5.12) using Taylor series method

Consider the nonlinear equations

$$\frac{d^2S}{d\chi^2} - \frac{\phi_S^2S}{1+\alpha S + \beta S^2} = 0 \tag{5.A1}$$

$$\frac{d^2P}{d\chi^2} + \frac{\phi_p^2 S}{1 + \alpha S + \beta S^2} = 0 \tag{5.A2}$$

The boundary conditions are given by:

$$\frac{dS}{d\chi} = 0, P = 0 \text{ when } \chi = 0 \tag{5.A3}$$

$$S = 1, P = 0 \text{ when } \chi = 1$$
 (5.A4)

Consider the Taylor's series at  $\chi = 1$  for dimensionless concentration of  $S(\chi)$  and  $P(\chi)$ .

$$S(\chi) \approx \sum_{q=0}^{3} \left( \frac{d^q S}{d\chi^q} \Big|_{\chi=1} \right) \frac{(\chi-1)^q}{q!}$$
 (5.A5)

$$P(\chi) \approx \sum_{q=0}^{3} \left( \frac{d^{q} P}{d\chi^{q}} \Big|_{\chi=1} \right) \frac{(\chi-1)^{q}}{q!}$$
 (5.A6)

Let  $\frac{d^q u}{d\chi^q}\Big|_{\xi=1} = A_q$ ,  $\frac{d^q v}{d\chi^q}\Big|_{\xi=1} = B_q$  and from the boundary conditions (Eq. (5.A3-5.A4)),

we get  $A_0=1$  and  $B_0=0$  . Let us consider,  $A_1=S'(1), B_1=P'(1)$  . Then

$$S(\chi) \approx \sum_{q=0}^{3} A_q \frac{(\chi - 1)^q}{q!}$$
 (5.A7)

$$P(\chi) \approx \sum_{q=0}^{3} B_q \frac{(\chi - 1)^q}{q!}$$
 (5.A8)

Substituting  $\chi = 1$  in Eq. (5.A1) and Eq. (5.A2), we get the following

$$A_2 = \frac{\phi_s^2}{1 + \alpha + \beta} \tag{5.A9}$$

$$B_2 = -\frac{\phi_P^2}{1 + \alpha + \beta} \tag{5.A10}$$

$$A_3 = \frac{\phi_s^2 l}{1 + \alpha + \beta} \left( 1 - \frac{\alpha + 2\beta}{1 + \alpha + \beta} \right) \tag{5.A11}$$

$$B_3 = -\frac{\phi_P^2 l}{1 + \alpha + \beta} \left( 1 - \frac{\alpha + 2\beta}{1 + \alpha + \beta} \right) \tag{5.A12}$$

Consider the approximation stops at third step, then we have

$$S(\chi) \approx A_0 + A_1(x - 1) + \frac{A_2}{2}(x - 1)^2 + \frac{A_3}{6}(x - 1)^3$$

$$= 1 + S'(1)(x - 1) + \frac{1}{2} \frac{\phi_s^2(x - 1)^2}{1 + \alpha + \beta} + \frac{\phi_s^2 S'(1)(x - 1)^3}{1 + \alpha + \beta} \left(1 - \frac{\alpha + 2\beta}{1 + \alpha + \beta}\right)$$
(5.A13)
$$P(\chi) \approx B_0 + B_1(x - 1) + \frac{B_2}{2}(x - 1)^2 + \frac{B_3}{6}(x - 1)^3$$

$$= P'(1)(x - 1) - \frac{1}{2} \frac{\phi_P^2(x - 1)^2}{1 + \alpha + \beta} - \frac{\phi_P^2 S'(1)(x - 1)^3}{1 + \alpha + \beta} \left(1 - \frac{\alpha + 2\beta}{1 + \alpha + \beta}\right)$$
(5.A14)

Now using the boundary conditions  $\frac{dS}{d\chi} = 0$ , P = 0 when  $\chi = 0$ , we can get

$$S'(1) = \frac{2\phi_s^2(1+\alpha+\beta)}{2(1+2\alpha+2\beta)+2(\alpha+\beta)^2+\phi_s^2(1-\beta)}; P'(1) = \frac{\phi_p^2(3+3\alpha+3\beta-l+\beta l)}{6(1+\alpha+\beta)^2} \quad (5.A15)$$

#### **Appendix 5.B:**

## Analytical solution of nonlinear equation (Eq.5.11 and Eq.5.12) using new homotopy perturbation method

In this Appendix, we indicate how Eq. (5.5) in this paper is derived.

$$\frac{d^2S}{d\chi^2} - \frac{\phi_s^2 S}{1 + \alpha S + \beta S^2} = 0 \tag{5.B1}$$

$$\frac{d^2P}{d\chi^2} + \frac{\phi_p^2 S}{1 + \alpha S + \beta S^2} = 0 \tag{5.B2}$$

The boundary conditions are given by:

$$\frac{dS}{d\chi} = 0, P = 0 \text{ when } \chi = 0 \tag{5.B3}$$

$$S = 1, P = 0 \text{ when } \chi = 1$$
 (5.B4)

we first construct a Homotopy as follows[34-37]:

$$(1-p)\left[\frac{d^2S}{d\chi^2} - \frac{{\phi_s}^2S}{1+\alpha S(\chi=1) + \beta S(\chi=1)^2}\right] + p\left[(1+\alpha S + \beta S^2)\frac{d^2S}{d\chi^2} - {\phi_s}^2S\right] = 0 \quad (5.B5)$$

$$(1-p)\left[\frac{d^{2}P}{d\chi^{2}} + \frac{\phi_{p}^{2}S}{1+\alpha S(\chi=1)+\beta S(\chi=1)^{2}}\right] + p\left[(1+\alpha S + \beta S^{2})\frac{d^{2}P}{d\chi^{2}} + \phi_{p}^{2}S\right] = 0 \quad (5.B6)$$

on simplification we get

$$(1-p)\left[\frac{d^2S}{d\chi^2} + \frac{\phi_s^2S}{1+\alpha+\beta}\right] + p\left[(1+\alpha S + \beta S^2)\frac{d^2S}{d\chi^2} - \phi_s^2S\right] = 0$$
 (5.B7)

$$(1-p)\left[\frac{d^{2}P}{d\chi^{2}} + \frac{\phi_{p}^{2}S}{1+\alpha+\beta}\right] + p\left[(1+\alpha S + \beta S^{2})\frac{d^{2}P}{d\chi^{2}} + \phi_{p}^{2}S\right] = 0$$
 (5.B8)

The approximate solution of Eqs. (5.B1) and (5.B2) are

$$S = S_0 + p S_1 + p^2 S_2 + \dots (5.B9)$$

$$P = P_0 + p P_1 + p^2 P_2 + \dots (5.B10)$$

Substituting Eq. (5.B9)in Eq. (5.B7) and Eq. (5.B10) in Eq.(5.B8)in, then comparing the coefficients of like powers of p yields:

$$p^{0}: \frac{d^{2}S_{0}}{d\chi^{2}} - \frac{\phi_{s}^{2}S_{0}}{1+\alpha+\beta} = 0$$
 (5.B11)

$$p^{0}: \frac{d^{2}P_{0}}{d\chi^{2}} + \frac{\phi_{p}^{2}S_{0}}{1+\alpha+\beta} = 0$$
 (5.B12)

The boundary conditions are

$$\chi = 0; \frac{dS_i}{d\chi} = 0; P_i = 0; i = 0,1,2,3 \dots$$
 (5.B13)

$$\chi = 1$$
;  $S_0 = 1$ ;  $P_0 = 0$ ;  $S_i = 0$ ;  $P_i = 0$ ;  $i = 1,2,3...$  (5.B14)

Solving the Eqs. (5.B11-5. B12), and using the above boundary conditions and we can find the following results.

$$S_0 = \frac{\cosh\left(\frac{\phi_s}{\sqrt{1+\alpha+\beta}}\chi\right)}{\cosh\left(\frac{\phi_s}{\sqrt{1+\alpha+\beta}}\right)} \tag{5.B15}$$

$$P_0 = \frac{{\phi_p}^2}{{\phi_s}^2} \left( \chi + \frac{1 - \chi - cosh\left(\frac{\phi_s}{\sqrt{1 + \alpha + \beta}}\chi\right)}{cosh\left(\frac{\phi_s}{\sqrt{1 + \alpha + \beta}}\right)} \right)$$
 (5.B16)

According to the HPM, we can conclude that

$$S(\chi) \approx \lim_{n \to 1} S = S_0 + S_1 + S_2 + \cdots$$
 (5.B17)

$$P(\chi) \approx \lim_{p \to 1} P = P_0 + P_1 + P_2 + \cdots$$
 (5.B18)

Considering the first iteration we have the solution of concentration of species

$$S(\chi) \approx S_0 = \frac{cosh(m\chi)}{cosh(m)}$$
 (5.B19)

$$P(\chi) \approx P_0 = \frac{\phi_p^2}{\phi_s^2} \left( \chi + \frac{1 - \chi - \cosh(m\chi)}{\cosh(m)} \right)$$
 (5.B20)

Where  $m = \frac{\phi_s}{\sqrt{1+\alpha+\beta}}$ 

# CHAPTER 6 CONCLUSION AND FUTURE ENHANCEMENTS

#### **CHAPTER - 6**

#### **Conclusion and Future Enhancements**

#### **6.1 Conclusions**

The solution approach accomplished in this thesis is based on the objective that at the maximum possible level. The analytical solutions should be achieved for the model nonlinear equations in applied chemical sciences since analytical solutions are the best for analysing experimental data if available or can be obtained.

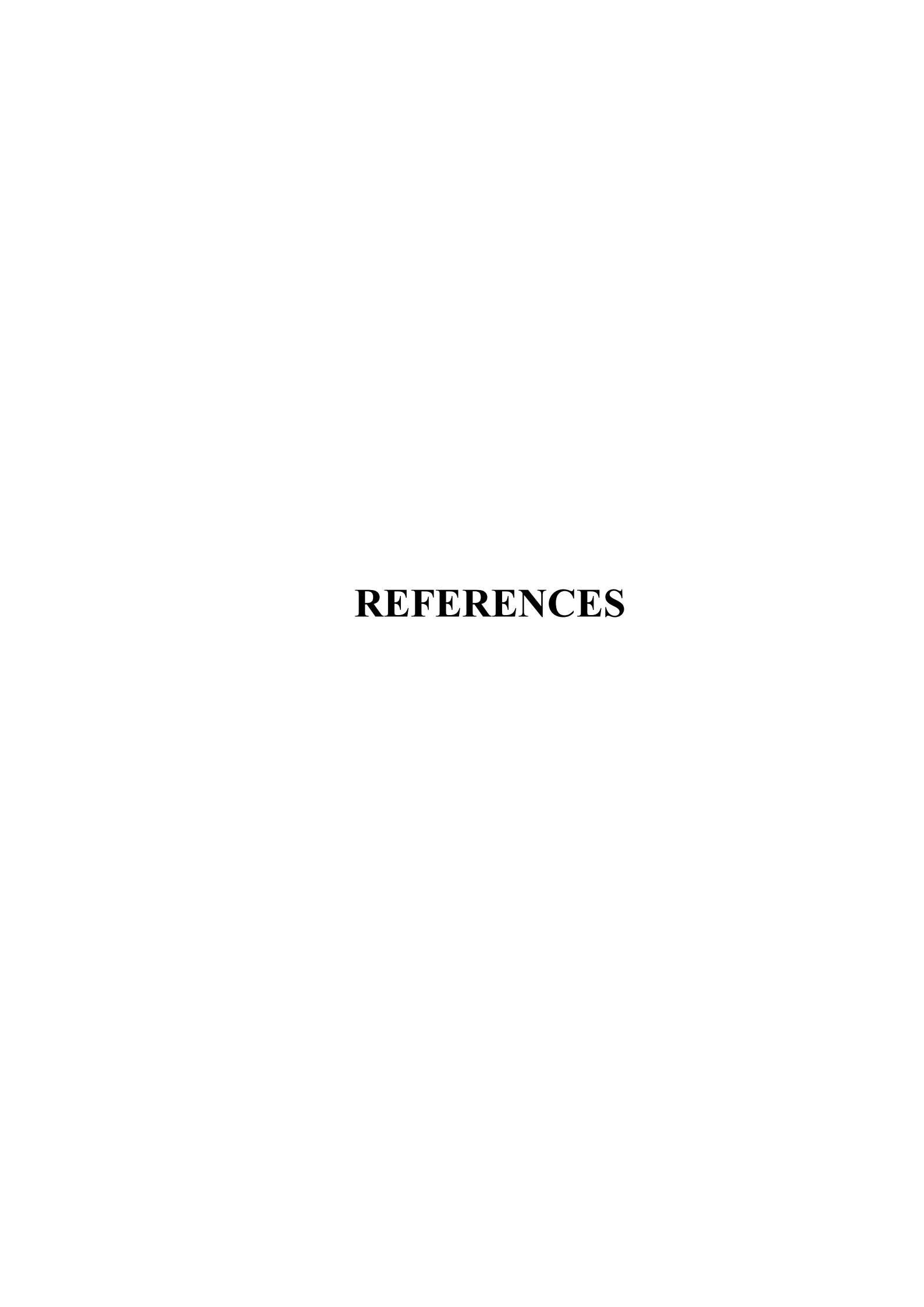
- The analytical expressions for the nonlinear differential equations with variable coefficients are adopted using a homotopy perturbation method and a variational iteration method.
- The system of nonlinear equations containing a nonlinear term related to reversible homogeneous reactions is solved. The concentration of species can be calculated by solving nonlinear equations with the homotopy perturbation method. Our rough analytical results are also compared to the simulation results. The agreement between our analytical and simulation results is satisfactory. The effects of the parameters on concentration are discussed and illustrated graphically.
- The reduction of hydrogen peroxide (H<sub>2</sub>O<sub>2</sub>) to water in a metal dispersed conducting polymer film is described mathematically. The model is based on a system of reaction-diffusion equations that includes a nonlinear term related to the enzymatic reaction's Michaelis–Menten kinetics. Approximate analytical expressions for substrate and product concentrations for steady and non-steady-state conditions were obtained.
- A theoretical model of the sensitivity and resistance of amperometry biosensors
  with substrate inhibition kinetics is discussed. This model is based on a system
  of non-stationary diffusion equations with a nonlinear term related to nonMichaelis-Menten kinetics of the enzymatic reaction. The influence of various
  parameters such as thickness of enzyme layer, bulk substrate concentration,

Michaelis-Menten and saturation constant on sensitivity and resistance of biosensor are discussed.

#### **6.2 Scope of the Future Work**

The thesis entitled "Theoretical analysis of nonlinear differential equations in applied chemical sciences "provides a significant contribution to the enhancement of procedures for solving nonlinear problems in chemical sciences with innovative solution techniques. The present investigation offers scope for future research on the following lines.

- Analytical solutions of nonlinear differential equations in chemical kinetics have been extended to nonlinear partial differential equations in physical, biological and medical sciences.
- Nonlinear problems in homogeneous reactions occur in the mass-transfer boundary layer can be extended to transient conditions in chemical and biotransformation processes by considering the convection and diffusion terms.
- The theoretical model based on a system of reaction-diffusion equations containing a nonlinear term related to Michaelis-Menten kinetics of the enzymatic reaction is extended to non-Michaelis-Menten kinetics.
- A theoretical model of the sensitivity and resistance of amperometry biosensors withnon-Michaelis—Menten kinetics is extended to all reaction mechanism.



#### **REFERENCES**

#### **CHAPTER I**

- [1] P. Doucet, P.B. Sloep, *Mathematical modeling in the life sciences*, EllisHorwood,1992.
- [2] J. Awrejcewicz, I.V. Andrianov, L.I. Manevitch, *Asymptotic approaches in the nonlinear dynamics: New Trends and Applications*. Springer, Berlin, 1998.
- [3] J.H. He, *Int. J. Modern phy. B* 20 (2006) 1141.
- [4] J.H. He, *Int. J. Nonl.Mech.* 34 (1999) 699.
- [5] J.H. He, *Phy. Lett.* A35 (2006) 87.
- [6] G. Domairry, H. Bararnia, Adv. Studies Theor. Phys. 2 (2008) 507.
- [7] G.Adomian, J. Math. Anal. & Appl. 135 (1988) 501.
- [8] B. Bülbül, M. Sezer, J. Appl. Math. 2013, 1-6 (2013).
- [9] M. Najafi, M. Moghimi, H.R. Massah, H. Khoramishad, M. Daemi, *Transactions on mathematics*. 3, 1429-1436 (2006).
- [10] F. Geng, Comput.Math. with Appl. 61, 1935-1938 (2011).
- [11] P. P. Boyle, W. Tian, Fred Guan, J. Symb. Comput. 33, (2002) 343-355.
- [12] D. Piriadarshani, P.L. Suresh, Glob. J. Pure Appl. Math. 12, 418-422 (2016).
- [13] M. Missaoui, H. Rguigui, S. Wannes, São Paulo J. Math. Sci. 14, 580-595 (2020).
- [14] X. Luo, H. Duan, L. He, *Energy*. 205, 118085 (2020).
- [15] Y. Khan, Int. J. Numer. Method H. 31, 1104-1109 (2021).

- [16] William E. Schiesser, "Hodgkin–Huxley and FitzHugh –Nagumo Models", in Differential Equation Analysis in Biomedical Science and Engineering: Partial Differential Equation Applications with R, First Edition, John Wiley & Sons, New York, United States, (2014). pp. 127-161
- [17] Pascal Wallisch, "FitzHugh -Nagumo Model: Traveling Waves", in *An Introduction to Scientific Computing in MATLAB, MATLAB for Neuroscientists* (Second Edition), Academic Press, (2014). pp. 425-438.
- [18] R. G. Parr and W. Yang, "Density-Functional Theory of Atoms and Molecules", *Oxford University Press*, Oxford, UK, (1989).
- [19] S. V. Pikulin, Comput. Math. and Math. Phys. 59, 1292-131 (2019).
- [20] Muhammad Asif Zahoor Raja, Aneela Zameer, Aziz Ullah Khan and Abdul Majid Wazwaz, *SpringerPlus* 5:1400 (2016).
- [21] Raka Jovanovic, Sabre Kais, Fahhad H. Alharbi, J. Appl. Math. 2014, (2014).
- [22] Hina Khan, Hang Xu, *Phys Lett A*, 365, (2007) 111-115.
- [23] Ji-Huan He, Appl. Math. Comput. 143, (2003) 533-535.
- [24] T. W. Chapman, A. P. Barrios, and Y.Meas, J. Electrochem. Soc.,154 (2007) 411.
- [25] Ongun MY, Math Comput Model: An International Journal, 53 (2011) 597.
- [26] R. Baronas, F. Ivanauskas, J. Kulys, Mathematical Modeling of Biosensors An Introduction for Chemists and Mathematicians, Springer, 2010.

#### **CHAPTER II**

- [1] B. Bülbül, M.Sezer, *J. Appl. Math.***2013**, 1-6 (2013).
- [2] M. Najafi, M. Moghimi, H.R. Massah, H. Khoramishad, M. Daemi, *Transactions on Mathematics.* **3**, 1429-1436 (2006).
- [3] F. Geng, Comput.Math. with Appl.**61**, 1935-1938(2011).
- [4] P. P. Boyle, W. Tian, Fred Guan, J. Symb. Comput. 33, (2002) 343-355.
- [5] D. Piriadarshani, P.L.Suresh, *Glob. J. Pure Appl. Math.* **12**, 418-422 (2016).
- [6] M.Missaoui, H.Rguigui, S.Wannes, *São Paulo J. Math. Sci.***14**, 580-595 (2020).
- [7] X. Luo, H. Duan, L. He, *Energy*. **205**, 118085 (2020).
- [8] Y. Khan, Int. J. Numer. Method H.31,1104-1109 (2021).
- [9] William E. Schiesser, "Hodgkin–Huxley and FitzHugh –Nagumo Models", in Differential Equation Analysis in Biomedical Science and Engineering: Partial Differential Equation Applications with R, First Edition, John Wiley & Sons, New York, United States, (2014). pp. 127-161
- [10] Pascal Wallisch, "FitzHugh -Nagumo Model: Traveling Waves", in *An Introduction to Scientific Computing in MATLAB, MATLAB for Neuroscientists* (Second Edition), Academic Press, (2014).pp. 425-438.
- [11] R. G. Parr and W. Yang, "Density-Functional Theory of Atoms and Molecules", *Oxford University Press*, Oxford, UK, (1989).
- [12] S. V. Pikulin, Comput. Math. and Math. Phys. **59**,1292-131(2019).
- [13] Muhammad Asif Zahoor Raja, AneelaZameer, Aziz Ullah Khan and Abdul Majid Wazwaz, *SpringerPlus* 5:1400(2016).
- [14] Raka Jovanovic, Sabre Kais, Fahhad H. Alharbi, J. Appl. Math. 2014, (2014).
- [15] Hina Khan, Hang Xu, *Phys Lett A*, **365**, (2007) 111-115.
- [16] Ji-Huan He, Appl. Math. Comput. 143, (2003) 533-535.

- [17] Abdul-Majid Wazwaz, Cent. Eur. J. Eng., 4, (2014) 64-71.
- [18] D.D. Ganji, Hafez Tari, M. BakhshiJooybari, *Comput. Math. with Appl.* **54**, (2007) 1018-1027.
- [19] MSM Selvi, L Rajendran, M Abukhaled, J. Phys. Commun. 4, (2020) 105017.
- [20] R Usha Rani, L Rajendran, AIP Conference Proceedings, 2277, (2020) 130006.
- [21] S Saravanakumar, A Eswari, L Rajendran, Marwan Abukhaled, *Appl. Math*, **14**,(2020) 967-976.
- [22] R Swaminathan, K Venugopal, P Jeyabarathi, L Rajendran, *Solid State Techno.***63**, (2020) 2464-2473.
- [23] S ThamizhSuganya, P Balaganesan, L Rajendran, Marwan Abukhaled, *EJPAM*, **13**, (2020) 631-644.
- [24] P Jeyabarathi, M Kannan, L Rajendran, *IJEAT*, **6**, (2020) 3332-3338.
- [25] K. Saranya, V. Mohan, L. Rajendran, *AJAC*, **11**, (2020) 15.
- [26] M Chitra Devi, P Pirabaharan, L Rajendran, Marwan Abukhaled, *Reac. Kinet. Mech. Cat.***130**, (2020) 35-53.
- [27] R. Swaminathan, K. Venugopal, M.Rasi, M. Abukhaled, L. Rajendran, *Quim Nova.***43**, (2020) 58-65.
- [28] R Angel Joy, L. Rajendran, Int. Rev. Chem. Eng. 4, (2012) 516-523.
- [29] A. Eswari, L. Rajendran, Application of variational iteration method and electron transfer mediator/catalyst composites in modified electrodes, *Nat. Sci.*, **2**,(2010) 612.
- [30] S Loghambal, L Rajendran, Int. J. Electrochem. Sci.5, (2010) 327-343.
- [31] G Rahamathunissa, L Rajendran, J. Math. Chem. 44, (2008) 849-861.
- [32] A. M. Wazwaz, Appl. Math. Comput. 212, (2009) 120-134.
- [33] A.M. Wazwaz, Appl. Math. Comput. 105, (1999) 11-19.

- [34] A.M. Wazwaz, Appl. Math. Comput. 118, (2001) 123-132.
- [35] J.H. He, Appl. math. Comput. 114, (2000) 115-123.
- [36] Andrei D. Polyanin Valentin F. Zaitsev, "Handbook of Exact Solutions for Ordinary Differential Equations", (second edition), *Chapman & Hall* (2003).
- [37] J.H. He, Comput. Methods Appl. Mech. Eng. 178, (1999) 257-262.
- [38] G.L. Liu, Proceedings of the 7th Conference of modern Mathematics and Mechanics, Shanghai (1997) 47–53.
- [39] J.H. He, Appl. Math. Comput. 135, (2003) 73-79.
- [40] J.H. He, Appl. Math. Comput. 151, (2004) 287-292.
- [41] S.J. Liao, Int. J. Non Linear Mech. 30, (1995) 371-380.
- [42] S.J. Liao, Eng. Anal. Bound Elem. 20, (1997) 91-99.
- [43] J.H. He, Appl. Math. Comput. 135, (2003) 73-79.
- [44] J.H. He, Appl. Mech. Eng. 167, (1998) 57-68.
- [45] J.H. He, X.H. Wu, Comput. Math. with Appl. 54, (2007) 881-894.
- [46] A.M. Wazwaz, Int. J. Comput. Math. 87, (2010) 1131–1141.

#### **CHAPTER III**

- [1] J. Newman and K. E. Thomas-Alyea, Electrochemical System, 3rd ed., Chap. 11and Appendix C, Prentice-Hall, Englewood Cliffs, NJ (2004).
- [2] V. G. Levich, Physicochemical Hydrodynamics, Prentice-Hall, Englewood Cliffs, NJ(1962).
- [3] A. J. Bard and L. R. Faulkner, Electrochemical Methods, John Wiley & Sons, New York (1980).
- [4] A. K. Hauser and John Newman, J. Electrochem. Soc., 136 (1989) 2820.
- [5] C. Hofseth and T. W. Chapman, J. Electrochem. Soc., 138 (1991) 2321.
- [6] C. M. Villa and T. W. Chapman, *Ind. Eng. Chem. Res.*, 34 (1995) 3445.
- [7] T. W. Chapman, A. P. Barrios, and Y.Meas, *J. Electrochem. Soc.*, 154 (2007) 411.
- [8] LC Mary, R.Usha Rani, A. Meena, L. Rajendran, *Int. J. Electrochem. Sci.*, 16 (2021) 151037.
- [9] K. Saravanakumar, L. Rajendran, Appl. Math. Model., 39,(2015) 117.
- [10] S. Liao, Appl. Math. Comput, 147 (2004) 490.
- [11] M. Abukhaled, J. Math., (2013) 1.
- [12] R. Saravanakumar, P. Pirabaharan, R. Swaminathan, Int. J. Res. 7 (2018) 342.
- [13] A. M. A. Wazwaz, Appl. Math. Comput. 102 (1999) 77.
- [14] M. Abukhaled, J. Comput. Nonlinear Dyn., 12 (2017) 051021.
- [15] M. Abukhaled, J. Electroanal. Chem., 792 (2017) 66.
- [16] J. H. He, Appl. Mech. Eng., 178 (1999) 257.
- [17] J.H. He, *Ind. J. Phy.*, 88 (2014) 193.
- [18] R.Saravanakumar, P.Pirabaharan, Marwan Abukhaled, and L. Rajendran, *J. Phys. Chem. B*, 124 (2020) 443.

- [19] R. Swaminathan, K. Venugopal, M. Rasi, M. Abukhaled, L.Rajendran, *Quim Nova*, 43 (2020) 58.
- [20] R. Swaminathan, K.L Narayanan, V. Mohan, K. Saranya, L. Rajendran, Int. J. Electrochem. Sci., 14 (2019) 37777.
- [21] K. Saranya, V. Mohan, L. Rajendran, J. Math. Chem., 58 (2020) 1230.
- [22] M. Chitra Devi, P. Pirabaharan, M. Abukhaled, L. Rajendran, *Electrochim. Acta*, 345 (2020) 136175.
- [23] B. Manimegalai, M.E.G. Lyons, L. Rajendran, *J. Electroanal. Chem.*, 880 (2020) 114921.
- [24] R. Usha Rani, L. Rajendran, Chem. Phys. Lett., 754 (2020) 137573.
- [25] R. Swaminathan, K. Venugopal, L. Rajendran, M. Rasi, M. Abukhaled, *Quim. Nova*, 43,1(2020)1-8.
- [26] K.P.V. Preethi, M.C. Devi, R. Swaminathan, R. Poovazhaki, *Int. J. Math. And Appl.*, 6 (2018) 359.

#### **CHAPTER IV**

- [1] S. Palanisamy, S. Cheemalapati, S. M. Chen, *Int. J. Electrochem. Sci.* 2012, 7, 8394.
- [2] K.E. Toghill, R. G. Compton, Int. J. Electrochem. Sci. 2010, 5, 1246.
- [3] S.B. Bankar, M.V. Bule, R.S. Singhal, L. Ananthanarayan, *Biotechnol. Adv.* 2009, 27, 489.
- [4] A. Pizzariello, M. Stred'ansky, S. Miertuš, *Bioelectrochemistry*. 2002, 56, 99.
- [5]. N. A. Choudhury, R. K. Raman, S. Sampath, A. K. Shukla, *J. Power Sources*. 2005, 143, 1.
- [6] R.R Bessette, M.G. Medeiros, CJ Patrissi, C. M. Deschenes, C. N. LaFratta, *J. Power Sources*. 2001, 96, 240.
- [7] Ichiro Yamanaka .; Takeshi Onizawa .; Sakae Takenaka .; Kiyoshi Otsuka .; Angew. *Chem. Int. Ed.* 2003, 42, 3653.
- [8] W. Yang, S. Yang, W. Sun, G. Sun, Q. Xin, Electrochim. Acta. 2006, 52, 9.
- [9] L. Han, S. Guo, P. Wang, S. Dong, Adv. Energy Mater. 2014, 1400424.
- [10] E. Kjeang, A. G. Brolo, D. A. Harrington, N. Djilali, D. Sinton, *Journal of Electrochemical Society*, 2007, 154, B1220.
- [11] B. D. Adams, C. K. Ostrom, A. Chen, *Journal of Electrochemical Society*, 2011, 1588, B434.
- [12] T.Q.N Do, M. Varničić, R. Hanke-Rauschenbach, T. Vidaković-Koch, K. Sundmacher, *Electrochim. Acta.* 2014, 137,616.
- [13] R. Benfeitas, G. Selvaggio, F. Antunes, P.M.B.M. Coelho, & A. Salvador, *Free Radical Biology and Medicine*, 2014, 74, 35.
- [14] C. Agnès, B.Reuillard, A. Le Goff, M. Holzinger, S. Cosnier, *Electrochem. Commun.* 2013, 34, 105.
- [15] L. An, T.S. Zhao, L. Zeng, X.H. Yan, Int. J. Hydrog. Energy. 2014, 39, 2320.

- [16] L. An, T.S. Zhao, Z. H. Chai, L. Zeng, P. Tan, Int. J. Hydrog. Energy. 2014, 39, 7407.
- [17] M.Somasundrum, A.Tongta, M. Tanticharoen, K. Kirtikara, *J. Electroanal. Chem.* 1997, 440, 259.
- [18] M.Y.Ongun, math comput model: An International Journal, 2011, 53, 597.
- [19] M. Rasi, K. Indira, L.Rajendran, J. Chem. Kinet. 2013, 45, 322.
- [20] A. M. Wazwaz, Cent. Eur. J. Eng. 2014, 4, 64.
- [21] A. Meena, & L. Rajendran, Chem. Eng. Technol. 2010, 33, 1999.
- [22] Y. Wu, J. H. He, results phys. 2018, 10, 270.
- [23] L. Rajendran, S. Anitha, Electrochim. Acta. 2013, 102, 474.
- [24] R. Swaminathan, K. LakshmiNarayanan, V. Mohan, K. Saranya, L. Rajendran, Int. J. Electrochem. Sci., 14 (2019) 3777 – 3791,
- [25] R. D. Skeel, M. Berzins, SIAM J. Sci. Comput, 1990, 11, 1.
- [26] M. Rasi, L. Rajendran, A. Subbiah, sensor actuat b-chem. 2015, 208, 128.
- [27] D.N. Rao, Resonance, 1998, 3, 38.
- [28] M. H. Sorouraddin, K. Amini, A. Naseri, J. Vallipour, J. Hanaee, M.R. Rashidi, *J. Biosci*. 2010,35, 395.
- [29] S. Schnell, P.K. Maini, Comments on Theoretical Biology, 2003, 8, 169.

#### **CHAPTER V**

- [1] R. Baronas, F. Ivanauskas, J. Kulys, Sensors. 3 (2003) 248–262.
- [2] R. Baronas, F. Ivanauskas, J. Kulys, M. Sapagovas, J. Math. Chem. 34 (2003) 227–242.
- [3] J. Kulys, R. Baronas, Sensors. 6 (2006) 1513–1522.
- [4] J. Kulys, Nonlinear Anal. Model. Control. 11 (2006) 285–292.
- [5] P. Manimozhi, A. Subbiah, L. Rajendran, Sensors Actuators, B Chem. 147 (2010) 290 -297.
- [6] A. Anitha, S. Loghambal, L. Rajendran, Am. J. Anal. Chem. 03 (2012) 495– 502.
- [7] M.E.G. Lyons, Int. J. Electrochem. Sci. 4 (2009) 77–103.
- [8] R. Baronas, J. Kulys, K. Petrauskas, J. Razumiene, J. Math. Chem. 49 (2011) 995–1010.
- [9] R. Baronas, F. Ivanauskas, J. Kulys, Springer, 2010. https://doi.org/978-90-481-3242-3.
- [10] L. Rajendran, R. Swaminathan, M. Chitra Devi, A Closer Look of Nonlinear Reaction-Diffusion Equations, Nova Science Publishers, Incorporated, New York, NY, 2020.
- [11] J.H. He, Y.O. El-Dib, J. Math. Chem. 58 (2020) 2245–2253.
- [12] A. Meena, L. Rajendran, J. Electroanal. Chem. 644 (2010) 50–59.
- [13] P. Jeyabarathi, M. Kannan, L. Rajendran, *Int. J. Eng. Adv. Technol.* 9 (2020) 1845–1853.
- [14] R. Swaminathan, K. Lakshmi Narayanan, V. Mohan, K. Saranya, L. Rajendran, *Int. J. Electrochem. Sci.* 14 (2019) 3777–3791.
- [15] K. Saranya, V. Mohan, L. Rajendran, J. Math. Chem. 58 (2020) 1230–1246.
- [16] J.H. He, F.Y. Ji, J. Math. Chem. 57 (2019) 1932–1934.

- [17] S. Vinolyn Sylvia, R. Joy Salomi, L. Rajendran, M. Abukhaled, *Solid State Technol*. 63 (2020) 10090–10106.
- [18] A.-M. Wazwaz, Appl. Math. Comput. 97 (1998) 37–44.
- [19] J. Visuvasam, A. Meena, L. Rajendran, J. Electroanal. Chem. 869 (2020) 114106.
- [20] M.E.G. Lyons, J. Solid State Electrochem. 24 (2020) 2751–2761.
- [21] B. Manimegalai, M.E.G. Lyons, L. Rajendran, J. Electroanal. Chem. 880 (2021) 114921.
- [22] K.M. Dharmalingam, M. Veeramuni, J. Electroanal. Chem. 844 (2019) 1–5.
- [23] M.C. Devi, P. Pirabaharan, M. Abukhaled, L. Rajendran, *Electrochim. Acta*. 345 (2020) 136175.
- [24] M.C. Devi, P. Pirabaharan, L. Rajendran, M. Abukhaled, *React. Kinet. Mech. Catal.* 130 (2020) 35–53.
- [25] J.Visuvasam, A. Meena, R. Swaminathan, L. Rajendran, *in: Adv. Chem. Eng.*, 2020: 1–12.
- [26] J.H. He, Ain Shams Eng. J. 11 (2020) 1411–1414.
- [27] C.-H. He, Y. Shen, F.-Y. Ji, J.-H. He, Fractals. 28 (2020) 2050011.
- [28] J.-H. He, J. Electroanal. Chem. 854 (2019) 113565.
- [29] J.-H. He, *Int. J. Mod. Phys. B.* 20 (2006) 1141–1199.
- [30] J.H. He, Comput. Methods Appl. Mech. Eng. 178 (1999) 257–262.
- [31] L. Rajendran, S. Anitha, [Electrochim. Acta (2013)], *Electrochim. Acta*. 102 (2013) 474–476.
- [32] J.H. He, Y.O. El-Dib, J. Math. Chem. 58 (2020) 2245–2253.
- [33] C. He, C. Liu, J. He, A.H. Shirazi, H. Mohammad-sedighi, Facta Universitatis: *Mechanical Engineering* (2021).

- [34] J.H. He, Y.O. El-Dib, *Numer. Methods Partial Differ. Equ.* 37 (2021) 1800–1808.
- [35] J.H. He, Y.O. El-Dib, Results Phys. 19 (2020).
- [36] K. Nirmala, B. Manimegalai, L. Rajendran, *Int. J. Electrochem. Sci.* 15 (2020) 5682–5697.



## LIST OF PUBLICATIONS IN PEER REVIEWED REPUTED INTERNATIONAL JOURNALS

#### **BASED ON THE THESIS**

- R. Swaminathan, B Manimegalai, K Venugopal, L Rajendran, Homotopy Perturbation Method and Variational Iteration Method for Solving the Nonlinear Equations with Variable Coefficients in Applied Sciences, AIP Conferences Proceedings. 2021 (In press).
- R. Swaminathan, R. Saravanakumar, Kothandapani Venugopal, L. Rajendran, Analytical Solution of Non Linear Problems in Homogeneous Reactions Occur in the Mass-Transfer Boundary Layer: Homotopy Perturbation Method, Int. J. Electrochem. Sci., 16 (2021) Article ID: 210644 (SCI Journal, IF=1.573)
- 3. **R. Swaminathan**, K. Venugopal, L. Rajendran M. Rasi, Marwan Abukhaled, Analytical Expressions For The Concentration and Current In The Reduction of Hydrogen Peroxide at a Metal-Dispersed Conducting Polymer Film, Quím. Nova 43 (1), (2020)58-65 (**SCI Journal, IF=0.668**)
- 4. **R. Swaminathan,** M. Chitra Devi, L. Rajendran, K. Venugopal, Sensitivity and Resistance of Amperometric Biosensors in Substrate Inhibition Processes, J. Electroanal. Chem., 895(2022) Article ID: 115527 (**SCI Journal, IF=4.464**)

## Reprint of Publications

International Journal of ELECTROCHEMICAL SCIENCE

www.electrochemsci.org

#### Analytical Solution of Non Linear Problems in Homogeneous Reactions Occur in the Mass-Transfer Boundary Layer: Homotopy Perturbation Method

Rajagopal Swaminathan<sup>1</sup>, R. Saravanakumar<sup>3</sup>, Kothandapani Venugopal<sup>2</sup>, L. Rajendran<sup>4,\*</sup>

Received: 3 February 2021/ Accepted: 27 March 2021 / Published: 30 April 2021

Mathematical models for mass transfer accompanied by a reversible homogeneous chemical reaction are discussed. This model is based on a system of nonlinear equations containing a nonlinear term related to reversible homogeneous reactions. When reactions arise in the mass-transfer boundary layer, the measurement of mass transfer to and from electrodes frequently needs the species concentrations. We can obtain the concentration of species by solving the nonlinear equations using the homotopy perturbation method. Our approximate analytical results are also compared with the simulation result. A satisfactory agreement is observed between our analytical and simulation results. The approximate analytical expression obtained here can be used to estimate the system's dynamical behaviour. The influence of the parameters on concentration is discussed and presented graphically.

**Keywords:** Mathematical modeling, Nonlinear equations, Homotopy perturbation method, Reversible homogeneous reactions.

#### 1. INTRODUCTION

Many electrode processes with homogeneous reactions that occur continuously in the mass-transfer boundary layer. These reactions involve splitting or forming in the process of deposition or degradation of metal-linking complexes, the interaction and dissociation of ions and redox soluble mediators. Quantitative studies of electrode-kinetics experiments as well as simulation of electrochemical reactor processes require the description of species concentrations at the electrode surface. Homogeneous reactions can strongly affect the concentration of species.

<sup>&</sup>lt;sup>1</sup> Department of Mathematics, VidhyaaGiri College of Arts and Science, Sivaganga - 630108, India

<sup>&</sup>lt;sup>2</sup> PG, Research & Department of Mathematics, Govt Arts College (Affiliated to Bharathidasan University), Kulithalai - 639120, India

<sup>&</sup>lt;sup>3</sup> Department of Mathematics, Anna University, University college of Engineering, Dindigul, India

<sup>&</sup>lt;sup>4</sup> Department of Mathematics, AMET (Deemed to be university), Kanathur, Chennai, India

<sup>\*</sup>E-mail: raj\_sms@rediffmail.com

The computation of concentration profiles near electrodes in the solution is based on the species conservation equation.

$$\frac{\partial c_i}{\partial t} = -\nabla \bullet N_i + R_i \tag{1}$$

where  $c_i$  is the molar concentration of species i, and  $R_i$  is the net rate of production of i locally by homogeneous reactions. The molar flux  $N_i$  and the rate of production of  $M_i^{z_i}$  usually represented by

$$N_i = -D_i \nabla c_i - z_i c_i D_i \frac{F}{RT} \nabla \phi + c_i v \text{ and } R_i = v_i \left[ k_r \prod_j c_j^{v_j} - k_f \prod_i c_i^{v_i} \right]$$
 (2)

This describes species transport through diffusion and convection and ion migration in an electric field [1]. When charged species are involved, equations 1-2 must be written for each species in solution and combined with the electroneutrality state  $\sum_{i} z_i c_i = 0$ , and  $\phi$  must be

determined.Implementation of appropriate boundary conditions on the electrode surface and in the bulk solution is needed for their solution. This kind of nonlinear problems occurs in many relevant situations, such as cyclic voltammetry, chronopotentiometry, rotating disk and ring-disk electrodes, and various boundary-layer flows with multiple geometries, system chemistries, flow and boundary conditions [2]-[6].

Recently Chapman et al [7] discuss the mass transfer at the electrodes for the homogeneous and fast reversible reaction. More recently the empirical expression of species concentration using the Taylor series method and hyperbolic function method was obtained by Mary et al. [8]. In this communication, we present a simple and effective homotopy perturbation approach for solving the nonlinear differential equation in the sense of mass transfer at the electrodes with reversible homogeneous reactions. An approximate analytical expression for the concentration of species in the homogeneous electrochemical reaction is obtained for various parameter values.

#### 2. MATHEMATICAL FORMULATION OF THE PROBLEM

Consider the reversible homogeneous reaction

$$A + B \underset{k_r}{\overset{k_f}{\longleftrightarrow}} C \tag{3}$$

A is formed at a known rate  $N_{Ao}$  at an electrode surface, and B is present in the bulk solution. The concentrations of A and C in the bulk solution are negligible, and the fluxes of B and C at the electrode surface are also zero. The homogeneous reaction forms the species C and diffuses into the bulk. For measuring concentration profiles, Eqs. (1) and (2) may be combined for each component. We assume the steady-state and ignore migration and convection in the diffusion layer [7]. In this case, the system of nonlinear one-dimensional reaction-diffusion equations becomes as follows [7]:

$$D\frac{d^{2}A(x)}{dx^{2}} = -k_{r}C(x) + k_{f}A(x)B(x)$$
(4)

$$D\frac{d^{2}B(x)}{dx^{2}} = -k_{r}C(x) + k_{f}A(x)B(x)$$
 (5)

$$D\frac{d^2C(x)}{dx^2} = k_r C(x) - k_f A(x)B(x)$$
(6)

The k coefficients denote the forward and reverse reaction rate constants, and A, B, and C represent the species concentrations. Both diffusion coefficients are assumed to be equal to a constant D for the sake of consistency. The boundary conditions are

$$D\frac{dA}{dx} = -N_{Ao}; \frac{dB}{dx} = \frac{dC}{dx} = 0 \text{ at } x = 0$$
 (7)

$$A = 0;$$
  $B = B_b;$   $C = 0$  at  $x = \delta$  (8)

By introducing the following dimensionless variables

$$a = \left[\frac{A}{B_{b}}\right], b = \left[\frac{B}{B_{b}}\right], S = \left[\frac{C}{B_{b}}\right], z = \left[\frac{x}{\delta}\right],$$

$$\varepsilon = \left[\frac{D}{\delta^{2}k_{f}B_{b}}\right]^{\frac{1}{2}}, K^{*} = \left[\frac{k_{f}B_{b}}{k_{r}}\right], \mu = \left[\frac{N_{Ao}\delta}{DB_{b}}\right]$$
(9)

Eqns. (4)-(6) becomes in dimensionless form as follows:

$$\varepsilon^2 \frac{d^2 a(z)}{dz^2} = a(z)b(z) - \frac{S(z)}{K^*} \tag{10}$$

$$\varepsilon^2 \frac{d^2 b(z)}{dz^2} = a(z)b(z) - \frac{S(z)}{K^*} \tag{11}$$

$$\varepsilon^2 \frac{d^2 S(z)}{dz^2} = \frac{S(z)}{K^*} - a(z)b(z) \tag{12}$$

The corresponding dimensionless boundary conditions are,

$$a'(z=0) = \mu, \ b'(z=0) = 0, \ S'(z=0) = 0$$
 (13)

$$a(z=1)=0, b(z=1)=1, S(z=1)=0$$
 (14)

where  $\varepsilon$  is the relative rates of diffusion and reaction. $K^*$  is the homogeneous equilibrium constant.  $\mu$  is the rate of injection of A relative to the limiting flux of B toward the electrode

### 3. ANALYTICAL EXPRESSION OF THE CONCENTRATION USING HOMOTOPY PERTURBATION METHOD

The nonlinear equations (10)-(12), in recent years, numerous methods have been developed to derive analytical or semi-analytical solutions regardless of how strong the nonlinearity maybe. Homotopy analysis method [9,10], variational iteration method[11,12], Adomian decomposition method[13] and Green's function iterative method[14,15] are used to solve the nonlinear equations. Due to its simpleimplementation and high accuracy, the homotopy perturbation method(HPM)[16-20], Residual method[21], Padé approximants method[22], Akbari-lGanji's method (AGM)[23] and Taylor series method[24], the new approach of homotopy perturbation method(NHPM)[25,26] has received great deal of attention.

By solving equations (10)-(12) using the homotopy perturbation approach (details in Appendix A), the following approximate analytical representation of ionic concentration is obtained.

$$a(z) = \mu(z-1) + \frac{\mu}{120K^*\varepsilon^4} \left[ (z-1)(z^2 - 2z - 4)^2 + 20K^*\varepsilon^2(z^3 - 3z^2 + 2) \right]$$
 (15)

$$b(z) = 1 + \frac{\mu}{120K^* \varepsilon^4} \left[ (z - 1)(z^2 - 2z - 4)^2 + 20K^* \varepsilon^2 (z^3 - 3z^2 + 2) \right]$$
 (16)

$$S(z) = 1 - b(z) \tag{17}$$

#### 4. PREVIOUS ANALYTICAL RESULTS

Chapman [7] derived approximate distributions of concentration. Consider the case of small  $\varepsilon$ , that is, the case where the homogeneous rate constant  $k_f$  is largeenough to make  $\varepsilon$  small. If the first term  $\varepsilon$  is neglected, the following solutions are obtained from a quadratic algebraic equation for S.

$$S(z) = \frac{1}{2} \left[ \left( \mu(1-z) + 1 + \frac{1}{K^*} \right) - \left( \left( \mu(1-z) + 1 + \frac{1}{K^*} \right)^2 - 4\mu(1-z) \right)^{1/2} \right]$$
 (18)

$$a(z) = \mu(1-z) - S(z)$$

$$b(z) = 1 - S(z)$$
(19)

$$b(z) = 1 - S(z) \tag{20}$$

Recently, Mary et al. [8] used Taylor's series method (TSM) to obtain the analytical representation of species concentration as follows:

$$a(z) = b(z) + \mu z - \mu - 1$$

$$b(z) = m + \frac{\alpha z^{2}}{2 \varepsilon^{2}} + \frac{(m\mu)z^{3}}{\varepsilon^{2} 3!} + \frac{\alpha \beta z^{4}}{\varepsilon^{4} 4!} + \frac{1}{\varepsilon^{4}} \left[ \beta \mu m + 3\alpha \mu \right] \frac{z^{5}}{5!} + \frac{1}{\varepsilon^{6}} \left[ \alpha \beta^{2} + 6 \alpha^{2} + 4\varepsilon^{2} m \mu^{2} \right] \frac{z^{6}}{6!}$$

$$S(z) = 1 - b(z)$$
(23)

where 
$$\alpha = m(m - \mu - 1) + \frac{m-1}{K^*}$$
  $\beta = 2m - \mu - 1 + \frac{1}{K^*}$  (24)

The value of m is obtained by solving the following equation.

$$m + \frac{\alpha}{2\varepsilon^2} + \frac{m\mu}{\varepsilon^2 3!} + \frac{\alpha\beta}{\varepsilon^4 4!} + \frac{1}{\varepsilon^4} \left[ \mu \beta m + 3\mu\alpha \right] \frac{1}{5!} + \frac{1}{\varepsilon^6} \left[ \alpha\beta^2 + 6 \alpha^2 + 4\varepsilon^2 m \mu^2 \right] \frac{1}{6!} - 1 = 0 (25)$$

But in this method, it is very difficult to find the constant m. Our analytical results (Eqs. (15)-(17)) are easily computable when compared with Taylor's series solution (Eqns. (21)-(23)).

#### 5. NUMERICAL SIMULATION AND DISCUSSION

**Table 1.** Comparison of numerical solution of concentration of species a(z) with the analytical solutions by Homotopy perturbation method and Taylor series method for  $K^* = 1, \mu = -3$  and for different values  $\varepsilon$ .

		ě	$\varepsilon = 0.7$	7			á	$\varepsilon = 0.8$	3				$\varepsilon = 0.9$	l	
Z	Num	Our HPM Eq.(15)	Error % of HPM	TSM Eq.(21)	Error % of TSM	Num	Our HPM Eq.(15)	Error % of HPM	TSM Eq.(21)	Error % of TSM	Num	Our HPM Eq.(15)	Error % of HPM	TSM Eq.(21)	Error % of TSM
0	2.500	2.494	0.24	2.483	0.70	2.538	2.527	0.44	2.483	0.56	2.573	2.568	0.21	2.563	0.40
0.2	1.922	1.920	0.11	1.907	0.79	1.957	1.949	0.42	1.907	0.48	1.991	1.997	0.31	1.985	0.28
0.4	1.390	1.380	0.70	1.371	1.38	1.420	1.415	0.37	1.371	0.69	1.449	1.436	0.90	1.445	0.26
0.6	0.894	0.889	0.53	0.867	3.08	0.917	0.909	0.82	0.867	1.41	0.938	0.929	0.95	0.935	0.39
0.8	0.427	0.424	0.88	0.399	6.53	0.440	0.436	0.84	0.399	2.39	0.451	0.444	1.51	0.451	0.04
1	0.000	0.000	0.00	0.000	0.00	0.000	0.000	0.00	0.000	0.00	0.000	0.000	0.00	0.000	0.00
Av	erage %	error	0.41		2.08			0.48		0.92			0.65		0.23

**Table 2.** Comparison of numerical solution of concentration of species b(z) with the analytical solutions by Homotopy perturbation method and Taylor series method for  $K^* = 1, \mu = -3$  and for different values  $\varepsilon$ .

			<i>ε</i> = 1					$\varepsilon = 1.5$	i				$\varepsilon = 2$		
z	Num	Our HPM Eq.(16)	Error % of HPM	TSM Eq.(22)	Error % of TSM	Num	Our HPM Eq.(16)	Error % of HPM	TSM Eq.(22)	Error % of TSM	Num	Our HPM Eq.(16)	Error % of HPM	TSM Eq.(22)	Error % of TSM
0	0.607	0.603	0.68	0.599	1.30	0.740	0.737	0.34	0.737	0.35	0.821	0.816	0.62	0.822	0.10
0.2	0.629	0.624	0.80	0.614	1.41	0.754	0.747	0.91	0.752	0.32	0.832	0.827	0.64	0.832	0.10
0.4	0.690	0.687	0.42	0.658	1.98	0.794	0.789	0.68	0.791	0.42	0.859	0.855	0.54	0.858	0.16
0.6	0.776	0.778	0.15	0.735	2.04	0.853	0.849	0.47	0.848	0.53	0.900	0.896	0.41	0.898	0.22
0.8	0.883	0.885	0.25	0.847	1.65	0.925	0.921	0.39	0.919	0.58	0.949	0.946	0.33	0.947	0.28
1	1.000	1.000	0.00	1.000	0.00	1.000	1.000	0.00	1.000	0.00	1.000	1.000	0.00	1.000	0.00
Av	erage %	error	0.38		1.40			0.46		0.37		•	0.43		0.14

**Table 3.** Comparison of numerical solution of concentration of species S(z) with the analytical solutions by Homotopy perturbation method and Taylor series method for  $\varepsilon = 2$ ,  $\mu = -1$  and for different values  $K^*$ .

		K	$X^* = 0.$	.1			1	$K^* = 0.$	2			I	$X^* = 0.5$	5	
Z	Num	Our HPM Eq.(17)	Error % of HPM	TSM Eq.(23)	Error % of TSM	Num	Our HPM Eq.(17)	Error % of HPM	TSM Eq.(23)	Error % of TSM	Num	Our HPM Eq.(17)	Error % of HPM	TSM Eq.(23)	Error % of TSM
0	0.039	0.038	0.78	0.039	0.52	0.050	0.050	0.20	0.050	0.26	0.061	0.061	0.49	0.061	0.26
0.2	0.036	0.036	0.84	0.036	0.55	0.047	0.047	0.04	0.047	0.43	0.057	0.058	0.35	0.058	0.35
0.4	0.030	0.030	0.34	0.030	2.02	0.039	0.039	0.93	0.039	0.77	0.048	0.048	0.42	0.048	0.63
0.6	0.021	0.021	0.42	0.022	2.37	0.028	0.027	0.91	0.028	1.81	0.034	0.034	0.58	0.035	1.47
0.8	0.011	0.011	0.46	0.011	3.67	0.014	0.014	0.14	0.015	5.00	0.017	0.017	0.58	0.018	4.65
1	0.000	0.000	0.00	0.000	0.00	0.000	0.000	0.00	0.000	0.00	0.000	0.000	0.00	0.000	0.00
Av			1.52			0.37		1.38			0.40		1.23		

The differential Eqns. (10)-(12) with the corresponding boundary conditions has also been solved numerically using SCILAB/MATLAB program (Appendix-B). The numerical solution is compared with our analytical results ( HPM method) and previously available results ( Taylors series method) in Tables 1–3. There is no much difference in average error percentage between HPM and TSM. But we can easily calculate the concentration for all values of the parameter in HPM.

Also, a comparison between the analytical and numerical results are shown in Figures 1.The maximum error between analytical (HPM) and the numerical result is 1.35%. It is evident from Tables 1-12 and Fig. 1 that our results are very close to the exact simulation results.

**Table 4.** Comparison of our analytical expression of concentration of species a with the numerical result for various values of the parameter  $\mu$  and some fixed values parameter  $\varepsilon = 2, \mu = -1$  using Eqn. (15).

		$K^* = 1$			$K^* = 10$		I	$X^* = 1000$	
z									% of
~	Numerical	Our	% of	Numerical	Our	% of	Numerical	Our	deviatio
	Result	Eq.(15)	deviation	Result	Eq.(15)	deviation	Result	Eq.(15)	n
0	0.934	0.925	0.98	0.929	0.918	1.26	0.929	0.917	1.28
0.2	0.736	0.729	0.92	0.731	0.722	1.24	0.731	0.721	1.28
0.4	0.544	0.541	0.64	0.540	0.535	1.03	0.540	0.534	1.06
0.6	0.357	0.358	0.09	0.354	0.353	0.29	0.354	0.353	0.35
0.8	0.173	0.178	2.66	0.172	0.176	2.21	0.172	0.175	2.18
1	0.000	0.000	0.00	0.000	0.000	0.00	0.000	0.000	0.00
	Average per	centage error	:: 0.88	Average per	centage erro	or: 1.00	Average percentage error: 1.02		

**Table 5.** Comparison of our analytical expression of concentration of species b with the numerical result for various values of the parameter  $\mu$  and some fixed values parameter  $\varepsilon = 2$ ,  $\mu = -1$  using Eqn. (16).

		$K^* = 1$			$K^* = 10$		$K^* = 1000$			
z	Numerical	Our	% of	Numerical	Our	% of	Numerical	Our	% of	
	Result	Eq.(16)	deviation	Result	Eq.(16)	deviation	Result	eq.(16)	deviation	
0	0.934	0.925	0.99	0.929	0.918	1.26	0.929	0.917	1.28	
0.2	0.938			0.933	0.922	1.19	0.933	0.921	1.22	
0.4	0.948	0.941	0.79	0.944	0.935	1.01	0.944	0.934	1.03	
0.6	0.963	0.958	0.59	0.960	0.953	0.75	0.960	0.953	0.76	
0.8	0.981	0.978	0.35	0.980	0.976	0.43	0.980	0.975	0.45	
1	1.000 1.000 0.00			1.000 1.000 0.00			1.000 1.000 0.00			
	Average perc	entage error	r: 0.61	Average per	entage erro	r: 0.77	Average percentage error: 0.79			

**Table 6.** Comparison of our analytical expression of concentration of species S with the numerical result for various values of the parameter  $\mu$  and some fixed values parameter  $\varepsilon = 4$ ,  $\mu = -1$  using Eqn. (17).

		$K^* = 1$			$K^* = 10$			$K^* = 1000$		
z	Numerical	Our	% of	Numerical	Our	% of	Numerical	Our	% of	
	Result	Eq.(17)	deviation	Result	Eq.(17)	deviation	Result	Eq.(17)	deviation	
0	0.020	0.019	0.89	0.020	0.020	0.73	0.020	0.020	0.23	
0.2	0.018	0.018	0.79	0.019	0.019	0.64	0.019	0.019	0.65	
0.4	0.015	0.015	0.51	0.015 0.016 3.19			0.016	0.016	0.29	
0.6	0.011	0.011	0.25	0.011	0.011	0.45	0.011	0.011	0.44	
0.8	0.006				0.006	3.09	0.006	0.006	3.11	
1	0.000 0.000 0.00			0.000 0.000 0.00			0.000 0.000 0.00			
	Average per	centage err	or: 0.89	Average percentage error: 1.35			Average percentage error: 0.79			

**Table 7.** Comparison of our analytical expression of concentration of species a with the numerical result for various values of the parameter  $\mu$  and some fixed values parameter  $\varepsilon = 2$ ,  $K^* = 1$  using Eqn. (15).

		$\mu = -1$			$\mu = -1.5$			$\mu = -2$		
z	Numerical	Our	% of	Numerical	Our	% of	Numerical	Our	% of	
	Result	Eq.(15)	deviation	Result	Eq.(15)	deviation	Result	Eq.(15)	deviation	
0	0.934	0.925	0.98	1.388	1.404	1.18	1.875	1.850	1.33	
0.2	0.736	0.729	0.92	1.094	1.106	1.10	1.478	1.459	1.32	
0.4	0.544	0.541	0.64	0.811	0.818	0.88	1.094	1.082	1.15	
0.6	0.357	0.358	0.10	0.536	0.537	0.15	0.718	0.715	0.38	
0.8	0.173	0.178	2.65	0.267	0.261	2.40	0.348	0.356	2.18	
1	0.000 0.000 0.00			0.000 0.000 0.00			0.000 0.000 0.00			
	Average perce	entage error	: 0.88	Average per	centage erro	or: 0.95	Average percentage error: 1.06			

**Table 8.** Comparison of our analytical expression of concentration of species a with the numerical result for various values of the parameter  $\varepsilon$  and some fixed values parameter  $\mu = -1$ ,  $K^* = 4$  using Eqn. (15).

		$\varepsilon = 2$			ε=5			$\varepsilon = 8$		
z	Numerical	Our	% of	Numerical	Our	% of	Numerical	Our	% of	
	Result	Eq.(15)	deviation	Result	Eq.(15)	deviation	Result	Eq.(15)	deviation	
0	0.930	0.919	1.22	0.987	0.987	0.04	0.995	0.995	0.01	
0.2	0.732	0.723	1.20	0.786	0.788	0.21	0.793	0.795	0.25	
0.4	0.541	0.536	0.96	0.586	0.590	0.63	0.592	0.596	0.67	
0.6	0.355	0.354	0.26	0.387	0.393	1.49	0.391	0.397	1.52	
0.8	0.172	0.176	2.31	0.188	0.196	4.18	0.191	0.199	4.18	
1	0.000 0.000 0.00			0.000 0.000 0.00			0.000 0.000 0.00			
	Average perce	ntage error:	0.99	Average per	centage erre	or: 1.09	Average percentage error: 1.11			

**Table 9.** Comparison of our analytical expression of concentration of species b with the numerical result for various values of the parameter  $\mu$  and some fixed values parameter  $\varepsilon = 2$ ,  $K^* = 10$  using Eqn. (16).

		$\mu = -1$			$\mu = -1.5$			$\mu = -2$		
$\mathcal{Z}$	Numerical	Our	% of	Numerical	Our	% of	Numerical	Our	% of	
	Result	Eq.(16)	deviation	Result	Eq.(16)	deviation	Result	Eq.(16)	deviation	
0	0.9272	0.9173	1.07	0.8967	0.8873	1.05	0.8661	0.8497	1.92	
0.2	0.9329				0.8936	0.94	0.8737	0.8582	1.81	
0.4	0.9435	**************************************			0.9186 0.9108 0.85			0.8810	1.51	
0.6	0.9594	0.9530	0.66	0.9420	0.9360	0.64	0.9212	0.9147	0.71	
0.8	0.9798				0.9667	0.40	0.9617	0.9555	0.65	
1	1.0000 1.0000 0.00			1.000 1.000 0.00			1.0000 1.0000 0.00			
	Average perce	ntage error	: 0.72	Average perc	entage erro	r: 0.65	Average percentage error: 1.10			

**Table 10.** Comparison of our analytical expression of concentration of species b with the numerical result for various values of the parameter  $\varepsilon$  and some fixed values parameter  $\mu = -2$ ,  $K^* = 50$  using Eqn. (16).

		<i>ε</i> =1			$\varepsilon = 4$			$\varepsilon = 7$		
Z	Numerical	Our	% of	Numerical	Our	% of	Numerical	Our	% of	
	Result	Eq.(16)	deviation	Result	Eq.(16)	deviation	Result	Eq.(16)	deviation	
0	0.8652	0.8437	2.55	0.9607	0.9456	1.60	0.9867	0.9815	0.53	
0.2	0.8729	0.8530	2.33	0.9630	0.9487	1.51	0.9874	0.9825	0.50	
0.4	0.8936	0.8783	1.75	0.9690	0.9569	1.26	0.9895	0.9853	0.42	
0.6	0.9242	0.9155	0.95	0.9780	0.9691	0.92	0.9925	0.9895	0.30	
0.8	0.9614				0.9839	0.50	0.9960	0.9945	0.15	
1	1.0000	1.0000 1.0000 0.00			1.0000 1.0000 0.00			1.0000 1.0000 0.00		
	Average perce	entage error	: 1.27	Average pero	centage erro	or: 0.96	Average percentage error: 0.32			

**Table 11.** Comparison of our analytical expression of concentration of species S with the numerical result for various values of the parameter  $\varepsilon$  and some fixed values parameter  $\varepsilon = 4$ ,  $K^* = 100$  using Eqn. (17).

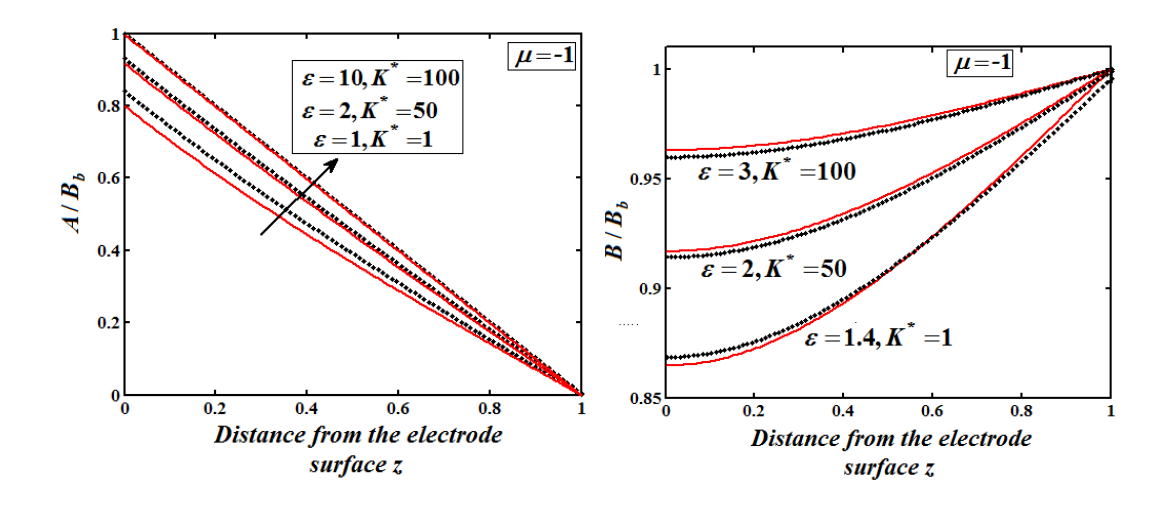
	$\mu = -1$			$\mu = -1.5$			$\mu = -2$		
z	Numerical	Our	% of	Numerical	Our	% of	Numerical	Our	% of
	Result	Eq.(17)	deviation	Result	Eq.(17)	deviation	Result	Eq.(17)	deviation
0	0.0200	0.0198	0.71	0.0297	0.0294	0.93	0.0393	0.0388	1.14
0.2	0.0189	0.0187	1.21	0.0280	0.0278	0.83	0.0370	0.0367	1.06
0.4	0.0157	0.0157	0.31	0.0234	0.0233	0.54	0.0310	0.0307	0.76
0.6	0.0115	0.0112	1.81	0.0167	0.0167	0.23	0.0220	0.0220	0.03
0.8	0.0057	0.0059	3.00	0.0085	0.0087	2.80	0.0112	0.0115	2.54
1	0.0000	0.0000	0.00	0.0000	0.0000	0.00	0.0000	0.0000	0.00
	Average percentage error: 1.17			Average percentage error: 0.89			Average percentage error: 0.92		

**Table 12.** Comparison of our analytical expression of concentration of species S with the numerical result for various values of the parameter  $\varepsilon$  and some fixed values parameter  $\mu = -2$ ,  $K^* = 500$  using Eqn. (17).

	$\varepsilon = 5$				$\varepsilon = 7$		$\varepsilon = 10$		
z	Numerical	Our	% of	Numerical	Our	% of	Numerical	Our	% of
	Result	Eq.(17)	deviation	Result	Eq.(17)	deviation	Result	Eq.(17)	deviation
0	0.0257	0.0255	0.63	0.0133	0.0133	0.27	0.0066	0.0066	0.09
0.2	0.0242	0.0241	0.51	0.0126	0.0126	0.17	0.0062	0.0062	0.59
0.4	0.0202	0.0202	0.17	0.0105	0.0105	0.24	0.0051	0.0052	1.61
0.6	0.0144	0.0145	0.63	0.0075	0.0076	1.03	0.0037	0.0037	1.87
0.8	0.0073	0.0075	3.18	0.0038	0.0039	3.60	0.0019	0.0020	2.75
1	0.0000	0.0000	0.00	0.0000	0.0000	0.00	0.0000	0.0000	0.00
	Average per	rcentage er	ror: 0.85	Average percentage error: 0.88			Average percentage error: 1.15		

The concentration of species depends upon the parameter relative rates of diffusion and reaction  $(\varepsilon)$ , rate of injection of A relative to the limiting flux of B toward the electrode  $(\mu)$  and homogeneous equilibrium constant  $(K^*)$ . Figure 1, shows the concentration of species a(z),b(z) and S(z) for various values of relative rates of diffusion and reaction and the homogeneous equilibrium constant.

From this fig.1, it is observed that an increase in equilibrium constant leads to increase in a(z) and b(z) and decreases in S(z). From this fig.2, it is noted that an increase in rate of injection leads to decrease in a(z), b(z) and S(z).



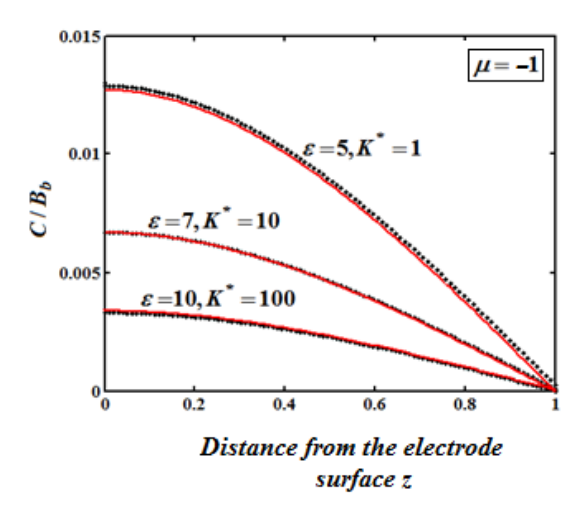


**Figure 1.** Comparison of concentrations a(z),b(z) and S(z) (Eqns. (15)-(17)) with simulation results for various values of parameters  $\varepsilon$ ,  $K^*$  and  $\mu$ .

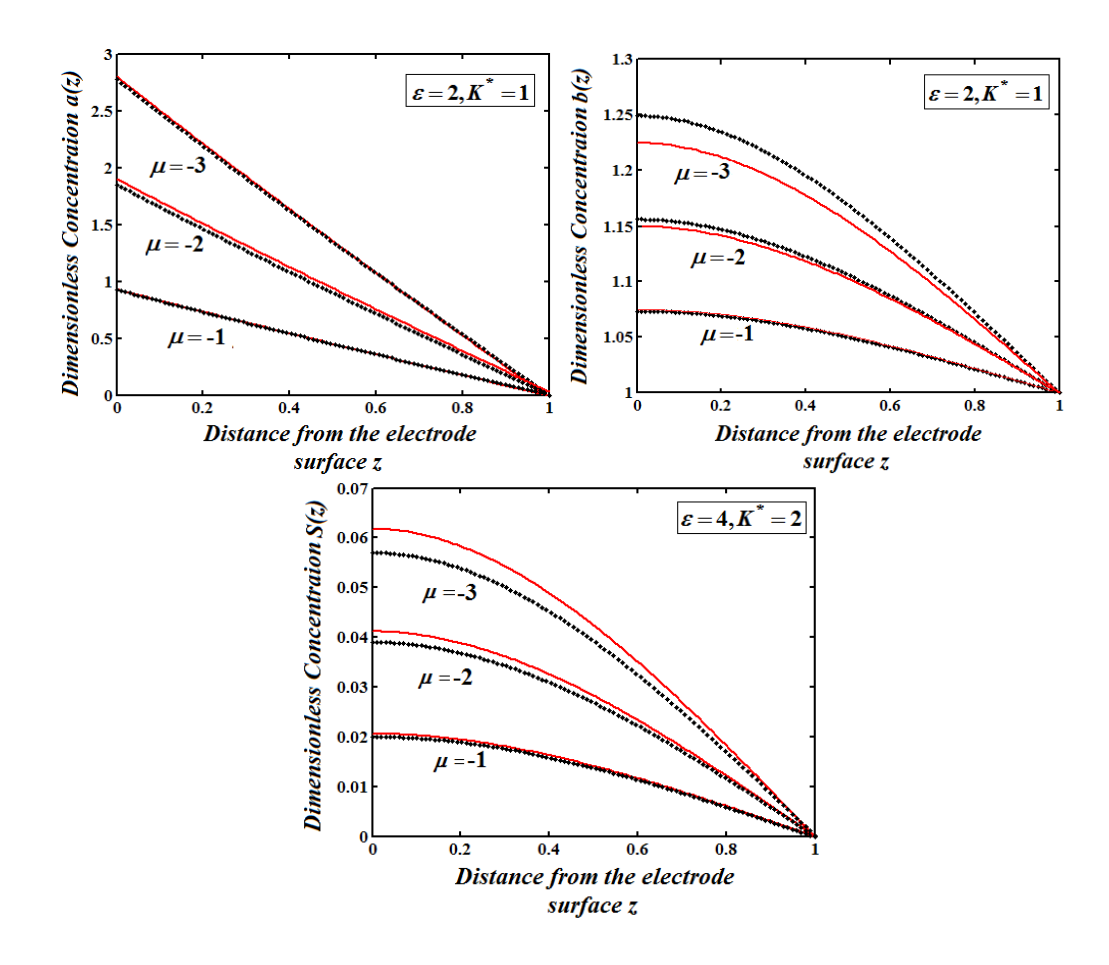


**Figure 2.** Comparison of concentrations a(z),b(z) and S(z) (Eqns. (15)-(17)) with simulation results for various values of parameters  $\varepsilon$ ,  $K^*$  and  $\mu$ .

#### 6. CONCLUSION

An analytical expression has effectively derived the concentration in the rotating disc electrode controlled by migration and convection in the diffusion layer for all values of the reaction rate constants. In this analysis, the model is apported to a rotating disk electrode in a one-dimensional situation. The nonlinear reaction-diffusion equations at steady-state are solved analytically by a new approach to HPM. There is a very good agreement between the analytical and the numerical solutions for all values of rate constant.

#### **ACKNOWLEDGMENT**

The Authors are also thankful to Shri J. Ramachandran, Chancellor, and Col. Dr G. Thiruvasagam, Vice-Chancellor, Dr. M. *Jayaprakashvel, Registrar*, Academy of Maritime Education and Training(AMET), Deemed to be University, Chennai, Tamilnadu, for their constant encouragement.

#### APPENDIX A: Analytical expression of the concentration using homotopy perturbation method

We construct the homotopy for the equations (10)-(12) as follows

$$(1-p)\left[\frac{d^2a}{dz^2}\right] + p\left[\frac{d^2a}{dz^2} - \frac{ab}{\varepsilon^2} + \frac{S}{K^*\varepsilon^2}\right] = 0 \tag{A1}$$

$$(1-p)\left[\frac{d^2b}{dz^2}\right] + p\left[\frac{d^2b}{dz^2} - \frac{ab}{\varepsilon^2} + \frac{S}{K^*\varepsilon^2}\right] = 0 \tag{A2}$$

$$(1-p)\left[\frac{d^2S}{dz^2} + \frac{ab}{\varepsilon^2}\right] + p\left[\frac{d^2S}{dz^2} + \frac{ab}{\varepsilon^2} - \frac{S}{K^*\varepsilon^2}\right] = 0$$
(A3)

where  $p \in [0,1]$  is an embedding parameter. Using Maclaurin series

$$a(z) = a(0) + za'(0) + z^2 \frac{a''(0)}{2!} + ...,$$
 (A4)

Now, assume that the solutions of Eqs. (A1) - (A3) is

$$a = a_0 + pa_1 + p^2 a_2 + \dots$$
  $b = b_0 + pb_1 + p^2 b_2 + \dots$  and  $S = S_0 + pS_1 + p^2 S_2 + \dots$  (A5)

Substituting Eq. (A5) into Eqs. (A1)-(A3) and equating the like coefficients of 'p' on both sides lead to the following linear differential equations:

$$p^0: \frac{d^2 a_0}{dz^2} = 0 {(A6)}$$

$$p^0: \frac{d^2b_0}{dz^2} = 0 (A7)$$

$$p^{0}: \frac{d^{2}S_{0}}{dz^{2}} + \frac{a_{0}b_{0}}{\varepsilon^{2}} = 0 \tag{A8}$$

Solving Eqs. (A6)-(A8) Subject to boundary conditions:

$$a_0(z=0) = \mu, b_0(z=0) = 0, S_0(z=0) = 0$$
 (A9)

$$a_0(z=1)=0, b_0(z=1)=1, S_0(z=1)=0$$
 (A10)

$$p^{1}: \frac{d^{2}a_{1}}{dz^{2}} - \frac{a_{0}b_{0}}{\varepsilon^{2}} + \frac{S_{0}}{K^{*}\varepsilon^{2}} = 0.$$
 (A11)

$$p^{1}: \frac{d^{2}b_{1}}{dz^{2}} - \frac{a_{0}b_{0}}{\varepsilon^{2}} + \frac{S_{0}}{K^{*}\varepsilon^{2}} = 0.$$
 (A12)

Solving Eqs. (A9) and (A10), subject to boundary conditions:

$$a_1(z=0) = \mu, b_1(z=0) = 0$$
 (A13)

$$a_1(z=1)=0, b_1(z=1)=1$$
 (A14)

The solution of the Eqns. (A6) to (A8) are given by

$$a_0(z) = \mu(z-1) \tag{A15}$$

$$b_0(z) = 1 \tag{A16}$$

$$S_0(z) = \frac{\mu(2 + z^3 - 3z^2)}{6\varepsilon^2}$$
 (A17)

and the solution of the Eqns. (A11) to (A12) are given by

$$a_1(z) = \frac{\mu}{120K^* \varepsilon^4} \left( (z - 1)(z^2 - 2z - 4)^2 + 20K^* \varepsilon^2 (z^3 - 3z^2 + 2) \right)$$
 (A18)

$$b_1(z) = \frac{\mu}{120K^*\varepsilon^4} \Big( (z - 1)(z^2 - 2z - 4)^2 + 20K^*\varepsilon^2 (z^3 - 3z^2 + 2) \Big)$$
 (A19)

With the use of these two iterations only, we obtain an approximate solution for the ionic concentration given by:

$$a(z) = a_0(z) + a_1(z)$$
  $b(z) = b_0(z) + b_1(z)$  (A20)

# APPENDIX B: Matlab program for the numerical solution of nonlinear differential equations (10)-(12)

function sol=ex6

ex6init=bvpinit(linspace(0,1),[0 1 1 0 0 0]);

sol = bvp4c(@ex6ode, @ex6bc, ex6init)

end

functiondydx=ex6ode(x,y)

dydx = [y(2)]

$$(1/(2)^2)*(y(1)*y(3)-((y(5))/(3)))$$

y(4)

$$(1/(2)^2)*(y(1)*y(3)-((y(5))/(3)))$$

y(6)

$$(1/(2)^2)*(((y(5))/(3)))-y(1)*y(3)];$$

end

Function res=ex6bc(ya,yb)

res=[ya(1)-0]

yb(2)-1

ya(3)-1

yb(4)-0

ya(5)-0

yb(6)-0];

end

#### NOMENCLATUREAND UNITS

Symbols	Name	Unit
$B_b$	Bulk concentration of species B	mol/cm <sup>3</sup>
A	Concentration of species A	mol/cm <sup>3</sup>
В	Concentration of species B	mol/cm <sup>3</sup>
С	Concentration of species C	mol/cm <sup>3</sup>
D	Diffusion coefficient	cm <sup>2</sup> /s
х	Distance from the electrode surface (Eqn.(2))	cm
δ	Diffusion layer thickness	cm
$k_r, k_f$	Reaction-rate constants	cm/s
$N_{Ao}$	Known rate constant	cm/s
$a = \frac{A}{B_b}, b = \frac{B}{B_b}, S = \frac{C}{B_b}$	Dimensionless concentration of the species A, B and C	None
z	Dimensionless distance from the electrode surface	None
ε	Dimensionless relative rates of diffusion and reaction	None
<i>K</i> *	Dimensionless homogeneous equilibrium constant	None
μ	Dimensionless rate of injection of A relative to the limiting flux of B toward the electrode	None

#### References

- 1. J. Newman and K. E. Thomas-Alyea, Electrochemical System, 3rd ed., Chap. 11and Appendix C, Prentice-Hall, Englewood Cliffs, NJ (2004).
- 2. V. G. Levich, Physicochemical Hydrodynamics, Prentice-Hall, Englewood Cliffs, NJ(1962).
- 3. A. J. Bard and L. R. Faulkner, Electrochemical Methods, John Wiley & Sons, New York (1980).
- 4. A. K. Hauser and John Newman, *J. Electrochem. Soc.*, 136 (1989) 2820.

- 5. C. Hofseth and T. W. Chapman, J. Electrochem. Soc., 138 (1991) 2321.
- 6. C. M. Villa and T. W. Chapman, *Ind. Eng. Chem. Res.*, 34 (1995) 3445.
- 7. T. W. Chapman, A. P. Barrios, and Y.Meas, J. Electrochem. Soc., 154 (2007) 411.
- 8. LC Mary, RU Rani, A Meena, L Rajendran, Int. J. Electrochem. Sci., 16 (2021) 151037.
- 9. K. Saravanakumar, L. Rajendran, Appl. Math. Model., 39,(2015) 117.
- 10. S. Liao, Appl. Math. Comput, 147 (2004) 490.
- 11. M. Abukhaled, J. Math., 2013 (2013) 1.
- 12. R. Saravanakumar, P. Pirabaharan, R. Swaminathan, Int. J. Res. 7 (2018) 342.
- 13. A. M. A. Wazwaz, Appl. Math. Comput., 102 (1999) 77.
- 14. M. Abukhaled, J. Comput. Nonlinear Dyn., 12 (2017) 051021.
- 15. M. Abukhaled, J. Electroanal. Chem., 792 (2017) 66.
- 16. J. H. He, Appl. Mech. Eng., 178 (1999) 257.
- 17. J.H. He, Ind. J. Phys., 88 (2014) 193.
- 18. R.Saravanakumar, P.Pirabaharan, Marwan Abukhaled, and L. Rajendran, *J. Phys. Chem. B*, 124 (2020) 443.
- 19. R. Swaminathan, K. Venugopal, M. Rasi, M. Abukhaled, L.Rajendran, Quim Nova, 43 (2020) 58.
- 20. R. Swaminathan, K.L Narayanan, V. Mohan, K. Saranya, L. Rajendran, *Int. J. Electrochem. Sci.*, 14 (2019) 37777.
- 21. K. Saranya, V. Mohan, L, Rajendran, J. Math. Chem., 58 (2020) 1230.
- 22. M. Chitra Devi, P. Pirabaharan, M. Abukhaled, L. Rajendran, *Electrochim. Acta*, 345 (2020) 136175.
- 23. B. Manimegalai, M.E.G. Lyons, L. Rajendran, J. Electroanal. Chem., 880 (2020) 114921.
- 24. R. Usha Rani, L. Rajendran, Chem. Phys. Lett., 754 (2020) 137573.
- 25. R. Swaminathan, K. Venugopal, L. Rajendran, M. Rasi, M. Abukhaled, *Quim. Nova*, 43,1(2020)1-8.
- 26. K.P.V. Preethi, M.C. Devi, R. Swaminathan, R. Poovazhaki, Int. J. Math. And Appl., 6 (2018) 359.
- © 2021 The Authors. Published by ESG (<u>www.electrochemsci.org</u>). This article is an open access article distributed under the terms and conditions of the Creative Commons Attribution license (http://creativecommons.org/licenses/by/4.0/).

## ANALYTICAL EXPRESSIONS FOR THE CONCENTRATION AND CURRENT IN THE REDUCTION OF HYDROGEN PEROXIDE AT A METAL-DISPERSED CONDUCTING POLYMER FILM

Rajagopal Swaminathan<sup>a</sup>, Kothandapani Venugopal<sup>b</sup>, Muthuramalingam Rasi<sup>c</sup>, Marwan Abukhaled<sup>d</sup>, Lakshmanan Rajendran<sup>c,\*,©</sup>

- <sup>a</sup>Department of Mathematics, Vidhyaa Giri College of Arts and Science, Sivaganga 630108, India
- <sup>b</sup>PG, Research & Department of Mathematics, Govt Arts College (Affiliated to Bharathidasan University), Kuliithalai 639120, India
- <sup>c</sup>Department of Mathematics, Lady Doak College, Madurai 625 002, India
- <sup>d</sup>Department of Mathematics and Statistics, American University of Sharjah, PO Box 26666 Sharjah, UAE
- <sup>e</sup>Department of Mathematics, Academy of Maritime Education and Training, Deemed to be University, Chennai 603 112, India

Recebido em 17/08/2019; aceito em 03/10/2019; publicado em 12/12/2019

A mathematical model describing the reduction of Hydrogen peroxide  $(H_2O_2)$  to water in a metal dispersed conducting polymer film is discussed. The model is based on a system of reaction-diffusion equations containing a non-linear term related to Michaelis—Menten kinetics of the enzymatic reaction. The approximate analytical expressions corresponding to the concentration of substrate and product for steady and non-steady state conditions have been obtained using a new approach to homotopy perturbation method (HPM). Approximate analytical expressions of the electrochemical oxidation current are also presented for steady and non-steady state conditions. The numerical simulation (Matlab program) response for concentration profiles was carried out and compared with the analytical results of this work and are found to be in good agreement. The influence of initial substrate concentration, the thickness of the film as well as the diffusion layer and kinetic parameters on the current response were investigated. A graphical procedure for estimating the kinetic parameters from the expression of the current response is also proposed.

**Keywords**: enzymatic biofuel cell; glucose oxidase; mathematical modeling; reaction-diffusion equation; homotopy perturbation method.

#### INTRODUCTION

Enzyme-based fuel cells can produce higher energy than conventional batteries utilizing significantly all the naturally good materials. Enzymatic biofuel cells rely on the oxidation of substrates such as hydrogen or glucose and reduction of oxygen to harvest energy from complex media. In particular, glucose biofuel cells (BFCs) represent a promising alternative to supply energy from living organisms to implanted electronic devices. Oxidase enzymes are widely used in energy devices (biosensor, enzymatic biofuel cell, bioreactor, etc.). In glucose oxidation-reduction process, oxygen is diminished to water (H<sub>2</sub>O) or hydrogen peroxide (H<sub>2</sub>O<sub>2</sub>). Glucose oxidase is found in nectar and goes about as a common additive. Enzymatic glucose biosensors utilize an electrode rather than oxygen to take up the electrons required to oxidize glucose and produce current in the extent to glucose fixation.1 Glucose oxidase is broadly used for the determination of free glucose in body liquids (diagnostics), in crude botanic material, and the nourishment business. Toghill and Compton discussed non-enzymatic glucose sensors.<sup>2</sup> It likewise has numerous applications in biotechnologies, commonly protein tests for natural chemistry incorporating biosensors in nanotechnologies.<sup>3</sup> Besides, glucose oxidase has damage the cancer tissue and cells as a result of hydrogen peroxide formation.

In recent times, many kinds of literature focused on glucose/hydrogen peroxide biofuel cell. Pizzariello *et al.* developed a glucose/hydrogen peroxide biofuel cell using a composite bulk modified bioelectrode based on a solid binding matrix.<sup>4</sup> Choudhury *et al.* discussed the effect of hydrogen peroxide as an oxidant in an alkaline direct borohydride fuel cell.<sup>5</sup> Bessette *et al.* reported the performance of the microfiber carbon electrode in magnesium—hydrogen

peroxide semi-fuel cell under optimum conditions and at a reduced concentration of  $H_2O_2$ .<sup>6</sup> Yamanaka *et al.* developed a three-phase  $H_2O_2$  fuel cell for the production of a concentrated aqueous solution of  $H_2O_2$  in an electrochemical reduction of  $O_2$ .<sup>7</sup>

Yang et al. investigated the influence of H<sub>2</sub>O<sub>2</sub> concentration in the performance of magnesium-hydrogen peroxide fuel cell with palladiumsilver deposited cathode and silver-nickel deposited electrode.8 Han et al. developed a hydrogen peroxide fuel cell with TiO<sub>2</sub> nanotube photoanode to increase the performance of the cell by make use of light and biomass.9 Also, Kjeang et al. demonstrated a microfluidic fuel cell incorporating hydrogen peroxide as oxidant. 10 Adams et al. reported an electrochemical reduction of hydrogen peroxide using highly active palladium platinum catalysts. 11 Do et al. developed a mathematical model which describes the bioelectrochemical reduction of hydrogen peroxide with direct electron transfer mechanism.<sup>12</sup> Benfeitas et al. investigated hydrogen peroxide metabolism in human erythrocytes.<sup>13</sup> The first example of glucose or hydrogen peroxide-based biofuel cell functioning under physiological conditions was reported in Agnès et al. 14 An et al. developed and tested the performance of an alkaline direct ethanol fuel cell with hydrogen peroxide as oxidant.<sup>15</sup> Also studied by An and coauthors, a one-dimensional mathematical model of the mixed potential in hydrogen peroxide fuel cell.<sup>16</sup>

Somasundaram *et al.* developed a kinetic model for the reduction of hydrogen peroxide to water in a metal-dispersed conducting polymer film.<sup>17</sup> This model is based on a system of the non-linear reaction-diffusion equation. Somasundaram *et al.* obtained the steady-state concentration and current for limiting cases (low and high substrate concentration) only.<sup>17</sup> In solving reaction-diffusion problems, there are mainly three types of methods: experimental, analytical, and numerical. Experiments are expensive, time-consuming, and usually, do not allow much flexibility in parameter variation. Numerical methods are popular for its computing

capabilities, although it provides only a long list of numbers, not an equation. Analytical methods are the most difficult ones, providing solutions with parameters. In this paper, we will consider the last two techniques to solve the coupled non-linear reaction-diffusion equation describing the reduction of hydrogen peroxide to water. The purpose of this communication is to derive the analytical expressions for the concentration of glucose (substrate), hydrogen peroxide (product) and current for non-steady state condition.

#### MATHEMATICAL FORMULATION

Figure 1 represents the schematic diagram for the reduction of hydrogen peroxide to water.

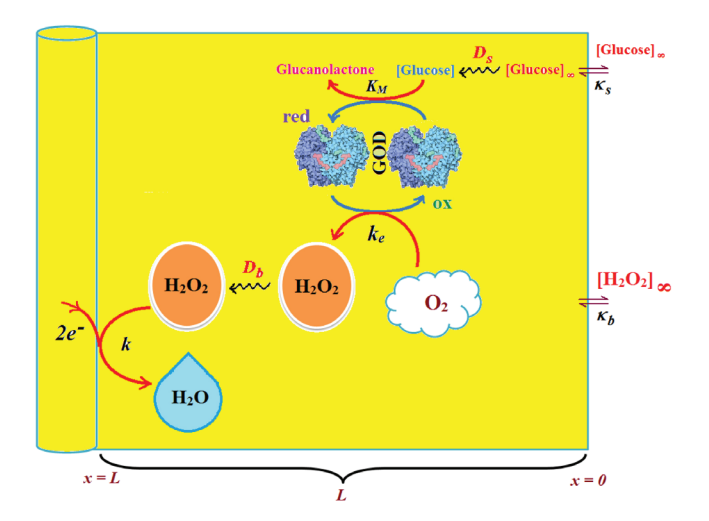


Figure 1. Schematic diagram for the reduction of hydrogen peroxide to water.

The reactions scheme occurring within the polymer film and in the bulk solution can be written as follows: 18

$$S + E_1 \underset{k}{\overset{k_1}{\longleftrightarrow}} E_1 S \xrightarrow{k_{cat}} P + E_2 \tag{1}$$

$$E_2 + A \xrightarrow{k_e} E_1 + B \tag{2}$$

$$B + 2e^{-} \xrightarrow{k} C \tag{3}$$

Eqn. (1) represents the oxidation of substrate (Glucose) S to product P (Hydrogen peroxide). Here  $E_1$  and  $E_2$  are the oxidized and reduced forms of the enzyme (oxidase) respectively. The reduction-oxidation process of the enzyme during the reduction of oxygen (A) to hydrogen peroxide (B) is shown in Eqn. (2). And the hydrogen peroxide which in turn reacts with microparticle in the presence of a pseudo first order rate constant k to produce water (C). Using Michaelis-Menten rate expression, the mass balance one dimensional equations for substrate and product within the polymer film can be written as follows: <sup>18</sup>

$$\frac{\partial s(x,t)}{\partial t} = D_S \frac{\partial^2 s(x,t)}{\partial x^2} - \frac{k_{cat} e_T s(x,t)}{K_M + s(x,t)} \tag{4}$$

$$\frac{\partial b(x,t)}{\partial t} = D_B \frac{\partial^2 b(x,t)}{\partial x^2} - kb(x,t) + \frac{k_{cat}e_T s(x,t)}{K_M + s(x,t)}$$
 (5)

where s(x,t) and b(x,t) are the concentrations of substrate and product respectively.  $D_S$  and  $D_B$  are the diffusion coefficients,  $k_{cat}$  is the catalytic reaction rate constant and  $K_M = (k_{cat} + k_{-1})/k_1$  is the

Michaelis-Menten rate constant. The initial and boundary conditions for the above equations are given by

$$t = 0, \ 0 < x < L$$
:  $s = k_s s_{\infty}, \ b = 0$  (6)

$$t > 0, \ x = 0: \quad \frac{\partial s}{\partial x} = 0, \quad \frac{\partial b}{\partial x} = 0$$
 (7)

$$t > 0, x = L: s = \kappa_s s_\infty, b = \kappa_b b_\infty$$
 (8)

Here  $s_{\infty}$  and  $b_{\infty}$  is the concentration of substrate and product in the bulk solution.  $k_s$  and  $k_b$  is the reaction rate constant for substrate and product respectively. L is the thickness of the polymer film. The current I of the product b at the electrode surface is given by

$$I = -nFAj_b = -nFAD_R(db/dx)_{x=L}$$
(9)

where  $j_b$  is the flux of the hydrogen peroxide at the electrode surface. Eqns. (4) and (5) can be written in dimensionless form using the following dimensionless parameters:

$$u = \frac{s}{\kappa_s s_{\infty}}, v = \frac{b}{\kappa_b b_{\infty}}, \chi = \frac{s}{L}, \tau = \frac{D_S t}{L^2}, \xi = \frac{D_B}{D_S},$$

$$\alpha = \frac{\kappa_s s_{\infty}}{K_M}, \beta = \frac{\kappa_b b_{\infty}}{K_M}, \gamma = \frac{kL^2}{D_S}, \varphi = \frac{k_{cat} e_T L^2}{D_S K_M}$$
(10)

Using Eqn. (10), equations (4) and (5) reduce to the following non-dimensional form:

$$\frac{\partial u(\chi,\tau)}{\partial \tau} = \frac{\partial^2 u(\chi,\tau)}{\partial \chi^2} - \frac{\varphi u(\chi,\tau)}{1 + \alpha u(\chi,\tau)}$$
(11)

$$\frac{\partial v(\chi,\tau)}{\partial \tau} = \xi \frac{\partial^2 v(\chi,\tau)}{\partial \chi^2} - \gamma v(\chi,\tau) + \frac{\alpha \varphi u(\chi,\tau)}{\beta (1+\alpha u(\chi,\tau))}$$
(12)

where  $u(\chi,\tau)$  and  $v(\chi,\tau)$  represents the dimensionless concentration of substrate and product respectively;  $\chi$  is a normalized distance;  $\tau$  is a dimensionless time;  $\xi$  is the ratio of the diffusion coefficient.  $\alpha$ ,  $\beta$ , and  $\gamma$  are the saturation parameters.  $\varphi$  is the Thiele modulus depends upon the enzyme concentration, diffusion coefficient of substrate  $D_S$  and the Michaelis-Menten constant  $K_M$ . The corresponding dimensionless initial and boundary conditions for equations (11) and (12) are as follows:

$$\tau = 0, \ 0 < \chi < 1: \ u = 1, \ v = 0$$
 (13)

$$\tau > 0, \ \chi = 0: \ \frac{\partial u}{\partial \chi} = 0, \ \frac{\partial v}{\partial \chi} = 0$$
 (14)

$$\tau > 0, \ \chi = 1: \ u = 1, \ v = 1$$
 (15)

The dimensionless current for hydrogen peroxide is

$$\Psi = -\frac{IL}{nFAk_b b_\infty D_B} = -\left(\frac{\partial v}{\partial \chi}\right)_{\gamma=1}$$
 (16)

# ANALYTICAL EXPRESSIONS FOR THE CONCENTRATION OF SUBSTRATE AND PRODUCT FOR GENERAL CASE UNDER NON STEADY CONDITION

Non-linear phenomena play a vital role in various zones of the sciences and engineering. Because of the expanding enthusiasm towards finding exact solutions for those problems, a variety of analytical methods are proposed. Recently Adomian decomposition

method, <sup>19</sup> homotopy analysis method, <sup>20</sup> variational iteration method, <sup>21,22</sup> homotopy perturbation method, <sup>23-26</sup> are used to solve the non-linear problems. Among such methods, a new approach of homotopy perturbation method is applied to solve the non-linear differential equations Eqns. (11) and (12). The focal point of this method is that it resulted in a simple approximate solution in the zeroth iteration itself. <sup>27</sup> This technique is appropriate for problems where transient effects, reaction-diffusion phenomena, and nonlinearity play important roles. The analytical expressions of concentrations of substrate and product can be obtained as follows (Appendix-A):

$$u(\chi,\tau) = \frac{\cosh(\sqrt{A}\chi)}{\cosh(\sqrt{A})} + \frac{16A}{\pi} \sum_{n=0}^{\infty} \frac{(-1)^n \cos[(2n+1)\pi\chi/2]e^{-[(2n+1)^2\pi^2 + 4A]^{\frac{\tau}{4}}}}{(2n+1)[(2n+1)^2\pi^2 + 4A]}$$
(17)

$$v(\chi,\tau) = \frac{\cosh(\sqrt{\gamma/\xi}\chi)}{\cosh(\sqrt{\gamma/\xi})} + \frac{\alpha_A}{\beta(\xi - A - \gamma)} \left(\frac{\cosh(\sqrt{\gamma/\xi}\chi)}{\cosh(\sqrt{\gamma/\xi})} - \frac{\cosh(\sqrt{A}\chi)}{\cosh(\sqrt{A/\xi})}\right) - \frac{\sum_{n=0}^{\infty} \mu_{An}(\tau)(-1)^n \cos[(2n+1)\pi\chi/2]}{\cosh(\sqrt{A/\xi})}$$
(18)

Using Eqns. (16) and (18), the dimensionless current is given by

$$\psi\left(\tau\right) = -\sqrt{\gamma/\xi} \ \tanh(\sqrt{\gamma/\xi}\,) - \frac{\alpha\mathcal{A}[\sqrt{\gamma/\xi} \ \tanh(\sqrt{\gamma/\xi}\,) - \sqrt{\mathcal{A}} \ \tanh(\sqrt{\mathcal{A}})]}{\beta\left(\xi \ \mathcal{A} - \gamma\right)} + \frac{\pi}{2} \sum_{n=0}^{\infty} \mu_{\mathcal{A}n}(\tau)(2n+1) \quad \text{(19)}$$

where

$$A = \varphi/(1 + \alpha) \tag{20}$$

$$\begin{split} \mu_{An}(\tau) &= \frac{4\pi\xi(2n+1)e^{-((2n+1)^2\pi^2\xi+4\gamma)\frac{\tau}{4}}}{[(2n+1)^2\pi^2\xi+4\gamma]} - \frac{64\alpha\,A^2e^{-((2n+1)^2\pi^2+4A)\frac{\tau}{4}}}{\pi\xi\beta\,(2n+1)[(2n+1)^2\pi^2+4A][(2n+1)^2\pi^2(\xi-1)-4(A-\gamma)]} \\ &\quad + \frac{64\pi\,\alpha\,A^2(2n+1)e^{-((2n+1)^2\pi^2\xi+4\gamma)\frac{\tau}{4}}}{\beta\,[(2n+1)^2\pi^2\xi+4\gamma][(2n+1)^2\pi^2\xi-4(A-\gamma)][(2n+1)^2\pi^2(\xi-1)-4(A-\gamma)]} \end{split} \tag{21}$$

When  $\tau \rightarrow \infty$ , equation (19) becomes

$$\psi_{ss} = -\sqrt{\gamma/\xi} \tanh(\sqrt{\gamma/\xi}) - \frac{\alpha A[\sqrt{\gamma/\xi} \tanh(\sqrt{\gamma/\xi}) - \sqrt{A} \tanh(\sqrt{A})]}{\beta(\xi A - \gamma)}$$
(22)

The above equation (Eqn. (22)) represents the new analytical expression of steady state current.

#### Limiting case

The consequences for the limiting situations of zero order kinetics  $(S >> K_M)$  and first order kinetics  $(S << K_M)$  arising from Eqns. (4) and (5) or (11) and (12) are reported below.

#### Case 1: Saturated (zero order) catalytic kinetics (High substrate)

In this case, the situation where the substrate concentration S is greater than the Michaelis-Menten constant  $K_M$  is considered. When  $S >> K_M$  or  $\alpha u >> 1$ , the non-linear Eqns. (11) and (12) reduces to the following dimensionless linear form:

$$\frac{\partial u(\chi,\tau)}{\partial \tau} = \frac{\partial^2 u(\chi,\tau)}{\partial \chi^2} - \frac{\varphi}{\alpha}$$
 (23)

$$\frac{\partial v(\chi,\tau)}{\partial \tau} = \xi \frac{\partial^2 v(\chi,\tau)}{\partial \chi^2} - \gamma v(\chi,\tau) + \frac{\varphi}{\beta}$$
 (24)

Solving the above Eqns. (23) and (24), the concentrations of substrate and product can be obtained as follows:

$$u(\chi,\tau) = 1 + \frac{\varphi}{2\alpha} (\chi^2 - 1) + \frac{16\varphi}{\pi^3 \alpha} \sum_{n=0}^{\infty} \frac{(-1)^n \cos[(2n-1)\pi\chi/2] e^{-[(2n-1)^2\pi^2]\frac{\tau}{4}}}{(2n-1)^3}$$
 (25)

$$\nu(\chi,\tau) = \frac{\cosh(\sqrt{\gamma/\xi}\chi)}{\cosh(\sqrt{\gamma/\xi})} + \frac{\varphi}{\beta\gamma} \left(1 - \frac{\cosh(\sqrt{\gamma/\xi}\chi)}{\cosh(\sqrt{\gamma/\xi})}\right) - \frac{4}{\pi} \sum_{n=0}^{\infty} \left\{ \frac{[\pi^2(2n+1)^2\xi - 4]e^{-i(2n+1)^2\pi^2\xi + 4\gamma}I_4^2}{(2n+1)[(2n+1)^2\pi^2\xi + 4\gamma]} \right\} \left[ -1\right)^n \cos[(2n+1)\pi\chi/2] \tag{26}$$

The expression for the current, in this case, is given by

$$\psi(\tau) = -\left(1 + \frac{\varphi}{\beta \gamma}\right) \sqrt{\gamma/\xi} \tanh(\sqrt{\gamma/\xi}) + 2 \sum_{n=0}^{\infty} \frac{[(2n+1)^2 \pi^2 \xi - 4]e^{-[(2n+1)^2 \pi^2 \xi + 4\gamma]^{\frac{\tau}{4}}}}{(2n+1)[(2n+1)^2 \pi^2 \xi + 4\gamma]}$$
(27)

From the above equation, the steady state  $(\tau \to \infty)$  current can be obtained as follows:

$$\psi_{ss} = -\left(1 + \frac{\varphi}{\beta \gamma}\right) \sqrt{\gamma/\xi} \tanh(\sqrt{\gamma/\xi})$$
 (28)

## Case 2: Unsaturated (first order) catalytic kinetics (Low substrate)

The situation where the substrate concentration S is less than the rate constant  $K_M$  is considered. In this case  $S << K_M$  or  $\alpha u << 1$ , the Eqns. (11) and (12) reduces to the following forms:

$$\frac{\partial u(\chi,\tau)}{\partial \tau} = \frac{\partial^2 u(\chi,\tau)}{\partial \chi^2} - \varphi u(\chi,\tau)$$
 (29)

$$\frac{\partial v(\chi,\tau)}{\partial \tau} = \xi \frac{\partial^2 v(\chi,\tau)}{\partial \chi^2} - \gamma v(\chi,\tau) + \frac{\varphi \alpha u(\chi,\tau)}{\beta}$$
(30)

The solutions for Eqns. (29) and (30) are given by

$$u(\chi,\tau) = \frac{\cosh(\sqrt{\varphi}\chi)}{\cosh(\sqrt{\varphi})} + \frac{16\varphi}{\pi} \sum_{n=0}^{\infty} \frac{(-1)^n \cos[(2n+1)\pi\chi/2]e^{-[(2n+1)^2\pi^2 + 4\varphi]^{\frac{\tau}{4}}}}{(2n+1)[(2n+1)^2\pi^2 + 4\varphi]}$$
(31)

$$\nu(\chi,\tau) = \frac{\cosh(\sqrt{\gamma/\xi}\,\chi)}{\cosh(\sqrt{\gamma/\xi}\,)} + \frac{\alpha\phi}{\beta(\xi\,\phi-\gamma)} \left(\frac{\cosh(\sqrt{\gamma/\xi}\,\chi)}{\cosh(\sqrt{\gamma/\xi}\,)} - \frac{\cosh(\sqrt{\phi}\chi)}{\cosh(\sqrt{\phi})}\right) - \sum_{n=0}^\infty \mu_{\phi,n}(\tau)(-1)^n \cos[(2n+1)\pi\chi/2] \right. \tag{32}$$

The current expression for this case is given by

$$\psi\left(\tau\right) = -\sqrt{\gamma/\xi} \tanh(\sqrt{\gamma/\xi}) - \frac{\alpha\phi[\sqrt{\gamma/\xi} \tanh(\sqrt{\gamma/\xi}) - \sqrt{\phi} \tanh(\sqrt{\phi})]}{\beta(\xi\phi - \gamma)} + \frac{\pi}{2} \sum_{n=0}^{\infty} \mu_{\phi n}(\tau)(2n+1) \tag{33}$$

where

$$\begin{split} \mu_{\phi,n}(\tau) &= \frac{4\pi\xi(2n+1)e^{-i(2n+1)^2\pi^2\xi+4\gamma]\frac{\tau}{4}}}{[(2n+1)^2\pi^2\xi+4\gamma]} - \frac{64\alpha\phi^2\,e^{-i(2n+1)^2\pi^2+4\phi]\frac{\tau}{4}}}{\pi\xi\beta(2n+1)[(2n+1)^2\pi^2+4\phi][(2n+1)^2\pi^2(\xi-1)-4(\phi-\gamma)]} \\ &\quad + \frac{64\pi\,\alpha\,\phi^2\,(2n+1)e^{-i(2n+1)^2\pi^2\xi+4\gamma]\frac{\tau}{4}}}{\beta\,[(2n+1)^2\pi^2\xi+4\gamma][(2n+1)^2\pi^2\xi-4(\phi-\gamma)][(2n+1)^2\pi^2(\xi-1)-4(\phi-\gamma)]} \end{split} \tag{34}$$

When  $\tau \rightarrow \infty$ , equation (33) becomes

$$\psi_{ss} = -\sqrt{\gamma/\xi} \tanh(\sqrt{\gamma/\xi}) - \frac{\alpha \phi \left[\sqrt{\gamma/\xi} \tanh(\sqrt{\gamma/\xi}) - \sqrt{\phi} \tanh(\sqrt{\phi})\right]}{\beta(\xi \phi - \gamma)}$$
 (35)

The analytical expressions of concentration of substrate, product and current for steady and non-steady state condition when  $\xi = 1$  for all the limiting cases are given in Table 1 and Table 2

#### NUMERICAL SIMULATION

To examine the accuracy of the solution obtained using the HPM method with a finite number of terms, the system of differential equations was solved numerically. Analytical solutions of equations (11) and (12) are challenging problems and can be obtained numerically with the help of Matlab software. The function pdex4 (Euler's method) in Matlab software, <sup>28</sup> which is a function for solving boundary value problems is used to solve Eqns. (11) and (12) numerically. Our results are compared with numerical results graphically in Figs. 2 and 3. The comparison confirmed that our obtained analytical results fitted very well with the numerical results. The maximum average relative error between the analytical and

**Table 1.** Summary of analytical expressions of concentrations of substrate, product and current for non-steady state condition when  $\xi = 1$ 

Conditions	This work	Previous work 18
	$u(\chi,\tau) = \frac{\cosh(\sqrt{A}\chi)}{\cosh(\sqrt{A})} + \frac{16A}{\pi} \sum_{n=0}^{\infty} \frac{(-1)^n \cos[(2n+1)\pi\chi/2]e^{-[(2n+1)^2\pi^2 + 4A]^{\frac{\tau}{4}}}}{(2n+1)[(2n+1)^2\pi^2 + 4A]}$	
Non steady state (HPM)	$v(\chi,\tau) = \frac{\cosh(\sqrt{\gamma}\chi)}{\cosh(\sqrt{\gamma})} + \frac{\alpha A}{\beta (A-\gamma)} \left(\frac{\cosh(\sqrt{\gamma}\chi)}{\cosh(\sqrt{\gamma})} - \frac{\cosh(\sqrt{A}\chi)}{\cosh(\sqrt{A})}\right) - \sum_{n=0}^{\infty} \mu_{An}(\tau)(-1)^n \cos[(2n+1)\pi\chi/2]$	
	$\psi(\tau) = -\sqrt{\gamma} \tanh(\sqrt{\gamma}) - \frac{\alpha A[\sqrt{\gamma} \tanh(\sqrt{\gamma}) - \sqrt{A} \tanh(\sqrt{A})]}{\beta(A - \gamma)} + \frac{\pi}{2} \sum_{n=0}^{\infty} \mu_{An}(\tau)(2n + 1)$	
	$u(\chi,\tau) = \frac{\cosh(\sqrt{\varphi}\chi)}{\cosh(\sqrt{\varphi})} + \frac{16\varphi}{\pi} \sum_{n=0}^{\infty} \frac{(-1)^n \cos[(2n+1)\pi\chi/2]e^{-[(2n+1)^2\pi^2 + 4\varphi]\frac{\tau}{4}}}{(2n+1)[(2n+1)^2\pi^2 + 4\varphi]}$	
High substrate	$v(\chi,\tau) = \frac{\cosh(\sqrt{\gamma}\chi)}{\cosh(\sqrt{\gamma})} + \frac{\varphi}{\beta\gamma} \left(1 - \frac{\cosh(\sqrt{\gamma}\chi)}{\cosh(\sqrt{\gamma})}\right) - \frac{4}{\pi} \sum_{n=0}^{\infty} \frac{(-1)^n [\pi^2 (2n+1)^2 - 4] \cos[(2n+1)\pi\chi/2]}{(2n+1)[(2n+1)^2\pi^2 + 4\gamma]} e^{-[(2n+1)^2\pi^2 + 4\gamma]\frac{\tau}{4}}$	
	$\psi (\tau) = -\left(1 + \frac{\alpha}{\beta \gamma}\right) \sqrt{\gamma} \tanh(\sqrt{\gamma}) + 2 \sum_{n=0}^{\infty} \frac{\left[\pi^{2} (2n+1)^{2} - 4\right] e^{-\left[(2n+1)^{2} \pi^{2} + 4\gamma\right]^{\frac{\tau}{4}}}}{\left[(2n+1)^{2} \pi^{2} + 4\gamma\right]}$	
Low substrate	$u(\chi,\tau) = \frac{\cosh(\sqrt{\varphi}\chi)}{\cosh(\sqrt{\varphi})} + \frac{16\varphi}{\pi} \sum_{n=0}^{\infty} \frac{(-1)^n \cos[(2n+1)\pi\chi/2]e^{-[(2n+1)^2\pi^2 + 4\varphi]\frac{\tau}{4}}}{(2n+1)[(2n+1)^2\pi^2 + 4\varphi]}$	
	$v(\chi,\tau) = \frac{\cosh(\sqrt{\gamma}\chi)}{\cosh(\sqrt{\gamma})} + \frac{\alpha\varphi}{\beta(\varphi-\gamma)} \left(\frac{\cosh(\sqrt{\gamma}\chi)}{\cosh(\sqrt{\gamma})} - \frac{\cosh(\sqrt{\varphi}\chi)}{\cosh(\sqrt{\varphi})}\right) - \sum_{n=0}^{\infty} \mu_{\varphi,n}(\tau)(-1)^n \cos[(2n+1)\pi\chi/2]$	
	$\psi(\tau) = -\sqrt{\gamma} \tanh(\sqrt{\gamma}) - \frac{\alpha \varphi \left[\sqrt{\gamma} \tanh(\sqrt{\gamma}) - \sqrt{\varphi} \tanh(\sqrt{\varphi})\right]}{\beta(\varphi - \gamma)} + \frac{\pi}{2} \sum_{n=0}^{\infty} \mu_{\varphi n}(\tau) (2n+1)$	

Table 2. Summary of analytical expressions of concentration of substrate, product and current for steady state condition when  $\xi = 1$ 

Conditions	This work	Previous work <sup>18</sup>
	$u(\chi) = \frac{\cosh(\sqrt{A}\chi)}{\cosh(\sqrt{A})}$	
Steady state (HPM)	$v(\chi) = \frac{\cosh(\sqrt{\gamma}\chi)}{\cosh(\sqrt{\gamma})} + \frac{\alpha A}{\beta (A - \gamma)} \left( \frac{\cosh(\sqrt{\gamma}\chi)}{\cosh(\sqrt{\gamma})} - \frac{\cosh(\sqrt{A}\chi)}{\cosh(\sqrt{A})} \right)$	
	$\psi_{ss} = -\sqrt{\gamma} \tanh(\sqrt{\gamma}) - \frac{\alpha A[\sqrt{\gamma} \tanh(\sqrt{\gamma}) - \sqrt{A} \tanh(\sqrt{A})]}{\beta (A - \gamma)}$	
	$u(\chi) = 1 + \frac{\varphi}{2\alpha} (\chi^2 - 1)$	
High substrate	$v(\chi) = \frac{\cosh(\sqrt{\gamma}\chi)}{\cosh(\sqrt{\gamma})} + \frac{\varphi}{\beta\gamma} \left( 1 - \frac{\cosh(\sqrt{\gamma}\chi)}{\cosh(\sqrt{\gamma})} \right)$	
	$\psi_{ss} = -\left(1 + \frac{\alpha}{\beta \gamma}\right) \sqrt{\gamma} \tanh(\sqrt{\gamma})$	
	$u(\chi) = \frac{\cosh(\sqrt{\varphi} \ \chi)}{\cosh(\sqrt{\varphi})}$	$u(\chi) = \frac{\cosh(\sqrt{\varphi} \ \chi)}{\cosh(\sqrt{\varphi})}$
Low substrate	$\nu(\chi) = \frac{\cosh(\sqrt{\gamma}\chi)}{\cosh(\sqrt{\gamma})} + \frac{\alpha\phi}{\beta(\phi - \gamma)} \left( \frac{\cosh(\sqrt{\gamma}\chi)}{\cosh(\sqrt{\gamma})} - \frac{\cosh(\sqrt{\phi}\chi)}{\cosh(\sqrt{\phi})} \right)$	$v(\chi) = \frac{\cosh(\sqrt{\gamma}\chi)}{\cosh(\sqrt{\gamma})} + \frac{\alpha\phi}{\beta(\phi - \gamma)} \left( \frac{\cosh(\sqrt{\gamma}\chi)}{\cosh(\sqrt{\gamma})} - \frac{\cosh(\sqrt{\phi}\chi)}{\cosh(\sqrt{\phi})} \right)$
	$\psi_{ss} = -\sqrt{\gamma} \tanh(\sqrt{\gamma}) - \frac{\alpha \phi \left[\sqrt{\gamma} \tanh(\sqrt{\gamma}) - \sqrt{\phi} \tanh(\sqrt{\phi})\right]}{\beta(\phi - \gamma)}$	$\psi_{ss} = -\sqrt{\gamma} \tanh(\sqrt{\gamma}) - \frac{\alpha \phi \left[\sqrt{\gamma} \tanh(\sqrt{\gamma}) - \sqrt{\phi} \tanh(\sqrt{\phi})\right]}{\beta(\phi - \gamma)}$

numerical results for substrate and product are 1.40% and 0.80%, respectively (Refer to Tables 3 and 4).

#### RESULTS AND DISCUSSION

Eqns. (17) to (19) represents the new analytical expressions for the dimensionless concentration of substrate, product and current respectively. Fig. 2 represents the dimensionless concentration of substrate  $u(\chi,\tau)$  versus dimensionless distance from the electrode  $\chi$  for different values of Thiele modulus  $\varphi$ , saturation parameter  $\alpha$  and time  $\tau$ . Thiele modulus is the ratio of the reaction rate to the rate of diffusion. From Fig. 2(a), it is inferred that the concentration of substrate decreases when Thiele modulus  $\varphi$  increases. When Thiele modulus  $\varphi < 0.1$ , the diffusion resistance is insufficient to limit the rate of reaction and the concentration remains the same within the film. The concentration of substrate reaches zero inside

62 Swaminathan et al. Quim. Nova

**Table 3.** Comparison of our analytical results of dimensionless substrate  $u(\chi, \tau)$  with numerical simulations for various values of  $\tau$  and  $\chi$  using Eqn. (17) when  $\varphi = 1$  and  $\alpha = 0.5$ 

		$\tau = 0.1$			$\tau = 0.5$			$\tau = 1$		$\tau = 100$		
χ	Analytical Eqn. (17)	Numerical	% of deviation	Analytical Eqn. (17)	Numerical	% of deviation	Analytical Eqn. (17)	Numerical	% of deviation	Analytical Eqn. (17)	Numerical	% of deviation
0	0.9365	0.9358	0.07	0.7961	0.7885	0.96	0.7513	0.7373	1.89	0.7394	0.7221	2.39
0.2	0.9372	0.9366	0.06	0.8032	0.7959	0.91	0.7606	0.7472	1.79	0.7493	0.7327	2.26
0.4	0.9401	0.9397	0.04	0.8251	0.8187	0.78	0.7888	0.7773	1.47	0.7792	0.7650	1.85
0.6	0.9478	0.9475	0.03	0.8633	0.8585	0.55	0.8369	0.8284	1.02	0.8300	0.8194	1.29
0.8	0.9653	0.9652	0.01	0.9204	0.9178	0.28	0.9066	0.902	0.50	0.9029	0.8973	0.62
1	1.0001	1	0.01	1	1	0	1	1	0	1	1	0
	Average % of deviation 0.04		0.04	Average % of deviation 0.58		0.58	Average % of deviation 1.11			Average % of deviation 1.40		

**Table 4.** Comparison of our analytical results of dimensionless product  $v(\chi, \tau)$  with numerical simulations for various values of  $\tau$  and  $\chi$  using Eqn. (18) when  $\varphi = 0.1$ ,  $\alpha = 0.5$ ,  $\beta = 0.05$ ,  $\gamma = 0.01$  and  $\xi = 1$ 

	$\tau = 0.7$				$\tau = 1$			$\tau = 2$			$\tau = 10$		
χ	Analytical Eqn. (18)	Numerical	% of deviation	Analytical Eqn. (18)	Numerical	% of deviation	Analytical Eqn. (18)	Numerical	% of deviation	Analytical Eqn. (18)	Numerical	% of deviation	
0	1.0237	1.037	1.28	1.1783	1.185	0.56	1.3063	1.309	0.20	1.3179	1.321	0.23	
0.2	1.0251	1.038	1.24	1.1725	1.179	0.55	1.2943	1.297	0.20	1.3053	1.308	0.20	
0.4	1.0289	1.04	1.06	1.1543	1.160	0.49	1.2579	1.260	0.16	1.2673	1.270	0.21	
0.6	1.0307	1.039	0.79	1.1218	1.126	0.37	1.1971	1.199	0.15	1.2039	1.206	0.17	
0.8	1.0237	1.028	0.41	1.0717	1.074	0.21	1.1113	1.112	0.06	1.1149	1.116	0.09	
1	0.9997	1	0.03	0.9998	1	0.02	0.9999	1	0.01	1	1	0	
	Average % of deviation 0.80		Average % of deviation 0.36		Average % of deviation 0.13		0.13	Average % of deviation		0.15			

the enzyme layer when the diffusion modulus i.e. Thiele module  $\varphi \ge 100$  which is observed at high film thickness L or enzymatic rate  $k_{cat}e_T$  or for low reaction rate constant  $K_M$  or diffusion  $D_s$ . This is because when  $\varphi$  is large, a significant diffusion modulus prevents a constant concentration of substrate within the film and thus lowers the concentration. The influence of the saturation parameter  $\alpha$  can be analyzed from Fig. 2(b), where it is shown that the concentration of substrate increases when the saturation parameter  $\alpha$  increases. This is because as the initial substrate concentration  $s_\infty$  increases obviously the concentration of substrate s increases. From Fig. 2(c), it is evident that the substrate concentration increases when time  $\tau$  decreases. For  $\tau \le 0.01$ , the concentration remains the same.

The change in product concentration with respect to dimensionless distance from the electrode for various values of parameters is shown in Figs. 3(a) – (f) respectively. Fig. 3(a) illustrates that for high catalytic activity, the concentration of substrate increases. By increasing the initial concentration of substrate  $\alpha$  or high catalytic activity, the product concentration increases as shown in Figs. 3(a) and 3(b). From Figs. 3(c) and 3(d), it is observed that, the concentration of product increases when the saturation parameters  $\beta$  and  $\gamma$  decreases. Compared to other parameters, time  $\tau$  has less influence over product concentration. Higher product concentration is obtained for steady- state time.

#### Differential sensitive analysis of kinetic parameters

Eqn. (19) represents the new approximate analytical expression for the non-steady state current  $\psi$  in terms of the parameters  $\alpha$ ,  $\beta$ ,  $\gamma$ ,  $\varphi$  and  $\xi$ . By differentiating the current partially with respect to these parameters, the impact of the parameters over current can be determined.<sup>29</sup> The percentages of change in current with respect to  $\gamma$ ,  $\beta$ ,  $\varphi$ ,  $\xi$  and  $\alpha$  are 46%, 35%, 14%, 3% and 2%, respectively. From

this, it is evident that parameters  $\gamma$  and  $\beta$  have more impact on current. These parameters are highly sensitive parameters. This implies that when the thickness of the film L or the concentration of product in the bulk  $b_{\infty}$  increases, the current increases. The parameter  $\varphi$  is called as moderately sensitive parameter as it has 14% of influence over current. The remaining two parameters  $\xi$  (ratio of diffusion coefficient) and  $\alpha$  (saturation parameter) are less sensitive. The spread sheet analysis of these results is described in Figure. 4. These results are also confirmed in Figures 5, 6(a)-6(e).

From Fig. 5, it is observed that the current initially increases with thickness and then decreases. After  $L \ge 2$  mm, the current reaches the steady state value. An interesting as well as important fact can be concluded from Figs. 6(a) - 6(e) regarding the influence of the kinetic parameters over current  $\psi(\tau)$  along time  $\tau$ . The current considerably depends on either the enzymatic rate within the film or the electron transport outside the film. From Fig. 6(a), it is confirmed that the current increases when the Thiele module  $\varphi$  increases. With increased initial concentration of substrate in bulk solution  $S_{\infty}$ , the corresponding current increases. This result is confirmed by Fig. 6(b). The influence of the saturation parameters  $\beta$  and  $\gamma$  on the current was shown in Figs. 6(c) and 6(d). Both parameters are inversely proportional to the current. Compared to  $\gamma$ ,  $\beta$  shows much deviation over current. From Fig. 6(e), it was found that the sharp decrease in the current with the increase of the ratio of diffusion coefficient  $\xi$ . And when  $\xi$  is small, the current decreases slowly. From this figure, it is observed that for high current, the diffusion coefficient of product should be less than the diffusion coefficient of substrate i. e.  $D_s < D_p$ .

#### Estimation of kinetic parameters k, $k_{cat}e_T$ and $K_M$

Numerous enzyme kinetics papers are dedicated for estimating

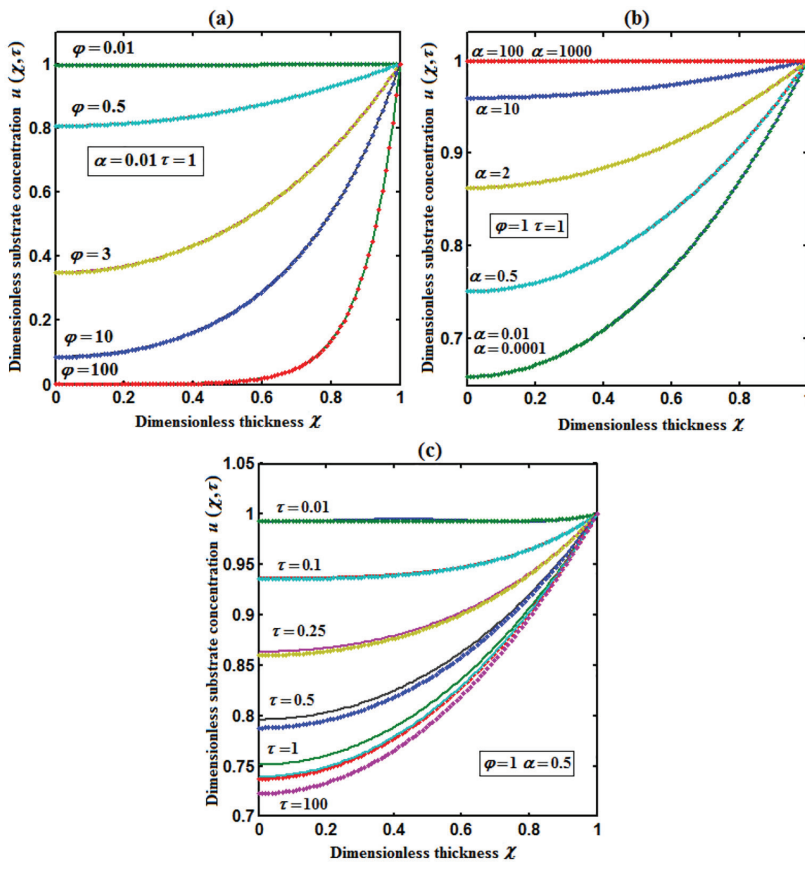


Figure 2. Plot of dimensionless concentration of substrate  $u(\chi,\tau)$  versus dimensionless thickness  $\chi$  calculated using Eqn. (17) for different values of (a) Thiele modulus  $\varphi$ , (b) saturation parameter  $\alpha$  and (c) time  $\tau$ . The key to the graph: (scattered line) represents the Eq. (17) and (dotted line) represents the numerical simulation.

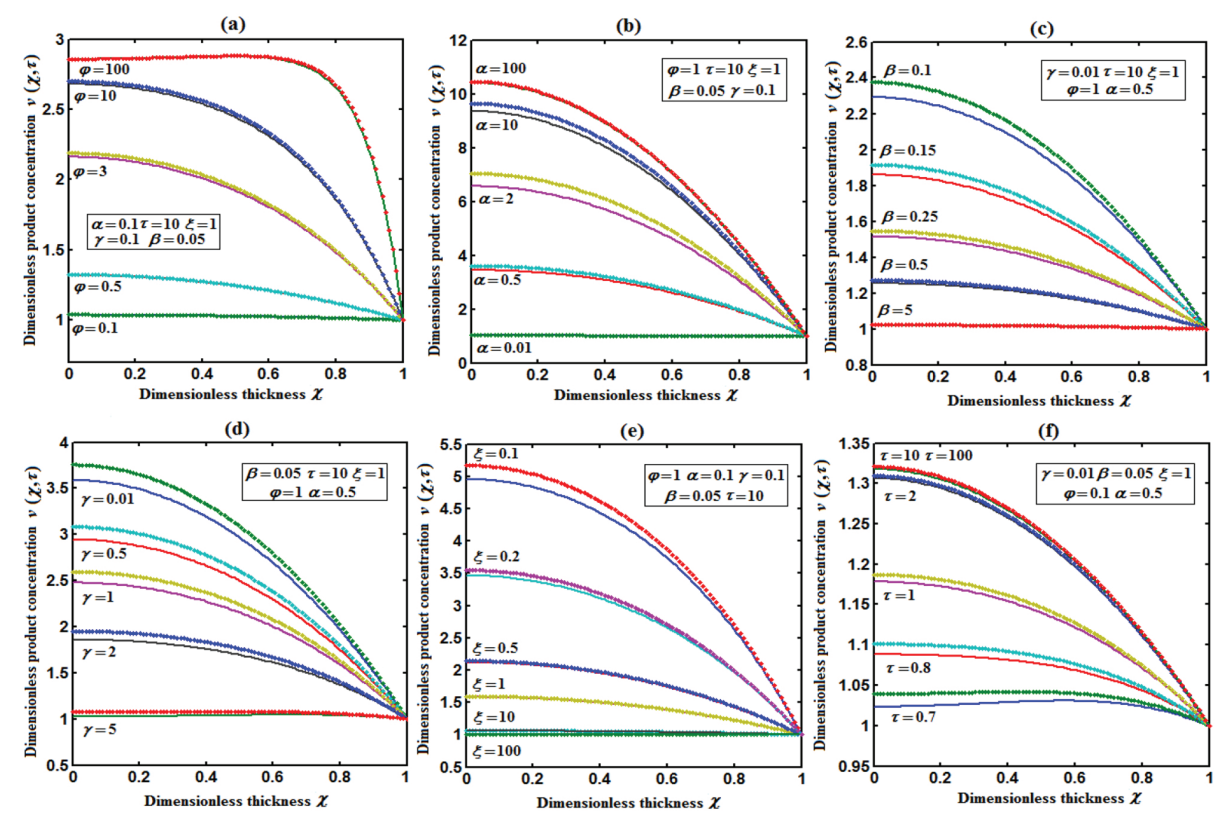


Figure 3. Plot of dimensionless concentration of product  $V(\chi,\tau)$  versus dimensionless thickness  $\chi$  calculated using Eqn. (18) for different values of (a) Thiele modulus  $\varphi$ , saturation parameters (b)  $\varphi$ , (c)  $\varphi$ , (d)  $\varphi$ , (e) diffusion parameter  $\varphi$  and (f) time  $\varphi$ . The key to the graph: (scattered line) represents the Eq. (18) and (dotted line) represents the numerical simulation.

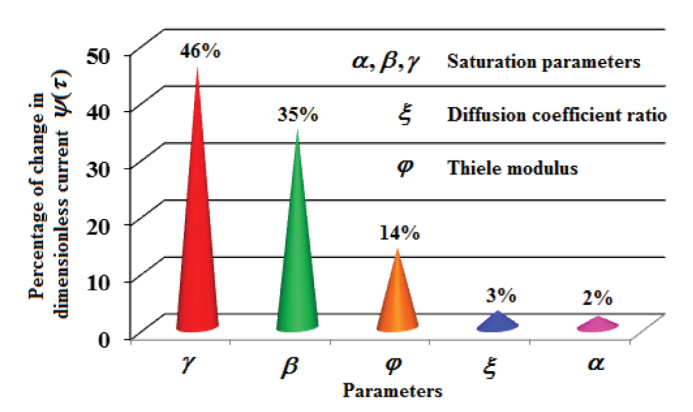


Figure 4. Sensitive analysis of parameters: Percentage change in current.

the kinetics parameters and distinguishing between reaction mechanisms.  $^{29\text{-}31}$  Pseudo first order constant k, helps us to quantify the rate of the chemical reaction. The Michaelis-Menten rate constant  $K_M$ , determines the relationship between the steady-state concentrations rather the equilibrium concentrations. The maximum velocity of the enzyme depends upon the catalytic rate constant  $k_{cat}$  and the total enzyme concentration  $e_T$ . The parameter  $k_{cat}$  is a very useful parameter that is employed for the breakdown of the enzyme substrate complex ES to product P when the enzyme is fully saturated with substrate. These kinetic parameters can be obtained from our analytical expression of current (Eqn. (28)). For small value of  $\gamma/\xi$ ,  $\tanh(\sqrt{\gamma}/\xi) \approx \sqrt{\gamma}/\xi$  and hence Eqn. (28) reduces to the following form:

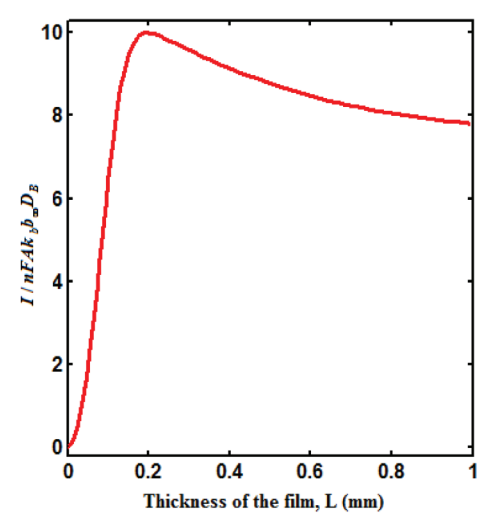
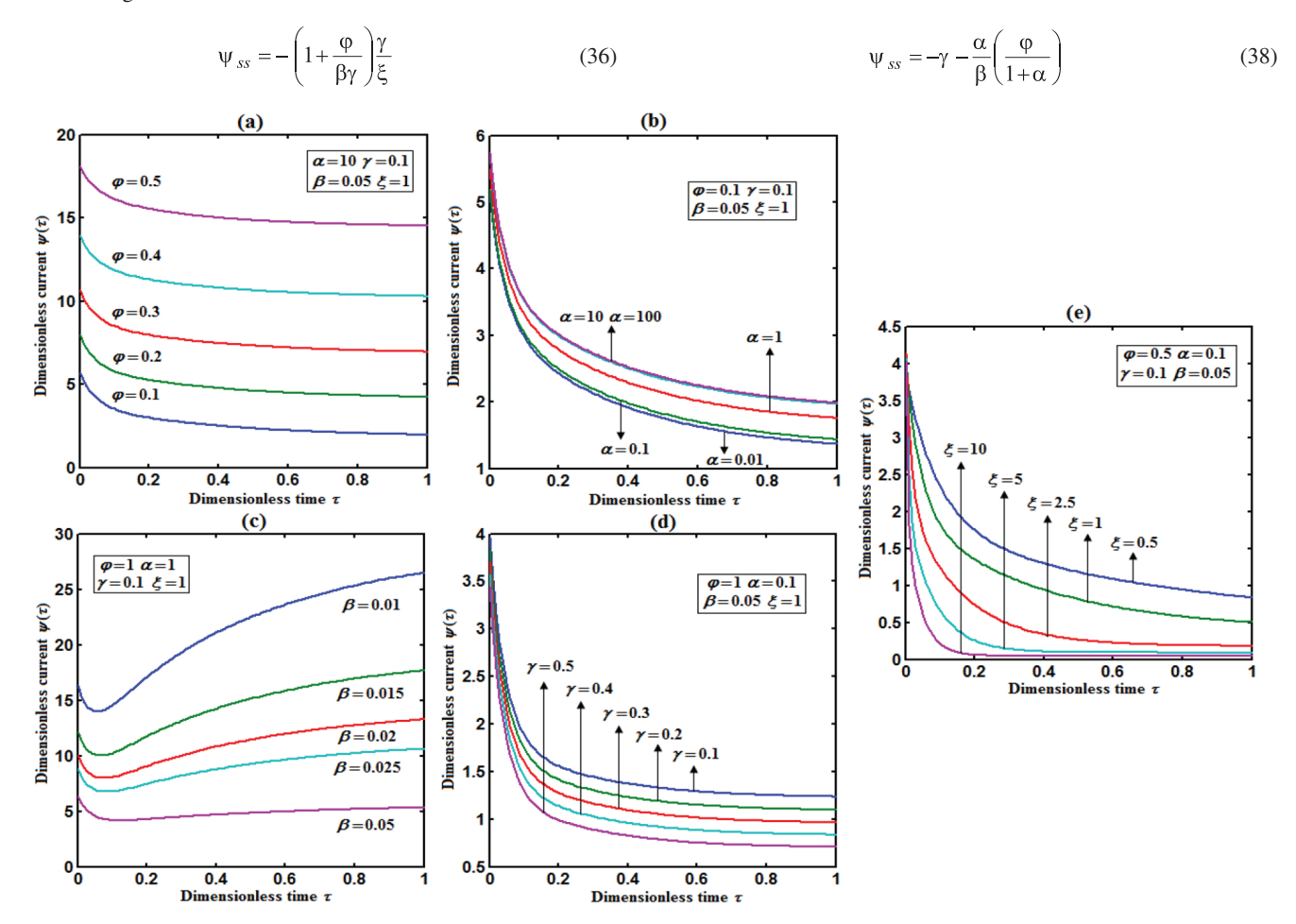


Figure 5. Plot of steady state current versus thickness of the film L.

Using Eqn. (10), the above equation can be rearranged as

$$\frac{I}{nFA\kappa_b b_{\infty}L} = k_{cat}e_T \left(\frac{1}{\kappa_b b_{\infty}}\right) + k \tag{37}$$

As in Fig. 7(a), plot of  $I/nFA\kappa_b D_{\infty}L$  versus  $1/\kappa_b D_{\infty}$  gives the slope = k, intercept =  $k_{cat}e_T$ . When the diffusion coefficient of substrate and product are equal i.e.  $\xi = 1$ , and  $\gamma$  is small, the current (Eqn. 22) becomes



**Figure 6.** Plot of dimensionless current  $\psi(\tau)$  versus dimensionless time  $\tau$  calculated using Eqn. (19) for different values of (a) Thiele modulus  $\varphi$ , saturation parameters (b)  $\alpha$ , (c)  $\beta$ , (d)  $\gamma$ , and (e) diffusion parameter  $\xi$ .

By substituting the value of  $\psi_{ss}$ ,  $\gamma$ ,  $\alpha$ ,  $\beta$  and  $\varphi$  from the Eqn. (10) and k,  $k_{cat}e_T$  from Eqn. (37), the parameter  $K_M$  can be obtained. Hence, we can obtain pseudo first order rate constant k, enzymatic rate  $k_{cat}e_T$  and Michaelis-Menten rate constant  $K_M$  from Eqns. (22) and (28).

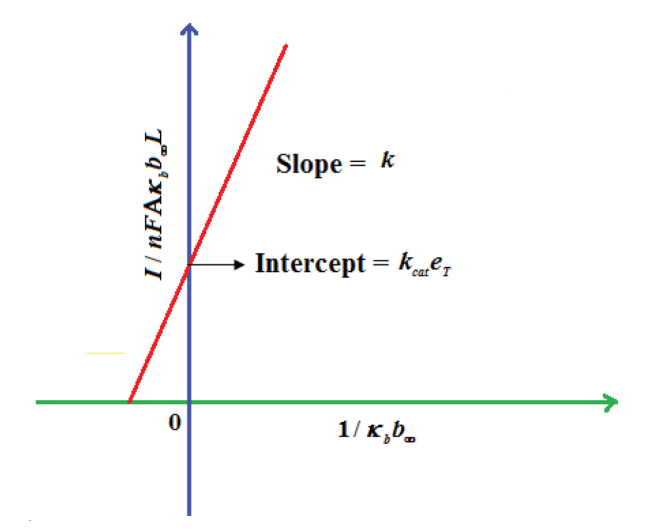


Figure 7. Estimation of kinetic parameter: pseudo first order rate constant k and enzymatic rate  $k_{cu}e_T$  using Eqn. (37).

#### **CONCLUSIONS**

A simple mathematical analysis of reaction and diffusion of glucose and hydrogen peroxide within the conducting film containing metal microparticles have been presented. Using a new approach to the Homotopy perturbation method, an approximate analytical expressions for the concentrations of substrate and product are obtained. Approximate analytical expressions for the steady and non-steady state current response produced during the reduction of  $\rm H_2O_2$  to water at the electrode surface are derived. The differential sensitive analysis for the steady-state current response for the controllable parameters: the thickness of the film, bulk substrate, and product concentration and enzymatic rate are analyzed. Also, the estimation of kinetic parameters is reported graphically.

#### SUPPLEMENTARY MATERIAL

The supplementary data associated with this article are available on http://quimicanova.sbq.org.br in the form of a PDF file, with free access.

#### ACKNOWLEDGMENTS

This work was supported by the Department of Science and Technology, SERB-DST (EMR/2015/002279) Government of India. The Authors are also thankful to Chancellor and Vice-Chancellor of the Academy of Maritime Education and Training (AMET), Deemed to be University, Chennai, India for their support and constant encouragement.

#### REFERENCES

- Palanisamy, S.; Cheemalapati, S.; Chen, S.M.; Int. J. Electrochem. Sci. 2012, 7, 8394.
- 2. Toghill, K. E.; Compton, RG.; Int. J. Electrochem. Sci. 2010, 5, 1246.
- Bankar, S. B.; Bule, M. V.; Singhal, R. S.; Ananthanarayan, L.; Biotechnol. Adv. 2009, 27, 489.
- Pizzariello, A.; Stred'ansky, M.; Miertuš, S.; Bioelectrochemistry. 2002, 56, 99
- Choudhury, N. A.; Raman, R. K.; Sampath, S.; Shukla, A. K.; *J. Power Sources* 2005, 143, 1.
- Bessette, R. R.; Medeiros, M.G.; Patrissi, C.J.; Deschenes, C. M.; LaFratta, C. N.; J. Power Sources 2001, 96, 240.
- Yamanaka I.; Onizawa T.; Takenaka S.; Otsuka K.; Angew. Chem. Int. Ed. 2003, 42, 3653.
- Yang, W.; Yang, S.; Sun, W.; Sun, G.; Xin, Q.; Electrochim. Acta 2006, 52, 9.
- Han, L.; Guo, S.; Wang, P.; Dong, S.; Adv. Energy Mater 2014, 5, 1400424.
- Kjeang, E.; Brolo, A. G.; Harrington, D.A.; Djilali, N.; Sinton, D.; Journal of Electrochemical Society 2007, 154, B1220.
- Adams, B. D.; Ostrom, C. K.; Chen, A.; Journal of Electrochemical Society 2011, 1588, B434.
- Do, T. Q. N.; Varničić, M.; Hanke-Rauschenbach, R.; Vidaković-Koch, T.; Sundmacher, K.; Electrochim. Acta. 2014, 137, 616.
- Benfeitas, R.; Selvaggio, G.; Antunes, F.; Coelho, P. M. B. M.; Salvador, A.; Free Radical Biology and Medicine, 2014, 74, 35.
- Agnès, C.; Reuillard, B.; Le Goff, A.; Holzinger, M.; Cosnier, S.; Electrochem. Commun. 2013, 34, 105.
- An, L.; Zhao, T. S.; Zeng, L.; Yan, X. H.; Int. J. Hydrog. Energy. 2014, 39, 2320.
- An, L.; Zhao, T. S.; Chai, Z. H.; Zeng, L.; Tan, P.; Int. J. Hydrog. Energy. 2014, 39, 7407.
- 17. Somasundrum, M.; Tongta, A.; Tanticharoen, M.; Kirtikara, K.; J. Electroanal. Chem. 1997, 440, 259.
- Ongun, M.Y.; Math Comput Model: An International Journal, 2011, 53, 507
- 19. Rasi, M.; Indira, K.; Rajendran, L.; J. Chem. Kinet. 2013, 45, 322.
- 20. Wazwaz, A.M.; Cent. Eur. J. Eng. 2014, 4, 64.
- 21. Meena, A.; Rajendran, L.; Chem. Eng. Technol. 2010, 33, 1999.
- Saravanakumar, R.; Pirabaharan, P.; Swaminathan, R.; International Journal of Research, 2018, 7, 342.
- 23. Wu, Y.; He, J. H.; Results Phys. 2018, 10, 270.
- 24. Rajendran, L.; Anitha, S.; *Electrochim. Acta* 2013, 102, 474.
- Swaminathan, R.; Lakshmi Narayanan, K.; Mohan, V.; Saranya, K.;
   Rajendran, L.; Int. J. Electrochem. Sci. 2019, 14, 3777.
- Preethi, K. P. V; Chitra Devi, M.; Swaminathan R.; Poovazhaki, R.; Int. J. Math. and Appl. 2018, 6, 359.
- 27. Skeel, R. D.; Berzins, M.; SIAM J. Sci. Comput. 1990, 11, 1.
- Rasi, M.; Rajendran, L.; Subbiah, A.; Sensor Actuat B-Chem. 2015, 208, 128
- 29. Rao, D.N.; Resonance, 1998, 3, 38.
- Sorouraddin, M.H.; Amini, K.; Naseri, A.; Vallipour, J.; Hanaee, J.; Rashidi, M.R.; J. Biosci. 2010, 35, 395.
- Schnell, S.; Maini, P. K.; Comments on Theoretical Biology, 2003, 8, 169.

FISEVIER

Contents lists available at ScienceDirect

### Journal of Electroanalytical Chemistry

journal homepage: www.elsevier.com/locate/jelechem



**Short Communication** 

# Sensitivity and resistance of amperometric biosensors in substrate inhibition processes



R. Swaminathan a, M. Chitra Devi b, L. Rajendran c,\*, K. Venugopal d

- <sup>a</sup> Department of Mathematics, Vidhyaagiri College of Arts and Science, Tamil Nadu, India
- <sup>b</sup> Department of Mathematics, Anna University, University College of Engineering, Dindigul, India
- <sup>c</sup> Department of Mathematics, AMET (Deemed to be University), Kanathur, Chennai, India
- <sup>d</sup> Government Arts College (Affiliated to Bharathidasan University, Tiruchirappalli), PG & Research Department of Mathematics, Kulithalai 639120, India

#### ARTICLE INFO

# Keywords: Mathematical modeling Non-linear equation Amperometric biosensor Sensitivity and resistance Non-michaelis-menten kinetics Substrate inhibition

#### ABSTRACT

A theoretical model of a sensitivity and resistance of amperometry biosensors with substrate inhibition kinetics is discussed. This model is based on the system of non-stationary diffusion equations containing a non-linear term related to non-Michaelis-Menten kinetics of the enzymatic reaction. This paper presents the approximate analytical expression of sensitivity and resistance of biosensor for small values of reaction diffusion parameters. The effect various parameters such as thickness of enzyme layer, bulk substrate concentration, Michaelis-Menten and saturation constant on sensitivity and resistance of biosensor are discussed.

#### 1. Introduction

Biosensors are approximate analytical devices that tightly combine biorecognition elements and physical transducer for the detection of the target compounds. An amperometric biosensor is a tool used in a solution to measure the concentration of a specific particular chemical or biochemical substances [1–4]. In biosensor, many enzymes are inhibited by their substrates. In the literature, the theoretical model has been widely applied as an essential tool to study and optimize the approximate analytical characteristics of biosensors. Practical biosensors contain a multilayer enzyme membrane; Exploratory monolayer membrane-containing biosensors are widely used to study the biochemical behavior of biosensors. The inhibition of substrates is often considered a biochemical oddity and experimental annoyance. This model is based on the system of non-stationary diffusion equations containing a nonlinear term related to non-Michaelis-Menten kinetics of the enzyme reaction [3].

The biosensor model with a substrate and product inhibition was constructed to reduce the number of biosensor properties. Manimozhi et al. [5] found the solution of steady-state substrate concentration in the case of substrate inhibition using the Homotopy perturbation method (HPM) and variational iteration method (VIM). Already the approximate analytical expression for steady-state concentrations of substrate and product with substrate inhibition using the Adomian decomposition method was discussed by Anitha et al. [6].

#### 2. Mathematical formulation of the problems

In the enzyme reaction,

$$E + S \leftrightarrow ES \to E + P \tag{1}$$

the substrate (S) binds to the enzyme (E) in order to form an enzymesubstrate complex ES. The substrate is converted to product (P) while it is part of this complex. The rate of the product's appearance depends on its substrate concentration.

For example, the simplest scheme of non-Michaelis-Menten kinetics may have been obtained by adding to the Michaelis-Menten scheme (Eq. (1)), a stage of enzyme-substrate complex (ES) interaction with another substrate molecule (S) (Eq. (2)) after the non-active complex (ESS) is generated as follows [10]:

E-mail address: raj\_sms@rediffmail.com (L. Rajendran).

A carbon nanotube based biosensor was mathematically modelled by Lyons [7,8]. The one-dimensional steady-state boundary value problem describing the transport and the kinetics of the substrate and the mediator in the two compartment domain was solved approximate analytically. Baronas et al. [9] proposed the mathematical model for the mediated biosensor with the CNT electrode deposited on the perforated membrane. In this paper, for small values of reaction/diffusion parameters, we have derived an approximate analytical expression of sensitivity and resistance of biosensor.

st Corresponding author.

$$ES + S \leftrightarrow ESS$$
 (2)

The steady-state non-linear differential equations for the substrate inhibition are [10]:

$$D_{s} \frac{\mathrm{d}^{2} s(x)}{dx^{2}} - \frac{V_{max} s(x)}{k_{m} + s(x) + \frac{(s(x))^{2}}{k}} = 0$$
(3)

$$D_{p} \frac{\mathrm{d}^{2} p(x)}{dx^{2}} + \frac{V_{max} s(x)}{k_{m} + s(x) + \frac{(s(x))^{2}}{k}} = 0$$
(4)

where  $D_s$ ,  $D_p$  are the diffusion coefficients of the substrate and product in the enzyme layer. s(x) and p(x) are the concentration of substrate and product in the enzyme layer.  $V_{max}$  is the maximal enzymatic rate,  $k_m$  denotes the Michaelis-Menten constant,  $k_s$  inhibition constant and d is the thickness of the enzyme layer. The corresponding boundary conditions are [10]

$$\frac{\mathrm{d}s(x)}{\mathrm{d}x} = 0, p(x) = 0 \text{ when } x = 0 \tag{5}$$

$$s(x) = s^*, p(x) = 0 when x = d$$
(6)

where  $s^*$  is the concentration of substrate at x=d and d is thickness of the enzyme layer. The modeling of the amperometric biosensor with the substrate inhibition reveals the complex kinetics of the biosensor response. At low substrate concentration, the kinetics looks like a simple substrate diffusion. When inhibition constant is large  $(k_s \to \infty)$ , the reaction kinetics is Michaelis-Menden model.

The steady-state current *I* of the biosensor is expressed as follows:

$$I = n_e F D_p \frac{dp(x)}{dx} \Big|_{x=0} \tag{7}$$

We introduce the set of dimensionless variables as follows:

$$\begin{split} S(\chi) &= \frac{s(x)}{s^*}, P(\chi) = \frac{p(x)}{s^*}, \chi = \frac{x}{d}, \phi_s^2 = \frac{V_{max}d^2}{D_s k_m}, \phi_p^2 = \frac{V_{max}d^2}{D_p k_m}, \\ \alpha &= \frac{s^*}{k_m}, \beta = \frac{(s^*)^2}{k_m k_s} \end{split} \tag{8}$$

where  $S(\chi)$  and  $P(\chi)$  indicate the dimensionless concentration of substrate and product respectively.  $\phi_s^2$  and  $\phi_p^2$  denote the corresponding reaction diffusion parameters.  $\chi$  represents the dimensionless distance.  $\alpha$  and  $\beta$  represents the saturation parameters. The governing non-linear reaction/diffusion Eqs. (3) and (4) are expressed in the following non-dimensionless form.

$$\frac{\mathrm{d}^2 S(\chi)}{\mathrm{d}\chi^2} - \frac{\phi_s^2 S(\chi)}{1 + \alpha S(\chi) + \beta (S(\chi))^2} = 0 \tag{9}$$

$$\frac{\mathrm{d}^2 P(\chi)}{\mathrm{d}\chi^2} + \frac{\phi_p^2 S(\chi)}{1 + \alpha S(\chi) + \beta (S(\chi))^2} = 0 \tag{10}$$

The boundary conditions are given by:

$$\frac{\mathrm{d}S}{\mathrm{d}\gamma} = 0, P = 0 \text{when} \gamma = 0 \tag{11}$$

$$S = 1, P = 0 when \gamma = 1 \tag{12}$$

The dimensionless current is reduced to

$$\psi = \frac{I}{n_e F D_P} \left[ \frac{d}{s^*} \right] = \frac{dP}{d\chi} \bigg|_{\chi = 0} \tag{13}$$

## 3. Approximate analytical expression of concentration of substrate and product

#### 3.1. Approximate solution using Taylor series method

Eqs. (9) and (10) are representing the system of nonlinear equations. It is very difficult to find the exact solution of these nonlinear

equations. Solving systems of nonlinear equations is perhaps one of the most difficult problems, especially in a diverse range of science and engineering applications. Recently so many approximate analytical methods [11] are used to solve the non-linear equations such as homotopy perturbation method [12–16], residual method [17], Taylor series method [18–21], AGM method [22–24],new approximate analytical method [25–27]. The concentration of substrate and product are obtained by solving the nonlinear Eqs. (9) and (10) using Taylor series method [28–30] (see Appendix A) as follows:

$$S(\chi) \approx 1 + S'(1)(x - 1) + \frac{1}{2} \frac{\phi_s^2(x - 1)^2}{1 + \alpha + \beta} + \frac{\phi_s^2 S'(1)(x - 1)^3}{1 + \alpha + \beta} \left( 1 - \frac{\alpha + 2\beta}{1 + \alpha + \beta} \right)$$
(14)

$$P(\chi) \approx P'(1)(x-1) - \frac{1}{2} \frac{\phi_p^2(x-1)^2}{1+\alpha+\beta} - \frac{\phi_p^2 S'(1)(x-1)^3}{1+\alpha+\beta} \left(1 - \frac{\alpha+2\beta}{1+\alpha+\beta}\right)$$
 (15)

where

$$S'(1) = \frac{2\phi_s^2(1+\alpha+\beta)}{2(1+2\alpha+2\beta)+2(\alpha+\beta)^2+\phi_s^2(1-\beta)}; P'(1)$$

$$= \frac{\phi_p^2(3+3\alpha+3\beta-l+\beta l)}{6(1+\alpha+\beta)^2}$$
(16)

#### 3.2. Approximate solution using new homotopy perturbation method

With the rapid development of nonlinear science, there appears an ever-increasing interest of scientists and engineers in the approximate analytical asymptotic techniques for nonlinear problems [31]. It is very difficult to solve nonlinear problems either numerically or theoretically. Perturbation methods provide the most versatile tools available in nonlinear analysis of engineering problems, and they are constantly being developed and applied to ever more complex problems. Homotopy perturbation method was first proposed by the He [32]. Recently, a new approach to HPM is presented to solve the nonlinear problem and this gives a simple approximate solution in the zeroth iteration [33]. By using this new homotopy perturbation [12,34,35] (Appendix B), the concentrations of substrate and products can be obtained as follows:

$$S(\chi) \approx \frac{\cosh(m\chi)}{\cosh(m)} \tag{17}$$

$$P(\chi) \approx \frac{\phi_p^2}{\phi_s^2} \left( \chi + \frac{1 - \chi - \cosh(m\chi)}{\cosh(m)} \right) \tag{18}$$

where 
$$m = \frac{\phi_s}{\sqrt{1 + \alpha + \beta}} = \sqrt{\frac{V_{max}d^2}{D_s(k_m + s^* + \frac{(s^*)^2}{D_s})}}$$
 (19)

The dimensionless current is

$$\psi = \frac{I}{n_e F D_P} \left[ \frac{d}{s^*} \right] = \frac{dP(\chi)}{d\chi} \Big|_{\chi=0} = \frac{\phi_p^2}{\phi_s^2} \left( 1 - \frac{1}{\cosh(m)} \right)$$
$$= \frac{D_s}{D_p} \left( 1 - \frac{1}{\cosh(m)} \right) \tag{20}$$

The value of steady-state current (I) is

$$\frac{I}{n_e F} = \frac{D_s s^*}{d} \left( 1 - \operatorname{sech} \left( \sqrt{\frac{V_{max} d^2}{D_s \left( k_m + s^* + \frac{\left( s^* \right)^2}{k_s} \right)}} \right) \right)$$
 (21)

The result obtained using new homotopy perturbation method is equivalent to approximate analytical expression derived by hyperbolic function method [36].

#### 3.3. Sensitivity of biosensor

The sensitivity is one of the most important characteristic of biosensors. The sensitivity  $B_S$  of a biosensor can be expressed as a gradient of the maximal biosensor current density with respect to the substrate concentration  $s^*$  [10]. The dimensionless sensitivity for the substrate concentration  $s^*$  is given by

$$B_{\mathcal{S}}(s^*) = \frac{s^*}{I(s^*)} \frac{\mathrm{d}I(s^*)}{\mathrm{d}s^*} = 1 + \left(\frac{1}{2} + \frac{s^*}{k_s}\right) \frac{s^*}{\left(k_m + s^* + \frac{(s^*)^2}{k_s}\right)} \frac{mtanh(m)}{1 - cosh(m)} \tag{22}$$

where  $B_S$  stands for the dimensionless sensitivity of the amperometric biosensor and  $I(s^*)$  is the density of the steady-state biosensor current calculated at the substrate concentration  $s^*$ . From the Eq. (22), it is conformed that the sensitivity  $B_S$  varies between -1 and 1.

#### 3.4. Resitance of biosensor

The resistance of the membrane-based biosensors to changes of the membrane thickness is introduced. The normalized dimensionless resistance  $B_R$  of the biosensor is expressed as the gradient of the steady-state biosensor current with respect to the enzyme layer thickness d [10],

$$B_R(d) = \frac{d}{I(d)} \frac{\mathrm{d}I(d)}{\mathrm{d}d} = \frac{mtanh(\mathrm{m})}{cosh(\mathrm{m}) - 1} - 1 \tag{23}$$

where  $B_R$  stands for the dimensionless sensitivity of the amperometric biosensor and I(d) is the steady- state biosensor current calculated at the thickness of the enzyme layer d. The resistance  $B_R$  varies between -1 and 1. The inverse of resistance is referred to as conductance, and such detection is referred to as conductometric electrochemical biosensor or simply conductometric biosensor [10]. The relationship between sensitivity and resistance are obtained from the Eqs. (22) and (23) as follows:

$$B_{S}(s^{*}) = 1 + \left(\frac{1}{2} + \frac{s^{*}}{k_{s}}\right) \frac{s^{*}}{\left(k_{m} + s^{*} + \frac{(s^{*})^{2}}{k_{s}}\right)} (B_{R}(d) + 1)$$
 (24)

#### 3.5. Thickness of the membrane

Using (18) we find approximate analytically the membrane thickness d, at which the steady-state current I gains the maximum at given parameters  $V_{max}$ ,  $D_s$ ,  $k_m$ ,  $k_s$  and  $s^*$ . We can rewrite the Eq. (18) as follows:

$$\frac{I(d)}{n_b F} = \frac{D_s \delta^*}{d} (1 - \operatorname{sech}(m))$$
(25)

We calculate a derivative of I(d) with the respect to the thickness d.

$$\frac{\partial I(d)}{\partial d} = n_e F D_s s^* \frac{1}{d^2} [(1 + m \tanh(m)) \operatorname{sech}(m) - 1]$$
(26)

And we're looking for *d*, where the derivative gets zero.

$$(1 + m \tanh(m))\operatorname{sech}(m) - 1 = -\cosh^{2}(m) + \cosh(m) + m \sinh(m)$$
$$= 0$$
(27)

Eq. (24) was solved numerically. A single solution  $m=m_{max}=1.5055$  was obtained. Consequentially, I gains the maximum at the membrane thickness d, where

$$d_{max} = m_{max} \sqrt{\frac{D_s \left(k_m + s^* + \frac{(s^*)^2}{k_s}\right)}{V_{max}}} = 285.65 \mu m$$
 (28)

at the values  $k_s = 10\mu M, k_m = 100\mu M, D_s = D_p = 300\mu m^2/s, s^* = 10\mu M$  and  $V_{max} = 1\mu M/s$  (values used in Fig. 4a).

#### 4. Result and discussion

Eqs. (14)–(19) are the simple and closed-form of approximate analytical expressions of sensitivity and resistance of amperometry biosensor with substrate inhabitation kinetics for the for different values of parameters such as substrate reaction–diffusion parameter ( $\phi_s^2$ ), product reaction–diffusion parameter ( $\phi_p^2$ ), thickness of membrane, diffusion coefficients and saturation parameters ( $\alpha$  and  $\beta$ ), respectively.

The error percentage between numerical and the approximate solution obtained by the Taylor series method and hyperbolic function method is less than 3.72% for small values of reaction–diffusion parameters (Tables 1 and 2). Here the analytical results are obtained

Table 1 Comparison of numerical solution of concentration of substrate with the analytical solutions obtained by hyperbolic function method and Taylor series method for  $\alpha = 0.1, \beta = 0.1$  and for different values of  $\phi_s^2$ .

χ	$\phi_s^2 = 0.$	5, m = 0.65				$\phi_s^2 = 1, m = 0.9$				
	NUM	NHPM Eq. (17)	TSM Eq. (14)	Error % for NHPM	Error % for TSM	NUM	NHPM Eq. (17)	TSM Eq. (14)	Error % for NHPM	Error % for TSM
0	0.8170	0.8226	0.8292	0.68	1.49	0.6768	0.6914	0.7156	2.15	5.73
0.25	0.8281	0.8333	0.8390	0.6	1.31	0.6959	0.7094	0.7303	1.94	4.94
0.5	0.8618	0.8658	0.8696	0.46	0.90	0.7540	0.7646	0.7784	1.41	3.24
0.75	0.9187	0.9209	0.9226	0.23	0.42	0.8539	0.8598	0.8663	0.69	1.44
1	1.0000	1.0000	1.0000	0.00	0.00	1.0000	1.0000	1.0000	0.00	0.00
	Average	Error %		0.40	0.82	Average	Error %		1.24	3.07

**Table 2** Comparison of numerical solution of concentration of product with the analytical solution obtained by hyperbolic function method and Taylor series method for  $\alpha = 0.1, \beta = 0.1, \phi_s^2 = 1$  and for different values of  $\phi_p^2$ .

χ	$\phi_p^{\ 2} = 0.5, m = 0.9$						$\phi_p^2 = 1, m = 0.9$					
	NUM	NHPM Eq. (18)	TSM Eq. (15)	Error % for NHPM	Error % for TSM	NUM	NHPM Eq. (18)	TSM Eq. (15)	Error % for NHPM	Error % for TSM		
0	0.0000	0.0000	0.0000	0.00	0.00	0.0000	0.0000	0.0000	0.00	0.00		
0.25	0.0309	0.0295	0.0282	4.41	8.69	0.0617	0.0591	0.0564	4.25	8.55		
0.5	0.0422	0.0405	0.0397	3.97	5.96	0.0844	0.0810	0.0794	3.97	5.96		
0.75	0.0327	0.0315	0.0313	3.65	4.24	0.0653	0.0630	0.0626	3.50	4.0		
1	0.0000	0.0000	0.0000	0.00	0.00	0.0000	0.0000	0.0000	0.00	0.000		
	Average	Error %		2.40	3.78	Average	Error %		2.34	3.72		

Here Num denotes numerical solution, NHPM- new homotopy perturbation method, TSM- Taylor series method.

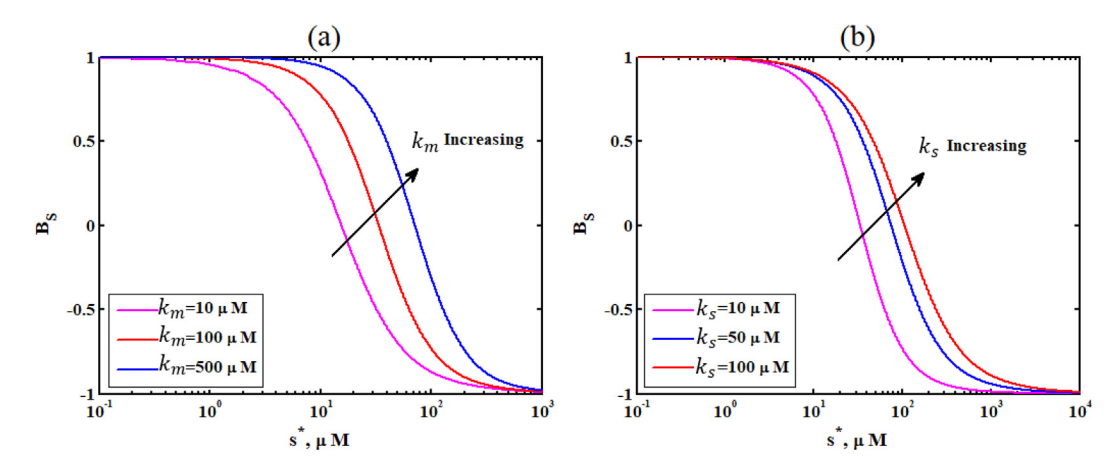


Fig. 1. The biosensor sensitivity using eqn. (22) for fixed values of  $D_s = D_p = 300 \mu m^2/s$ ,  $V_{max} = 1 \mu M/s$ ,  $d = 100 \mu m$ .(a).  $k_s = 10 \mu M$  and various values of  $k_s \mu M$ . (b).  $k_m = 100 \mu M$  and various values of  $k_s \mu M$ .

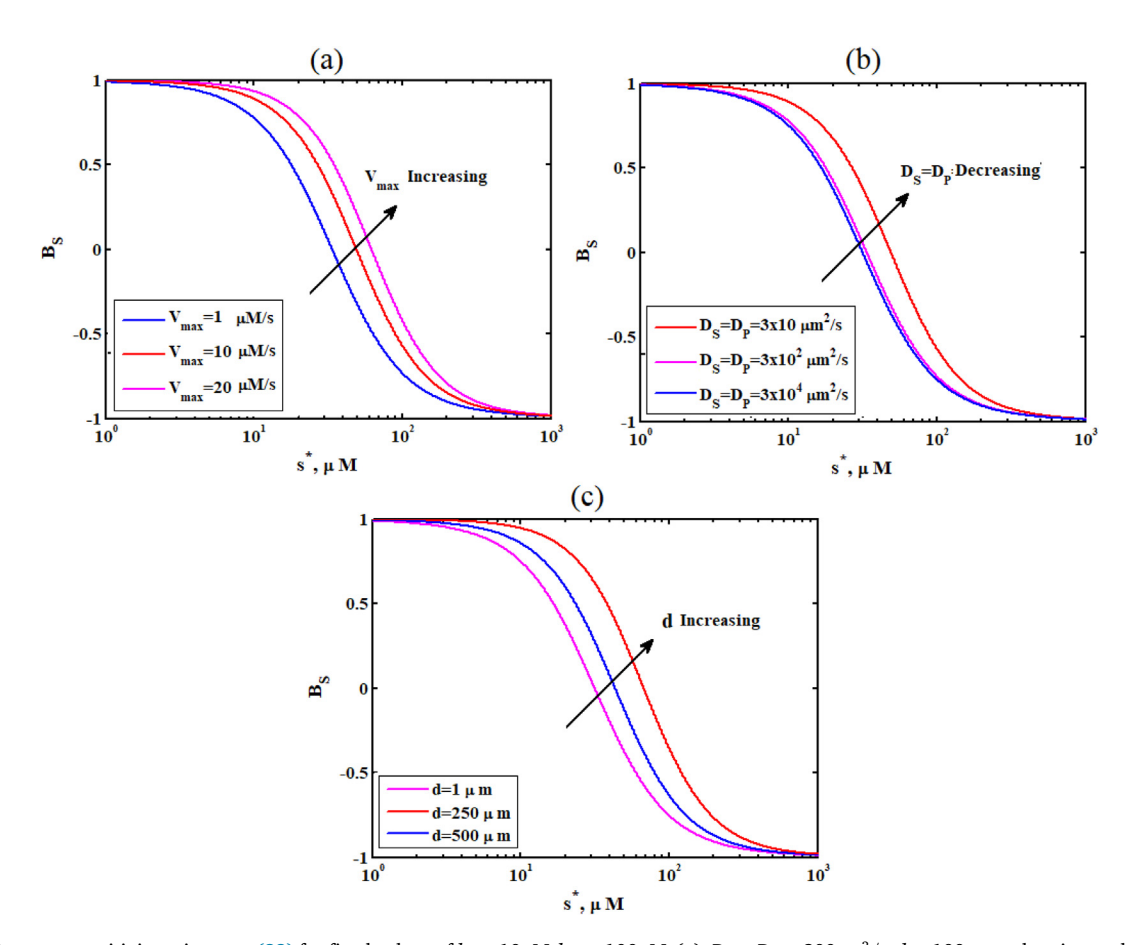


Fig. 2. The biosensor sensitivity using eqn. (22) for fixed values of  $k_s = 10\mu M$ ,  $k_m = 100\mu M$ . (a).  $D_s = D_p = 300\mu m^2/s$ ,  $d = 100\mu m$  and various values of  $V_{max}\mu M/s$ . (b).  $V_{max} = 1\mu M/s$ ,  $d = 100\mu m$  and various values of  $D_s = D_p\mu m^2/s$ . (c).  $D_s = D_p = 300\mu m^2/s$ ,  $V_{max} = 1\mu M/s$  and various values of  $V_{max}\mu M/s$ .

using three terms for the Taylor series and zeroth-order iteration for NHPM. The approximation accuracy should be increased by increasing high order terms in the Taylor series and iteration in NHPM.

#### 4.1. Sensitivity

The sensitivity is also one of the most important characteristics of the biosensors [10]. The biosensor sensitivity can be expressed as the gradient of the steady-state current with respect to the substrate concentration. Since the biosensor current as well as the substrate concentration varies even in orders of magnitude, especially when comparing different sensors, another useful parameter to consider is a dimensionless sensitivity.

The biosensor sensitivity for different values of the parameter are displays in the Figs. 1(a, b) and 2(a–c). It is notice that a decrease in all parameter leads to decrease in sensitivity. When  $s^* \approx 10^3 \mu M$  the sensitivity.

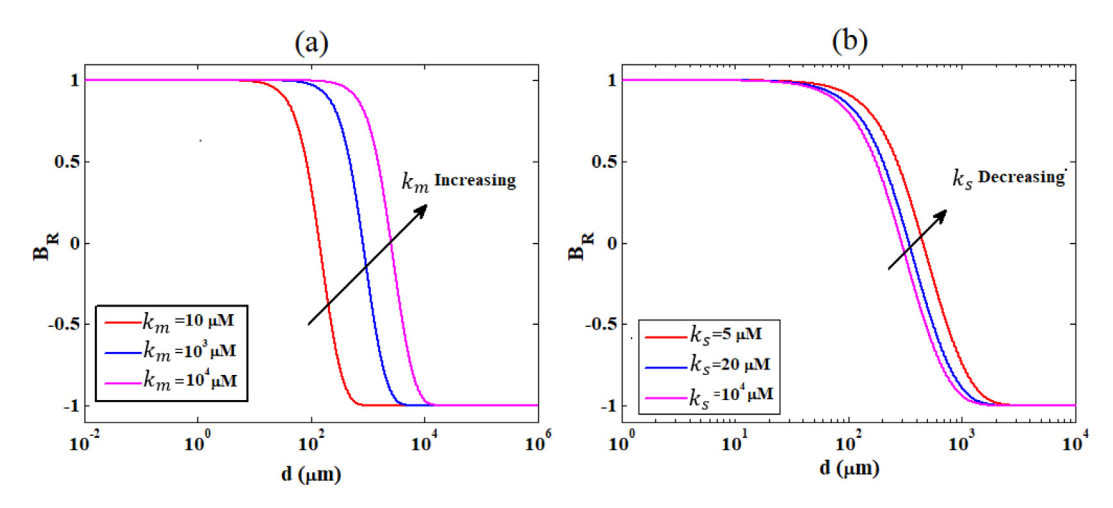


Fig. 3. The biosensor resistance using eqn. (23) for fixed values of  $D_s = D_p = 300 \mu m^2/s$ ,  $V_{max} = 1 \mu M/s$ .(a). $k_s = 10 \mu M$ ,  $s^* = 10 \mu M$  and various values of  $k_m \mu M$ . (b).  $k_m = 100 \mu M$ ,  $s^* = 30 \mu M$  and various values of  $k_s \mu M$ .

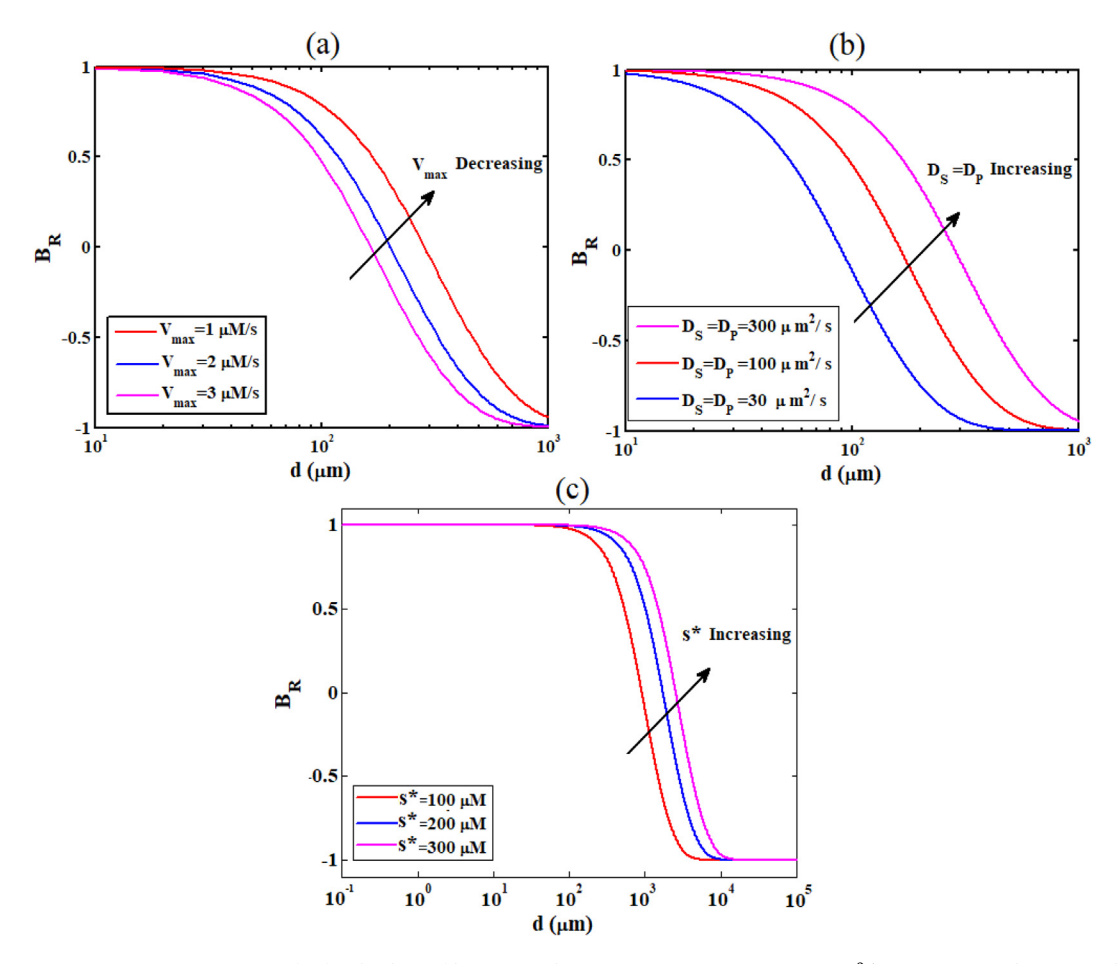


Fig. 4. The biosensor resistance using eqn. (23) for fixed values of  $k_s = 10\mu M$ ,  $k_m = 100\mu M$ . (a).  $D_s = D_p = 300\mu m^2/s$ ,  $s^* = 10\mu M$  and various values of  $V_{max}\mu M/s$ . (b).  $V_{max} = 1\mu M/s$ ,  $s^* = 10\mu M$  and various values of  $D_s = D_p\mu m^2/s$ . (c).  $D_s = D_p = 300\mu m^2/s$ ,  $V_{max} = 1\mu M/s$  and various values of  $s^*\mu M$ .

sitivity reaches the minimum value -1. Due to the substrate inhibition, the sensitivity differs notably only at intermediate concentrations of the substrate i.e  $1\mu M < s^* < 100\mu M$ .

#### 4.2. Resistance

Figs. 3 and 4 illustrate the biosensor resistance  $B_R$  versus the membrane thickness d for different values of the parameter. One can see

from the figures that the shape of all the curves of the normalized resistance is very similar. The results show that the effect of increasing values of the membrane thickness d, results in a deceasing resistivity. It means that the maximal as well as minimal biosensor resistance  $B_R$  is directly proportional to  $\phi_s^2 (= V_{max} d^2/D_s k_m)$ .

Since I is a non-monotonous function of d, the  $B_R$  varies between -1 and 1. The cases when  $B_R$  is close to -1 or 1 correspond to the biosensors the response of which is very sensitive to changes in the

thickness d of the enzyme membrane. The noticeable change in the behavior of the biosensor resistance at the moderate substrate concentrations due to the transition from the kinetic-limited to the diffusion-controlled mode of the biosensor action.

As one can see in Figs. 3 and 4 an increase in the electrochemical reaction rate constant  $k_m$ , substrate concentration  $s^*$  or decrease in  $k_s$  and  $V_{max}$  proportionally shifts the curve representing the resistance  $B_R$  to the right. Thus, an increase in the diffusion coefficient proportionally prolongs the linear part of the biosensor resistance calibration curve.

#### 5. Conclusion

The mathematical model of the amperometric biosensor can be successfully used to investigate the biosensor's sensitivity and resistance. Simple and closed-form the approximate analytical expression for the sensitivity and resistance are obtained for substrate inhibition kinetics. The current function *I* gain the maximum at the membrane thickness

$$d_{max}=1.5055\sqrt{D_s\left(k_m+s^*+rac{(s^*)^2}{k_s}
ight)/V_{max}}$$
. The effect of thickness of the

membrane, concentration of substrate at x=d, diffusion coefficient, Michaelis-Menten constant, inhibition constant on sensitivity and resistance are discussed. The biosensor sensitivity and the linear range of the calibration curve can be increased when substrate concentration  $s^* < 1 \mu Mors^* > 10^3 \mu M$  and all values of other parameters.

Enzyme concentration can significantly reduce biosensor resistance. By decreasing the concentration of the substrate, biosensor resistance may also be greatly reduced (Fig-4). When the biosensor operates in the diffusion-limiting mode instead of in the enzyme reaction-controlled mode, the linear portion of the calibration curve is longer.

#### CRediT authorship contribution statement

**R. Swaminathan:** Data curation, Software, Formal analysis, Writing - original draft. **M. Chitra Devi:** Methodology, Visualization, Resources, Investigation. **L. Rajendran:** Conceptualization, Supervision, Validation, Writing - review & editing, Investigation, Project administration. **K. Venugopal:** Validation, Investigation, Supervision.

#### **Declaration of Competing Interest**

The authors declare that they have no known competing financial interests or personal relationships that could have appeared to influence the work reported in this paper.

#### Acknowledgement

The authors express their gratitude to Shri J. Ramachandran, Chancellor, Col. Dr. G. Thiruvasagam, Vice-Chancellor and Dr. M. Jayaprakashvel, Registrar, Academy of Maritime Education and Training (AMET), Chennai, Tamil Nadu for their encouragement.

#### Appendix A

Analytical solution of nonlinear Eq. (Eqs. (11) and (12)) using Taylor series method

Consider the nonlinear equations

$$\frac{d^2S}{d\chi^2} - \frac{\phi_s^2S}{1 + \alpha S + \beta S^2} = 0 \tag{A1}$$

$$\frac{d^{2}P}{dy^{2}} + \frac{{\phi_{p}}^{2}S}{1 + \alpha S + \beta S^{2}} = 0 \tag{A2}$$

The boundary conditions are given by:

$$\frac{dS}{d\gamma} = 0, P = 0 \text{ when } \chi = 0 \tag{A3}$$

$$S = 1, P = 0 when \chi = 1$$
 (A4)

Consider the Taylor's series at  $\chi=1$  for dimensionless concentration of  $S(\chi)$  and  $P(\chi)$ .

$$S(\chi) \approx \sum_{q=0}^{3} \left( \frac{d^{q} S}{d \chi^{q}} \Big|_{\chi=1} \right) \frac{(\chi - 1)^{q}}{q!}$$
(A5)

$$P(\chi) \approx \sum_{q=0}^{3} \left( \frac{d^{q} P}{d \chi^{q}} \Big|_{\chi=1} \right) \frac{(\chi - 1)^{q}}{q!}$$
(A6)

let  $\frac{d^{q}u}{d\chi^{q}}\Big|_{\xi=1}=A_q$ ,  $\frac{d^{q}v}{d\chi^{q}}\Big|_{\xi=1}=B_q$  and from the boundary conditions (Eq. (A.3-A.4)), we get  $A_0=1$  and  $B_0=0$ . Let us consider,  $A_1=S'(1), B_1=P'(1)$ . Then

$$S(\chi) \approx \sum_{q=0}^{3} A_q \frac{(\chi - 1)^q}{q!} \tag{A7}$$

$$P(\chi) \approx \sum_{q=0}^{3} B_q \frac{(\chi - 1)^q}{q!} \tag{A8}$$

Substituting  $\chi = 1$  in Eq. (A1) and Eq. (A2), we get the following

$$A_2 = \frac{{\phi_s}^2}{1 + \alpha + \beta} \tag{A9}$$

$$B_2 = -\frac{\phi_p^2}{1 + \alpha + \beta} \tag{A10}$$

$$A_3 = \frac{\phi_s^2 l}{1 + \alpha + \beta} \left( 1 - \frac{\alpha + 2\beta}{1 + \alpha + \beta} \right) \tag{A11}$$

$$B_3 = -\frac{\phi_p^2 l}{1 + \alpha + \beta} \left( 1 - \frac{\alpha + 2\beta}{1 + \alpha + \beta} \right) \tag{A12}$$

Consider the approximation stops at third step, then we have

$$S(\chi) \approx A_0 + A_1 (x - 1) + \frac{A_2}{2} (x - 1)^2 + \frac{A_3}{6} (x - 1)^3$$

$$= 1 + S'(1)(x - 1) + \frac{1}{2} \frac{\phi_s^2(x - 1)^2}{1 + \alpha + \beta} + \frac{\phi_s^2 S'(1) (x - 1)^3}{1 + \alpha + \beta} \left(1 - \frac{2\beta}{1 + \alpha + \beta}\right)$$
(A13)

$$P(\chi) \approx B_0 + B_1 (x - 1) + \frac{B_2}{2} (x - 1)^2 + \frac{B_3}{6} (x - 1)^3$$

$$= P'(1)(x - 1) - \frac{1}{2} \frac{\phi_p^2 K'(1)}{1 + \alpha + \beta} - \frac{\phi_p^2 K'(1)}{1 + \alpha + \beta} \left(1 - \frac{\alpha + 2\beta}{1 + \alpha + \beta}\right)$$
(A14)

Now using the boundary conditions  $\frac{dS}{d\chi}=0, P=0$  when  $\chi=0$ , we can get

$$S'(1) = \frac{2\phi_s^2(1+\alpha+\beta)}{2(1+2\alpha+2\beta)+2(\alpha+\beta)^2+\phi_s^2(1-\beta)}; P'(1)$$

$$= \frac{\phi_p^2(3+3\alpha+3\beta-l+\beta l)}{6(1+\alpha+\beta)^2}$$
(A15)

#### Appendix B

Analytical solution of nonlinear equation (Eq.11 and Eq.12) using new homotopy perturbation method

In this Appendix, we indicate how Eq. (5) in this paper is derived.

R. Swaminathan et al.

$$\frac{d^2S}{dr^2} - \frac{\phi_s^2 S}{1 + \alpha S + \beta S^2} = 0 \tag{B1}$$

$$\frac{d^2P}{d\chi^2} + \frac{\phi_p^2 S}{1 + \alpha S + \beta S^2} = 0 \tag{B2}$$

The boundary conditions are given by:

$$\frac{dS}{d\gamma} = 0, P = 0 \text{ when } \chi = 0 \tag{B3}$$

$$S = 1, P = 0 when \chi = 1$$
 (B4)

we first construct a Homotopy as follows [34-36]:

$$(1-p)\left[\frac{d^2S}{d\chi^2} - \frac{\phi_s^2S}{1+\alpha S(\chi=1) + \beta S(\chi=1)^2}\right]$$

$$+p\left[\left(1+\alpha S + \beta S^2\right)\frac{d^2S}{d\chi^2} - \phi_s^2S\right]$$

$$= 0 \tag{B5}$$

$$\begin{split} &(1-p)\left[\frac{d^{2}P}{d\chi^{2}} + \frac{{\phi_{p}}^{2}S}{1 + \alpha S(\chi = 1) + \beta S(\chi = 1)^{2}}\right] \\ &+ p\left[\left(1 + \alpha S + \beta S^{2}\right)\frac{d^{2}P}{d\chi^{2}} + {\phi_{p}}^{2}S\right] \\ &= 0 \end{split} \tag{B6}$$

on simplification we get

$$(1-p)\left[\frac{d^2S}{d\chi^2} + \frac{\phi_s^2S}{1+\alpha+\beta}\right] + p\left[\left(1+\alpha S + \beta S^2\right)\frac{d^2S}{d\chi^2} - \phi_s^2S\right] = 0 \tag{B7}$$

$$(1-p)\left[\frac{d^2P}{d\chi^2} + \frac{{\phi_p}^2S}{1+\alpha+\beta}\right] + p\left[\left(1+\alpha S + \beta S^2\right)\frac{d^2P}{d\chi^2} + {\phi_p}^2S\right] = 0 \tag{B8}$$

The approximate solution of Eqs. (B1) and (B2) are

$$S = S_0 + pS_1 + p^2S_2 + \dots (B9)$$

$$P = P_0 + pP_1 + p^2P_2 + \dots ag{B10}$$

substituting Eq. (B9) in Eq. (B7) and Eq. (B10) in Eq. (B8) in, then comparing the coefficients of like powers of p yields:

$$p^{0}: \frac{d^{2}S_{0}}{d\chi^{2}} - \frac{\phi_{s}^{2}S_{0}}{1 + \alpha + \beta} = 0$$
 (B11)

$$p^0: \frac{d^2P_0}{d\chi^2} + \frac{\phi_p^{\ 2}S_0}{1+\alpha+\beta} = 0 \tag{B12} \label{eq:B12}$$

The boundary conditions are

$$\chi = 0; \frac{dS_i}{d\chi} = 0; P_i = 0; i = 0, 1, 2, 3 \cdots$$
(B13)

$$\chi = 1; S_0 = 1; P_0 = 0; S_i = 0; P_i = 0; i = 1, 2, 3 \cdots$$
 (B14)

Solving the Eqs. ((B11) and (B12)), and using the above boundary conditions and we can find the following results.

$$S_{0} = \frac{\cosh\left(\frac{\phi_{s}}{\sqrt{1+\alpha+\beta}}\chi\right)}{\cosh\left(\frac{\phi_{s}}{\sqrt{1+\alpha+\beta}}\right)}$$
(B15)

$$P_{0} = \frac{\phi_{p}^{2}}{\phi_{s}^{2}} \left( \chi + \frac{1 - \chi - cosh\left(\frac{\phi_{s}}{\sqrt{1 + a + \beta}}\chi\right)}{cosh\left(\frac{\phi_{s}}{\sqrt{1 + a + \beta}}\right)} \right)$$
(B16)

According to the HPM, we can conclude that

$$S(\chi) \approx \lim_{p \to 1} S = S_0 + S_1 + S_2 + \cdots$$
 (B17)

$$P(\chi) \approx \lim_{n \to 1} P = P_0 + P_1 + P_2 + \cdots$$
 (B18)

Considering the first iteration we have the solution of concentration of species

$$S(\chi) \approx S_0 = \frac{\cosh(m\chi)}{\cosh(m)}$$
 (B19)

$$P(\chi) \approx P_0 = \frac{\phi_p^2}{\phi_s^2} \left( \chi + \frac{1 - \chi - \cosh(m\chi)}{\cosh(m)} \right)$$
 (B20)

where 
$$m=rac{\phi_s}{\sqrt{1+lpha+eta}}$$

#### **Appendix C Nomenclature**

Symbol	Meaning
s	Concentration of substrate
p	Concentration of product
$s^*$	Concentration of substrate at $x = d$
$k_m$	Michaelis-menten constant
$k_s$	Inhibition constant
$V_{max}$	Maximal enzymatic rate
d	Thickness of the enzyme layer
F	Faraday constant
$D_s$	Diffusion coefficient of the substrate
$D_p$	Diffusion coefficient of the product
I	Current density of the biosensor
x	Distance
$\mathcal{S}$	Dimensionless concentration of substrate
P	Dimensionless concentration of product
χ	Dimensionless distance
$\phi_s^2$	Substrate reaction diffusion parameter
${\phi_p}^2$	Product reaction diffusion parameter
$\alpha$	Saturation parameter
β	Saturation parameter
$B_S$	Biosensor sensitivity
$B_R$	Biosensor resistance.
$\psi$	Dimensionless current
$n_e$	Number of electrons involved in charge transfer at the
	electrode surface
Unit	Experimental values []
$\mu M$	-
$\mu M$	-
$\mu M$	10–100
$\mu M$	100
$\mu M$	10
$\mu M/s$	1–1000
μm	10–100
C/mol	96,485
$\mu m^2/s$	300
$\mu m^2/s$	300
$\mu A/cm^2$	-
cm	_
None	_
None	_
None	-
None	0.5–300
None	0.5–300

(continued on next page)

#### Appendix C Nomenclature (continued)

Symbol	Meaning
None	0.1–1
None	0.1–10
None	_

#### References

- R. Baronas, F. Ivanauskas, J. Kulys, The influence of the enzyme membrane thickness on the response of amperometric biosensors, Sensors 3 (2003) 248–262, https://doi.org/10.3390/s30700248.
- [2] R. Baronas, F. Ivanauskas, J. Kulys, M. Sapagovas, Modelling of amperometric biosensors with rough surface of the enzyme membrane, J. Math. Chem. 34 (3/4) (2003) 227–242, https://doi.org/10.1023/B;JOMC.0000004072.97338.12.
- [3] J. Kulys, R. Baronas, Modelling of amperometric biosensors in the case of substrate inhibition, Sensors 6 (2006) 1513–1522, https://doi.org/10.3390/s6111513.
- [4] J. Kulys, Biosensor response at mixed enzyme kinetics and external diffusion limitation in case of substrate inhibition, Nonlinear Anal. Model. Control. 11 (2006) 285–292. https://doi.org/10.15388/na.2006.11.4.14740.
- [5] P. Manimozhi, A. Subbiah, L. Rajendran, Solution of steady-state substrate concentration in the action of biosensor response at mixed enzyme kinetics, Sens. Actuat. B Chem. 147 (1) (2010) 290–297, https://doi.org/10.1016/j. snb.2010.03.008.
- [6] A. Anitha, S. Loghambal, L. Rajendran, Analytical expressions for steady-state concentrations of substrate and product in an amperometric biosensor with the substrate inhibition—The adomian decomposition method, Am. J. Anal. Chem. 03 (08) (2012) 495–502, https://doi.org/10.4236/ajac.2012.38066.
- [7] M.E.G. Lyons, Transport and kinetics at carbon nanotube Redox enzyme composite modified electrode biosensors, Int. J. Electrochem. Sci. 4 (2009) 77–103.
- [8] M.E.G. Lyons, Transport and kinetics at carbon nanotube redox enzyme composite modified electrode biosensors part 2. redox enzyme dispersed in nanotube mesh of finite thickness, Int. J. Electrochem. Sci. 4 (2009) 1196–1236.
- [9] R. Baronas, J. Kulys, K. Petrauskas, J. Razumiene, Modelling carbon nanotube based biosensor, J. Math. Chem. 49 (5) (2011) 995–1010, https://doi.org/ 10.1007/s10910-010-9791-2.
- [10] R. Baronas, F. Ivanauskas, J. Kulys, Mathematical Modeling of Biosensors An Introduction for Chemists and Mathematicians, Springer, 2010. https://doi.org/ 978-90-481-3242-3.
- [11] L. Rajendran, R. Swaminathan, M. Chitra Devi, A Closer Look of Nonlinear Reaction-Diffusion Equations, Nova Science Publishers, Incorporated, New York, NY 2020
- [12] J.-H. He, Y.O. El-Dib, Homotopy perturbation method for Fangzhu oscillator, J. Math. Chem. 58 (10) (2020) 2245–2253.
- [13] A. Meena, L. Rajendran, Mathematical modeling of amperometric and potentiometric biosensors and system of non-linear equations – Homotopy perturbation approach, J. Electroanal. Chem. 644 (1) (2010) 50–59.
- [14] P. Jeyabarathi, M. Kannan, L. Rajendran, Mathematical Modelling of Double Chamber Microbial Fuel Cell using Homotopy Perturbation Method, Int. J. Eng. Adv. Technol. 9 (2020) 1845–1853. https://doi.org/10.35940/ijeat. c5542.029320.
- [15] R. Swaminathan, K. Lakshmi Narayanan, V. Mohan, K. Saranya, L. Rajendran, Reaction/diffusion equation with Michaelis-Menten kinetics in microdisk biosensor: Homotopy perturbation method approach, Int. J. Electrochem. Sci. 14 (2019) 3777–3791. https://doi.org/10.20964/2019.04.13.

- [16] R. Swaminathan, K. Venugopal, M. Rasi, M. Abukhaled, L. Rajendran, Analytical expressions for the concentration and current in the reduction of hydrogen peroxide at a metal-dispersed conducting polymer film, Quim. Nova 43 (2020) 58\_65
- [17] K. Saranya, V. Mohan, L. Rajendran, Steady-state concentrations of carbon dioxide absorbed into phenyl glycidyl ether solutions by residual method, J. Math. Chem. 58 (6) (2020) 1230–1246, https://doi.org/10.1007/s10910-020-01127-0.
- [18] J.-H. He, F.-Y. Ji, Taylor series solution for Lane-Emden equation, J. Math. Chem. 57 (8) (2019) 1932–1934, https://doi.org/10.1007/s10910-019-01048-7.
- [19] S. Vinolyn Sylvia, R. Joy Salomi, L. Rajendran, M. Abukhaled, Poisson-boltzmann equation and electrostatic potential around macroions in colloidal plasmas: Taylor series approach, Solid State Technol. 63 (2020) 10090–10106.
- [20] A.-M. Wazwaz, A comparison between Adomian decomposition method and Taylor series method in the series solutions, Appl. Math. Comput. 97 (1998) 37-44
- [21] J. Visuvasam, A. Meena, L. Rajendran, New analytical method for solving nonlinear equation in rotating disk electrodes for second-order ECE reactions, J. Electroanal Chem. 869 (2020) 114106
- [22] M.E.G. Lyons, Transport and kinetics in electrocatalytic thin film biosensors: bounded diffusion with non-Michaelis-Menten reaction kinetics, J. Solid State Electrochem. 24 (2020) 2751–2761.
- [23] B. Manimegalai, M.E.G. Lyons, L. Rajendran, A kinetic model for amperometric immobilized enzymes at planar, cylindrical and spherical electrodes: the Akbari-Ganji method, J. Electroanal. Chem. 880 (2021) 114921, https://doi.org/ 10.1016/j.jelechem.2020.114921.
- [24] K.M. Dharmalingam, M. Veeramuni, Akbari-Ganji's Method (AGM) for solving non-linear reaction - Diffusion equation in the electroactive polymer film, J. Electroanal. Chem. 844 (2019) 1–5.
- [25] M.C. Devi, P. Pirabaharan, M. Abukhaled, L. Rajendran, Analysis of the steadystate behavior of pseudo-first-order EC-catalytic mechanism at a rotating disk electrode, Electrochim. Acta 345 (2020) 136175.
- [26] M.C. Devi, P. Pirabaharan, L. Rajendran, M. Abukhaled, An efficient method for finding analytical expressions of substrate concentrations for different particles in an immobilized enzyme system, React. Kinet. Mech. Catal. 130 (2020) 35–53.
- [27] J. Visuvasam, A. Meena, R. Swaminathan, L. Rajendran, Mathematical Modelling of Rotating Disc Electrodes and Nonlinear Diffusion, in: Adv. Chem. Eng., 2020: pp. 1–12.
- [28] J.-H. He, Taylor series solution for a third order boundary value problem arising in Architectural Engineering, Ain Shams Eng. J. 11 (4) (2020) 1411–1414, https://doi.org/10.1016/j.asej.2020.01.016.
- [29] C.-H. HE, Y. Shen, F.-Y. Ji, J.H. He, Taylor series solution for fractal bratu-type equation arising in electrospinning process, Fractals 28 (01) (2020) 2050011, https://doi.org/10.1142/S0218348X20500115.
- [30] J.-H. He, A simple approach to one-dimensional convection-diffusion equation and its fractional modification for E reaction arising in rotating disk electrodes, J. Electroanal. Chem. 854 (2019) 113565, https://doi.org/10.1016/ j.jelechem.2019.113565.
- [31] JI.-H. HE, Some asymptotic methods for strongly nonlinear equations, Int. J. Mod. Phys. B. 20 (10) (2006) 1141–1199, https://doi.org/10.1142/ S0217979206033796.
- [32] J.-H. He, Homotopy perturbation technique, Comput. Methods Appl. Mech. Eng. 178 (3-4) (1999) 257–262, https://doi.org/10.1016/S0045-7825(99)00018-3.
- [33] L. Rajendran, S. Anitha, Reply to "comments on analytical solution of amperometric enzymatic reactions based on Homotopy perturbation method," by Ji-Huan He, Lu-Feng Mo [Electrochim. Acta (2013)], Electrochim. Acta. 102 (2013) 474–476. https://doi.org/10.1016/j.electacta.2013.03.163.
- [34] J.-H. He, Y.O. El-Dib, The reducing rank method to solve third-order Duffing equation with the homotopy perturbation, Numer. Methods Partial Differ. Eq. 37 (2) (2021) 1800–1808, https://doi.org/10.1002/num.v37.210.1002/num.22609.
- [35] J.-H. He, Y.O. El-Dib, Periodic property of the time-fractional Kundu–Mukherjee–Naskar equation, Results Phys. 19 (2020) 103345, https:// doi.org/10.1016/j.rinp.2020.103345.
- [36] K. Nirmala, B. Manimegalai, L. Rajendran, Steady-state substrate and product concentrations for non-michaelis-menten kinetics in an amperometric biosensorhyperbolic function and padeapproximants method, Int. J. Electrochem. Sci. 15 (2020) 5682–5697. https://doi.org/10.20964/2020.06.09.